Inhibitory actions of electrolysed water on food spoilage fungi

Franziska Wohlgemuth

Thesis submitted to the University of Nottingham

for the degree of Doctor of Philosophy

School of Life Sciences

2021

Abstract

Chemical sanitisers are needed for controlling microbial contamination and growth in various settings, including healthcare, domestic settings and the food industry. One promising sanitiser with proposed applications in the food industry is the oxidising sanitiser electrolysed water (EW). For EW applications to be effective, a more in-depth understanding of EW mode-of-action is needed, together with the identification of limiting factors associated with the chemical matrices in relevant EW applications.

This study investigated the reactivity of EW with different organic substances. For this purpose, the common food spoilage fungus *Aspergillus niger* was treated with EW in the presence or absence of the organic materials. The sanitiser retained partial fungicidal activity at high levels of added soil, commonly associated with freshly harvested produce. By narrowing down the reactivity of EW from complex matrices to specific organic molecules, proteins and amino acids were found to strongly suppress EW fungicidal activity.

The potential implications of EW reactivity with proteins and amino acids within cells were investigated in the fungal model organism *Saccharomyces cerevisiae*. This capitalised on the advanced understanding of the uptake and metabolism of diverse compounds and the availability of convenient genetic tools in this model organism. Pre-culture with methionine but not with other tested amino acids increased yeast resistance to subsequent treatments (in the absence of methionine) with sanitisers (EW, sodium hypochlorite, ozonated water). Further tests suggested a direct role of the methionine molecule itself, as opposed to downstream products of methionine metabolism or methionine misincorporation in proteins, in increasing yeast EW resistance. Intracellular methionine oxidation

can disturb FeS cluster proteins and this study found that EW treatment impairs FeS cluster protein activity.

Because active species in EW can be inactivated by organic compounds, microorganisms may be exposed to low effective EW doses during EW treatments where organic matter is present. When low, sub-lethal EW doses were applied to *A. niger*, early germination events and colony growth post-treatment were delayed and there was increased variation in size among resultant colonies. The delay and increased variation were non-heritable and were observed with chlorine-containing sanitisers (EW, sodium hypochlorite) but not the chlorine-free oxidant ozonated water. The collective findings led to a hypothesis that chloramine formation within spores during EW treatment may contribute to the observed phenotypes.

This study increases the understanding of limiting chemical factors for EW applications and sheds light onto the cellular mode-of-action of EW and the fungal response mechanisms to sanitiser treatments. Such insights can improve the rational development of EW application processes and contribute to understanding and prediction of antimicrobial efficacy in diverse settings.

Publications

Davies, C. R., Wohlgemuth, F., Young T., Violet, J., Dickinson, M., Sanders, J.-W., Vallieres, C., Avery, S. V., 2021. Evolving challenges and strategies for fungal control in the food supply chain. *Fungal Biol. Rev.*, 36, 15-26.

Wohlgemuth F., Gomes, R. L., Singleton, I., Rawson, F. J., Avery, S. V., 2020. Top-down characterisation of an antimicrobial sanitiser, leading from quenchers of efficacy to mode of action. *Front. Microbiol.*, 11, 575157.

Acknowledgements

First, I would like to thank my supervisor Prof Simon Avery for inviting me to work on this project and for his excellent scientific guidance and support throughout my PhD. Thank you also to my co-supervisors Prof Rachel Gomes, Dr Frankie Rawson and Prof Ian Singleton for their valuable discussions and inputs.

I am indebted to B44 and the fungal group for helping me through the last four years by offering technical, emotional and, notably, culinary support. Everyone helped in different ways, but some people deserve a special mention: Thank you to Matt Kokolski for being the reason the fungal group is running smoothly. I cannot thank Dr Cindy Vallières enough, for being the "fountain of knowledge" (Foster, 2019) that she is, but also for her friendship, support and her striking efforts to create a positive environment in our group. I thank my PhD brother Dr Harry Harvey for many useful discussions. Thank you to Taran Young, Catheryn Davies and everyone else who made working in the fungal group more fun.

I thank the EPSRC for funding this project. I would also like to thank Ozo Innovations for providing technical guidance, financial support and, most importantly, the electrolysed water for this study. Further thanks go to John Grubb at GreenTeck Global for providing an ozonated water spray bottle.

Finally, I want to thank my family and friends for offering support and for reminding me that there is a life outside of the lab. Lockdown added additional challenges to PhD projects everywhere, and I am grateful for many video calls throughout those strange times and, last but not least, for being exceptionally lucky with my lockdown companion.

Table of Contents

List of figures

Appendix figures

List of tables

Appendix tables

List of abbreviations and symbols

ε	extinction coefficient
aa	amino acid
Abs	absorbance
AEW	acidic electrolysed water
AMM	*Aspergillus* minimal media
Amp	ampicillin
APF	aminophenyl fluorescein
ars	sodium arsenite
asc	ascorbic acid
AspGD	*Aspergillus* Genome Database
BEW	basic electrolysed water
BLAST	basic local alignment search tool (NCBI)
BSA	bovine serum albumin
cfu	colony forming unit(s)
CGR	Centre of Genomic Research, University of Liverpool
CIA	cytosolic iron sulphur protein assembly
ctrl	control
CV	coefficient of variation
DCF	2',7'-dichloro-dihydro-fluorescin diacetate
DE	differentially expressed
DEPC	diethyl pyrocarbonate
DHE	dihydroethidium
DMF	dimethylformamide
DMSO	dimethyl sulphoxide
DTT	dithiothreitol
EDTA	ethylenediaminetetraacetic acid
EMBL-EBI	European Bioinformatics Institute, part of the European Molecular Biology Laboratory
EW	electrolysed water
FA	formic acid
FAC	free available chlorine
FDR	false discovery rate
FeS cluster	iron sulphur cluster
FPKM	fragments per kilobase per million reads
fRMsr	see MSR; reduces free (*R*)-MetO
FSC	forward scatter
g	relative centrifugal force
GAP	glyceraldehyde-3-phosphate dehydrogenase
GFP, yEGFP	green fluorescent protein, yeast-enhanced GFP
GO	gene ontology
GSH	glutathione
HPF	hydroxyphenyl fluorescein
HPLC grade water	high-purity water suitable for high-performance liquid chromatography
ISC	mitochondrial iron sulphur cluster assembly
ITS	internal transcribed spacer

kGy	kilo Gray
LB	lysogeny broth
Li-Acetate	lithium acetate
log reduction	decadic logarithm of the ratio of microorganisms before and after a treatment (1 log corresponds to 10-fold reduction)
logFC	log2 fold change
LOI	loss on ignition
MES	2-(N-morpholino)ethanesulphonic acid
MetO	methionine sulphoxide
MetRS	Met-tRNA-synthetase
MSR	methionine sulphoxide reductase
MsrA (Mxr1)	reduces free and protein-bound (*S*)-MetO
MsrB (Mxr2)	reduces protein-bound (*R*)-MetO
NAC	N-acetyl cysteine
NADPH	nicotinamide adenine dinucleotide phosphate
NaOCl	sodium hypochorite
NCBI	National Center for Biotechnology Information
NEB	New England Biolabs
NEW	neutral electrolysed water
ns	not significant
OD_{600}	optical density at 600 nm
ORF	open reading frame
ORP	oxidation-reduction potential
PAA	peracetic acid
PBS	phosphate buffered saline
PCA	principal component analysis
PCR	polymerase chain reaction
PDA	potato dextrose agar
PEG	polyethylene glycol
PI	propidium iodide
PM	paromomycin
ppm	parts per million
PQ	primaquine
px	pixel(s)
repl	replicate
rev min^{-1}	revolutions per minute
RFI	relative fluorescence intensity
RNase	ribonuclease
ROS	reactive oxygen species
RT	room temperature
s	second(s)
SAEW	slightly acidic electrolysed water
SAM	S-adenosyl methionine
SD	standard deviation
SDS	sodium dodecyl sulphate
SDW	sterile distilled water
seq	sequence
SOC	super optimal broth with catabolite repression

SSC	sideward scatter
TBE buffer	tris/borate/EDTA
Tris-HCl	tris(hydroxymethyl)aminomethane pH adjusted with hydrochloric acid
U	enzyme unit(s)
UV	ultraviolet radiation
UV-C	ultraviolet radiation with wavelengths below 280 nm
v/v	volume per volume
w/v	weight per volume
w/w	weight per weight
WHO	world health organization
YE	yeast extract
YEPD (YEP)	yeast extract peptone supplemented (or not) with glucose
YNB	yeast nitrogen base

1 Introduction

1.1 Fungi in the environment

1.1.1 Characteristics

Fungi represent one of the eukaryotic kingdoms of life, distinct from other kingdoms such as plants or animals (Hawksworth, 1991). The group encompasses highly diverse species, from single-cell yeasts to moulds to mushrooms (Bridge and Spooner, 2001, Walker and White, 2017). Many fungal species form a mycelium that can stretch over large areas up to several hectars, contributing to the spread of fungal cells and spores (Bridge and Spooner, 2001). These mycelia are formed by hyphae, which are filamentous structures of interconnected cells that provide cytoplasmic connectivity (Dighton, 2016). Hyphae are however compartmentalised by septa which can be closed by Woronin bodies, blocking the connectivity (Bleichrodt et al., 2012). Yeast cells divide mitotically by cell division either as diploid and haploid cells and the conversion between the two states occurs by meiosis of diploid cells and mating of haploids, respectively (Gimeno and Fink, 1992, Fischer et al., 2020). On the other hand, the hyphae of filamentous fungi grow apically by cell-wall extension and exocytosis processes, while specialised structures produce spores (either sexually or asexually) which disperse into the environment and can grow into a new hyphal network upon germination (Riquelme et al., 2018). The spores can survive in dry conditions for many years (Zukiewicz-Sobczak, 2013).

1.1.2 Occurrence, benefits of fungi and the fungal threat

Fungi occur in aquatic, terrestrial and marine ecosystems, generating nutrients and food for plants and animals, and they can withstand extreme conditions such as freezing temperatures at the poles or low-nutrient environments (Dighton,

2016). In soil, fungi take part in degradation processes and in mycorrhizal relationships with plant roots but can also act as pathogens (Bridge and Spooner, 2001). Symbiotic associations between fungi and green algae or cyanobacteria are known as lichens (Asplund and Wardle, 2017). Fungi can also be used for bioremediation of pollutants (Priyadarshini et al., 2021) or for industrial production of food products, pharmaceuticals, biofuels and more (Walker and White, 2017). Fungal species are found in samples from the healthy human gut, such as *Saccharomyces cerevisiae*, species of *Candida*, *Cladosporium*, *Aspergillus* and *Penicillium*, usually identified by *in-vitro* cultivation and/or molecular methods (Hallen-Adams and Suhr, 2017).

Airborne fungal spores are abundant in outdoor and indoor air and some of these fungi can present health risks for immunocompromised patients (Rainer et al., 2001). Several mould species also have allergenic properties (Zukiewicz-Sobczak, 2013). Many different fungal species, especially moulds, have been found in drinking water samples, for instance in hospital air and water systems, including pathogenic, toxigenic and allergenic species (Hageskal et al., 2009, Rainer et al., 2001). Generally, pathogenic fungi globally result in an estimated 1.6 million deaths per year (Bongomin et al., 2017). Plant-pathogenic fungi can cause diseases in crop plants or forests which necessitates the application of control strategies such as fungicides to protect crops (van der Does and Rep, 2017). Fungal crop diseases represent a serious problem for maintaining food security and they cost billions of dollars due to crop loss every year (Savary et al., 2012). Damage by fungi also plays a role in the deterioration of paintings, stone monuments, buildings and other materials (Singh, 1994, Sterflinger, 2010, Sterflinger and Pinzari, 2012).

1.2 Fungi and the food industry

1.2.1 Food spoilage as a global concern

Fresh food such as fruits and vegetables are part of a healthy diet but are also susceptible to spoilage. Food losses due to fungal spoilage are common for perishable foods such as fruits and vegetables, with sources of contamination ranging from pre-harvest (irrigation water, soil, contaminated seeds) to post-harvest steps (handling, storage and transportation, cross-contamination) (Bhilwadikar et al., 2019). Warm and humid climates or extreme weather events further increase the risk of spoilage (FAO, 2019). According to the Food and Agriculture Organization of the United Nations, around 50% of fruits and vegetables are lost at different stages of the food supply chain from agriculture up to and including the consumer level (FAO, 2011). The food supply chain describes all the steps that are necessary to produce and bring foods such as fresh fruits and vegetables to the consumer (Figure 1-1). In food processing factories, fungal contamination can persist on food handling surfaces, containers, walls and floor surfaces, increasing the risk of postharvest contamination of the produce (Bernat et al., 2017, Snyder and Worobo, 2018). Food losses at the post-harvest, processing and distribution stages amount to between 10 and 40% of the initial fruit and vegetable production, depending on the geographical region (FAO, 2011). More recently, it has been estimated that at least 14% of global food production is lost at the post-harvest level up to (not including) the retail level. Roots, tubers, oil-bearing crops, fruits and vegetables contribute the most to these food losses, with 20–25% of the produced weight being lost (FAO, 2019).

Figure 1-1: Food supply chain. Adapted from Longfield (2017).

Food losses are an important economic problem. For instance, it has been estimated that grain losses in Eastern and Southern African countries alone correspond to a value of US$1.6 billion per year (the estimated value of total production is US$11 billion) (The World Bank et al., 2011). In addition, the loss of food represents a waste of land, water, resources and energy. Considering that 815 million people suffered from malnutrition worldwide in 2016 (FAO et al., 2017), the loss of edible food also becomes an ethical problem. The urgency of providing sufficient amounts of food to all people was underlined by the award of the 2020 Nobel Peace Prize to the World Food Programme. To reduce the risk of microbial spoilage, the main principles developed by the US Food and Drug Administration focus on preventing the exposure of food to contaminating organisms at every point of the production and supply chain (FDA, 1998). This includes the implementation of good agricultural practices, the prevention of contamination from water, proper handling of manure as well as workers' hygiene.

1.2.2 Principles of microbial food spoilage

Microorganisms naturally degrade organic matter and this is essential for nutrient recycling (Blackburn, 2006). The general term for this is biodegradation, and it is used actively by some food industries, e.g., in fermentation. If unwanted degradation and microbial growth occur on food, this is generally regarded as spoilage. One key group of food spoilage microorganisms are moulds (filamentous fungi). Moulds produce a diversity of degradative enzymes and their actions can lead to off-flavours, discoloration, rotting and formation of toxins or allergenic particles (Filtenborg et al., 1996). Other food spoilage microorganisms include bacteria (e.g., *Pseudomonas*, *Clostridium*) and yeasts (e.g., *Candida*, *Saccharomyces*) (Blackburn, 2006). Yeasts and moulds are important in food spoilage because they are able to grow on a wide range of products. This is due to their ability to grow on various chemical substrates while also exhibiting a high

tolerance to low pH, low water activity, low temperature and the presence of preservatives (Huis in't Veld, 1996). In general, harvested vegetables will often (but not exclusively) become spoiled by bacteria, whereas the low pH of fruits favours the growth of fungi (Brackett, 1987, Oms-Oliu et al., 2010). Spoilage yeasts such as *Zygosaccharomyces bailii* are a common problem in soft drink preservation (Stratford et al., 2020).

In addition to food spoilage that is visible or detectable after sensory inspection, food (including fruits and vegetables) can be a carrier for pathogenic microorganisms (Steele and Odumeru, 2004). In recent years, there have been several well-documented outbreaks of food related diseases in western countries. Examples include the presence of enterohemorrhagic *Escherichia coli* O104:H4 (EHEC) on sprouts (Burger, 2012) and the contamination of yoghurt with the pathogenic fungus *Mucor circinelloides* (Lee et al., 2014b). However, food borne illnesses pose an especially big threat in developing countries, due to low or missing regulatory standards in combination with a growing food production industry (WHO, 2015). Worldwide, the WHO report recorded 600 million foodborne illnesses and 420,000 related deaths in 2010.

1.2.3 Food spoilage fungi and mycotoxin production

Many filamentous fungi cause spoilage of harvested produce. *Penicillium* strains like *P. digitatum* or *P. italicum* can cause green and blue mould on citrus fruits, leading to significant economic losses (Palou, 2014). Peach and nectarine fruits are most commonly spoiled post-harvest by species of *Monilinia*, *Rhizopus* and *Botrytis cinerea* (Bernat et al., 2017). A range of *Aspergillus* species can spoil various fresh fruits and vegetables, dried fruits, nuts and coffee beans, such as *A. niger* and *A. carbonarius* (Perrone et al., 2007), and *A. flavus* is also well known to spoil grains, nuts and pulses, including animal feed commodities (Fakruddin et

al., 2015). A major concern relating the consumption of (especially non-visibly) spoiled produce is the production of mycotoxins by filamentous fungi, mainly *Aspergillus*, *Alternaria*, *Fusarium* and *Penicillium*, with cytotoxic, carcinogenic or mutagenic effects (Martinović et al., 2016, Barkai-Golan, 2008c). Among the *Aspergilli*, maybe the most important food spoilage species is *A. flavus* which produces aflatoxins including the highly carcinogenic aflatoxin B_1 (Klich, 2007). Other toxins produced by *Aspergilli* include aflatoxins B_2, G_1 and G_2, produced by *A. flavus*, *A. parasiticus* and *A. nomius*, and ochratoxin A, the latter being produced by species in the *Aspergillus* sections *Circumdati* and *Nigri* (see 1.3.1) (Perrone et al., 2007, Barkai-Golan, 2008a). A common spoilage organism of apples and other fruits, *P. expansum*, produces patulin and a range of other toxic metabolites (Andersen et al., 2004). Apart from patulin, *Penicillium* species also produce ochratoxin A, citrinin, penicillic acid, cyclopiazonic acid and penitrem (Barkai-Golan, 2008b). Because spoilage fungi can also infect animal feed, the mycotoxins may even find their way into human food consumption through animal-derived products such as dairy or eggs (Martinović et al., 2016).

1.3 The food spoilage fungus *Aspergillus niger*

1.3.1 Biology of *A. niger*

In the present study, the food spoilage organism *A. niger* was studied because it spoils commodities such as onions (Kumar et al., 2015), and internal conversations with Ozo Innovations Ltd. had indicated an industrial interest in control strategies against this fungus. The genus *Aspergillus* consists of filamentous fungi that produce mitotic conidiospores for reproduction (Figure 1-2) (Klich, 2009). For many *Aspergillus* species, sexual reproduction has been reported, involving fruiting bodies called cleistothecia and the formation of ascospores (O'Gorman et al., 2009). *A. niger* is one of more than 250 *Aspergillus*

species, and nowadays, 27 *Aspergillus* species have been grouped in the *Nigri* section (split into seven clades including the *A. niger* clade). These *Nigri* species are distinguishable with molecular methods and are highly similar in morphology (Massi et al., 2021). So far, a sexual cycle has not been shown for *A. niger* although research is ongoing due to findings such as the existence of mating type genes in this species (Ellena et al., 2020). *A. niger* grows aerobically and can be found on organic matter such as soil, litter, compost and decaying plant material (Schuster et al., 2002). The fungus expresses enzymes for the degradation of lignocellulose and is important for the global carbon cycle (Baker, 2006). Industrially, *A. niger* has been cultivated as a source of citric acid and various enzymes since 1919 (Schuster et al., 2002).

A range of mycotoxins are produced by different *Aspergilli* (such as ochratoxins, gliotoxin and fumonisin in *A. niger*), and they can lead to mycotoxicoses when ingested or inhaled (Klich, 2009, Noonim et al., 2009). At least 40 *Aspergillus* species are clinically important (Klich, 2006). Alongside *A. fumigatus*, *A. flavus* and *A. terreus*, *A. niger* is one of the *Aspergillus* species that are found most often in soil and that are also the most relevant in allergies, whereas invasive aspergillosis is mainly caused by *A. fumigatus* and *A. flavus*, with only few cases being related to *A. niger* (Klich, 2009). Furthermore, *A. niger* can be involved in ear infections (Schuster et al., 2002). However, *A. niger* spores are widely distributed in our every-day surroundings and rarely manage to colonise the body unless the patient is susceptible due to an immunodeficiency (Schuster et al., 2002).

1.3.2 Contamination and degradation issues associated with *A. niger*

Within buildings, *A. niger* and other *Aspergillus* species commonly occur in damp or wet areas (Klich, 2009). In the context of food, *A. niger* commonly occurs on

tomatoes (Hasan, 1995), onions (Massi et al., 2021), grapes (Cabañes et al., 2002, Logrieco et al., 2009) and coffee beans (Figure 1-2) (Noonim et al., 2009). Colonisation with *A. niger* can lead to degradation of the edible parts of plants (mostly post-harvest) and potentially mycotoxin production, such as ochratoxin A or fumonisin B_2 formation on grape berries (Taniwaki et al., 2018, Logrieco et al., 2009). Apart from dangers related to mycotoxin formation by *A. niger*, the fungal growth can result in decay, rotting, off-flavours and colourations (Perrone et al., 2007). Aside from fruits and vegetables, *A. niger* is also a common contaminant of yoghurt (Gougouli and Koutsoumanis, 2017). Outbreaks of *A. niger* resulting in black mould disease have been reported in agriculture (e.g., in onions) (Lorbeer et al., 2000). While exact numbers are difficult to obtain, post-harvest onion losses have been estimated to amount to 25–40% in India, the second-largest onion producing country in the world, with microbial spoilage contributing 10–12% of the losses, mainly caused by fungi including *A. niger* (Kumar et al., 2015).

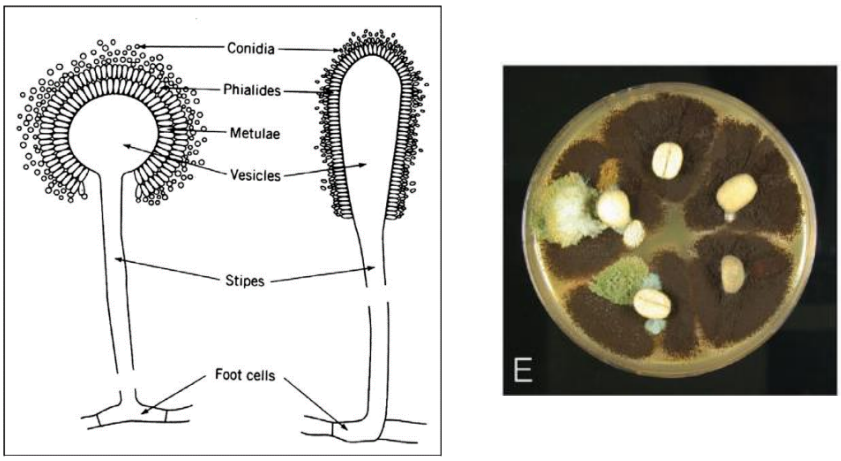

Figure 1-2: *Aspergillus niger*. Left: Schematic of *Aspergillus* condiophores. From Klich (2009). Right: Agar plate cultivation of *A. niger* and other fungal species from coffee beans. From Perrone et al. (2007).

1.4 Preventing microbial contamination: Sanitisation, disinfection and sterilisation

Different terms describe the reduction or elimination of microorganisms on or in inanimate materials and foods. Generally, disinfection refers to the killing of all microorganisms except spores, whereas sanitisation means the reduction of microbial counts to acceptable levels (Block, 2001). For sanitisers, the reduction requirements lie between 5 log reduction for food surfaces and 3 log reduction for non-food surfaces within 30 seconds, whereas disinfectants must be effective within 10 minutes (Pfuntner, 2011). A similar definition for sanitisers against suspended microorganisms (5 log in 30 s) and biofilms (3 log in 30 s) has been given (Hricova et al., 2008). Sterilisation, on the other hand, describes the removal or destruction of all viable microorganisms, including spores (Block, 2001). In the food industry, "commercial sterility" is often used as a verifiable definition for the safety of sterile food. Commercially sterile products such as canned food have to be free of microorganisms capable of growing at normal room temperature storage, and the sterilisation process is usually validated by a ≥12 log reduction of *Clostridium botulinum* (Anderson et al., 2011). The requirements are summarised in Table 1-1.

Table 1-1: Requirements for reducing and eliminating the microbial load.

Criteria[a]	**Sanitisation**	**Disinfection**	**Sterilisation**
Reduction of microbial load?	✓	✓	✓
Free of vegetative microbial cells?	×	✓	✓
Free of spores?	×	×	✓
Reduction requirements	5 log in 30 s (food surfaces, suspended microorganisms), 3 log in 30 s (non-food surfaces, biofilms)	10 min	Commercially sterile: ≥12 log for *C. botulinum*

[a] Criteria as reported by Pfuntner (2011), Hricova et al. (2008), Block (2001) and Anderson et al. (2011).

1.5 Food preservation and sanitisation

1.5.1 Challenges of fresh produce treatments

Fruits and vegetables are commonly washed with tap water to remove dirt and microorganisms. Wei et al. (2017) found that the efficiency of tap water washing of strawberries, cherry tomatoes and bayberries was limited to a maximum 1 log reduction of yeasts and moulds. Water can be contaminated with microorganisms and this can also introduce microbial load to the produce during the washing step (Pichel et al., 2019). There are other postharvest treatments that are applied to help maintain the fresh quality of fruits and vegetables. Additionally, sanitising treatments must be used on food handling utensils or surfaces.

The treatment of fresh produce faces the challenges of preserving taste, colour, texture and smell of the product and avoiding harmful chemical residues, while being efficient and economically feasible (Al-Haq et al., 2005). Some conventional preservation techniques include lowering the water activity (drying/curing) and fermentation (Gould, 1996, Ross et al., 2002). However, these treatments cannot be used on fresh fruits and vegetables without markedly altering the properties of the produce. Different treatments can be combined to give additive or synergistic inhibitory effects. This concept is known as the hurdle technology (Figure 1-3) and allows the use of less stringent treatments (Leistner, 1992, Leistner and Gould, 2002).

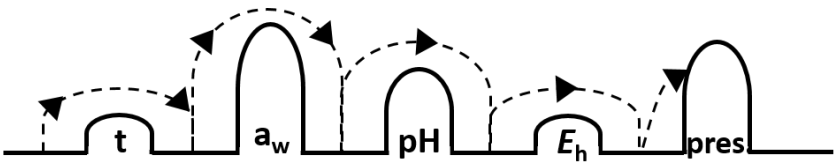

Figure 1-3: Visualization of the hurdle technology. Microorganisms can overcome individual hurdles, but the combination of different hurdles prevents microbial growth. t, temperature; a_w, water activity; pH, acidification; E_h, redox potential; pres., preservatives. Re-drawn from Leistner (1992).

1.5.2 Physical treatments

Heat treatment is used to inactivate microorganisms and insects as well as degradative enzymes that play a role in fruit ripening processes (Mahajan et al., 2014). Often, heat is applied by hot water dipping, which significantly reduces fungal growth on fruits, resulting in up to 4–20 x lower numbers of spoiled fruits (Hong et al., 2014, Maxin et al., 2012). In contrast, cold storage of food decreases the rate of metabolic reactions and thereby slows down microbial growth (Jay, 1995). Treating milk with heat and gamma radiation (described below) resulted in 5 log and 7 log reductions of *E. coli*, respectively (D'Aoust et al., 1988, Garin-Bastuji et al., 1990) and approx. 3 log reductions of *Bacillus* spores in milk products (Hashisaka et al., 1990). Such efficiencies vary for different microbial species and food matrices and are compared for the different treatment methods in Table 1-2. To allow a simplified comparison between treatment methods and microbial reduction rates, treatment efficiencies reviewed in Table 1-2 were rated in this study according to their reported $\log_{10}$ reduction rate against the test requirements of the European disinfection standards, where 5 log reduction (bacteria) and 4 log reduction (fungi) are required in suspension to pass the European norm for disinfectants, and 4 log and 3 log for surface tests (Fraise, 2008, Sandle, 2017).

To circumvent the possibility of heat-related damage to the produce, emerging non-thermal technologies such as pulsed electric fields, oscillating magnetic fields, high power ultrasound, high hydrostatic pressure and non-thermal plasma (a type of ionised gas) have been studied (Afshari and Hosseini, 2013). Atmospheric cold plasma may find applications for in-package sanitisation of fresh produce (Deng et al., 2019). Plasma treatments reduced fungal contamination on nuts although long treatment times (>10 min) were necessary to achieve one log reduction (Devi et al., 2017). Better fungal reduction (~3 log) was achieved with in-package

plasma treatments (5 min) of strawberries, where the plasma is generated and retained within the packaging container, enabling prolonged exposure of microorganisms to microbicidal plasma species (Misra et al., 2014). Other studies reported reductions of approx. 3–4 log for bacteria and *S. cerevisiae* on different food matrices (apples, melons, mangoes, egg shells, apple juice, cheese) after plasma treatment (Afshari and Hosseini, 2013).

Ultrasonic treatments can be combined with chemical treatments (e.g., chlorine based) to increase the sanitisation efficacy (Demirci et al., 2020). Accordingly, ultrasound alone gave low reductions of yeasts and moulds on green asparagus (~0.3 log) but combination with acetic acid + gibberellic acid increased the effect to ~1.3 log (acids alone: ~0.6 log) (Wang and Fan, 2019). Other potential methods are high hydrostatic pressure or pulsed electric fields but so far they are reported mostly for processed produce such as fruit juices (Demirci et al., 2020, Pinto et al., 2020). Combining heat treatment with high pressure markedly improved inactivation of fungal ascospores in a strawberry puree (Timmermans et al., 2020).

UV radiation can be applied to decontaminate surfaces by causing DNA damage in microbial cells (Lado and Yousef, 2002). UV exposure also activates plant defence mechanisms in harvested fruits and vegetables (Charles and Arul, 2007, Zhang and Jiang, 2019). Pulsed light consists of broad spectrum electromagnetic radiation (from the UV to the infrared range) and is more effective than continuous UV treatments, and commercial pulsed light systems are available (Deng et al., 2019). Fungal spoilage of strawberries after 8 days of storage was reduced by 16–42% after pulsed light treatment for 2–40s (Duarte-Molina et al., 2016).

Alternatively, fruits and vegetables can be treated with gamma radiation. Ionising irradiation is more common for killing of microflora on dry food products but has

gained interest for fresh produce more recently (both for direct killing of pathogens and stimulation of plant defence), although negative effects on quality and critical consumer perception are ongoing challenges (Demirci et al., 2020, Jeong and Jeong, 2018). An additional concern can be regulatory, especially in the EU, where some countries limit the use of irradiation to dried herbs, spices and vegetable seasonings, while the application extends to fresh produce in the US and other parts of the world (Eustice, 2018). Medium doses (1–10 kGy) lead to reductions in microbial counts, and high doses (>10 kGy) are effective in killing bacteria and fungi (Ferrier, 2010). However, high doses often affect the fruit quality negatively (Mahajan et al., 2014). Low doses (<1 kGy) have been shown to delay ripening and extend shelf life (Mahto and Das, 2013, Pandey et al., 2013). Irradiation of quince fruit (1.2–2.1 kGy) reduced spoilage by yeasts and moulds after 5–15 days by up to 3.8–4.9 log (Hussain et al., 2019). On cucumbers, irradiation (2–3 kGy) delayed fungal spoilage (by one week) but finally resulted in higher fungal spoilage (after 28 days), potentially due to tissue softening (Khalili et al., 2017).

Physical treatments are also commonly applied to sanitise food packaging, reducing the risk of spoilage during storage and transport (Demirci et al., 2020). In comparison to chemical treatments, physical methods do not remove dirt and plant debris and they may lead to physical (e.g., thermal) damage to the produce. Additionally, some of the described methods may be challenging to scale-up and implement in high-throughput industrial settings (Deng et al., 2019, Ali et al., 2018, Demirci et al., 2020).

Table 1-2: Comparison of the efficiency of sanitisation and disinfection methods on food and fresh produce.

Method	Organism	Produce	Efficiency[a]	Reference
Heat treatment	*Escherichia. coli*, *Campylobacter* spp., *Yersinia enterocolitica*	milk	high	(D'Aoust et al., 1988)
Heat+high pressure	*Talaromyces macrosporus, A. fischeri* ascospores	strawberry puree	high	(Timmermans et al., 2020)
γ-radiation	*E. coli*, *Salmonella* Dublin	milk	high	(Garin-Bastuji et al., 1990)
	Bacillus spp. spores	cheese, ice cream, frozen yoghurt	sufficient	(Hashisaka et al., 1990)
	yeasts and moulds	quince fruit	sufficient	(Hussain et al., 2019)
Plasma treatment	*E. coli*, *Salmonella* spp.	fruits, egg shells	low/sufficient	reviewed by (Afshari and Hosseini, 2013)
	S. cerevisiae	mango, melon	sufficient	
	total yeasts and moulds, *A. flavus*, *A. parasiticus*	peanuts	low	(Devi et al., 2017)
	yeasts and moulds	strawberries	sufficient	(Misra et al., 2014)
	E. coli, *Salmonella* spp., *S. cerevisiae*	apples, melons, mangoes, egg shells, apple juice, cheese	low/sufficient	reviewed by (Afshari and Hosseini, 2013)
Ultrasound	yeasts and moulds	green asparagus	low	(Wang and Fan, 2019)
Chlorine treatment (free available chlorine)	*E. coli*	lettuce	low	(Beuchat, 1999)
	Listeria monocytogenes	food contact surfaces or suspensions	high	reviewed by (Hoelzer et al., 2012)
	yeasts and moulds	sugar snaps	low	(Van Haute et al., 2013)
	yeasts and moulds	oyster mushrooms	low	(Ding et al., 2011)
	yeasts and moulds, *Aspergillus* section *Flavi*	Brazil nuts	low	(Ribeiro et al., 2020)

Table 1-2 (cont.)

Ozone	bacteria (*E. coli*, *Salmonella* spp., *L. monocytogenes*)	berries, apples, dried figs, pistachios, potatoes, spinach, cantaloupes	mostly low, sometimes sufficient/high in fruits	reviewed for bacteria and fungi by (Horvitz and Cantalejo, 2014)
	yeasts and moulds	strawberries, apples, spinach	low	
Peracetic acid (PAA)	*Enterobacter sakazakii*	apples, tomato, lettuce	sufficient/high	(Kim et al., 2006)
	yeasts and moulds	carrots	low/sufficient	(Landfeld et al., 2010)
Electrolysed water (EW)	bacteria and fungi	fruits and vegetables	mostly low/sufficient	see Table 1-3

[a] The efficiency is given as a rating of relative efficiency according to the log reductions of microbial counts described in the cited literature reports (high: ≥5 log reduction; sufficient: 4 log for bacteria, 3 log for fungi and spores; low: lower than sufficient). The rating system was employed in this study based on the European norms for disinfectant requirements, see main text for details (Fraise, 2008, Sandle, 2017).

1.5.3 Chemical treatments

Fresh produce can be washed with chemical sanitisers to reduce the fungal load. The most common choice for many years has been chlorine treatment in the form of washes with dissolved hypochlorite salts; the application and efficacy of which have been reviewed (Kaczmarek et al., 2019, Bhilwadikar et al., 2019). Alternative chemical treatments include chlorine dioxide (ClO_2), alcohols, copper sulphate ($CuSO_4$), organic acids, hydrogen peroxide (H_2O_2), ozone gas (O_3) and peracetic acid (PAA). A common challenge with most chemical treatments is their effectiveness at dosages and treatment times that do not also adversely affect the produce. Additional concerns with specific treatments are low chemical stability (H_2O_2, PAA, O_3), safety concerns in factories (ClO_2, PAA, O_3) and toxicity of residues ($CuSO_4$, ClO_2) (Bastarrachea et al., 2019, Deng et al., 2019); these concerns contribute to the ongoing use of hypochlorite salts. The efficiencies of common chemical treatments in food applications are compared in Table 1-2.

Sanitisers based on hypochlorite salts are used at a range of 50 to 200 mg L^{-1} free available chlorine (FAC; pH-dependent mix of ^{-}OCl, HOCl and Cl_2) (Olaimat and Holley, 2012). A review of 11 different studies estimated an average log reduction of 5.5 (95% confidence interval: 4.4–6.6) for killing of *Listeria monocytogenes* in food applications, with exposure times between 8 seconds and 30 min (one study additionally tested 48 h exposure) (Hoelzer et al., 2012). Elsewhere, it has been shown that FAC treatment reduces bacterial concentrations on lettuce moderately (up to 2.5 log reduction) and not sufficiently to eliminate bacterial growth (Beuchat, 1999). Yeast and moulds on sugar snaps, brazil nuts and oyster mushrooms were reduced by only up to 1–2 log by FAC treatment at 100–250 mg L^{-1} (Van Haute et al., 2013, Ding et al., 2011, Ribeiro et al., 2020). Chlorine may play a bigger role in keeping the washing water itself free of contaminants (Aruscavage et al., 2006). The presence of organic materials (such as blended lettuce leaves or proteins) can decrease the sanitising effect of FAC in the processing water and on food surfaces (Zhang et al., 2009, Hoelzer et al., 2012). Importantly, high levels of FAC are expected to leave residues on treated items and might impact the quality of fresh products (Artés et al., 2009), see also 1.5.4.

Alternatively, fumigation with sulphur dioxide or ozone can be used for sanitisation (Mahajan et al., 2014). Food treatments with ozone were reviewed (Horvitz and Cantalejo, 2014) and the specific application of aqueous ozone (ozonated water) is described below (1.8.3). Ozone is a highly reactive oxidizing gas that, compared to chlorine, is effective on a wider spectrum of microorganisms. The efficiency varies with different microorganisms, food matrices and ozone concentrations, but often lies between 2–3 log microbial reductions, with exposure times usually between 1 min and 1 h (Horvitz and Cantalejo, 2014).

Peroxyacetic acid (PAA) has strong oxidizing properties and can be used on fruits and vegetables without the production of harmful by-products (Carrasco and Urrestarazu, 2010). Fungal contaminants were shown to be decreased by up to 3.5 log after PAA treatment, and bacterial concentrations were reduced by up to 5 log (Kim et al., 2006, Landfeld et al., 2010).

Exposure of fruits and vegetables to (optimised levels of) nitric oxide (NO), a plant signalling molecule, slows down the maturation and senescence process and thereby delays fruit ripening and the occurrence of postharvest diseases (Singh et al., 2013). Following the same principle, inhibitors of ethylene action, a ripening-inducing plant hormone, are available (Martinez-Romero et al., 2007).

Fruits and vegetables can be covered with edible coatings that protect against spoilage, which requires safe-to-eat coating materials that do not negatively affect the taste (Dhall, 2013, Lin and Zhao, 2007). Non-edible waxes or edible, biodegradable coatings (e.g., chitosan) can be applied to citrus fruits, preventing fungal growth and preserving the physiological quality and integrity of the fruit, and representing a potential fungicide delivery route (Palou et al., 2015). Modified atmosphere packaging after the harvest, processing and potential sanitising treatments can further increase the shelf life of fresh produce (Mahajan et al., 2014). Different packaging technologies can influence factors such as CO_2 levels or moisture passively or actively. For instance, the incorporation of oxygen scavenger material into packaging reduced the amount of fungal decay on berries (Niazmand and Yeganehzad, 2020). Choosing the right sanitisation and preservation method(s) will depend on the application parameters, such as the produce type or the organic load during the sanitisation treatment (Van Haute et al., 2015).

1.5.4 Chemical contamination arising during sanitisation processes

Generally, chemical components from sanitiser solutions can be deposited on treated produce or accumulate in effluent water. Depending on the concentration, chemical stability and toxicity of the compounds, this can pose a serious problem and may limit the allowable dosage and therefore effectiveness of a given treatment. For instance, these considerations limit the concentrations of ClO_2 that can be applied in fresh produce treatments and necessitate subsequent water rinses (Deng et al., 2019). This in turn produces more contaminated water that may need to undergo remediation. In addition to direct toxic effects from the sanitiser chemistry, the reactivity of the sanitiser with organic and inorganic compounds during the sanitising process can lead to the formation of by-products with harmful effects. For instance, the redox reaction between ClO_2 and matrix constituents yields harmful chlorite (ClO_2^-) and chlorate (ClO_3^-) (Van Haute et al., 2017). Chlorate can also form during sodium hypochlorite treatments (Tudela et al., 2019).

When free available chlorine (FAC) reacts with organic matter, so-called chlorinated disinfection by-products can form, including trihalomethanes, haloacetic acids, chlorates and amino acid chlorination products (such as aldehydes, nitriles and carboxylic acids) (Tudela et al., 2019, Gil et al., 2019, How et al., 2018). This represents a health risk both in the processing water and on the washed produce due to the genotoxicity and carcinogenicity of some by-products (Villanueva et al., 2015). Maximum levels of certain disinfection by-products are therefore regulated by the EU (EU, 1998, EU, 2020b), the US (USEPA, 2009), and in WHO guidelines (WHO, 2017). The progress towards more stringent regulations (EU, 2020b) and demands for clearer food labelling (Gracia and de-Magistris, 2016) underline the importance of controlling by-product formation during food sanitisation.

An FAC of at least 10 mg L^{-1} has been recommended for sufficient microbial (bacterial) reduction in industrial produce washing (Luo et al., 2018). Higher levels are commonly used up to 200 mg L^{-1} (Kaczmarek et al., 2019), the maximum level allowed by the US food and drug administration for washing food for human consumption (FDA, 2019). The level of accumulation of different disinfection by-products in processing water was shown to depend on the produce type (lettuce, red cabbage, onion, mixed baby leaves) and the FAC level, but can exceed the drinking water limits of the EU, US and WHO even at 10 mg L^{-1} FAC (Tudela et al., 2019). Accumulation of disinfection by-products on lettuce, strawberries and cabbage has also been shown after sodium hypochlorite washing (Lee et al., 2019). Removal of chlorine and disinfection by-products in the effluent water can be achieved using dechlorination chemicals or activated carbon filters (Hermant and Basu, 2013, Gil et al., 2019). However, these measures add a processing step, and do not help with residues already deposited on the washed produce.

1.6 Electrolysed water

1.6.1 Production technologies

In conventional chlorine treatment of post-harvest produce, calcium hypochlorite is shipped in dry form and needs to be fully dissolved in water to limit damage to the produce, whereas sodium hypochlorite is only stable in solution, making shipping more expensive (Mishra et al., 2018). Using electrochemistry, solutions of the required free available chlorine concentration can instead be produced on-site and in response to demand, from cheap, safe ingredients (water and NaCl) (Zhang et al., 2018). The product, electrolysed water (EW), is a sanitiser that was first developed in Russia and has been used extensively for medical applications in Japan since the 1980s (Hricova et al., 2008, Rahman et al., 2016). It can be produced in electrochemical cells (Figure 1-4). The chambers of the cell are filled

with water and dissolved salts (if applicable). The two chambers are separated by a semi-permeable membrane, and they both contain an electrode. When electric current is applied, electrons flow from the anode to the cathode, with oxidation events taking place at the anode, reductions at the cathode. This electrolysis process results in acidic electrolysed water (AEW) with a high oxidation-reduction potential (ORP) in the anode chamber and basic electrolysed water (BEW) with a very negative ORP at the cathode (Hricova et al., 2008).

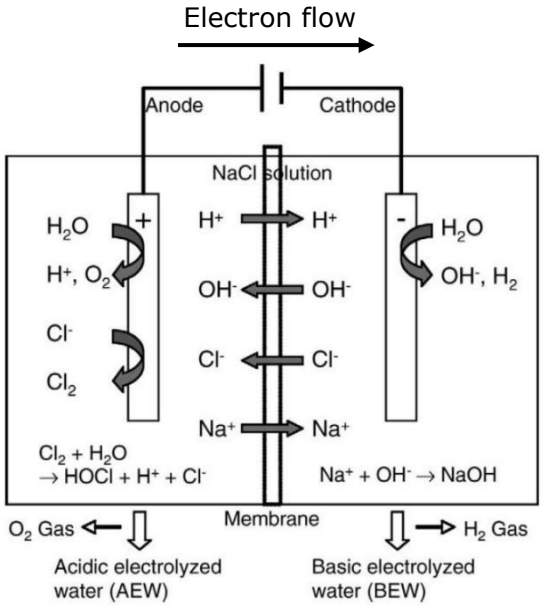

Figure 1-4: Water electrolysis in an electrochemical cell. The chamber is filled with a salt solution. When electric current is applied, acidic electrolysed water is produced at the anode and basic electrolysed water is formed at the cathode. From Hricova et al. (2008).

AEW can be used as a sanitiser, whereas BEW is more suitable for cleaning purposes as it removes grease and dirt (Rahman et al., 2016). In many applications, such as household use, cosmetic applications and drinking water treatment, extreme pH values and corrosiveness pose a problem. In these cases, neutral electrolysed water (NEW) is favourable (Deza et al., 2005). NEW is obtained by increasing the pH of AEW by adding OH^- ions or by electrolysis in single-cell systems without a membrane (Deza et al., 2007, Izumi, 1999, Gil et al., 2015). Electrolysis in flow-through electrolysers that continuously produce EW

is preferred over the use of non-flow-through single-chamber systems because the latter decrease the electrolysis efficiency and increase chlorate formation (Zhang et al., 2018). The EW that is a focus of the present study is produced in a flow-through cell without a membrane where direct current is applied across layers of boron-doped diamond electrodes, producing a single type of EW, instead of separate AEW and BEW production (specifications by Ozo Innovations Ltd.).

1.6.2 Formation of active species in EW

The initial electrochemical reactions that take place at the electrodes during EW production are shown in Figure 1-4 and can be summarised as follows (Hricova et al., 2008):

Anode: $2\,H_2O \rightarrow 4\,e^- + O_2\uparrow + 4\,H^+$

$2\,Cl^- \rightarrow 2\,e^- + Cl_2\uparrow$

Cathode: $2\,H_2O + 2\,e^- \rightarrow 2\,OH^- + H_2\uparrow$

The chlorine molecule can then disproportionate to form hypochlorous acid:

$$Cl_2 + H_2O \rightarrow HOCl + H^+ + Cl^-$$

Due to these and additional reactivities, generation of EW involves the formation of free chlorine species (Cl_2, HOCl, ^-OCl), and other active compounds at low levels, including chlorine dioxide (ClO_2) and reactive oxygen species (ROS) such as ozone, hydrogen peroxide, superoxide and hydroxyl radicals through varied oxidation reactions of water molecules (Jeong et al., 2009, Zhang et al., 2018). Many of the non-chlorine components are unstable. Among the chlorine species

found in EW, hypochlorous acid (HOCl) has the strongest antimicrobial effect but dissociates to hypochlorite ($^{-}$OCl) between pH 6.5 and 8.5 and forms Cl_2 gas at very low pH (<3) (Rahman et al., 2016), and the pH-dependent mix of these three species is commonly referred to as free available chlorine (FAC, see 1.5.3). Chlorine in the form of HOCl is 80 x more effective at sanitisation than the dissociated $^{-}$OCl, and the highest amounts of HOCl can be found in EW solutions at pH 5.0 to 6.5, sometimes referred to as slightly acidic electrolysed water (SAEW) (Cao et al., 2009).

The antimicrobial activity of EW is attributed to either the chlorine compounds, ROS, the high oxidation-reduction potential, the pH (for AEW) or most likely a combination of these (Al-Haq et al., 2005, Li et al., 2014). Compared to conventional sanitisation with dissolved hypochlorite salts such as NaOCl, the additional non-chlorine active species can increase the efficacy of EW (Graça et al., 2020). These additional chemical species may help attain fungal killing at lower FAC concentrations, so allowing decreased formation of chlorinated disinfection by-products while maintaining antimicrobial efficacy during the sanitisation process.

1.6.3 Chlorine based disinfection kinetics

The free available chlorine of chlorine-based sanitisers reacts with organic compounds and inorganic species (such as Fe^{2+}, NH_3) present during the sanitisation process (Tchobanoglous et al., 2003). This chlorine demand of the matrix has to be met before reaching a "breakpoint" where free chlorine accumulates and is then available for antimicrobial activity. The process can be divided into four steps (Figure 1-5). First, chlorine (in the form of FAC) is "introduced" into a water sample, either by adding concentrated chlorine solution or hypochlorite salts, or by electrochemical generation in-solution (in the case of

EW production), and reducing agents that may be present in the water sample (e.g., Fe^{2+}, H_2S, some organic substances; present in non-purified water or waste water streams) can inactivate the FAC by reducing it to chloride ions (Cl^-) (step 1 leading up to point A in Figure 1-5). Once these reducing agents are oxidised, any additional (non-reacted) free chlorine in the solution can react with ammonia and organic compounds, forming combined chlorine such as mono- and di-chloramines (step 2, shown between point A and B in Figure 1-5; this second step occurs provided that the initial free chlorine concentration exceeds the level necessary to satisfy the chlorine demand of step 1). If the chlorine concentration in the solution is even higher (due to a high initial FAC dose, or continuous increase by ongoing electrochemical generation), the formed mono- and di-chloramines (combined chlorine) will react with the additional (yet unreacted) FAC (free chlorine) to form nitrogen trichloride (NCl_3) or chloride ions with the formation of nitrous oxide (N_2O) and nitrogen (N_2). This is represented by the loss of combined chlorine in step 3 (between B and C in the figure). At the breakpoint (C in the figure), the described processes are satisfied. If the free chlorine concentration that was initially added to the solution exceeds the level that is necessary to reach the breakpoint, or if additional free chlorine is generated electrochemically in the solution after reaching the breakpoint, free (unreacted) chlorine (FAC) can accumulate in the solution, in addition to any non-destructed combined chlorine, in step 4. It should be noted that the precise shape of the chlorine curve can depend on the matrix e.g., the extent of step 3 may be less pronounced when organic nitrogen compounds are present (Tchobanoglous et al., 2003).

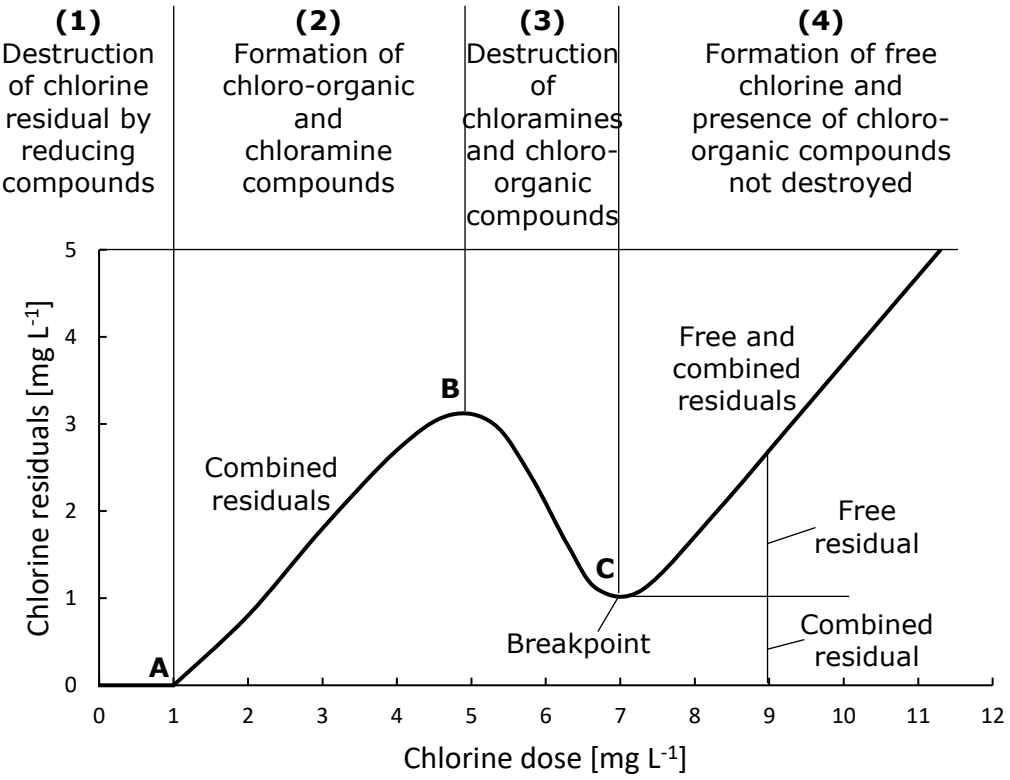

Figure 1-5: Schematic breakpoint chlorination. The graph describes the order of processes after free chlorine (FAC) is introduced into a water sample, either by adding concentrated solution or by electrochemical generation in-solution. Step 1, free chlorine is reduced by any reducing agents already present in the water sample. 2, any amino compounds already present in the water sample react with free chlorine that was not used up in step 1, generating combined chlorine. 3, combined chlorine compounds generated in step 2 react with free chlorine that was not used up in steps 1+2, resulting in the destruction (reduction) of the combined chlorine. 4, reactions between water constituents and the introduced free chlorine are satisfied at the breakpoint, and any free chlorine that was not used up by steps A–C can accumulate. See text for details. Re-drawn from Tchobanoglous et al. (2003).

If hypochlorous acid or hypochlorite salts are dissolved in residue-free water, the final concentration of free chlorine species should be similar or identical to the added dose. Similarly, if residue-free water is electrolysed, the generated chlorine species should all be in the form of free (unreacted) chlorine. However, if in either case the water (that is used for dissolving the salts or for electrolysis) contains chemical residues, the final concentration of free chlorine species (FAC) in the water will be lower, depending on those residues and their reactivity with free chlorine species. If the objective is to sanitise the water sample directly, or to

introduce chlorine into the water and then use it for secondary sanitisation (e.g., in the case of EW production), then the efficacy of the sanitisation will therefore also depend on the chemical residues in the original water sample. This means that in order to achieve a required level of sanitisation, a higher dose of hypochlorite salts may need to be added, or longer electrolysis may need to be applied, in order to reach sufficient levels of free chlorine species (FAC) in a residue-containing water sample. This is because in order to reach the chlorination breakpoint, the chlorine demand of the matrix needs to be satisfied. Such a chlorine demand could occur either when a water sample is being disinfected directly (by adding concentrated sanitiser), such as waste water which usually contains organic or inorganic constituents, or when the water used for generating EW contains chemical constituents due to limited prior purification, or when a chlorine solution (containing FAC) is used to sanitise contaminated surfaces, and the free chlorine species reacts with contaminants such as organic compounds.

Importantly, the formation of harmful by-products such as trihalomethanes occurs during the pre-breakpoint steps after the chlorine demand of ammonium ions has been satisfied (see 1.5.4 for details about by-products) (Liu et al., 2018, Stefán et al., 2019). The chlorination reactions further depend on different factors such as pH, temperature and chlorine-to-ammonia ratio, and a high organic matter content will increase the disinfection by-product formation (Devi and Dalai, 2021). On the other hand, breakpoint chlorination can be used to remove high ammonium levels from drinking water sources to prevent the formation of high nitrite levels (Stefán et al., 2019).

Some of the reaction products such as chloramines may retain mild oxidising activity (Hawkins et al., 2003). Chloramines can also be used as sanitisers and are referred to as combined chlorine as opposed to free chlorine (FAC) (Tchobanoglous et al., 2003). In drinking water distribution systems, especially in

the United States, monochloramine (NH_2Cl) is used as a residual sanitiser. This means that water leaving the treatment plants contains a controlled chloramine level in order to reduce the growth of microorganisms in the distribution system, although some problematic microorganisms can survive such conditions (Waak et al., 2019).

1.6.4 Antimicrobial properties

The antimicrobial efficacy of EW products depends on different factors. Generally, a lower pH favours killing (consistent with shifting the equilibrium to more HOCl and less ^-OCl), as do a higher chlorine concentration (FAC) and higher oxidation-reduction potential; water temperature and hardness can further influence the process (Ding and Liao, 2019). Different mechanistic effects have been suggested, including oxidation and damage to membranes, proteins, enzymes and DNA and modification of ATP production by the oxidation-reduction potential of EW (Ramírez Orejel and Cano-Buendía, 2020).

Electrolysed water is active against a range of bacterial and fungal species and the efficacies have been reviewed (Hricova et al., 2008, Huang et al., 2008). In suspension, treatment with AEW or NEW usually leads to reductions of microbial counts >5 log, but lower efficiencies have been reported in some experiments for *Bacillus* spp., *Salmonella typhimurium*, *L. monocytogenes*, *Staphylococcus aureus* and conidia of *Aspergillus* and *Penicillium*. Treatments are usually short (0.5–15 min) with low FAC (10–90 mg L^{-1}). Some evidence suggests that Gram-positive bacteria are more resistant to EW treatment than Gram-negative bacteria, and spores more resistant than vegetative cells (Ding and Liao, 2019). Electrolysed water was shown to be effective against *A. niger* in suspension, as well as against other important human- or plant-pathogenic fungi such as *A. fumigatus*, different *Candida* species, *Alternaria* sp. and *Botrytis cinerea* (Buck et al., 2002, Ünal et al.,

2014, Gunaydin et al., 2014). Furthermore, other food spoilage species (*A. flavus* and *P. digitatum*) in suspension and/or on orange surfaces were successfully inactivated with electrolysed water (Xiong et al., 2014, Xiong et al., 2010, Youssef and Hussien, 2020). This underlines the potential of using electrolysed water to help prevent food spoilage by fungal species such as *A. niger*.

As noted above, the additional active species in EW compared to pure free available chlorine sanitisers (e.g., dissolved hypochlorite salts) may result in stronger fungicidal activities and lower required FAC concentrations. Accordingly, yeast populations on apple slices were reduced more strongly (~1 log difference) by EW than NaOCl (Graça et al., 2020). A greater effectiveness of EW compared to NaOCl has been also observed against yeasts and filamentous fungi (by ~0.3 log) despite the fact that the chlorine concentration (FAC) of the EW solution was lower than the FAC of the NaOCl solution (20 mg L^{-1} versus 150 mg L^{-1}) (Koide et al., 2009). However, the pH of the NaOCl solution in the cited study was higher than the pH of EW, shifting the chemical equilibrium to the less damaging ^{-}OCl, which could potentially explain the lower effectiveness of NaOCl compared to EW in the cited study. Similarly, EW (30 mg L^{-1}) inactivated *S. aureus* on leafy vegetables at least as well as or better than NaOCl (100 mg L^{-1}, higher pH than the EW) (Kim et al., 2018). EW also reduced *E. coli* populations more strongly than NaOCl (up to 0.3 log more for planktonic cells and 0.8 log more in biofilms), although NaOCl was found to act faster (the superior EW effect occurred after approx. ≥1 h treatment) (Meireles et al., 2017). In contrast, stronger and also faster inactivating effects on bacteria have been reported with EW compared to NaOCl at the same FAC (Ersoy et al., 2019). Similarly, Ogunniyi et al. (2019) showed that EW inactivated bacteria as well as or better than NaOCl. On spring onions, a greater antibacterial effect of EW compared to NaOCl was reported (difference of approx. 1 log reduction) although the effects of both sanitisers were more similar on other tested produce (chives, chicory, tomatoes) (Ju et al., 2017).

1.7 Applications of EW

1.7.1 Versatile role as a sanitiser and beyond

Electrolysed water is used as a sanitiser in medical applications, agriculture, food and livestock industries (Huang et al., 2008, Kim et al., 2000a). For instance, EW can be used to disinfect medical equipment contaminated with viral particles (Sakurai et al., 2003), and for bacterial decontamination of surfaces (Boyce, 2016). In 2020, EW was found to inactivate SARS-CoV-2 particles in a FAC concentration-dependent manner (Takeda et al., 2020). EW-sprays reduced the bacterial surface load in a residential care home in one study (Meakin et al., 2012). EW has also been proposed for direct patient contact in wound care, as an antibacterial nasal spray, for hand sanitising, and as a mouthwash (Yan et al., 2021, Lux et al., 2021). Electrolysis units that produce alkaline (basic) EW (BEW) from tap or mineral water are widely used in Japan to produce EW for drinking or cooking (Koseki et al., 2007). Alkaline electrolysed water can be consumed by drinking and has been suggested to be beneficial for gastrointestinal symptoms and general well-being (Tanaka et al., 2019). Electrolysis may improve the taste of water with a high calcium concentration but worsen the taste in case of low calcium concentrations (Koseki et al., 2007).

Waste water that contains high levels of oxidisable constituents and ammonia nitrogen can be treated by electrolysis, resulting in the oxidation of the chemical constituents and removal of ammonia by oxidation to N_2 and NCl_3 (Meng et al., 2020), as described above for the principles of breakpoint chlorination (1.6.3). Furthermore, nitrate and nitrite can be removed by cathodic reduction (Yao et al., 2019). Blackwater (untreated waste water from toilet systems) can be sanitised by electrolysis and optimisation of the electrolysis process is ongoing (Thostenson et al., 2018).

The application of EW as a sanitiser in the food industry is described below. In addition, EW can be used to degrade pesticides on fruits and vegetables (Wu et al., 2019b, Qi et al., 2018). Fungal mycotoxins such as aflatoxins on peanuts or maize feed, ochratoxin in grape berries or deoxynivalenol in wheat grains can be degraded by EW although the formation of chlorinated by-products may be a concern (Pankaj et al., 2018, Lyu et al., 2018, Gómez-Espinosa et al., 2017, Magistà et al., 2021). EW has also been reported as an elicitor for the accumulation of beneficial bioactive compounds in broccoli sprouts (Li et al., 2018). Apart from applications in medical settings, the food industry and waste water treatments, further potential uses of EW have been proposed, e.g, as a tool for harvesting microalgae by flocculation (Lee et al., 2018).

1.7.2 Electrolysed water as a sanitiser in the food industry

EW has been in use for a number of years, but its potential for treating fresh produce is still being explored and developed (Youssef and Hussien, 2020). Several companies currently offer commercial EW generating systems that are recommended for fresh produce washing or food handling surface decontamination, for use by the food industry or at home, e.g., EcoloxTech, TaeyoungE&T, Ozo Innovations. The development of portable EW generators has also been described (Zhang et al., 2018), and hand-held EW spray bottles are already available on the UK market, e.g., the H2O e3 eActivator Cleaning System.

EW treatment efficiency has been evaluated for microbial inactivation on different vegetables (lettuce, cucumber, spinach, carrots, alfalfa seeds and sprouts, green onions, mushrooms, cabbage and more), and the efficiencies lie mostly between 1 and 4 log reduction (Huang et al., 2008, Rahman et al., 2016, Afari and Hung, 2018). On fruits (apples, strawberries, tomatoes), similar reductions can be achieved, with higher reductions (5–7 log) for tomatoes (note that log reduction

tests are often performed on produce after inoculation with the organism(s) of interest, allowing the application of high microbial loads and the determination of high log reduction rates) (Rahman et al., 2016, Hricova et al., 2008). EW can also be used on minimally processed (fresh-cut) fruits and vegetables, with reductions mostly between 1 and 3 log (Ali et al., 2018). Apart from fruits and vegetables, other applications include the sanitisation of shelled eggs (2–6 log microbial reduction, see Table 1-3), treatment of drinking water for chickens or dairy ewes (Bodas et al., 2013, Bugener et al., 2014) and spray disinfection in layer breeding houses (Hao et al., 2013). Microbial contamination on surfaces can also be sanitised effectively with EW, e.g., on plastic or wooden cutting boards (4–8 log reduction) (Deza et al., 2007, Hricova et al., 2008), whereas the reported efficiencies on ceramics, glass and stainless steel were lower in some studies (2–5 log reduction) (Jiménez-Pichardo et al., 2021, Hricova et al., 2008).

Efficiencies of different EW applications are summarised in Table 1-3. As in Table 1-2 above, for ease of comparison the outcomes are rated as 'high' (≥5 log reduction), 'sufficient' (4 log for bacteria, 3 log for fungi) and 'low' (below sufficient). The efficiency of EW in tests can depend on several parameters, including the EW properties, the sanitising method as well as the method and concentration of microbial inoculation on the food surface (Koseki et al., 2003). Different studies apply varying EW concentrations, treatment times and washing procedures, making direct comparisons difficult. However, many of the studies indicate reductions of cell counts between 1–4 log. EW can therefore be expected to reduce spoilage and extend shelf life, but not completely disinfect the produce, depending partly on the initial microbial load. Accordingly, the fungal load on vegetables can increase over the storage period despite an initial killing effect (Martínez-Hernández et al., 2013). This underlines the need for additional measures such as reducing the microbial contamination of food during growth,

harvest and processing of fruits and vegetables, as well as adequate storage and/or packaging post-treatment.

Table 1-3: Comparison of the efficiency of EW treatment of fresh produce.

Organism	Produce	Efficiency[a,b]	Reference
Total bacteria	pea sprouts	low (1.6)	(Zhang et al., 2019)
	fresh-cut carrot, spinach, bell pepper, radish, potato	low (2.6)	(Izumi, 1999)
	fresh-cut cabbage	high (5)	(Chen et al., 2018)
Common food spoilage bacteria (*E. coli*, *Salmonella spp.*, *L. monocytogenes*)	carrots, cucumbers, leaf vegetables, mushrooms	low (~1–3)	reviewed for various fruits and vegetables by (Hricova et al., 2008, Rahman et al., 2016, Afari and Hung, 2018)
	fruits (apples, strawberries)	low (~2)	
	tomatoes, green onions	high (7.5, >5)	
	lettuce, spinach	low (~1)	(Ogunniyi et al., 2021)
Common food spoilage bacteria (*E. coli*, *Salmonella spp.*, *L. monocytogenes*)	lettuce	low-sufficient (4.5)	(Koseki et al., 2003)
	egg shells	low-sufficient (4)	(Park et al., 2005)
L. monocytogenes	apples	low (1)	(Sheng et al., 2020)
	egg shells	low (2.2)	(Rivera-Garcia et al., 2019)
Salmonella Enteritidis	egg shells	high (5.5)	(Cao et al., 2009)
E. coli	egg shells	high (>6.4)	(Medina-Gudiño et al., 2020)
S. aureus	lettuce, chicory, cabbage	low (1.5)	(Kim et al., 2018)
Brettanomyces bruxellensis	grapes	low (1.4)	(Cravero et al., 2018)
Fungi (yeasts/moulds)	cucumber, strawberries	low (1.6–2)	(Koseki et al., 2004)
	carrot pieces	low (2)	(Rahman et al., 2011)

Table 1-3 (cont.)			
Fungi (yeasts/moulds)	fresh-cut cabbage	sufficient (3)	(Chen et al., 2018)
	pea sprouts	low (1.2)	(Zhang et al., 2019)
	broccoli	sufficient (3)	(Martínez-Hernández et al., 2013)
	broccoli	sufficient (3.5)	(Navarro-Rico et al., 2014)
	mung bean sprouts	low (2)	(Liu and Yu, 2017)

[a] The efficiency is given as a rating of relative efficiency according to the log reductions of microbial counts described in the cited literature reports (high: ≥5 log reduction; sufficient: 4 log for bacteria, 3 log for fungi and spores; low: lower than sufficient). The rating system was employed in this study based on the European norms for disinfectant requirements, see main text for details (Fraise, 2008, Sandle, 2017).
[b] In brackets: maximum log reduction achieved. Note that ratings lower than the maximum log reduction indicate that lower efficiencies were achieved in some conditions.

1.8 EW and water resilience

1.8.1 Advantages of the on-site generation and chemistry

A major advantage of electrolysed water, compared to other chemical sanitisers, is that it is simple to produce (Rahman et al., 2016). Apart from the production unit, the process only requires water, salt (often NaCl) and electricity, which makes EW easily accessible, less expensive than other chemical disinfectants and enables production on demand (Robinson et al., 2013, Yukihiro et al., 2003). The on-site production from cheap, safe substrates eliminates the need for transport, handling and storage of concentrated chemical disinfectant (Gil et al., 2015). The commercial availability of EW generators (see 1.7.2) makes this technology widely accessible and could provide sanitising solutions even in remote areas. The low requirements render the production of EW environmentally-friendly, energy-saving and independent of non-renewable resources, subject to the electricity source (Al-Haq et al., 2005).

The active components of EW can also react back to the substrates salt and water and the oxidising/sanitising effects of EW can be easily inactivated by mixing with organic matter, e.g., after use (Huang et al., 2008). These reversion processes may allow the re-use of the water. The caveats of this process (i.e., by-product formation) are discussed below (1.8.2). In the food industry, the continuous electrolysis of produce wash water or chilling brine can allow the recirculation and re-use of water and help prevent cross-contamination (Gómez-López et al., 2015, Liu et al., 2006). Similarly, electrolysis can be applied to water recirculation systems in aquaculture such as fish ponds (Ben-Asher and Lahav, 2016). Such re-use can help address the problems of water scarcity and improve access to clean water. The on-site, on-demand production allows generation of only as much EW as is needed, reducing the waste of water resources which may occur when surplus stored liquid sanitiser has to be disposed of after the end of its shelf life.

Furthermore, some studies claim that EW is non-toxic and does not pose a health threat (Huang et al., 2008), however a cytotoxic effect of acidic EW has been shown in a dose-dependent manner (Reis et al., 2020) (the alkaline EW produced at the cathode did not have a cytotoxic effect in the cited study, and the drinking water application cited in 1.7.1 was for alkaline EW, too). Like with many other chemical sanitisers, the effect of EW on human health and environmental organisms will therefore depend on the EW dosage. Encouragingly, results from animal and *in-vitro* studies suggest that usage of low concentrated EW (≤60 mg L^{-1} FAC) could have beneficial health effects in medical applications such as beneficial effects on mammalian cells during wound healing (resulting in faster *in-vitro* wound closure) or as a mouthwash while having no or low cytotoxic effects (Reis et al., 2020, Morita et al., 2011).

1.8.2 Challenges of EW applications

1.8.2.1 Formation of by-products during the electrolysis process

During the water electrolysis, chlorate (ClO_3^-) and perchlorate (ClO_4^-) are formed at the anode or from reactions between FAC and ozone or hydroxyl radicals in solution (Jung et al., 2010). Those compounds, especially perchlorate, pose serious health threats (Richardson et al., 2007, Srinivasan and Sorial, 2009). During FAC-based sanitisation, chlorates can accumulate in the wash water and the produce, with levels depending on the type of washed produce (López-Gálvez et al., 2019). EW treatment of irrigation water increased the chlorate levels in the water, and resulted in chlorate accumulation on irrigated lettuce (López-Gálvez et al., 2018, Garrido et al., 2020). The levels measured in these studies were below but close to the updated (now less stringent) regulatory limits in the EU (EU, 2020a). It is therefore important to control and limit the formation and deposition of those residues on treated products. Removal of chlorates from effluent water is difficult due to their high water solubility and persistence (Jung et al., 2010).

Another concern is the possibility of chlorine gas emission, especially during the generation of AEW (Al-Haq et al., 2005, Huang et al., 2008), see also 1.6.2. To prevent the formation of the health-adverse chlorine gas, production of neutral or slightly-acidic EW is preferred to acidic EW (Ali et al., 2018). On the other hand, formation of chlorate/perchlorate increases with increasing pH due to the shift from HOCl to ^-OCl, with the highest levels recorded at pH 7.2 and above (Jung et al., 2010). This indicates that the pH conditions during electrolysis have to be carefully chosen.

1.8.2.2 Shelf life of EW

Another challenge might be the limited shelf life of electrolysed water. The oxidation-reduction potential of one AEW product was only stable for 1−2 months,

and the free chlorine (570 mg L^{-1} FAC) decreased strongly from the first day of storage (Robinson et al., 2013). At 4°C, the AEW was more stable than at 20°C. After one year of storage at 4°C, the AEW still achieved high bactericidal activity (>5 log reduction) in the absence of FAC, which may be due to the stable low pH of about 1.5. The bactericidal efficacy of a more neutral low-chlorine EW (pH 6–7, 10 mg L^{-1} FAC) decreased by 1–3 log within 7–14 days of room temperature storage in the dark (Rahman et al., 2012). Open storage and light both decreased the chlorine content of EW (pH 6–7, 20–200 mg L^{-1} FAC) over the first two weeks of storage (Xuan et al., 2016). In stored solutions, non-FAC oxidative species may be less relevant (compared to FAC) due to their short-lived chemical stability, whereas they may play a bigger role in direct electrolyser systems where microorganisms are present during the electrolysis itself (Jeong et al., 2007). In line with the manufacturer's recommendations (Ozo Innovations Ltd.), the EW in this study was stored in the dark at 4°C and used within 2.5 weeks of its generation. While the on-site production from simple substrates is an advantage of EW compared to conventional sanitisers, the above data also suggest it may be a necessity.

1.8.2.3 Chemical inactivation of EW and formation of by-products during EW application

The use of EW for sanitisation and disinfection is likely to be limited by the reactivity of EW with organic substances (Oomori et al., 2000). A lowered fungicidal efficiency of EW should be expected for treatment of dirty surfaces or liquids containing dissolved organic compounds. The presence of proteins lowers the efficacy of several common sanitisers (e.g., PAA, quaternary ammonium compounds) but chlorine (FAC) based sanitisers tend to be the most strongly affected (Hoelzer et al., 2012). The effect of relevant organic compounds on the fungicidal activity of EW will be discussed and investigated further in Chapter 2.

The potential by-products of FAC based sanitisers are described above (1.5.4, 1.6.3). A promising result following irrigation of lettuce with AEW was that only low levels of trihalomethanes were present in both the water and lettuce (López-Gálvez et al., 2018). However, other studies detected higher levels of trihalomethane formation when treating process water with EW, likely due to the increased levels of chemical constituents of such water (Gil et al., 2015). While the addition of organic matter to EW can increase the formation of disinfection by-products, the exact level of by-product formation depends on the chemistry of the organic compounds (Lee et al., 2017). Compared to NaOCl, conflicting results have been reported about higher or lower disinfection by-product accumulation following EW treatment (Clayton et al., 2019, Gil et al., 2019). Food-industry specific by-products can also form when EW is applied: EW treatment of grapes may result in higher levels of the off-flavour compound 2,4,6-trichloroanisole in wine post-fermentation (Gabrielli et al., 2020, Giacosa et al., 2019).

1.8.3 Alternatives: ozonated water

Although EW might allow the use of lower free available chlorine concentrations (see preceding sections), disinfection by-products remain a potential concern (Gil et al., 2019, Wang et al., 2019, Clayton et al., 2019), underlining the desirability for FAC-free alternatives. Ozonated water can be produced by electrolysis using water alone (Sekido and Kitaori, 2008, Lutz et al., 2017). Therefore, it shares with EW the benefits of on-site production from safe substrates, but not the disadvantage of FAC content. Instead, ozone is formed that first decomposes to other reactive species, e.g., hydroxyl radicals, and finally to oxygen and water (Baggio et al., 2020, Wang et al., 2020). Therefore, ozonated water treatment does not usually leave residues on the produce (Brodowska et al., 2018), although certain by-products such as carbonyls or bromates might form in the presence of organic matter or bromide ions (Papageorgiou et al., 2017, Wu et al., 2019a).

Similar levels of yeast killing were reported when comparing grapes treated with EW or ozonated water, at only 5 mg L^{-1} ozone versus 400 mg L^{-1} FAC in the EW (Cravero et al., 2018). However, ozonated water (0.7–5 mg L^{-1} ozone) was less effective than EW (5–34 mg L^{-1} FAC) in inactivating fungi on various fresh-food surfaces (Degala et al., 2020, Koseki and Isobe, 2007). This may reflect the difficulty of maintaining sufficient ozone levels due to its low stability, which may require cooling below room temperature to increase the stability and water solubility of ozone (Deng et al., 2019, Galdeano et al., 2018). Ozone in aqueous and gaseous phases has been approved by the US food and drug administration for use in food for human consumption (FDA, 2001). Ozonated water generators are commercially available (e.g., Absolute Ozone, GreenTeck Global) and several food brands use ozone treatments (Hinkle, 2017). Challenges of ozone treatment include its short half-life (seconds to hours, depending on parameters like water quality), health concerns associated with ozone gas formation and risk of corrosion (Baggio et al., 2020, Brodowska et al., 2018).

1.9 Need for further understanding of antimicrobial EW efficacy

As discussed above, chemical sanitisers and disinfectants have applications for control of microbial contamination and growth in diverse settings, with a global market exceeding US$20 billion per year. That looks set to increase with the heightened public awareness and concern arising from the Covid-19 pandemic. For applications of antimicrobial sanitisers to be effective, there is a need to understand limiting factors associated with chemical matrices presented by the relevant applications, ideally supported by understanding of antimicrobial mode-of-action.

Several mechanisms of EW action against microorganisms have been suggested, including damage (e.g., oxidative) to proteins, membranes and DNA, perturbation of electron flow and inhibition of steps in central metabolism (Ramírez Orejel and Cano-Buendía, 2020, Ali et al., 2018, Gil et al., 2015). Mode-of-action studies have generally focussed on bacteria. More research is needed to pinpoint and validate potential mechanisms in fungi, especially those with relevance for the food industry. Growth of moulds such as *A. niger* is difficult to control and can result in severe food losses and adverse health effects (see 1.3.2). It is important to identify molecular targets of EW as well as fungal response and defence mechanisms for a better understanding and prediction of EW efficacy in different application scenarios. The FAC and ROS in EW can cause oxidative stress in organisms (discussed further in Chapter 3) and consideration of this in relation to other pro-oxidants could further the understanding of fungal response to oxidative stress. Furthermore, variability in the stress resistance of spores or cells within one (genetically identical) population can influence the survival of microorganisms in stress conditions, and such phenotypic heterogeneity is further described in the context of EW action in Chapter 4.

Whereas the FAC is generally believed to be the main factor in antimicrobial EW action, other ROS can be formed (1.6.2) and studies have also shown an influence of the oxidation-reduction potential and pH (Li et al., 2014, Kim et al., 2000b). While there are likely to be parallels with the actions of pure FAC sanitisers such as NaOCl, the additional properties of EW may modulate the effects. Furthermore, the EW produced in different generators can differ in composition, e.g., depending on the production technology (anodic/acidic or neutral EW) or the electrode material (Zhang et al., 2018). It is therefore important to assess new EW technologies, as they may compare with previously-studied types of EW.

As discussed above, efficacy of sanitisers such as NaOCl or EW is negatively affected by the presence of organic contaminants (1.6.3, 1.8.2.3). At the same time, access to clean drinking water and microbial food safety are primary concerns in countries with poor sanitation systems (Roche et al., 2017). Climate change-related events such as flooding can increase the contamination of drinking water resources (Pichel et al., 2019). While EW can theoretically be generated in remote areas, given a generating unit and access to electricity, the effects of different organic contaminants need to be better understood in order to assess realistic limits for such chemicals in applications. Otherwise, EW treatment may increase disinfection by-product concentrations while not achieving microbial killing and could, in the worst case, do more harm than good.

1.10 Aims and objectives

This thesis aims to further the understanding of the fungicidal action of EW, with particular regard to food industry applications. For this purpose, electrolysed water from Ozo Innovations (brand name eloclear™) was studied and applied to treat the common food spoilage organism *A. niger* as well as the fungal model organism *Saccharomyces cerevisiae*. EW applications used here were short-term treatments (5 min) to model short contact times between sanitiser and surface (i.e., produce) in the food industry or in other (industrial) settings.

The efficacy of EW treatments can be affected by the presence of organic materials (1.8.2.3), and the aim of Chapter 2 was to elucidate such reactivity between EW and different organic substances, in order to better understand the matrix-dependent efficacy of EW. Treatment of freshly harvested produce with EW is likely to occur in the presence of incidental environmental soil load and the impact of soil samples on EW efficacy against *A. niger* was studied in this thesis. There is a need to identify specific molecules that interact with EW, and this study used a

top-down approach that led to the identification of proteins and specific amino acids that were highly reactive with the EW.

Based on the identified reactivities between EW and amino acids as well as proteins, it was hypothesised that EW might also react with these compounds within cells and that this may underpin cellular mechanisms of EW toxicity. The aim of Chapter 3 was to identify cellular targets and EW mode-of-action by studying the effects of EW in the model organism *S. cerevisiae*. This capitalised on the advanced understanding of the metabolism and uptake mechanisms of diverse compounds in this model organism, and the availability of different deletion and overexpression strains.

Because active species in EW can be inactivated by organic compounds, microorganisms may be exposed to low effective EW doses during EW treatments where organic matter is present. In Chapter 4, the response of *A. niger* to EW treatments, specifically to low doses, was studied. Effects of EW treatments on fungal growth behaviour and spore-to-spore variation were detected and further investigated, with the aim to better understand the fungal response to EW and to assess potential consequences for sanitiser application settings.

2 EW and organic substances: reactivity and inactivation

2.1 Introduction

2.1.1 Presence of organic compounds during sanitising treatments

When EW is used in its potential industrial or domestic applications, it will often come into contact with both organic and inorganic matter. In the case of food-washing with EW, this could be soil or dirt on the surface of freshly harvested fruits and vegetables, components of the fresh produce (especially in the case of cuts/damage to the surface) or water contaminants. The latter may be deposited on the produce from a water washing step prior to EW treatment, or may be present in the water used to generate or dilute the EW. This is especially relevant in parts of the world that lack reliable access to high-quality clean drinking water. Examples of inorganic water constituents are ammonia, nitrite and nitrate ions, metals, chloride and sulphate ions, whereas organic constituents in water samples are often proteins, carbohydrates and fats or their constituent parts (Tchobanoglous et al., 2003). It is well known that high levels of organic matter can decrease the FAC concentration and antimicrobial effects of FAC based sanitisers (Kaczmarek et al., 2019). This represents a problem when reliable, consistent sanitising results are required.

2.1.2 Reactivity of EW components

The FAC in chlorine based sanitisers (such as EW) can react with inorganic and organic compounds, e.g., ammonia and amino acids, resulting in decreases in both the FAC and antimicrobial effect (Oomori et al., 2000). Such a chlorine demand of the matrix has to be met before FAC accumulates that is then available

for antimicrobial activity (discussed in more detail in 1.6.3) (Tchobanoglous et al., 2003). The chloramines resulting from the reaction of FAC with organic or inorganic nitrogen compounds can retain mild oxidizing activity (Mood, 1950, Hawkins et al., 2003). This highlights the importance of survival-based tests compared to FAC analysis for a more complete assessment of EW efficacy. The effect of organic compounds on the activity of EW will also depend on the reactivity of such compounds with the different EW components (including non-chlorine species) whose relative contributions to overall EW action are unclear. In addition to the inactivation of EW species, potentially toxic by-products from the reactivity of EW with organic compounds present a safety concern regarding the treated produce or water (see 1.5.4 and 1.8.2.3).

2.1.3 Reactivities of relevant organic materials

The initial focus of this chapter is on investigating the effect of soil on EW, which is particularly important as residual surface soil is common on many types of fruits and vegetables subject to sanitisation treatments. Based on the results obtained and because previous studies indicated strong reactivities between EW and amino acids, peptides and protein-rich foods (Oomori et al., 2000, Jo et al., 2018), the second focus will be on proteins and amino acids. However, it should be noted that other compounds such as lipids (abundant in many foods) can also be oxidised by reactive oxygen species, leading to peroxidation of unsaturated fatty acids (Avery, 2011), and could therefore influence the activity of EW and the success of a sanitising treatment.

2.1.3.1 Soil composition

Generally, the minerals or compounds in soil are composed of the elements oxygen, silicon, aluminium, iron, calcium, sodium, potassium, magnesium and other elements in small quantities (Lade, 2001). But different soil types vary in

their chemical and physical properties, which may influence their reactivity with EW. For instance, soil is often characterised based on its textural fractions. In a common classification system (as used by the United States Department of Agriculture), sand, silt and clay correspond to large (50–2000 μm), medium (2-50 μm) and small (<2 μm) particle sizes (Martín et al., 2018). The individual soil particles can interact to form aggregates which result in local microenvironments in soil ecosystems (Harvey et al., 2020) and which could also alter the accessibility of soil components to EW during a sanitising treatment. Organic matter in soil stems from plant litter and microbial biomass and their degradation products (Kögel-Knabner, 2002). Functional classes of soil organic matter are varied, including aliphatic, aromatic, phenol, carboxylate, polysaccharide, hydroxyl, amine and amide compounds (Margenot et al., 2015)., and some of these are likely to be reactive with EW. Processing techniques such as soil sterilisation can affect the soil properties, e.g., by reducing the aggregation and increasing the dissolved organic matter fraction (Berns et al., 2008). In the cited study, the authors found that sterilisation by γ-irradiation produced less change than sterilisation by autoclaving. Consequently, the soil in the present study was γ-irradiated to achieve sterilisation.

2.1.3.2 Effect of ROS on proteins and amino acids

As mentioned above, the second focus of this chapter is to study the reactivity between EW and proteins or amino acids, because such reactivity has previously been indicated and also because proteins and amino acids are oxidation-sensitive, and EW contains oxidising chemical species (chlorine species and non-chlorine ROS). Sensitivity of proteins to oxidative damage depends on protein properties such as amino acid composition, conformation, accessibility of redox-sensitive sites, charge distributions and potential metal-binding sites (Chang et al., 2020, Avery, 2011). Oxidation of proteins by hydroxyl radicals leads to radical formation at α-carbon atoms or in the side chains. Subsequent reactions with superoxide or

Fe(II) can result in peptide bond cleavage (Stadtman and Levine, 2003). Proteins are also highly reactive with FAC, leading to chlorination of amino groups and side chains and further downstream modification reactions (Hawkins et al., 2003).

Protein oxidation at certain residues (e.g., arginine, histidine, proline, lysine, threonine, tryptophan) results in irreversible carbonylation (Avery, 2011, Fedorova et al., 2014). Phenylalanine and tyrosine are also oxidised by various ROS types (Stadtman and Levine, 2003). The main oxidation product of methionine is methionine sulphoxide (Hawkins et al., 2003). Cysteine can be oxidised at the thiol(ate) group by various oxidants, yielding the sulphenic acid form (Poole, 2015). The reactivity of amino acids with specific ROS depends on the conditions, for instance at neutral pH (~7), cysteine is more reactive with H_2O_2 than methionine (Davies, 2005, Winterbourn and Metodiewa, 1999), but at low pH (<5), H_2O_2 is more likely to oxidise methionine than cysteine because cysteine is usually protonated at low pH (Levine et al., 2000).

2.1.4 Aims

It is known that NaOCl or EW can react with organic compounds, depending on the chemistry of those compounds. However, a clear understanding of the reactivities of EW with organic constituents of environmental samples is missing. This work focused on the reactivity of soil and EW to help understand and predict the feasibility of EW treatments in the food industry and beyond. Furthermore, a complex mix of organic compounds (YEPD broth medium) was used to dissect which compound classes produce the inactivation of EW, and in that way leading to characterisation of proteins and specific amino acids that are highly reactive with EW. Most previous studies focused on the bactericidal effect of EW in the presence of organic compounds, however extensive data on the fungicidal effect is lacking. Therefore, the impacts on EW efficacy were studied by assessing the

efficacy against the common food spoilage fungus *A. niger*, including both a standard laboratory strain (*A. niger* N402) and *A. niger* isolates from contaminated Indian onions.

2.2 Materials and methods

Unless otherwise specified, chemicals were obtained from Sigma-Aldrich or Oxoid Ltd., Thermo Fisher Scientific.

2.2.1 Fungal strains and growth conditions

The study used the filamentous fungus *Aspergillus niger* N402 (ATCC 64974). *A. niger* was maintained and grown at 28°C on Potato Dextrose Agar (PDA, Oxoid) or YEPD (2% [w/v] bacteriological peptone (Oxoid, Basingstoke, UK), 1% [w/v] yeast extract (Oxoid), 2% [w/v] D-glucose). Conidia were harvested in 0.1% [v/v] Tween 80 from PDA slopes after one week of growth, filtered through a 40 µm cell strainer and spore densities were counted in a haemocytometer. If applicable, conidia were cultivated in YEPD for 2–4 h (allowing activation/swelling) or germinated and grown for 2 days (150 rev min^{-1}, 28°C, initial inoculum adjusted to 10^5 spores mL^{-1}), and swollen conidia (after 2–4 h) were harvested by centrifugation (537*g*, 10 min) followed by washing twice (9000*g*, 4 min) and resuspending in 0.1% Tween 80 (see 2.2.2.1 for harvest of mycelium after 2 days). Where necessary, YEPD was solidified with 2% [w/v] agar (Sigma-Aldrich, St. Louis, MO).

2.2.2 Isolation of wild fungal strains and ITS sequencing

2.2.2.1 Strain isolation and preparation of genomic DNA

Onion samples with black mould contamination were kindly provided by Jain Farm Fresh Foods Ltd. in Jalgaon, India. Swabs of the fungal contamination were streak plated onto YEPD agar, incubated at 28°C for 2 days and 8 colonies that showed *A. niger*-like morphology were selected (isolates 1–8). Spores from these colonies were grown on PDA slopes as described above. Genomic DNA from the 8 wild isolates and the *A. niger* N402 lab strain was extracted using the Wizard® Genomic

DNA Purification Kit, following the manufacturer's protocol for isolation of genomic DNA from plant tissue, as follows: Mycelium from 2-day old YEPD cultures (10^5 spores mL^{-1}, 50 mL, 28°C, 150 rev min^{-1}) was harvested by filtration through Miracloth and ground to a powder in liquid nitrogen. In a 1.5 mL reaction tube, 600 µL Nuclei Lysis Solution was mixed with the powder, followed by incubation at 65°C for 15 min. After cooling down to room temperature, 3 µL RNase Solution was added, the tubes inverted 2–5 times and incubated at 37°C for 15 min. After centrifugation (15,000*g*, 3 min), the supernatant was mixed with 200 µL Protein Precipitation Solution and vortexed for 20 s at high speed. After another centrifugation step to separate the precipitated proteins from the DNA in solution (15,000*g*, 3 min), the supernatant was added to 600 µL isopropanol, mixed by inversion and centrifuged (15,000*g*, 1 min). The pellet was washed by adding 600 µL 70% ethanol and inverting several times. After centrifugation (15,000*g*, 1 min), the supernatant was removed, and the pellet left to air-dry. The pellet was then rehydrated at 4°C overnight in 100 µL DNA Rehydration Solution (10 mM Tris-HCl, pH 7.4, with 1 mM EDTA), and the obtained genomic DNA was stored at –20°C.

2.2.2.2 PCR amplification and DNA sequencing

Internal Transcribed Spacer (ITS) regions were amplified by PCR using the primers ITS1 (5'-TCCGTAGGTGAACCTGCGG-3') and ITS4 (5'-TCCTCCGCTTATTGATATGC-3'), described previously (White et al., 1990). The PCR conditions were as follows:

Table 2-1: PCR conditions for the amplification of ITS regions.

Ingredient	Final concentration in PCR reaction	Final amount (50 µL PCR reaction)
10 µL genomic DNA	2 ng μL^{-1}	100 ng
1 µL dNTPs	0.2 mM	10 nmol
2.5 µL ITS1 primer	0.5 µM	0.025 nmol
2.5 µL ITS4 primer	0.5 µM	0.025 nmol
2.5 µL DMSO	5%	2.5 uL
10 µL 5X Phusion® HF reaction buffer	1X	1X
0.5 µL Phusion® HF DNA polymerase	0.02 U μL^{-1}	1 U
21 µL water	–	

PCR programme	Cycles
98°C (5 min)	1x
98°C (0.5 min)	35x
55°C[a] (0.5 min)	
72°C (0.5 min)[b]	
72°C (10 min)	1x
10°C (hold)	1x

[a] 50°C for isolate 1 and 2
[b] 2.5 min for isolate 1 and 2 (these conditions were chosen after previous PCR at above conditions was unsuccessful for isolates 1 and 2)

PCR products were purified using the NucleoSpin® Gel & PCR CleanUp Kit (Macherey-Nagel), following the manufacturer's instructions. Samples were sent for sequencing with primer ITS4 to Eurofins Genomics EU Sequencing GmbH (Cologne, Germany). The sequencing results obtained were analysed using: (i) the NCBI BLAST® blastn tool (using standard settings) to identify matches of the obtained sequences with ITS sequences from known fungal species, and (ii) the EMBL-EBI Clustal Omega Multiple Sequence Alignment tool (https://www.ebi.ac.uk/Tools/msa/clustalo/) (Madeira et al., 2019). Sequences and alignments were visualised using SnapGene® Viewer 5.1.7.

2.2.3 Electrolysed water (EW), NaOCl and ozonated water

Eloclear® electrolysed water (EW) was provided by Ozo Innovations (Kidlington, UK). The EW was manufactured electrochemically in single-cell units with a pH ~8.7–9.3 and a free available chlorine (FAC) concentration between 1800–

2000 mg L^{-1}. The FAC concentration was checked prior to experiments using the HACH® DPD Free Chlorine Reagent (Permachem®) in a HACH® Pocket Colorimeter™ II. EW was stored in plastic containers in the dark at 4°C for up to 2.5 weeks. Dilutions (v/v) were prepared in HPLC grade water (unless stated otherwise) immediately prior to use. NaOCl solution (5% chlorine) was purchased from ACROS Organics™, Fisher Scientific, stored at 4°C and the FAC concentration was checked using the DPD reagent prior to experiments. Ozonated water was produced using an Enozo Sanitizing Spray Bottle (SB-100HD) from Enozo Technologies, Inc. (North Andover, MA), kindly provided by GreenTeck Global (Wallingford, UK). The bottle was filled with sterile filtered tap water (4°C) and ozonated water was produced by spraying for 5 s. The water was used within 30 s (Chapter 2, Chapter 4) or 2 min (Chapter 3) of its generation.

2.2.4 Soil samples

Soil samples from arable land with varying chemical and textural properties were kindly provided by Hannah Cooper (University of Nottingham). The soil properties are listed in Table 2-2. An additional uncharacterised sample ("soil 8") was autoclaved soil from an untreated control site at the Woburn long-term sludge experiment, UK (http://www.era.rothamsted.ac.uk/Other#SEC11) (Gibbs et al., 2006). All samples (including the previously-autoclaved sample) were sterilised using γ-irradiation for 4 days, corresponding to a total dose of 22–26 kGy. Samples were then passively dried at 37°C for 4 weeks until a constant weight was reached.

Table 2-2: Soil type characterisation. Data and samples were kindly provided by Hannah Cooper (University of Nottingham).

#	Particle Size Characterisation	LOI[a] [%]	Sand [%]	Silt [%]	Clay [%]	pH
1	Sandy_Silt_Loam	7.76	24.6	64.4	10.9	7.71
2	Sandy_Clay_Loam	7.66	66.8	12.6	20.6	7.9
3	Sandy_Clay_Loam	3.82	65.8	10.6	23.6	7.88
4	Sandy_Clay_Loam	13.68	59.3	21.7	18.9	7.73
5	Clay	7.78	34.4	30.5	35.1	6.38
6	Sandy_Clay_Loam	6.18	66.8	12.6	20.6	7.71
7	Sandy_Clay_Loam	5.85	55.5	24.3	20.2	8.1

[a] LOI (loss on ignition) is a measure for organic matter content.

2.2.5 Fruits and vegetables

Blueberries, tomatoes and spinach leaves were purchased from Sainsbury's (SO Organics brand) and washed in sterile distilled water (SDW) before use. To reduce potential microbial contamination of the produce surface, UV treatment was applied using the Sterilisation programme (90 s) of a GS Gene Linker® UV Chamber (BioRad).

2.2.6 EW or NaOCl treatment of *A. niger*

Electrolysed water was diluted in sterile water to 22.5% [v/v] (equals 400–450 mg L^{-1} FAC) and either mixed or not with different organic substrates (either fruits or vegetables, soil samples, Tween 80, YNB (0.69% yeast-nitrogen base without amino acids, Formedium, Norfolk, UK), YEPD components, proteins [as specified later] or amino acids). Five minutes after mixing with EW, the solutions or suspensions were used to treat freshly harvested conidia (final density 10^5 spores mL^{-1} unless stated otherwise) at final concentrations of 20% EW [v/v], ≤0.01% [v/v] Tween 80 (0.1 mg mL^{-1}). Treatment volumes were between 0.1–1 mL (0.1 mL when treatment and recovery were in 96-well plates, 0.5–1 mL in reaction tubes for agar plating experiments) except for experiments where fruits and vegetables were added which required 20 mL EW to cover the surface area. The surface area per treatment was approximately 14 cm^2 (blueberries, 2 fruits),

30 cm^2 (spinach, 1 leaf) and 22 cm^2 (tomatoes, 1 fruit), and fruits and leaves were intact during the treatments. After defined periods (1–7 min), EW treatments were stopped by mixing with an equal or higher volume of two-times concentrated (2X) YEPD. After appropriate dilution in YEPD, 100 µL samples were plated onto YEPD agar and incubated for at least 2 days, 28°C before colony counting. For recovery in broth after EW treatment, 100 µL samples were transferred to 96-well plates and incubated statically at 30°C. Growth was determined by OD_{600} readings at appropriate time points in either a BioTek® EL800 or a PowerWave XS2 microplate reader. In certain experiments, sodium hypochlorite (NaOCl) treatment was used for comparison (7.8-fold dilution of the purchased solution). NaOCl was diluted in sterile water as specified and used as described above for EW.

2.2.7 Heat treatment after EW treatment to assess potential synergistic effect of combined treatments

After EW treatment of *A. niger* spores (0.23–9.5% EW, 0.1 mL treatment volume), spores suspended in YEPD (0.15 mL) were transferred into 0.2 mL reaction tubes and heat treated for 1 min (actively cooling down to 18°C for a 1 min hold after the treatment) in a Prime Thermal Cycler, Techne (Cole-Parmer, Stone, UK). Different temperatures were achieved with a gradient setting (settings on PCR cycler: temperature: 59°C, gradient: 20°C, resulting in 50.3°C [1st column from the left on the heating block], 52.5°C [3rd], 54.6°C [4th], 58.2°C [6th], 60.1°C [7th], 63.8°C [9th] and 67.3°C [11th]). Heat treatment was carried out ~15–20 min after the EW treatment. Aliquots of 100 µL were subsequently incubated statically for OD_{600} determination over time, as described above (2.2.6).

2.2.8 Determination of protein and humic acid contents of soil samples

A citrate extraction and a modified Lowry assay were performed as described previously (Redmile-Gordon et al., 2013). Briefly, 8 mL of 20 mM citrate buffer (pH 7) was added to 1 g of dried soil in 15 mL polypropylene centrifuge tubes and autoclaved for 30 min (117°C). After autoclaving, the tubes were cooled on ice and then centrifuged (3500*g*, 20 min, 4°C). The supernatant was stored at 4°C for the Lowry assay ("citrate extract").

In an alternative citrate + SDS extraction protocol (Chen et al., 2009), 10 mL of 250 mM citrate buffer (pH 8) was added to 1 g dried soil in 50 mL centrifuge tubes and shaken for 4 h (Stuart® see-saw rocker SSL4, 70 rev min^{-1}, with vortexing at 0 h, 2 h and 4 h). After centrifugation (2876*g*, 15 min, 4°C), the supernatant was collected as "citrate extract II". 10 mL SDS buffer (1% [w/v] SDS, 0.1 M Tris-HCl (pH 6.8), 20 mM DTT) was added to the pellet, shaken for 30 min (see-saw rocker, as above), and centrifuged to obtain the supernatant ("SDS extract"). The "citrate extract II" and the "SDS extract" were combined for the Lowry assay ("citrate+SDS extract").

The modified Lowry assay was performed separately for both extracts. For the assay, 50 µL extract samples ("citrate extract" or "citrate+SDS extract", diluted between 1:5 and 1:12.5 depending on the assay signal of the extract) were transferred to 96-well plates and mixed with 50 µL of PBS containing either BSA as protein standard or a humic acid (Sigma-Aldrich) standard (standard concentrations in PBS: BSA, 40–640 mg L^{-1}; humic acid, 160–640 mg L^{-1}). Assay reagents A and B were prepared by mixing solutions 1, 2 and 3. Solution 1: 0.35 g mL^{-1} $CuSO_4.5H_2O$ in deionised water. Solution 2: 0.07 g mL^{-1} sodium potassium tartrate in deionised water. Solution 3: 0.07 g mL^{-1} Na_2CO_3 in 0.35 N

NaOH. Reagent A was prepared by mixing solutions 1, 2 and 3 in the ratio 1:1:100, and reagent B was the same except solution 1 was substituted with deionised water. To each extract + standard combination, 100 µL of $CuSO_4$-containing reagent A (in plate A, for protein and humic acid determination) or of $CuSO_4$-free reagent B (in plate B, for humic acid determination) was added. Samples were incubated for 10 min in the dark, followed by the addition of 100 µL 1X Folin-Ciocalteu Phenol reagent (ThermoFisher) and 30 min incubation in the dark. The absorbance at 750 nm was determined with a BioTek® microplate reader (Epoch2). After subtraction of a blank (PBS + reagents), the absorbances corresponding to protein (Abs_{prot}) and humic acid (Abs_{hum}), respectively, were calculated from the absorbance readings for plates A and B (Abs_A and Abs_B) (Frølund et al., 1995):

$$Abs_{prot} = 1.25\ (Abs_A - Abs_B) \qquad Abs_{hum} = Abs_B - 0.2Abs_{prot}$$

2.2.9 Determination of protein content in YEPD

The Pierce™ Modified Lowry Protein Assay (ThermoFisher) was performed according to the manufacturer's Microplate Procedure. Samples (20 µL of either YEP, peptone or yeast extract, diluted to between 100–600 mg L^{-1}) were mixed with 20 µL BSA standard (25–750 mg L^{-1}). Modified Lowry Reagent (200 µL) was added, before incubation for 10 min in the dark and subsequent addition of 20 µL 1X Folin-Ciocalteu Phenol Reagent. After 30 min incubation in the dark, absorbance at 750 nm was determined with a BioTek® microplate reader (Epoch2).

2.2.10 *In-vitro* assays with fluorescent dyes

The fluorescent probes hydroxyphenyl fluorescein (HPF) and aminophenyl fluorescein (APF) (Setsukinai et al., 2003) were supplied by Sigma-Aldrich at

5 mM in dimethylformamide (DMF). These were diluted in HPLC grade water to 50 µM. Dye (10 µL of the 50 µM dilution) was mixed with 10 µL water or diluted amino acids or antioxidants (final assay concentration 0.3–10 µM), and 80 µL oxidant (diluted EW, NaOCl, pure ozonated water or 30% H_2O_2) was added. Fluorescence was recorded immediately (within 2 min of oxidant addition) and at further time points up to 1 h, with excitation at 485/20 nm and emission at 528/20 nm (BioTek® microplate reader Synergy HTX).

Dihydroethidium (DHE) was obtained from Thermo Fisher Scientific and 2',7'-dichloro-dihydro-fluorescin diacetate (DCF) from Sigma-Aldrich. These dyes were diluted in water to 5 µM for DCF and 5–3000 µM for DHE (no fluorescence was detected at any of these concentrations), and used as described for APF and HPF above.

2.2.11 Statistical analysis and software

Tests for statistical significance were according to a two-tailed paired *t*-test, correcting for multiple comparisons by controlling the false discovery rate at FDR <5%, using a two-stage step-up method (Benjamini et al., 2006). The calculations were performed within GraphPad Prism 8 software. Paired tests were used to control for observed between-experiment variation in EW effect-size. At least three independent replicates were analysed in each case. Significance was defined by a p-value <0.05. Linear regressions were calculated in Prism 8, to determine R^2 and p-values. Correlation analysis was performed within MATLAB® 2018a, calculating Pearson's correlation coefficient and significance with the command "corrplot(y,'testR','on')" [y being a matrix of soil characteristics and spore survival].

2.3 Results

2.3.1 EW efficacy against *A. niger*

2.3.1.1 Killing of laboratory strain (N402) and wild isolates of *A. niger* by EW treatment

Freshly harvested conidia of *A. niger* were killed by short-term EW treatment (5 min), when the EW was used at full strength (1800–2000 mg L^{-1} FAC, detection limit ~1–2% survival, Figure 2-1 A). Dilutions of EW and shorter treatment times allowed more survival. Concentrations between 0.3–1% EW (5.4–20 mg L^{-1} FAC) were found to result in intermediate killing effects (<1 log) after 5 min and these conditions were selected for subsequent experiments requiring partial survival. The effect of high concentrations (≥3% EW [≥54–60 mg L^{-1} FAC]) was assessed further (see below). It was also noted that germinating conidia were more sensitive than dormant spores to EW treatment (Figure 2-1 B).

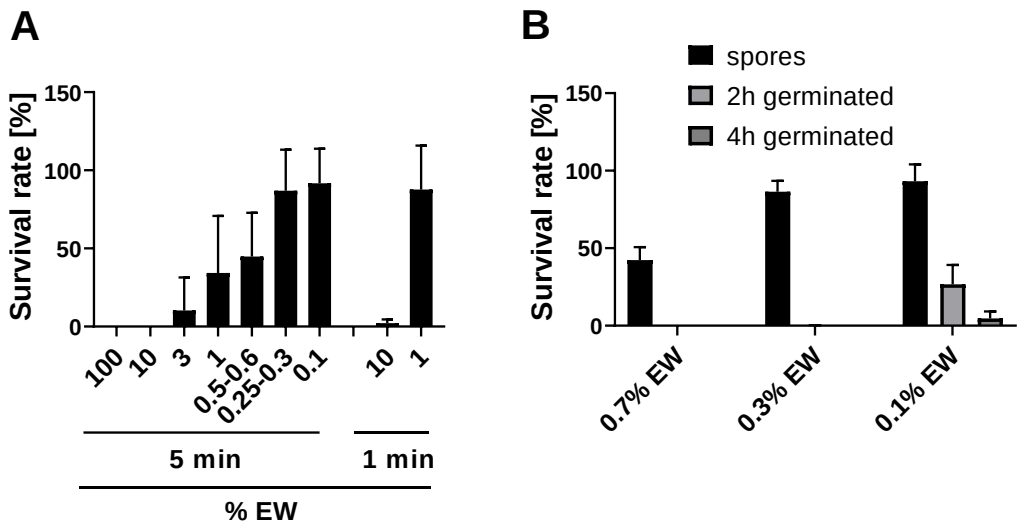

Figure 2-1: Survival rates of *A. niger* N402 treated with EW. Conidia (A,B) or germinating conidia (B, 2 h or 4 h germination in YEPD, 150 rev min^{-1}, 28°C) were treated with the specified EW dilutions (% [v/v], in sterile tap water or HPLC grade water (A) or HPLC grade water (B)), for 1 or 5 min as specified (A) or 5 min (B). Survival was determined by plating 100 µL of appropriate dilutions on YEPD agar and subsequent colony enumeration, calculated as a percentage relative to an untreated control. The detection limit was ~1–2% survival. Mean data ± SD are shown for at least 3 biological replicates.

The EW sensitivity of the laboratory strain (N402) was compared to wild isolates of *A. niger* from Indian onion samples. To assess the strain identities, the internal transcribed spacer (ITS) regions between the 18S and 28S rRNA genes (including the 5.8S gene) were amplified with the primers ITS1 and ITS4 and sequenced with ITS4 (sequences can be found in Appendix A, 6.1.1) (White et al., 1990). Alignments of the resulting sequences with the EMBL-EBI Clustal Omega Multiple Sequence Alignment tool (Madeira et al., 2019) showed that the ITS sequences of the wild *A. niger* isolates closely matched the laboratory strain sequence: when strains with short sequencing lengths were excluded (isolates 5 [27 bp] and 7 [133 bp]), the multiple sequence alignment revealed a 422 bp-consensus sequence that matched all other strains (isolates 1–4, 6, 8 and N402), except for two 1 bp-differences that were detected in the sequence for isolate 4 (more differences were observed towards the start and end of the sequences, where sequencing inaccuracies may occur, see Appendix A, 6.1.2).

The NCBI BLAST® blastn tool revealed sequence matches to existing *A. niger* ITS sequences of various *A. niger* strains and isolates (MBL1511, BFW, Asp-7136, AR2, An3-2, JS-1, MSR3, MSR4) in the top-two matches (sorted by ascending E values, a statistical parameter which describes how likely a match was obtained by chance) for all isolates (these matches had 95–100% sequence identity, see Appendix A, 6.1.3; see text below for the top-two matches sorted by descending % sequence identity), except isolate 5 which matched best to a *Penicillium* ITS sequence (2nd best match was *Aspergillus tubingensis*, no *A. niger* sequence was detected in the top 100 hits), most likely due to the very low sequencing length for this isolate (27 bp). In some other cases, the best match (sorted by E value) was to an unclassified fungal species (isolate 6) or to an *A. tubingensis* ITS sequence (isolate 2, 8 and strain N402; the 2nd best match was *A. niger* in all these cases), most likely due to a high ITS sequence similarity between *A. niger* and *A. tubingensis* (Accensi et al., 1999) and potential sequencing errors at the

beginning and end of the obtained sequencing reads, which would explain the *A. tubingensis* match for the N402 strain. In the case of isolate 7, the top two hits matched an uncultured *Aspergillus* clone and *A. terreus*, respectively. When the BLAST matches were sorted by % sequence identity, the % identity of the first two hits was higher (99–100%), and in this case, the first two hits were *A. niger* strains or isolates (bendaryC, TSE15.2, AHBR3, AR2, RS_10, 7M1, DUCC5709, CM_MY17_59) for all the isolates in this study, except for isolates 5 and 7.

With the exception of isolates 5 and 7, the most frequent organism among all significant blast-hits were *A. niger* matches (57–76% of all significant matches). In conclusion, the ITS data suggest that isolates 1–4, 6 and 8 may be *A. niger* strains. However, it should be noted that ITS sequencing alone is not sufficient for precise species identification and should ideally be combined with sequencing of protein-coding loci such as the calmodulin and β-tubulin genes (Alshehri and Palanisamy, 2020), which may have helped to better distinguish between closely related species. Here, it was deemed sufficient that some of the wild isolates were likely true *A. niger* isolates to allow comparison with the EW sensitivity of *A. niger*, so further steps for more precise strain identification were not taken. The organisms were assayed with EW. All of the isolates showed similar EW sensitivity compared to the N402 laboratory strain (Figure 2-2; isolate 7 was tested in one biological replicate only and showed survival similar to isolates 6, 8 and N402 [not shown]). Some strains seemed to survive better compared to N402 (e.g., survival of strains 1 and 2 at 0.6% EW was on average ~50–60% and ~40% for N402), but there was high variation between biological replicates and the killing effect was still in a similar order of magnitude for the different strains. This suggests that the lab strain is a suitable model for assessing the EW response of *A. niger*. However, it is possible that some wild strains of *A. niger* such as the ones isolated here would show somewhat increased levels of EW resistance compared to the results obtained for *A. niger* N402 in other experiments throughout this thesis.

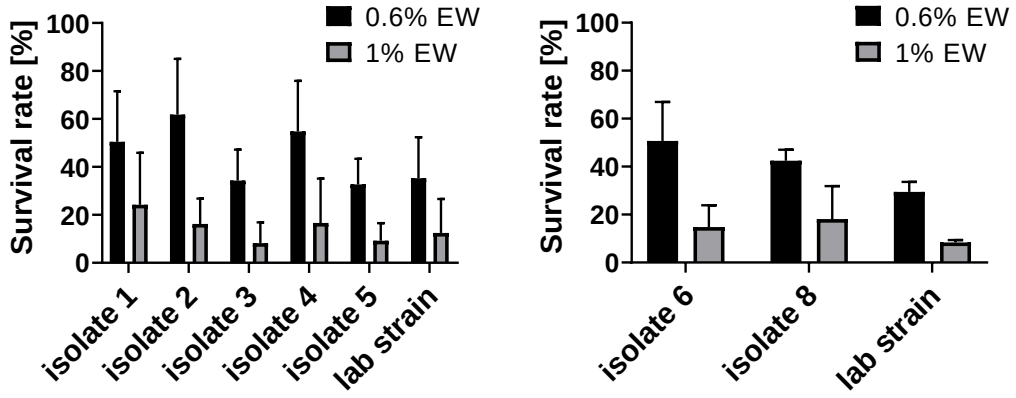

Figure 2-2: Survival rates of wild *A. niger* isolates from Indian onions compared to the laboratory strain *A. niger* N402. Conidia were treated for 5 min with the specified EW dilutions (% [v/v] in HPLC grade water) and survival was determined by plating 100 µL of appropriate dilutions on YEPD agar (in technical duplicates) and subsequent colony enumeration. The data show mean values ± SD for at least 3 biological replicates. See main text for strain details.

2.3.1.2 Log reduction rates of spore viability on agar

To assess further the efficacy of EW against *A. niger* N402, after EW treatment (10^5 spores mL^{-1} in the treatment mix), diluted samples (~100–200 spores) as well as concentrated samples (x 25 and x 200 concentrated) were spread plated onto YEPD agar plates. The survival was assessed by colony enumeration and calculated relative to an untreated control. 10–100% EW resulted in approx. 3–4 log reduction in spore outgrowth after 5 min treatment, with some variation between replicates including reductions >4 log in some cases (Figure 2-3). Electrolysed water at a concentration of 20% (360–400 mg L^{-1} FAC; 5 min exposure) was used throughout to give high killing with 10^5 spores mL^{-1} in the treatment mix, achieving >3 log killing (confirmed in specific experiments as stated, see 2.3.2.2 and 2.3.3).

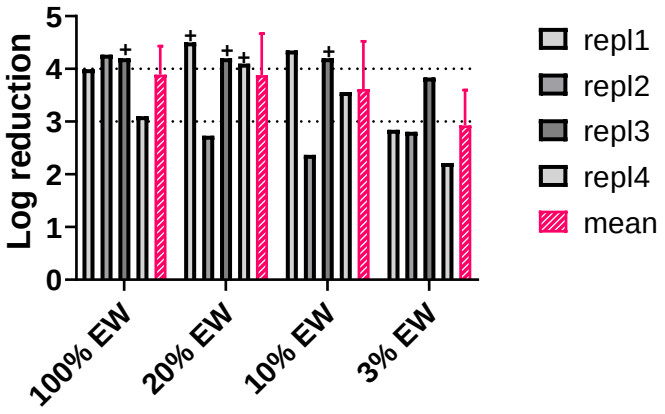

Figure 2-3: Log reduction rates for EW treatments of *A. niger* spores as determined by recovery on agar plates. *A. niger* suspensions were treated for 5 min with full strength or diluted EW (3–100% [v/v] in HPLC grade water; spore concentration in treatment mix was 10^5 spores mL^{-1}). Treatments were stopped by inactivation with 2X YEPD and three different dilutions were plated onto YEPD agar (~2–4 x 10^4, ~2–5 x 10^3 and 1–2 x 10^2 spores per plate, in technical duplicate). Log reduction rates were calculated from the resulting survival (colony forming units relative to no-EW control). If colonies were distinguishable and reliable for more than one dilution (between ~10 and 200 colonies), the average of the resulting reduction rates was used. If no colonies were found on any of the plates, the theoretical reduction rate for 1 cfu per plate (on both technical duplicates) at the highest spore concentration was calculated and is given in the graph, indicated by a "+" above the bar, to represent the minimum log reduction achieved by the treatment condition (the real reduction rate is > the given value). Results are shown for 4 independent biological replicates separately and also the mean of each set of replicates (in pink).

2.3.2 Influence of environmental organic substances on EW efficacy

2.3.2.1 Fruits and vegetables

Because EW may be used on fresh fruits and vegetables, the effect of the presence of these products on EW efficacy against *A. niger* was tested. Adding intact blueberries, spinach or tomatoes did not impact the killing by EW of *A. niger* spores in suspension (20% EW [360–400 mg L^{-1} FAC], 5 min treatment, Figure 2-4). UV treatment was employed to prevent contamination from natural microorganisms on the purchased produce, however no contamination from non-UV-treated samples was detected when plating EW treatment and control samples on YEPD agar for *A. niger* outgrowth post-treatment (30 µL samples from 20 mL treatment volumes, diluted 1:33.3 before plating). UV-treated produce also did not influence the EW efficacy. It should be noted that in an application process,

the ratio of produce to EW may be higher and damaged fruits and vegetables may influence the EW effect more due to increased accessibility of reacting organic substances in tissue wounds and juices (no macerated or damaged fruits were tested in this study). Adding soil (100 mg mL^{-1} wet soil) resulted in slightly increased survival of EW treatment in one replicate (0.5%; no detectable growth in the other two replicates), so the effect of soil was studied further (2.3.2.2). The positive control YEPD is discussed below (2.3.3).

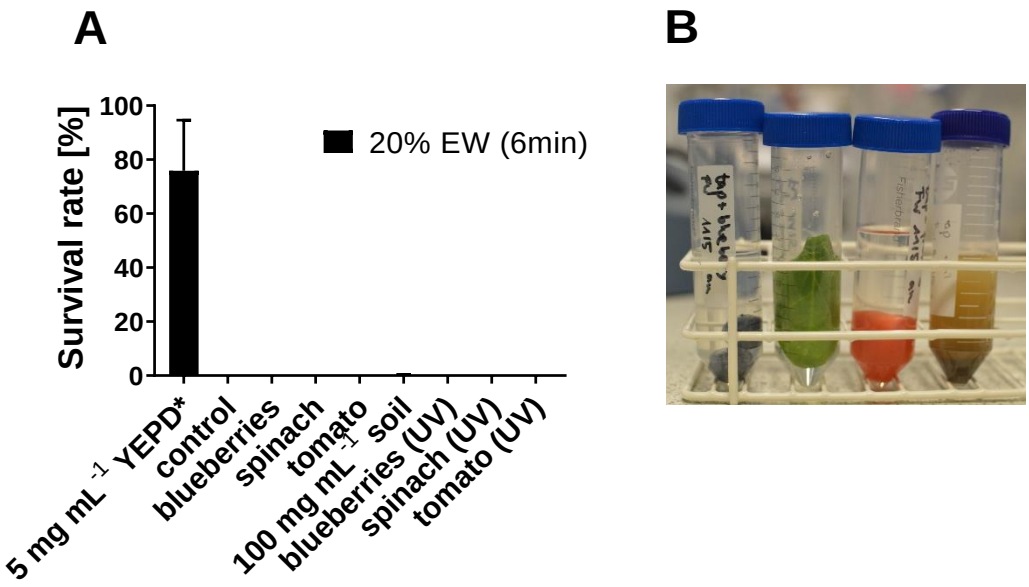

Figure 2-4: Influence of the presence of fruits, vegetables and soil on the EW efficacy. *A. niger* spores were treated with 20% [v/v] EW (dilution in sterile tap water) for 6 min in the presence or absence of different organic materials and survival was determined by spread plating aliquots containing ~100 spores (~60 in one replicate) in technical duplicate on YEPD agar and subsequent colony enumeration. A) Data are mean values ± SD from at least 3 biological replicates, except UV treated produce: n = 2. B) Example of an EW treatment with added fruits, vegetables or soil. Blueberries: surface area approx. 14 cm^2 (2 berries in 20 mL EW), spinach: approx. 30 cm^2 (1 leaf), tomatoes: approx. 22 cm^2 (1 fruit). UV treatments were carried out in a GS Gene Linker® UV Chamber (BioRad) for 90 s. The soil sample was soil "8" (see 2.2.4), used here without γ-irradiation or drying. *Outgrowth from YEPD-containing treatments was delayed compared to non-EW controls (by up to 4 additional days of growth at room temperature after the initial 2 day incubation at 28°C); the data shown are for this longer incubation time.

2.3.2.2 Soil samples

Potential applications of EW in the fresh food industry, among other applications, may be affected by soil residues on produce or other contaminants; a factor that could alter EW activity. Effects of soil on EW activity were therefore tested. In standard experimental conditions, EW at a 20% [v/v] dilution (360–400 mg L^{-1} FAC) was sufficient to kill >3 log spores of *A. niger* in 5 min (see "control" in Figure 2-5; no colony formation was detected when plating ~2000 spores per plate after EW treatment). Adding soil (dried and γ-sterilised) to EW treatments inactivated EW-dependent killing only at high soil levels (Figure 2-5 A,C). The soil concentration (750 mg mL^{-1}) shown in the figure was chosen after preliminary tests with soil "8" showed that smaller soil additions were insufficient for suppressing EW activity (not shown). The data are presented both as log reduction rates (Figure 2-5 panels C,D) and as survival rates (linear scale, panels A,B) as this helps visualize differences in the sizes of the inactivation effects between the soil types. Four out of eight tested soils did not give full EW inactivation even at 750 mg mL^{-1}. The strongest inactivation effect was observed for one soil sample (soil 4) which gave full inactivation of EW at 100 mg mL^{-1} and more limited EW action (<2 log killing) at 30 mg mL^{-1} (Figure 2-5 B,D). At 750 mg mL^{-1} added soil, sample 7 seemed to inactivate EW the strongest, however at lower soil additions (100 mg mL^{-1}), soil 7 had a weaker inactivation effect than soil 4 (Figure 2-5). The soil concentrations necessary to inactivate EW were compared to a complex mix of organic compounds (YEPD, a fungal growth medium). This mix at only 5 mg mL^{-1} was sufficient to inactivate EW fully.

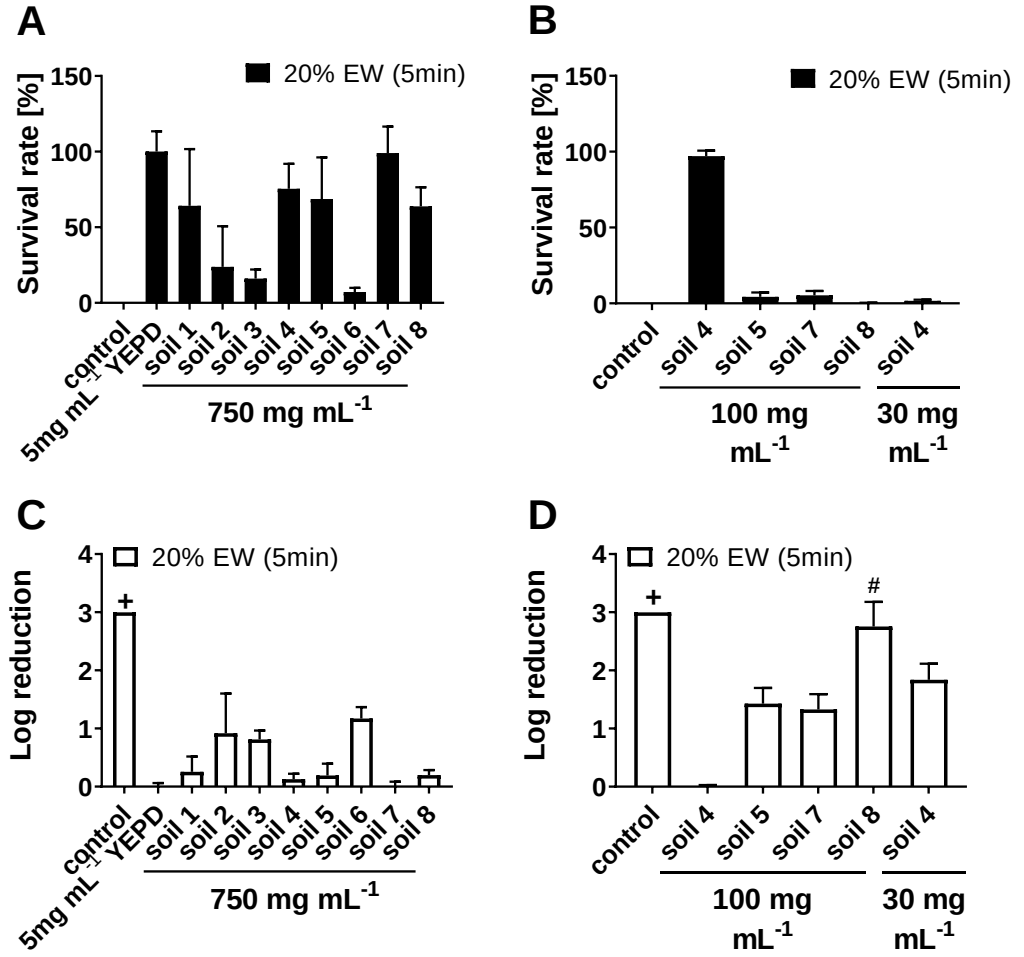

Figure 2-5: Inactivation of fungicidal EW activity by soil material. Soil (characteristics of soils 1–7 listed in Table 2-2), YEPD or water (control) were added as specified to 22.5% [v/v] EW and incubated for 5 min, before exposing *A. niger* spores to the (supplemented) EW for 5 min, final concentration 20% EW. Survival rates (A,B) and log reduction rates (C,D) were determined by colony growth on YEPD agar after up to 3 days. A,C) Soil added to a final concentration of 750 mg mL^{-1}. B,D) Soil added to final concentrations of 100 or 30 mg mL^{-1}. Data are means ± SD from at least 3 biological replicates (except soil 8 in A: n = 2). The log reduction was >3 in control samples (+, no cfu detected when plating ~2000 spores). In panels B,D >3 log reduction was detected with soil 8 in two out of 3 biological replicates (#).

To explain the differences observed for the different soil types, and because YEPD gave strong EW inactivation and contains high protein levels (see below), the organic content of the soil samples was dissected. The protein content and the humic substance content of the soils were determined in citrate extracts and, to increase the range of extracted proteins, also in citrate+SDS extracts (Chen et al., 2009). Protein levels were low (below 5–10 mg g^{-1} soil) compared to the humic

substance levels (>12 mg g^{-1}; Figure 2-6 B) and these low protein levels for the different soil types did not appear to correspond with their relative EW inactivation efficiencies (Figure 2-5 A,C). Soil 4 showed a high level of humic substances (in both types of extract; Figure 2-6 A) and had the strongest inactivating effect on EW (Figure 2-5 B,D). Humic substances in soil extracts are formed by accumulation, aggregation and degradation of organic molecules (Lehmann and Kleber, 2015). The extraction methods used here do not claim full representation of all soil organic matter, but the comparison between the soil types indicates a higher organic content in soil 4 compared to the other soil types (see Discussion 2.4.3).

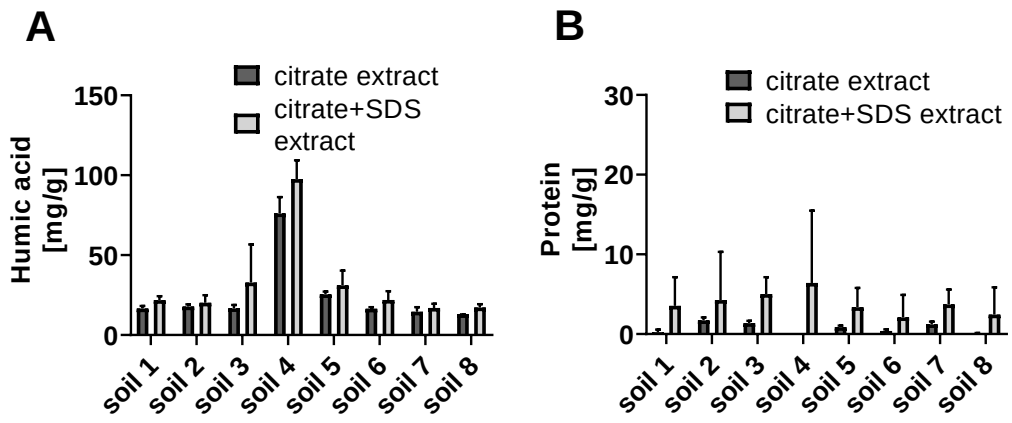

Figure 2-6: Determination of organic and protein content in soil extracts. Organic compounds from soil samples (characteristics listed in Table 2-2) were extracted with protocols using either citrate or citrate+SDS (see 2.2.8). With a modified Lowry assay, both the organic content, measured as humic acid (A), and the protein content (B) were measured (Redmile-Gordon et al., 2013). Values are means of 2 technical replicates ± SD. B) No protein was detected in at least one of the technical replicates for soils 1, 4 and 8 (with both extraction methods) and soil 2 (citrate + SDS extract).

A Pearson's correlation analysis revealed no significant correlation between any of the soil characteristics (textural properties, pH and organic content as given in Table 2-2 and Figure 2-6) and the effect on EW efficacy against *A. niger* spores (Figure 2-7). However, a moderate (non-significant) correlation between spore

survival and sand content or silt content was found, where spore survival increased with decreasing particle size (i.e., decreasing sand content/increasing silt content). In soil particle characterisation, sand represents large and silt smaller particles, see 2.1.3.1 (Martín et al., 2018). Fungal survival of the treatments (i.e., EW inactivation by soil) increased with decreasing particle size, i.e., with increasing total surface area of particles in the treatments. Furthermore, a moderate, non-significant positive correlation between LOI (measure of soil organic content) and the survival was found, consistent with the findings above regarding the high organic-content of soil 4.

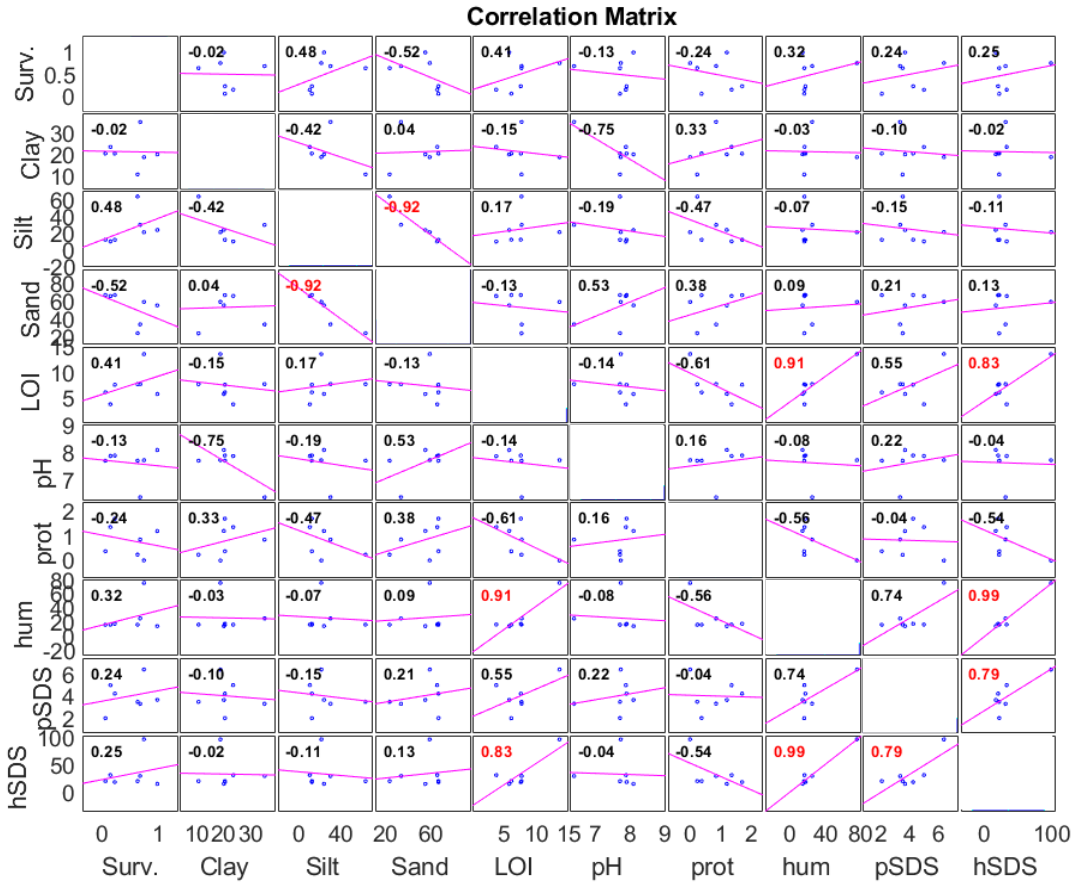

Figure 2-7: Correlation matrix for soil characteristics and EW inactivation by the soil. Data from Table 2-2, Figure 2-6 and Figure 2-7 (excluding soil 8). Numbers indicate Pearson's correlation coefficient and a red colour indicates significance ($p \leq 0.05$, two-tailed). Surv., survival rates of *A. niger* treated with 20% EW with 750 mg mL^{-1} added soil sample (1.0 = 100% survival). prot., protein content in citrate extracts of the soil samples. hum, organic content in citrate extracts. pSDS, protein content in citrate+SDS extracts. hSDS, organic content in citrate+SDS extracts. LOI: loss on ignition (measure of organic content). Correlation calculated and plotted in MATLAB® 2018a.

2.3.3 Influence of YEPD medium, a 'model' complex mix of organic substances

Because of the above indication of a relationship between soil organic load and EW inactivation, YEPD, a complex mix of organic substances, was selected for investigating the effects of different organic constituents of this fungal growth medium. Increasing additions of YEPD progressively inactivated the fungicidal activity of EW (20% EW [360–400 mg L^{-1} FAC], Figure 2-8 A; 1 min EW treatment in the control without added substances resulted in at least 2.5 log spore killing). YEPD consists of peptone (40% [w/w] of the YEPD dry weight), yeast extract (YE, 20% [w/w]) and glucose (40% [w/w]). Further testing showed that two of the individual components (peptone and YE) each had inactivating effects on EW, but glucose did not (Figure 2-8 B). Both peptone and YE contain high protein concentrations, determined as 98% and 52% [w/w], respectively (Table 2-3; these are estimates as non-protein substances can interfere with the Lowry reaction in complex mixtures, Everette et al. (2010)). The inactivating effect was then examined with purified proteins (Figure 2-9; 5 min EW treatment resulted in at least 3 log spore killing). Lysozyme and bovine serum albumin (BSA) inactivated EW at a concentration range similar to peptone and YE (0.5–1 mg mL^{-1}) but achieved a more complete inactivation (~100% inactivation at 1 mg mL^{-1} BSA or lysozyme). Lysozyme seemed to inactivate EW better than BSA. With peptone and YE, colony formation by surviving spores was delayed by up to 4–5 additional days compared to control growth without treatment, whereas with BSA or lysozyme, most colonies were small but visible after the usual 2 day growth period. Spore suspensions in this study were prepared in Tween 80 (final concentration in EW treatments is 0.01–0.1 mg mL^{-1} Tween 80) and it was confirmed that the presence of Tween did not interfere with EW efficacy (Figure 2-8 A,B). A different fungal growth medium, YNB, did not reduce the EW efficacy

(Figure 2-8 B), although it should be noted that the concentration of its constituents was lower compared to the YEPD components tested in the same experiment, but the YNB concentration was comparable to the concentrations tested in Figure 2-9, where YE, BSA and lysozyme reduced the EW efficacy.

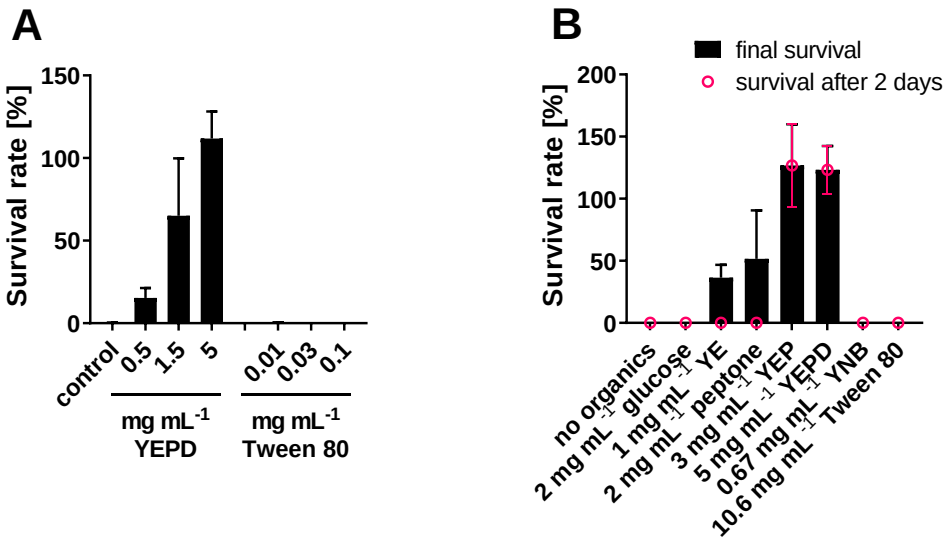

Figure 2-8: Inactivation of fungicidal EW activity by YEPD. Organic constituents were included at the indicated concentrations in EW preparations (20% EW, [v/v]) used to treat *A. niger* spores. A) YEPD [consisting of peptone (40% [w/w] of the dry weight), yeast extract (20%), glucose (40%)], B) YEPD components (YE, yeast extract; YEP, YE + peptone; YEPD, YEP + glucose), YNB (without added glucose), Tween 80. The organic components were added 5 min prior to use of the EW for short-exposure (A, 1 min; B, 7 min) treatments of spores. Survival rates were determined by colony counts on YEPD agar. Values shown are means from biological triplicates ± SD, except Tween additions in A: n = 2. B) Appearance of colonies was delayed after some treatments, as specified where % survival after up to a week (black) is greater than from counts at 2 days (pink; growth was at 28°C for the first 2 days and then at room temperature).

Table 2-3: Protein concentrations in YEP components.

	YEP[b]	**Peptone**	**YE**[c]
Protein concentration (w/w) [%][a]	82.3 ± 5.9	98.4 ± 23.0	52.0 ± 4.4

[a] Determined using the Pierce™ Modified Lowry Protein Assay (ThermoFisher). Data are means from technical triplicates ± SD.
[b] YEP comprised 66.7% peptone and 33.3% YE, reflecting the relative compositions of these components in YEPD medium.
[c] YE, yeast extract.

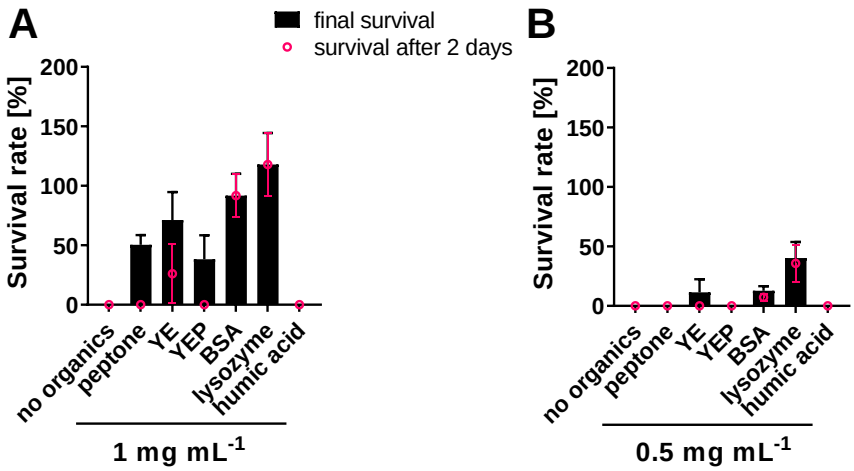

Figure 2-9: Inactivation of fungicidal EW activity by pure proteins, yeast extract and peptone. Organic constituents were included at the indicated concentrations (A, 1 mg mL^{-1}; B, 0.5 mg mL^{-1}) in EW preparations (20% EW, [v/v]) used to treat *A. niger* spores. YE, yeast extract; YEP, YE+peptone; BSA, bovine serum albumin. The organic components were added 5 min prior to use of the EW for 5 min treatments of spores. Survival rates were determined by colony counts on YEPD agar. Values shown are means from biological triplicates ± SD. Appearance of colonies was delayed after some treatments, as specified where % survival after up to a week (black) is greater than from counts at 2 days (pink; growth was at 28°C for the first 2 days and then at room temperature).

2.3.4 Influence of amino acids

2.3.4.1 Comparing the 20 main proteinogenic amino acids

To dissect protein constituents that may contribute to EW inactivation, the effects of the protein building blocks, amino acids, were tested. To compare their effects, the amino acid concentrations necessary to inactivate EW were determined at an EW concentration that, on its own, results in >3 log reduction of *A. niger* spores (20% EW [360–400 mg L^{-1} FAC]). All 20 tested amino acids supplied at between 5 to 7 mM at least partly inactivated fungicidal EW activity (Figure 2-10 A). The strongest inactivating effects on EW (i.e., at amino acid concentrations lower than 2.5 mM) were found for tryptophan (Trp), tyrosine (Tyr, for which 2.5 mM was the highest concentration attainable due to low Tyr solubility in water), cysteine (Cys) and methionine (Met). Certain other amino acids [arginine (Arg), histidine (His), asparagine (Asn)] also showed a mild elevation in EW inactivation compared to the remaining amino acids, evident at later time points (Figure 2-10 B).

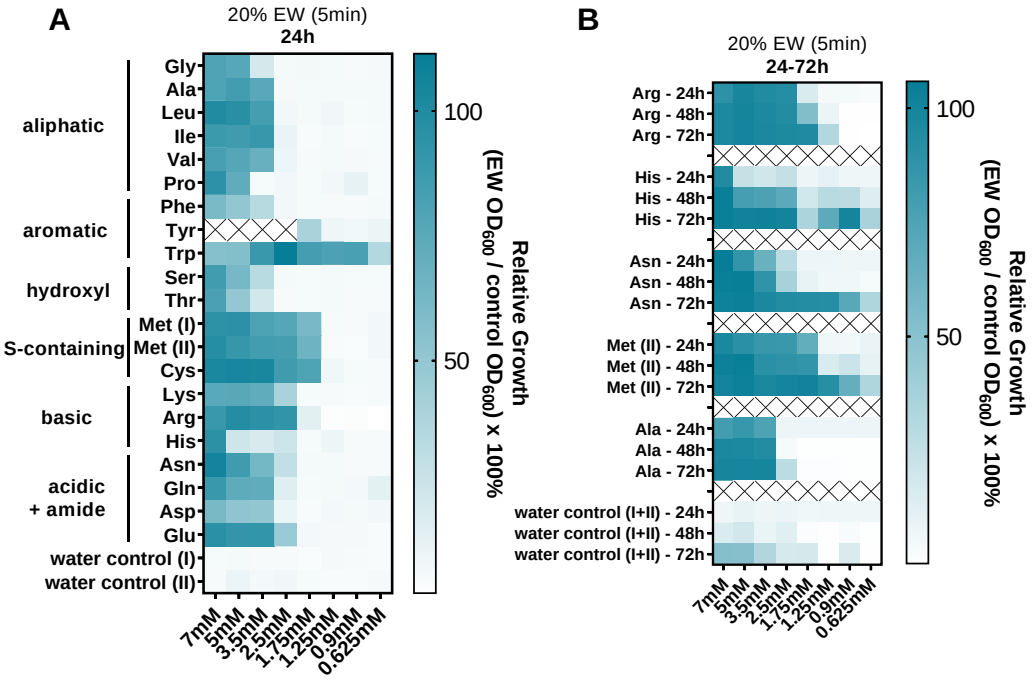

Figure 2-10: Inactivation of fungicidal EW activity by amino acids. Amino acids were included at the indicated concentrations in EW preparations (20% EW, [v/v]) 5 min prior to 5 min EW treatment of *A. niger* spores. Growth was determined in YEPD broth by OD_{600} readings and normalised to control growth without EW treatment. A) Readings after 24 h for all tested amino acids. B) Readings after 24 h, 48 h and 72 h for selected amino acids to highlight growth delays. Mean values are shown from 3 biological replicates (except lysine: n = 2). Within each replicate experiment, assays were split across two 96-well plates, both of which contained Met and a no-amino acid (water) control as internal controls, shown as (I) and (II). Tyrosine values ≥2.5 mM are missing due to limited water solubility. Numerical values and standard deviations are listed in Appendix B (6.2.1).

2.3.4.2 The effect of oxidised methionine

Because Met can be oxidised to methionine sulphoxide (MetO) and Met was among the amino acids that were the most reactive with EW (2.3.4.1), the inactivating effects of Met and MetO were compared. EW and also NaOCl were inactivated by lower concentrations of Met than MetO (Figure 2-11 A,B), consistent with a lower oxidant scavenging capacity of the oxidised form. Surprisingly, high concentrations of MetO (5–7 mM) in combination with EW treatment resulted in partial growth inhibition whereas intermediate MetO concentrations (2.5–3.5 mM) showed EW inactivation (better fungal growth), and such a difference between the effect of high and intermediate concentrations was not observed with (reduced)

Met. The growth inhibitory effect was even more pronounced when MetO concentrations between 21–42 mM were mixed with EW (one replicate; Figure 2-11 C; absolute OD_{600} values are shown here to demonstrate the absence of inhibition with MetO alone in the water control). When spores were diluted 1:10 in YEPD instead of 1:2 after treatments, the inhibition at high MetO concentrations disappeared, whereas without the dilution, an inhibition was visible even when the pre-mixed EW and MetO were inactivated by YEPD addition before addition to the *A. niger* spores (Figure 2-12 A,B). One explanation for the growth inhibition could be the potential formation of a toxic product in the medium upon oxidation of MetO by EW. This product may be less susceptible to inactivation by YEPD than the EW active chemical species, which would explain the growth inhibition that was observed when adding spores to the EW-MetO mix after the YEPD inactivation step.

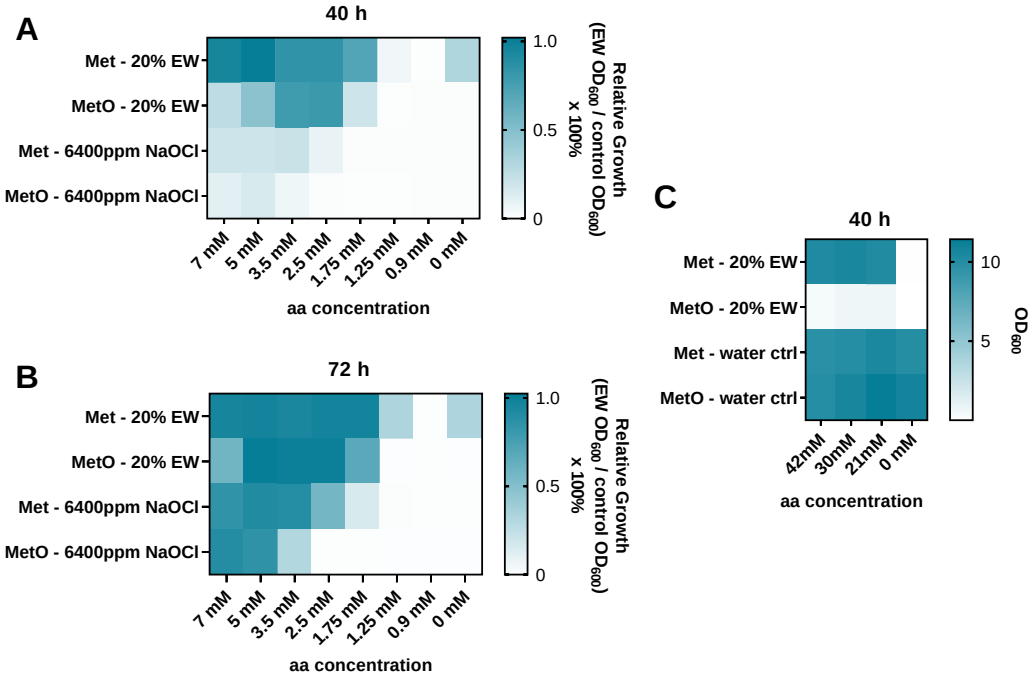

Figure 2-11: Inactivation of fungicidal EW activity by Met and MetO. Amino acids were included at the indicated concentrations in EW preparations (20% EW, [v/v]) or NaOCl dilutions (6400 mg L^{-1}, see comment at the end of this legend) 5 min prior to 5 min EW treatments of *A. niger* spores. Outgrowth of treated spores was determined in YEPD broth by OD_{600} readings after 40 h or 72 h. A,B) Two time points of the same experiments. Readings are normalised to control growth without EW treatment. C) Separate experiment with higher amino acid concentrations. Mean values are shown from 3 biological replicates (A,B) or data from 1 replicate (C). Numerical values and standard deviations for A and B are listed in Appendix B (6.2.2). MetO, methionine sulphoxide. ctrl, control (no EW). aa, amino acid. Regarding the NaOCl concentration, it should be noted that this concentration was calculated after diluting a purchased 5% NaOCl solution 1:7.8 but was not confirmed by FAC measurement. In other experiments, the measured FAC of dilutions of the purchased NaOCl solution was lower than the calculated FAC, therefore it is likely that the actual NaOCl concentration was lower than stated.

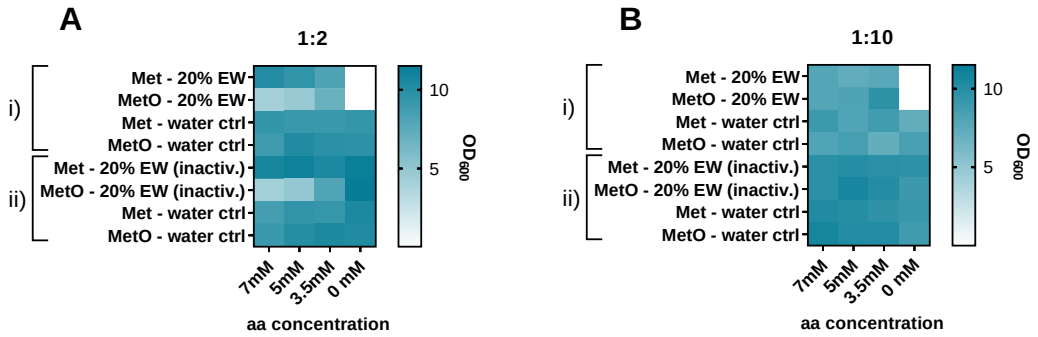

Figure 2-12: Investigating potential toxic product formation from MetO-EW-reactivity that may persist after YEPD inactivation of EW. i) Amino acids were included at the indicated concentrations in EW preparations (20% EW, [v/v]) 5 min prior to 5 min EW treatment of *A. niger* spores. ii) Amino acids and EW were incubated for 5 min, followed by YEPD addition to inactivate the EW, and subsequent treatment of *A. niger* spores with the inactivated EW (inactiv.), to assess whether fungal growth inhibition at high MetO levels (mixed with EW) occurs even when fungal spores are not exposed to active EW. In both cases, outgrowth of treated spores was determined in YEPD broth by OD_{600} readings after 40 h. A) Inactivating the EW with YEPD (either before or after the spore treatments) dilutes the treatments (and Met/MetO concentrations) by 1:2. B) Samples from the same experiments as in A were further diluted with YEPD before assessing the outgrowth in broth (final dilution 1:10), to determine whether dilution of a proposed toxic product would abolish the growth inhibition effect. Mean values are shown from biological duplicates. Numerical values and standard deviations are listed in Appendix B (6.2.2). MetO, methionine sulphoxide. aa, amino acid. ctrl, control (no EW); inactiv., EW inactivated prior to spore treatment by mixing with 2X YEPD.

2.3.5 Amino acids inactivate the oxidising properties of EW

2.3.5.1 Reactivity of Met and Cys with the FAC in EW

Methionine and other amino acids might be directly oxidised by EW, with simultaneous depletion of oxidising species in EW. The oxidising properties of EW were assayed with the oxidation-sensitive fluoroprobes HPF and APF. These probes enable the distinction between FAC ($^{-}$OCl/HOCl) and other ROS (mainly $^{\bullet}$OH and $ONOO^{-}$). While the reactivity of APF and HPF with other ROS is of a similar order (albeit up to 5x stronger with APF), APF reactivity with FAC is up to 600x stronger than HPF (Setsukinai et al., 2003). HPF fluoresces strongly only at ≥5-fold excess of FAC (Flemmig et al., 2012). To test selective detection of FAC with APF but not HPF, equimolar levels of probe and oxidant were used (5 µM probe; the FAC of EW [~1800 mg L^{-1}] would correspond to ~5.5 µM HOCl at 0.016% [v/v] EW [~0.3 mg L^{-1} FAC]). Only APF was fluorescent at these levels,

whereas EW concentrations ≥0.8% resulted in both APF and HPF fluorescence (Figure 2-13 A). A similar pattern was observed for diluted NaOCl (0.008% [0.24–0.25 mg L^{-1} FAC], 3.2–3.3 µM, Figure 2-13 D), indicating that the FAC might be (one of) the main oxidising agent(s) in the EW. The strong correlation between fluorescence signals in response to NaOCl and EW (Figure 2-14) further supports that the FAC in EW may be the main oxidising species.

The amino acids His, Ala, Arg, Asn, Trp, Met and Cys (chosen based on a stronger EW inactivation effect compared to other amino acids, see Figure 2-10, plus Ala as a negative control) were added to the EW and NaOCl oxidant solutions, to test effects on APF oxidation. At 1.2 µM added amino acid, only methionine and cysteine produced significant decreases in the APF-oxidising properties of either EW or NaOCl (Figure 2-13 B,E). Interestingly, this differed from the results obtained by the growth assay in Figure 2-10 where Trp inactivated EW more strongly than Met and Cys.

Because Met is expected to be oxidised and the work above indicated that reduced L-Met inactivated EW better than MetO (2.3.4.2), these molecules along with the D-isomer of Met were compared also for effects on APF oxidation by EW and NaOCl (Figure 2-13 C,F). L-Met and D-Met resulted in an equally strong reduction of the oxidising properties of both EW and NaOCl. MetO had a weaker effect on APF oxidation by EW and NaOCl, in keeping with a model in which oxidation of Met to MetO by EW or NaOCl reduces FAC species which are then no longer available for oxidation of APF.

Increasing concentrations of Met and Cys additions decreased the APF fluorescence signal, consistent with a concentration-dependant quenching of EW and NaOCl oxidising activity (Figure 2-15 A,B). The quenching effect of Cys was stronger than that of Met at all tested concentrations.

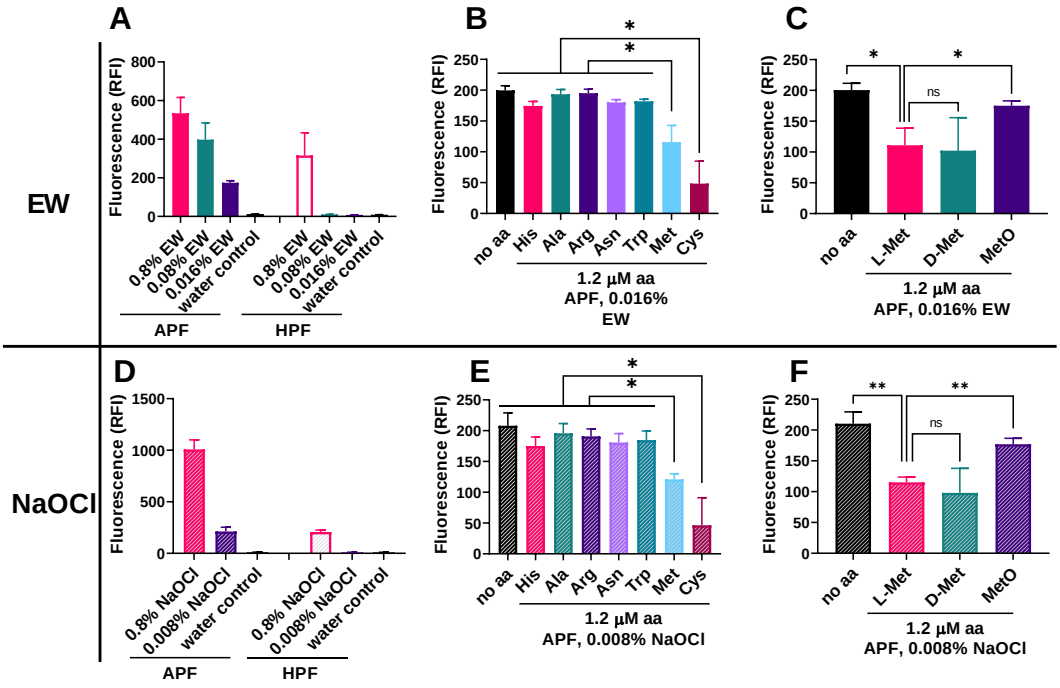

Figure 2-13: Influence of amino acids on the oxidising properties of EW and NaOCl. A,D) The fluorescent ROS probes APF and HPF (5 µM) were mixed with different dilutions of EW (A) or NaOCl (D) [100% (v/v) EW = 1800–2000 mg L^{-1} FAC; 100% NaOCl = 3000–3100 mg L^{-1} FAC]. Fluorescence (RFI, relative fluorescence intensity) was recorded within two minutes of mixing. B,C,E,F) The effect of amino acids (1.2 µM) supplemented in the APF-oxidant mix on the fluorescence signal was tested at approximately equimolar concentrations of dye (5 µM) and EW (0.016% EW; ~5.5–6.1 µM HOCl [FAC expected to be primarily HOCl]; B,C), or NaOCl (0.008% = 3.2–3.3 µM; E,F). Mean values ± SD are shown for at least 3 replicates. aa, amino acid. *p<0.05; **p<0.01; ns, not significant; according to paired *t*-test (two-tailed) with correction for multiple comparisons by controlling the false discovery rate at 5% FDR (Benjamini et al., 2006).

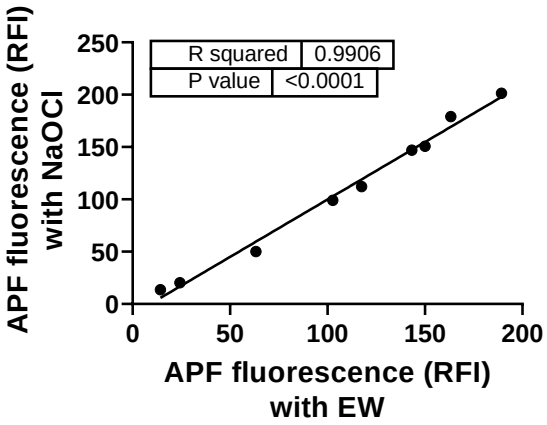

Figure 2-14: Correlation between NaOCl and EW induced APF fluorescence. Data from Figure 2-15. Fluorescence of APF mixed with NaOCl or EW and increasing concentrations of Met or Cys was recorded within two minutes of mixing and resulting values are plotted (RFI, relative fluorescence intensity). The linear regression, coefficient of correlation (R^2) and p-value of the regression are given.

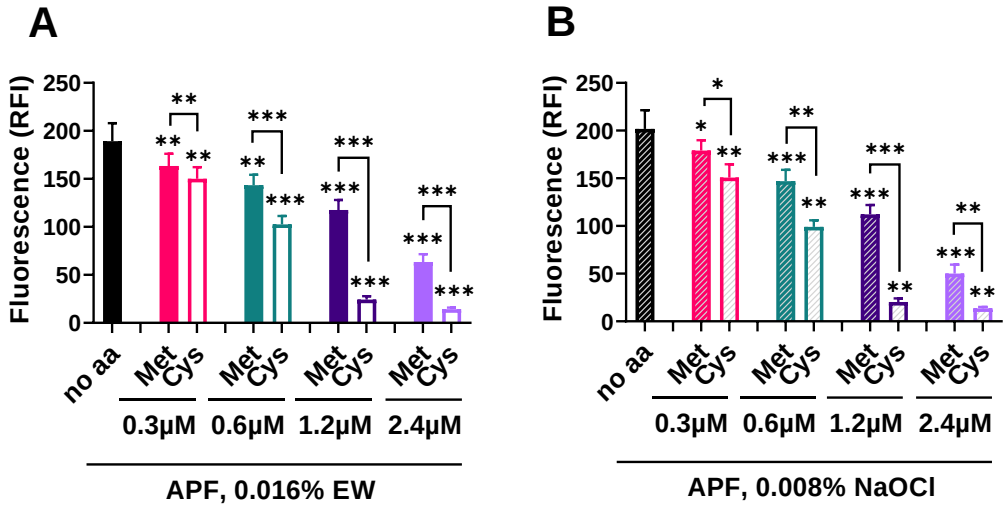

Figure 2-15: Influence of increasing Met and Cys concentrations on the oxidising properties of EW and NaOCl. The fluorescent ROS probe APF (5 µM) was mixed with Met or Cys and 0.016% EW (~5.5–6.1 µM HOCl) (A) or 0.008% NaOCl (3.2–3.3 µM) (B). Fluorescence (RFI, relative fluorescence intensity) was recorded within two minutes of mixing. Mean values ± SD are shown for at least 3 replicates. aa, amino acid. *p<0.05; **p<0.01; ***p<0.001; according to paired *t*-test (two-tailed) with correction for multiple comparisons by controlling the false discovery rate at 5% FDR (Benjamini et al., 2006). Comparisons are between amino acid addition and amino acid free control (no aa) unless specified by a connecting line.

2.3.5.2 Comparing effects of Met and Cys to other antioxidants

The strength of inactivation of the oxidising properties of EW and NaOCl by Met and Cys was compared to that of other common antioxidants. Cys and Cys-containing antioxidants (reduced glutathione, N-acetyl-cysteine) decreased the APF-oxidising properties of both oxidants the most (Figure 2-16). The effect of Met was in a similar range as dithiothreitol (DTT) and ascorbate.

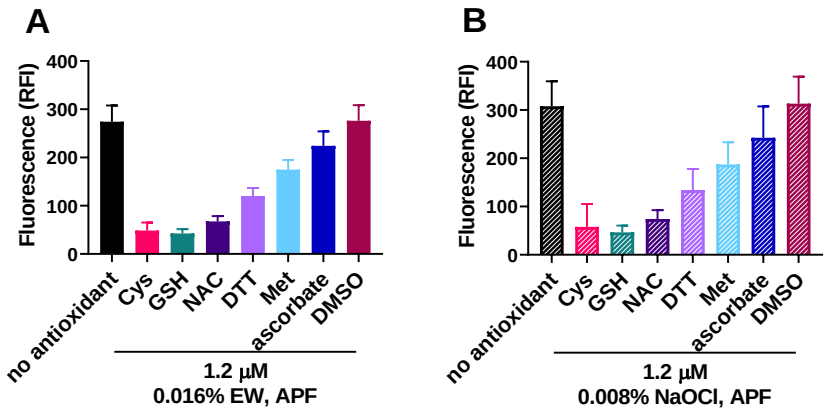

Figure 2-16: Reactivity of antioxidants with EW and NaOCl. The fluorescent ROS probe APF (5 µM) was mixed with antioxidants (1.2 µM) and 0.016% EW (~5.5–6.1 µM HOCl) (A) or 0.008% NaOCl (3.2–3.3 µM) (B). Fluorescence (RFI, relative fluorescence intensity) was recorded within two minutes of mixing. Mean values ± SD are shown for at least 3 replicates. GSH, reduced glutathione. NAC, N-acetyl-cysteine. DTT, dithiothreitol. Ascorbate, sodium L-ascorbate. DMSO, dimethyl sulphoxide.

2.3.5.3 Testing other dyes and oxidants

Other probes for reactive oxygen species were tested. The fluoroprobe DCF (2',7'–dichlorofluorescin diacetate) was much less sensitive in this assay than APF and HPF (above) whereas no fluorescence was detected with the dye DHE even at high EW concentrations (Figure 2-17 A). It was noted that with high EW concentrations, such as 80% (1440–1600 mg L^{-1} FAC; 27–30 mM HOCl), the fluorescence of DCF, APF and HPF decreased within minutes after the first reading (not shown), suggesting oxidative damage to the dyes. In contrast, the fluorescence signal in the experiments above where lower FAC was used (2.3.5.1, 0.016% EW and 0.008% NaOCl) was stable over a 1 h period. Additionally, high EW concentrations required the use of higher amino acid concentrations (1.5–6 mM) in order to see their effect, which in the case of some amino acids stabilised the fluorescence or even led to a slow fluorescence increase over a 1 h period in oxidant-free water controls (with all tested dyes, not shown). This suggested reactivities of the dyes with amino acids when the latter were supplied at high concentrations, likely to interfere with measurements of oxidation by EW or NaOCl (there was no evidence

for such artefacts at the low oxidant and amino acid concentrations used in the APF experiments above). Due to the high EW concentrations required for a DCF signal, this dye was not used to further investigate the reactivity of EW and amino acids. Similarly, NaOCl only resulted in DCF fluorescence at high oxidant concentrations (Figure 2-17 B) and fluorescence was lost within 10 min after the first measurement.

As a non-chlorine oxidant, H_2O_2 was tested. Only APF resulted in a fluorescence signal but it was of much lower intensity than the signals achieved with EW and NaOCl (Figure 2-17 C, with undiluted H_2O_2 [30%; 8.8 M]). APF fluorescence was stable or increased over time, ruling out oxidative damage to the dye as was seen with high EW concentrations. 6 mM Cys quenched the APF fluorescence whereas 6 mM Met did not (15 mM Met was tested in one additional replicate [not shown] and did not decrease the APF fluorescence). Due to the low signal intensity, no further tests were carried out with H_2O_2.

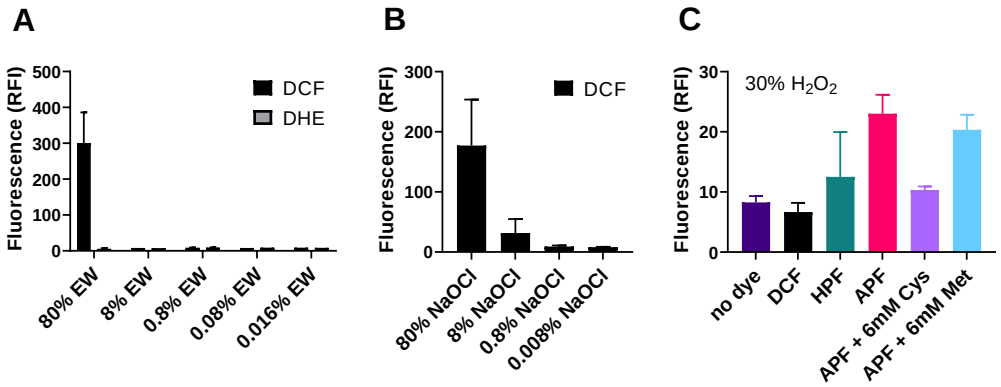

Figure 2-17: Reactivity of EW, NaOCl and H_2O_2 with ROS-/FAC-fluoroprobes. A) EW dilutions (100% [v/v] EW = 1.8–2.0 g L^{-1} FAC, 34–38 mM HOCl) were mixed with the fluorescent dyes DCF (5 µM) and DHE (pooled data from experiments with 5–3000 µM dye, no fluorescence recorded at any tested concentration in this range). B) NaOCl dilutions (100% [v/v] NaOCl = 3.0–3.1 g L^{-1} FAC, 40–42 mM) were mixed with DCF. C) 30% H_2O_2 (8.8 M) was mixed with the fluorescent dyes DCF, HPF, APF. Met and Cys were included as specified. Fluorescence (RFI, relative fluorescence intensity) was recorded within two minutes of mixing. Dye concentrations were 5 µM for DCF, APF and HPF and 5–3000 µM for DHE (no fluorescence was detected at any of these concentrations). Mean values ± SD are shown for at least 3 replicates, except for A: concentrations between 0.016% and 8% EW are 1–2 replicates.

2.3.5.4 Reactivity of Met and Cys with ozonated water

Ozonated water was applied as a different, non-chlorine oxidant, to help dissect effects that may be attributed to FAC versus ROS. In contrast to EW, ozonated water produced similar fluorescence responses with APF and HPF (Figure 2-18 A), consistent with the relative ROS selectivity of the probes (Setsukinai et al., 2003). No DCF or DHE fluorescence could be detected with ozonated water (not shown). Met and Cys could suppress the oxidising actions of ozonated water on APF and HPF (Figure 2-18 B,C; note Figure 2-19 for details about the choice of time points for HPF fluorescence readings). However, this suppression required higher concentrations of the amino acids (10 µM) than for EW inactivation (1.2 µM). At 10 µM amino acid, fluoroprobe oxidation by EW was nearly fully suppressed by Met and Cys and partially suppressed by Asn (Figure 2-18 D). These results may suggest a lower reactivity of the amino acids with ozonated water than with EW (Figure 2-13 vs. Figure 2-18), although it is also possible that the concentration of active species was higher in ozonated water than in EW (note however that the fluorescence intensity of APF mixed with ozonated water was lower than when APF was mixed with EW, suggesting less active species in ozonated water, although this could also be due to differences in the reactivity of the two oxidants with APF). The strong reactivity of both NaOCl and EW with Met and Cys suggests that FAC, as opposed to other potential ROS components of EW, is likely the main EW component reacting with these amino acids.

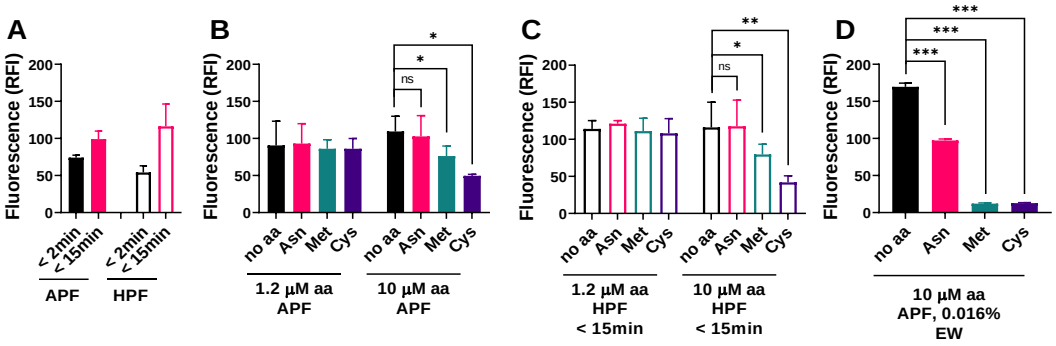

Figure 2-18: Influence of amino acids on the oxidising properties of ozonated water. The fluorescent ROS probes APF and HPF (5 µM) were mixed with ozonated water. Fluorescence (RFI, relative fluorescence intensity) was recorded within two minutes of mixing and again 13 min later. B,C) Effects of amino acids supplied at the specified concentrations in the APF-ozonated water mix (B) or HPF-ozonated water mix (C). Because HPF fluorescence strongly increased within the first few minutes, and no significant effect of the amino acids was visible at the first time point (<2 min), data for the 15 min time point are shown for HPF (cf. Figure 2-19). D) Effect of high amino acid concentrations (10 µM) supplied in an APF-EW mix (experimental details as described in Figure 2-13). Mean values ± SD are shown for at least 3 replicates. *p<0.05; **p<0.01; ***p<0.001; ns, not significant; according to paired *t*-test (two-tailed) with correction for multiple comparisons by controlling the false discovery rate at 5% FDR (Benjamini et al., 2006).

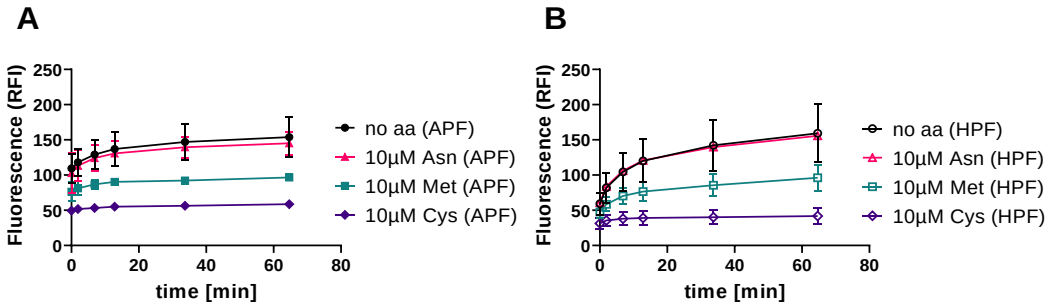

Figure 2-19: APF and HPF fluorescence with ozonated water over a 1 h period. Ozonated water was mixed with the fluorescent dyes APF (A) or HPF (B) and 10 µM amino acids, as specified. Fluorescence (RFI, relative fluorescence intensity) was recorded over a 1 h period. Selected time points are shown in Figure 2-18 B and C. Whereas APF fluorescence increased slightly in all samples over time (preserving relative relationships between the different treatments), differences between conditions became more pronounced over time with HPF. The forth of the plotted time points (t<15 min) was used to compare the conditions in Figure 2-18. Data are mean ± SD for at least 4 replicates.

2.3.6 Heat treatment

Different sanitising treatments are often applied in combination to increase the antimicrobial efficacy, and previous studies had indicated a beneficial effect of EW combined with heat treatment (Ovissipour et al., 2018, Han et al., 2018). The EW in this study was combined with subsequent heat treatment (Figure 2-20). Synergies for drug combinations are usually assessed by calculating the FIC (fractional inhibitory index) but this requires 2-fold concentration differences between tested dosages in a series. With heat treatment, this was not achievable as the thermal killing effect takes place over a small range of temperatures. Instead, here the EW concentration and heat treatment that resulted in the lowest detectable growth (when combined) were compared separately and in combination. In both biological replicates, the growth in the combination appeared to be lower than expected from (the product of the fractional growth obtained for) each treatment individually (repl1: combination of 2.16% EW [~40 mg L^{-1} FAC] and 60.1°C — relative growth 0.76 [effect of EW alone] x 0.48 [effect of heat treatment alone] = 0.36, versus 0.08 measured; repl2: combination of 4.54% EW [~95 mg L^{-1} FAC] and 60.1°C — 0.50 x 0.66 = 0.33 versus 0.04 measured; Figure 2-20). Therefore, the combination of EW and heat treatment may be beneficial in an application setting, although the presented data alone do not establish that the effect size is necessarily large enough to make this a commercially-viable strategy. It may be also beneficial to test heat treatment prior to or simultaneously with EW treatment.

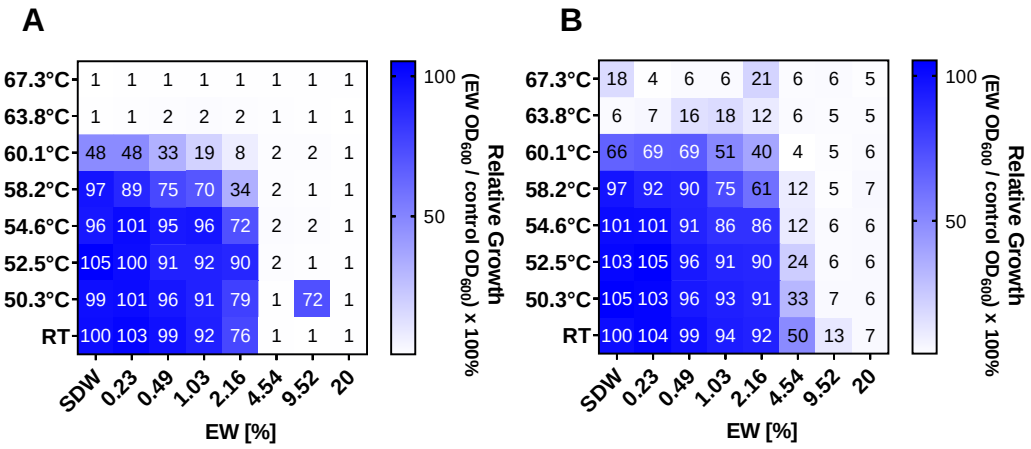

Figure 2-20: *A. niger* EW treatment followed by heat treatment. Spores of *A. niger* N402 were treated with EW (0.23–20% [v/v] in SDW, ~4–400 mg L^{-1} FAC, 5 min). Treatments were stopped by adding equal volumes of 2X YEPD and 150 µL aliquots were heat treated (50.3–67.3°C) for 1 min (Prime Thermal Cycler, Techne). Growth was determined in YEPD broth by OD_{600} readings after 48 h and normalised to control growth without EW treatment. Fields are labelled with the numerical value. Data from 1 biological replicate each in A and B. RT, room temperature.

2.4 Discussion

Sanitisers are widely used in many industrial and domestic settings. In the food industry, *A. niger* is a relevant spoilage fungi, and this study showed EW to be effective in killing *A. niger* spores of a laboratory strain and of *A. niger* isolates from contaminated onions. One key consideration of EW applications is the potential for incidental dampening of activity, e.g., by contaminating organic matter. This study used a top-down approach, starting from complex substances and narrowing down reactivity to specific organic molecules. The EW retained partial fungicidal activity with high levels of added soil, and soil with higher organic load gave stronger inactivation of EW. The fungal growth medium YEPD, a complex mix of organic substances, strongly inhibited EW activity, and this was linked to the protein-rich components of YEPD. Pure proteins and amino acids strongly inactivated EW, and specific amino acids were identified that were specifically reactive with EW, compared to the rest of the amino acids. Knowledge of such reactivities is important for estimating the outcome of potential EW applications where organic materials may be present.

2.4.1 EW efficacy

The EW used in this study resulted in (on average) 3–4 log killing of *A. niger* spores at FAC concentrations between 180–2000 mg L^{-1} (10–100%) (with 10^5 spores mL^{-1} in the treatment mix and 5 min treatment). Other studies found EW (55 or 80 mg L^{-1}, pH 2.8 or 6) to be effective against *A. niger* spores (5 or 1.2 x 10^5 spores mL^{-1} in the treatment mix) so that no growth was observed after 30 s or 5 min treatment, respectively (Buck et al., 2002, Gunaydin et al., 2014). In those studies, the growth assays after the treatment assessed % germination (assessed by microscopy) from 200 spores or colony formation from 120 spores and showed full inhibition. Due to the low number of assessed spores, a meaningful log reduction rate cannot be determined. The EW in this study at a

similar FAC (54–60 mg L^{-1}, 3% EW) achieved slightly less than 3 log killing (on average 2.9 log). In a recent study, EW (121 mg L^{-1} FAC, pH 2.8, 15 min) resulted in less than 2 log killing of *A. niger* spores (and less than 1 log for one tested strain) (Gonçalves Lemos et al., 2020). However, this study used a European Standard protocol for assessing disinfectants in which spores are suspended in a 1 g L^{-1} peptone solution with added milk powder. Both of these additives would be expected to strongly interfere with the EW efficiency, considering the results presented here for similar types of additions in EW treatments.

Generally, early germinating conidia (2 or 4 h germination in YEPD) were more sensitive to the EW in the present study than dormant conidia (treated within ~1 h after harvesting, in 0.1% Tween), consistent with the role of spores as stabilised cells that are formed in adverse conditions and that exhibit increased stress resistance (Dijksterhuis, 2017). In application settings, a mixture of germinating and un-germinated spores may be present (e.g., on onion surfaces). The results here indicate that the effectiveness of an EW treatment should be modelled based on the response of dormant spores in order to ensure killing of either stage. The sensitivity of later germination stages or mycelium was not tested here.

Different natural environments will select for fungal strains with different phenotypes and genotypes. Different fungal strains from the same species isolated from different locations can display different behaviour and stress tolerance depending on their site of isolation, and compared to common lab strains (Ashu et al., 2018, Kvitek et al., 2008). Environmental isolates obtained from contaminated onions showed ITS-sequence similarity with known *A. niger* strains and some of the isolates may be *A. niger* strains. However, these isolates showed similar EW sensitivity as the laboratory strain *A. niger* N402. This result supports the use of EW for effective control of *A. niger* spores present during industrial treatments, e.g., on contaminated onions. However, it should be kept in mind that

strains may behave differently depending on their environment (e.g., growing on artificial media vs. fruit/vegetable surfaces) which could affect their stress resistance.

2.4.2 Inactivation of EW by organic compounds

In the case of processing applications relevant to the food industry, sanitisation may be influenced by soil and complex organic mixtures derived from fresh produce or from processing and irrigation water. Prior removal of soil with water washing steps would increase the water consumption and require subsequent sanitisation of the wash water. It has previously been reported that different complex organic substances (peptone, glycine, milk, minced meat, chopped cabbage, and river natural organic matter) can react with the FAC in EW, depleting the FAC and forming combined chlorine with lower sanitising activity than FAC (Oomori et al., 2000, Ogunniyi et al., 2019). Combined chlorine compounds such as chloramines (from reaction of FAC with amines) can retain mild oxidising activity (Hawkins et al., 2003). Therefore, survival-based tests were used in this study instead of FAC analysis in order to assess the EW efficacy in the presence of organic substances.

Results of the present study indicated that fungicidal EW activity is not affected by the presence of intact fruits and vegetables. While this is promising for potential applications, the EW:fruit ratio in an industrial setting may differ from that tested here, and microorganisms attached to the fruit surface or in crevices may be more protected from EW than spores in suspension (spores were treated in suspension in the experiments here). Damage to the fruit surfaces would alter the pH (influencing the FAC-composition) and allow juices to interact with the EW. It is likely that these factors would increase the risk of inactivating the active species in EW during an industrial washing/sanitising process. Notably, electrolysed water

has been successfully applied to reduce the microbial contamination of freshly cut vegetable pieces, with the relative efficacy of treatment depending on the vegetable type (Izumi, 1999). In a different study, EW did not prevent mould spoilage around wounds on apples, but was effective at reducing cross-contamination between apples (Okull and Laborde, 2004). The risk of inactivation of EW activity will need to be determined with the specific produce or produce group in mind, and food properties such as antioxidant contents may help to predict the inactivation risk. However, in this study, the chosen focus was the reactivity of EW with soil, seeing as soil contamination is likely to be present in the washing process of many different types of fruits and vegetables, marking the relevance of further understanding the effects of such soil contamination.

2.4.3 Inactivation of EW by soil

Unexpectedly large additions of soil (30–750 mg mL^{-1}) were needed to decrease the fungicidal activity of EW in this study. Smaller amounts of soil had little or no effect. This result resonates with the high levels of NaOCl (6%) used to remove organic compounds from soil samples (Margenot et al., 2015) and indicates that EW can be used for sanitisation in the presence of moderate levels of soil, or even for the sanitisation of soil samples (Harvey et al., 2020). Reactive oxygen species can be scavenged in soil by plant-derived tannins and other phenolic compounds (Rimmer, 2006). The FAC, hydrogen peroxide or other ROS present in EW could be similarly inactivated after direct oxidation of soil organic compounds. On the other hand, potential reactions with inorganic metal species (hydroxyl radical formation involving H_2O_2 [Fenton chemistry] or HOCl [Fenton-type reaction]) could lead to reactivities with a broader range of aromatic and other organic compounds due to the high reactivity of hydroxyl radicals (Mikutta et al., 2005, Panasenko et al., 2013). Consistent with the proposed scavenging of reactive EW species (or secondarily derived hydroxyl radicals) by soil organic compounds, the

soil type with the highest organic content in this study (a sandy clay loam soil) had the strongest inactivating effect on EW. Its high organic content was supported both by analyses performed here, as well as a higher loss-on-ignition value (LOI, an indicator of soil organic matter) (Table 2-2).

Previously, the bactericidal activities of EW and NaOCl were reported to be inactivated to a similar extent by complex natural organic matter (Ogunniyi et al., 2019). Whereas NaOCl targets certain soil organic constituents (sterols, long-chained lipids, lignin dimers), other soil compounds (such as alkylaromatics, short-chain lipids, carbohydrates and peptides) are less reactive (Sleutel et al., 2009). The latter finding was explained by potential protective effects of the soil minerals and structure that may shield molecules such as peptides from NaOCl exposure. Interestingly, a moderate (but not significant) correlation between decreasing particle size and EW activity (spore inactivation) was apparent for the soil samples tested here [Pearson's correlation coefficient for spore survival versus silt (smaller) or sand (larger) particle content were 0.48 or -0.52, respectively]. This is consistent with less shielding of molecules by smaller particles. It is clear from the results that some fungicidal activity of EW persisted at moderate levels of soil contamination, although this could be coincident with the formation of by-products of concern, such as trihalomethanes from the reaction of soil organic compounds with the FAC (Jackman and Hughes, 2010).

It is important to note that soil particles form aggregates and microorganisms within these aggregates can be protected from some (but not all) external stressors (Harvey et al., 2020). Microorganisms within environmental soil samples may therefore be somewhat protected from EW killing, despite the proposed low inactivation of EW by soil additions. In the present experiments, *A. niger* spores were added to the EW-soil suspension externally, although it is still possible that mixing steps by vortexing and settling processes of soil components resulted in

partial enclosure of fungal spores in protected soil aggregations. Therefore, when loss of fungicidal EW activity was detected in experiments, this may not always be caused by chemical reactivity and inactivation of FAC (or other) species, but may also be caused by physical protection of the fungal spores by soil structures against the active EW.

2.4.4 Inactivation of EW by proteins and amino acids

2.4.4.1 Reactivity with complex organic substances and proteins

In the literature, partial or full inactivation of EW occurred over a wide concentration range for different organic substances (0.04–100 g L^{-1}): Tests on natural river organic matter showed full removal of the FAC of EW (5 mg L^{-1}) at about 0.04 g L^{-1} organic matter whereas the EW retained partial bactericidal activity at 0.04 g L^{-1} organic matter (Ogunniyi et al., 2019), potentially due to formation of bactericidal by-products from reactions between the EW and organic matter. In a different study, the FAC of EW (50 mg L^{-1}) was removed within 10 min by 100 g L^{-1} chopped cabbage, and more slowly (over 60 min) by 1 g L^{-1} minced meat or 5 g L^{-1} milk (Oomori et al., 2000). Dry manure on eggshells partially inactivated the bactericidal activity of EW with 10–30 mg L^{-1} FAC (Bing et al., 2019).

These varied results underscore the need to understand further EW reactivity with different chemical components of complex organic mixes. Inactivation of the FAC and the bactericidal activity of EW (31–50 mg L^{-1} FAC) has been reported with 0.1–1 g L^{-1} peptone (Oomori et al., 2000, Jo et al., 2018). Results in the present study indicated comparable reactivity of the EW (at 360–400 mg L^{-1} FAC) with ~1 g L^{-1} peptone, yeast extract or pure proteins, according to fungicidal activity. As proteins are highly abundant in all living organisms and in many foods or as surface-contaminants, these are important considerations for EW applications.

Purified lysozyme inactivated EW fungicidal activity slightly better than BSA, which may be due to the smaller size of lysozyme (higher surface area, more terminal amino groups per g protein) or differences in amino acid composition. If EW also reacts with cellular proteins (e.g., exposed membrane proteins), fungi that produce proteins with higher EW reactivity may inactivate EW more efficiently, thereby potentially preventing severe (intra-)cellular EW-induced damage and surviving treatment better.

It is well known that FAC readily reacts with proteins (Hawkins et al., 2003). In a study that investigated the inactivation of NaOCl by BSA, it was found that the sanitising potency of 300 mg L^{-1} FAC was inactivated by ~4 g L^{-1} BSA (higher BSA concentrations up to ~70 g L^{-1} were needed in some experiments) (Pappen et al., 2010). The higher BSA concentration required compared to the present study (1 g L^{-1} BSA) may be explained by a difference between the assays used: the cited study pre-mixed BSA and bacteria and added NaOCl (6 min incubation) whereas here, EW and BSA (or other protein samples) were pre-mixed and allowed to react for 5 min before proceeding to a 5 min treatment of the fungal spores, most likely leading to a more complete inactivation of the active EW species before the start of the treatment. Taken together, it is likely that the inactivation of EW by proteins and protein-rich mixtures is (at least partly) due to the reaction of the FAC in EW with the proteins.

In contrast to the effects of proteins, EW (360–400 mg L^{-1} FAC) retained its fungicidal activity when 2 g L^{-1} glucose was added. Consistent with these results, Oomori et al. (2000) found no decrease of the FAC of EW (50 mg L^{-1}) when adding glucose (0.1 g L^{-1}). In a different study, glucose addition (0.005–0.010 g L^{-1}) accelerated the decay of the FAC of EW (starting at 6–7 mg L^{-1}) over 120 h, with very little effect visible at the first time point at 2h (Duan et al., 2016). This raises an interesting point, as certain compounds that are less reactive (and/or reacting

more slowly) with EW than proteins may still affect its long-term activity. While this would be less relevant for the treatment of fruits and vegetables (which require short treatment times to reduce adverse effects on the quality), it may be more important if EW is stored for a few days and the water that is used to generate or dilute EW contains contaminants with such decay-accelerating effects.

2.4.4.2 Reactivity of the FAC with amino acids

The reactivity of amino acids, the components of proteins, with FAC ($HOCl/^{-}OCl$, at pH 7.4) is reported to decrease in the order: Cys > Met > cystine ≈ His ≈ α-amino group (in free amino acids) ≈ terminal amino group (in proteins) > Trp > Lys > Tyr ≈ Arg > backbone amides > Asn ≈ Gln (Pattison and Davies, 2001, Storkey et al., 2014). Here, amino acids with the strongest EW-inactivation effects were Cys, Met, His, Trp, Tyr, Arg and Asn, with Met and Cys found to suppress most strongly the oxidising properties of EW and NaOCl. The results were in close agreement with the above reactivity data for FAC, suggesting that the FAC component of EW could at least partly account for EW reactivity with (and inactivation by) proteins and amino acids. The pH of the amino acid solutions may influence the chemical reactivities, for instance Cys is less prone to oxidation at low pH than at high pH (Levine et al., 2000), and the reactivity of FAC depends on the pH, as HOCl is typically more reactive than ^{-}OCl (Hu et al., 2017). However, the pHs of the different amino acid stock solutions (which were between pH 3.2 and 10.9 for the different solutions) were not correlated with their effect on EW activity (Appendix C, 6.3). Interestingly, the results obtained for effects of amino acids on EW activity as assessed by spore survival (2.3.4.1) differed somewhat from effects of amino acids on the oxidative properties of EW determined *in-vitro* (2.3.5.1). Namely, Trp seemed to inactivate EW more strongly (allowing survival at lower levels of added amino acid) than Met and Cys, whereas the latter were the most reactive with EW in the *in-vitro* assays. It is possible that the oxidation of Met and Cys yields toxic by-products that inhibit spore survival, as was

hypothesised for MetO oxidation (2.3.4.2). For instance, FAC-mediated oxidation of free cystine (the oxidation product of 2 x Cys) yields the chloramine N,N-dichlorocystine which retains oxidative activity (Nagy and Ashby, 2005), although the oxidative activity of this product may not be strong enough to react with the fluorescent dye in the *in-vitro* assay. A lower oxidative activity of the product compared to FAC would be expected because the oxidised product [i.e., the chloramine] in a redox reaction will have a lower oxidising potential than the oxidising substrate [i.e., the FAC] (otherwise the redox reaction would not occur in this direction). For several chloramines, reaction rates with reducing agents that are ~10^5 x lower than the reaction rates of HOCl with the same reducing agents have been reported (Peskin and Winterbourn, 2001), indicating a large difference between the oxidising potential of FAC and chloramines.

These considerations could mean that in the presence of low amino acid levels, Cys reacts with EW to form cystine, and remaining reactive EW species further oxidise cystine to form the chloramine (or other possible oxidation products). This would reduce the fluorescence signal in the *in-vitro* assay due to the assumed lower oxidising activity of the product (consistent with the observed low fluorescence at low additions of Cys in this assay), whereas in the survival assay the presence of the chloramine (or other possible toxic products) could inhibit the fungal growth. At higher levels of Cys addition, the active species in EW can be fully consumed by the reaction of Cys with EW, so that no (or less) secondary reactions take place and no (or only low levels of the) chloramine is formed, consistent with fungal survival at higher Cys additions. This again highlights the importance of survival-based assays, because Cys levels higher than suggested by *in-vitro* assays may be tolerated during a sanitising treatment without losing the fungicidal effect of EW. But the formation of by-products and their toxicity should be considered, especially when treating food surfaces or drinking water.

Among the other tested antioxidants, reduced glutathione inactivated EW and NaOCl to a similar extent as Cys, and this is consistent with reported reactivity rates for both compounds with FAC (Peskin and Winterbourn, 2001, Storkey et al., 2014). Lower reactivities were reported for NAC, in a similar order of magnitude to the reactivity of Met with FAC (Storkey et al., 2014), whereas the present results indicate that NAC had higher EW-reactivity than Met. For DTT and ascorbate, the reactivity with FAC is lower compared to glutathione (at neutral pH) (Peskin and Winterbourn, 2001, Folkes et al., 1995), and this is consistent with the results here. Overall, both Met and especially Cys inactivated EW and NaOCl to a similar extent as the common antioxidants that were tested in this study, indicating the potential importance of these amino acids for influencing the FAC of such sanitisers.

2.4.4.3 Reactivity of non-chlorine ROS with amino acids

Non-chlorine products of electrolysis were tested here by using ozonated water. Amino acid reactivity of ozone is reported to decrease in the order Cys > Trp ≈ Met > Phe ≈ His (Sharma and Graham, 2010). The rate constants for Cys and Met reactivity with ozone are of the order 10^6 M^{-1} s^{-1} (pH 8) whereas reactivities of Met and Cys with FAC are of the order 10^7–10^8 M^{-1} s^{-1} (pH 7.4) (Storkey et al., 2014). This supports the present data, which indicate that Met and Cys have greater inactivating effects on NaOCl and EW than on ozonated water, consistent with a primary role for the FAC in the reactivity of EW with these amino acids.

Several amino acids are known to be especially prone to oxidation, such as Pro, Arg, Lys, Thr, Trp, Phe, Tyr, Cys and Met (Baraibar et al., 2013). However, the data presented here on EW reactivity and amino acids matches better the specific reactivities of FAC (little particular effect with Pro, Lys, Thr or Phe was observed here). While non-chlorine ROS may contribute to the antimicrobial effect of EW, a major role is less likely in stored EW solutions (as used here) due to the short life

time of these ROS (Jeong et al., 2007). Within cells, FAC species may also lead to formation and conversion of other ROS species which arise as respiratory by-products: HOCl reacts with superoxide radicals and with iron to form hydroxyl radicals, and with hydrogen peroxide to form singlet oxygen (Panasenko et al., 2013). Hydroxyl radicals are highly reactive and can oxidise most cellular molecules, including all proteinogenic amino acids (rate constants $>10^7$ M^{-1} s^{-1}), the most reactive of which include Met and Cys ($>10^9$ M^{-1} s^{-1}) (Xu and Chance, 2005).

To further model the formation of both FAC and chlorine-free ROS during the electrolysis process, the fungicidal activity of a mixture of NaOCl and H_2O_2 was tested (Appendix D, 6.4). However, adding H_2O_2 resulted in spore survival at NaOCl concentrations that, applied alone, were effective at killing *A. niger* spores. Hypochlorite compounds can oxidise H_2O_2 to O_2 (initially forming highly reactive, unstable singlet oxygen $^1O_2$), while being reduced to Cl^- in the process (Held et al., 1978). This reduction of the active FAC would explain the loss of killing observed upon H_2O_2 addition to NaOCl. Interestingly, a different study has shown a synergistic effect of NaOCl and H_2O_2 against bacteria (Lontsi Djimeli et al., 2014). This different outcome may be related to differences in the experimental design including the applied concentrations, which were not specified in the cited study, but may have been lower to achieve a bactericidal effect compared to the spore treatment here. A different study supported a synergistic fungicidal effect of NaOCl and H_2O_2 but used sequential treatment, possibly to avoid the chemical reactivity of the two compounds (Cerioni et al., 2009). Other approaches of mixing oxidants to mimic EW (e.g., including O_3 and ClO_2) have been reported (Bradford, 2011). In the present study, it was decided that the approach of comparing EW, NaOCl and ozonated water was more feasible and at the same time avoided the problem of chemical reactivity within oxidant mixtures, so providing for a clearer interpretation of the data.

2.4.5 Conclusions

The electrolysed water used in this study shows good sanitisation efficiency against *A. niger* spores (>3 log). A >4 log reduction was reached in several experiments (with 10–100% EW), which is the requirement of the European disinfection standard for fungi in suspension (Sandle, 2017). The EW was effective against environmental food spoilage isolates identified as *A. niger*. However, the efficiency is highly dependent on the chemical matrix of a treatment. The presence of relatively high levels of soil still allow partial killing. Adverse effects of soil in EW treatments will depend on whether very high levels of soil are reached, and high organic content in the soil will decrease the EW activity more strongly. Conversely, the presence of proteins or amino acids (especially Cys, Met, Trp, Tyr), even at low levels (~1–5 mM for EW at ~360–400 mg L^{-1} FAC), during EW treatments should be expected to strongly reduce the killing efficiency. The reactivity of amino acids with FAC specifically has been studied extensively, and this study indicates similar reactivities for EW. These findings increase the understanding of inactivation of EW by proteins or protein-rich mixtures. Proteins are highly abundant in all living organisms and many foods, such as meat, dairy, soy, potatoes (Slavin and Lloyd, 2012, Hoffman and Falvo, 2004), so assessment of protein levels is highly relevant for using EW in the food industry. It is also relevant for regions of the world that lack access to clean drinking water, where water treated with or coming into contact with EW may contain such constituents as the ones tested here. An additional risk of the reactivity between EW and organic compounds is the formation of toxic by-products such as trihalomethanes or chloramines which have been reported both for conventional FAC treatment and EW. Depending on the application, the reactivity of EW with relevant organic substances should be determined, ideally using studies such as the present one to predict reactivities followed by testing the reactivity in the specific (industrial) treatment setting. Based on these reactivities, the accumulation of potential by-products then needs to be monitored.

3 EW in a yeast model: cellular targets and mode of action of EW

3.1 Introduction

3.1.1 Oxidative stress in cellular systems

When organisms grow aerobically, so-called reactive oxygen species (ROS) such as the superoxide anion radical ($O_2^{\bullet -}$) and hydrogen peroxide (H_2O_2) can be formed when oxygen undergoes incomplete (monoelectron) reduction at the respiratory chain complexes (Larosa and Remacle, 2018). Other ROS species are singlet oxygen ($^1O_2$) and hydroxyl radicals ($^{\bullet}OH$) (Breitenbach et al., 2015). Reactions occur between the different ROS types, often producing more ROS (Aguirre et al., 2006, Fedorova et al., 2014). The free chlorine species hypochlorous acid can undergo reactions that yield ROS (Panasenko et al., 2013). EW treatment has been shown to result in ROS accumulation in fungal cells (Mokudai et al., 2015). ROS can oxidise most cellular molecules, causing damage to DNA, RNA, proteins, lipids, polysaccharides and small metabolites (Breitenbach et al., 2015). Oxidative reactions include the oxidation of amino acid residues such as Lys, Arg, Pro, Thr, Met, Cys and Tyr, some of them resulting in carbonyl formation (see 2.1.3.2), as well as oxidation of low-density lipoprotein or poly-unsaturated fatty acids, and oxidative modification of DNA bases which can lead to mutagenesis events (Liguori et al., 2018). However, in addition to damage caused by ROS, the formation of ROS can also serve important cellular functions, such as signalling and immune response (Foyer and Noctor, 2005, Lau et al., 2008, Spooner and Yilmaz, 2011).

3.1.2 Cellular defences against oxidative stress

Oxidative stress occurs when ROS accumulate inside cells and cannot be scavenged sufficiently by the different defence mechanisms. This is often caused by external factors such as ionizing radiation, ROS inducing chemicals, hydrogen peroxide, ozone, hypochlorous acid, heavy metals or heat stress (Angelova et al., 2005, Abrashev et al., 2008, Dukan and Touati, 1996, Sies et al., 2017). Cells use a range of mechanisms to prevent, detoxify or repair ROS and oxidative damage. Preventative measures include packaging DNA in more ROS-resistant chromatin structures containing proteins or the accumulation of ROS-scavenging pigments (Sies et al., 2017). ROS-scavenging mechanisms are widely conserved and include enzymatic defence mechanisms such as superoxide dismutases, catalases, peroxidases (Angelova et al., 2005, Zadrąg-Tęcza et al., 2018) and non-enzymatic ROS buffering systems such as glutathione, α-tocopherol, ascorbic acid, pyruvate, methionine, cysteine or mannitol (Piedrafita et al., 2015, Ruijter et al., 2003). Generally, filamentous fungi have a greater variety of ROS defence mechanisms than unicellular fungi due to a larger number of antioxidant enzymes and the production of antioxidant secondary metabolites (Aguirre et al., 2006). In addition to systems that target ROS directly, other ROS defence mechanisms repair damage caused by ROS (Boiteux et al., 2017, Avery and Avery, 2001, Delaye et al., 2007).

3.1.3 Role of methionine in oxidative stress conditions

3.1.3.1 Methionine sulphoxide reductase (MSR) system

Whereas carbonylation of different amino acid residues during oxidative stress is irreversible, one major repair mechanism for oxidised proteins focuses on oxidised methionine residues (Sideri et al., 2009). Several oxidants such as hypochlorous acid readily oxidise free and protein-bound Met at the sulph-hydryl group, yielding methionine sulphoxide (MetO) (Storkey et al., 2014, Khor et al., 2004b). MetO

can be reduced to Met by the highly conserved methionine sulphoxide reductases, abbreviated as MSR or MXR enzymes (Figure 3-1) (Brot et al., 1981, Grimaud et al., 2001, Delaye et al., 2007). MetO has a chirality centre at the sulphur atom and MsrA (Mxr1) reduces the (*S*)-stereoisomer, whereas MsrB (Mxr2) reduces the (*R*)-stereoisomer (Kryukov et al., 2002). In yeast, MsrA can reduce free and protein-bound (*S*)-MetO, whereas MsrB reduces protein-bound (*R*)-MetO and the free (*R*)-MetO molecule is reduced by an additional fRMsr enzyme (Le et al., 2009). Other enzymes with MetO reducing capabilities have been reported in bacteria (MetP, DMSO reductases) (Tarrago et al., 2020). Previously, it was believed that yeast MsrA is localised in the cytoplasm and MsrB in the mitochondria, but a recent study challenges this compartmentalisation, showing that MsrB can also be found in the cytoplasm and suggesting yet unknown regulatory mechanisms regarding the localisation (Nicklow and Sevier, 2020). In proteins, surface exposed methionine residues are believed to help scavenge ROS, preserving the protein's functionality by protecting other residues from damage (Levine et al., 1996). However, Met residues can also be a liability during oxidative stress: certain Met residues in the *Aspergillus niger* glucose oxidase were experimentally substituted with other amino acids, and this variant showed increased stability in oxidative conditions (Kovačević et al., 2019). In addition to a ROS scavenging function, the reversible oxidation of methionine can regulate and modulate protein function (Drazic et al., 2013, Wang and Pan, 2016, Nicklow and Sevier, 2020).

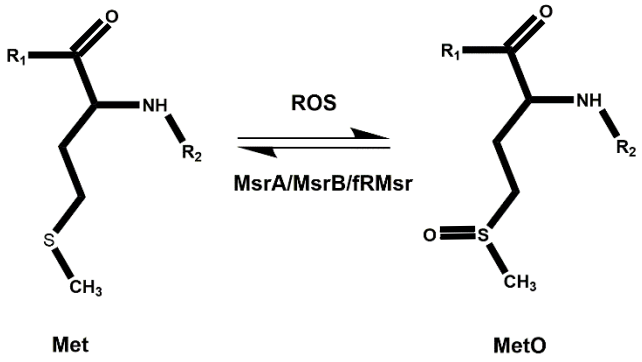

Figure 3-1: Oxidation and reduction of methionine in yeast. Methionine (Met) can be oxidised to methionine sulphoxide (MetO) by various pro-oxidant agents. MSR enzymes revert MetO back to Met. R_1: hydroxyl group for free Met, C-terminal protein backbone for protein-bound Met. R_2: hydrogen for free Met, N-terminal protein backbone for protein bound Met. Structure drawn in ChemDraw® Professional.

3.1.3.2 Methionine biosynthesis and uptake

Methionine-prototrophic strains of *S. cerevisiae* can synthesise Met starting from exogenous sulphate which, after uptake and multi-step reduction to sulphide, is incorporated into homocysteine (catalysed by Met15), followed by conversion to Met (Figure 3-2) (Ljungdahl and Daignan-Fornier, 2012). Met conversion to SAM (a universal methyl group donor) is carried out by two enzymes and methylation reactions involving SAM yield S-adenosyl-homocysteine which can be converted back to homocysteine, completing a Met cycling mechanism (Loenen, 2006). In the *S. cerevisiae* BY4741 strain used in this study, the *MET15* (also called *MET17* or *MET25*) gene is disrupted, making the strain Met auxotrophic due to the lack of homocysteine synthesis.

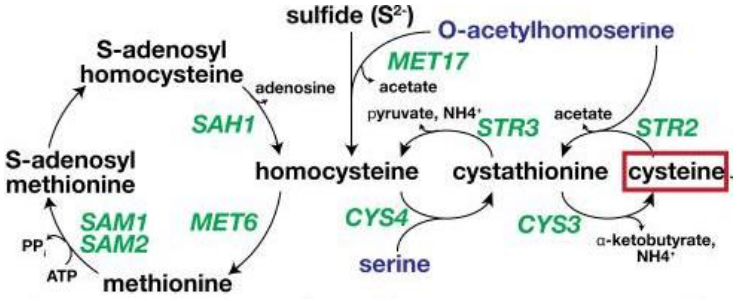

Figure 3-2: Methionine biosynthesis and cycling. Modified from Ljungdahl and Daignan-Fornier (2012).

Regulation of the Met biosynthesis (and uptake) genes (the *MET* regulon) is carried out by the transcription factor Met4, together with the DNA-binding proteins Cbf1 and Met31/Met32 and the cofactor Met28: Met4-dependent genes are downregulated in the presence of high Met levels (Sadhu et al., 2014, McIsaac et al., 2012). This sensing relies on intracellular Cys (another downstream product of homocysteine) and potentially SAM (Sadhu et al., 2014, Hansen and Johannesen, 2000). In *S. cerevisiae*, two methionine-specific transporters take up exogeneous Met, called Mup1 (high affinity transporter) and Mup3 (low affinity) (Gits and Grenson, 1967, Isnard et al., 1996). Five additional broad-specificity transporters contribute to the Met uptake: Agp3, Agp1, Bap2, Bap3 and Gnp1. Upon switching yeast to high Met medium, Mup1, Mup3 and Agp3 are down-regulated (by Met4-dependent transcriptional regulation combined with ubiquitylation of the transporter proteins), whereas Agp1, Bap2, Bap3 and Gnp1 are upregulated by the amino acid sensing system SPS (Menant et al., 2006).

3.1.4 FeS cluster proteins

3.1.4.1 Roles of FeS clusters in cellular function

A group of proteins that is generally highly sensitive to oxidative stress are proteins with iron sulphur (FeS) cofactors. FeS clusters consist of iron atoms (Fe^{2+} or Fe^{3+}) connected by sulphides (S^{2-}). The most common cluster formations are [2Fe-2S], [3Fe-4S] and [4Fe-4S] (Imlay, 2006). The presence of FeS cofactors is highly conserved and required for diverse protein functions, some of them essential for viability (Alhebshi et al., 2012). They are important for processes including redox enzyme activity and electron transfer (e.g., in mitochondrial respiration), iron homeostasis, DNA maintenance, replication and repair, translation and ribosome metabolism (Imlay, 2006, Lill and Freibert, 2020). FeS cluster protein synthesis is highly conserved in eukaryotes and relies on two

processes: the mitochondrial iron-sulphur cluster (ISC) assembly and the cytosolic iron-sulphur protein assembly (CIA) (Braymer and Lill, 2017).

Examples of FeS cluster proteins (and the ones analysed in the present study) are aconitase (encoded by *aco1* and *aco2* in yeast), Rli1 and Yah1. The essential [2Fe-2S] ferredoxin Yah1 is involved in the ISC, but it also functions in other pathways such as the biosynthesis of coenzyme Q (Pierrel et al., 2010). Rli1 is an essential, highly conserved [4Fe-4S] protein involved in critical cellular functions such as translation initiation, ribosome export from the nucleus during biogenesis and ribosome recycling (Schuller and Green, 2017, Kispal et al., 2005). Aconitase, a [4Fe-4S] enzyme, is part of the citric acid cycle where it catalyses the conversion of citrate, via *cis*-aconitate, to isocitrate by a dehydration/hydration reaction (Beinert et al., 1996). Other aconitase functions include a role in lysine biosynthesis (Aco2 in yeast), in the methylcitrate cycle, and, after FeS cluster disassembly in iron depletion conditions, conversion of aconitase into a regulatory iron-responsive element-binding protein (Fazius et al., 2012, Brock et al., 2002, Narahari et al., 2000).

3.1.4.2 Sensitivity of FeS clusters to oxidative stress

FeS clusters in proteins can be oxidised by ROS which can result in the release of Fe from the cluster (Imlay, 2006). This renders certain FeS cluster proteins sensitive to oxidation, with two main consequences: (i) loss of function of FeS proteins; (ii) release of iron from FeS clusters can contribute to the Fenton reaction yielding hydroxyl radicals, resulting in additional ROS damage (Avery, 2011). In line with this increase in ROS, overexpression of the FeS protein Yah1 has been shown to increase pro-oxidant sensitivity of cells, potentially related to increased Fe release upon oxidative damage (Vallières et al., 2017). Examples of oxidative damage to FeS cluster proteins are the oxidation sensitivity of aconitase,

isopropylmalate isomerase, 6-phospho-gluconate dehydratase and homoaconitase (Jang and Imlay, 2007, Lalève et al., 2016, Wallace et al., 2004).

An interesting link between methionine oxidation and FeS cluster damage has been reported (Sideri et al., 2009). Accumulation of MetO in yeast (due to deletion of the *MSR* genes) resulted in increased FeS cluster damage, suggesting that MSR proteins may exhibit an indirect protective function of FeS clusters. In addition, overexpression of the FeS protein Rli1 rescued a ROS sensitive phenotype of an *msrΔ* deletion strain (Alhebshi et al., 2012). Further connections between Met and iron metabolism have been found in the present study and reported previously and are addressed in the discussion (3.4.7).

3.1.5 Aims

Results from the previous chapter suggested that EW is highly reactive with amino acids, and among all tested amino acids, Met was one of the more reactive amino acids. As discussed, this result matches the known reactivity of FAC, suggesting also an important role of FAC in the EW mode of action. Furthermore, EW is known to have oxidising properties and to induce ROS accumulation. However, exact targets of EW and response mechanisms in fungi are not known (see 1.9) and were therefore addressed in this chapter. Because amino acids are abundant in cells, it was hypothesised that EW may react with intracellular amino acids, including with Met. This hypothesis was tested in the yeast model organism *S. cerevisiae* because it readily takes up amino acids from its growth medium and the uptake mechanisms are well researched, with genetic tools and auxotrophic strains available as convenient research tools. Based on the observed reactivity of amino acids with EW, the effect of providing increased levels of amino acids to the yeast cells were tested here. Methionine pre-culture was found to provide protection against EW, and this effect was further studied to determine whether

the protective effect was associated with the Met molecule itself, Met metabolism products or Met misincorporation into proteins. Moreover, it was tested whether EW treatment may lead to FeS cluster protein damage. These proteins are known to be oxidation sensitive and damage to FeS cluster proteins has also previously been observed in conditions of increased Met oxidation (Sideri et al., 2009). The study was carried out to provide new knowledge on the fungicidal mode of EW action that could help to rationally improve the generation and application of EW, while also adding to the understanding of the yeast response to oxidative stress.

3.2 Materials and methods

3.2.1 Fungal strains and growth conditions

The study used the yeast strains *Saccharomyces cerevisiae* BY4741 (*MAT*a; *his3-1*; *leu2-0*; *met15-0*; *ura3-0*), BY4742 (*MAT*α; *his3-1*; *leu2-0*; *lys2-0; ura3-0*), BY4743 (*MAT*a/α; his3-1/his3-1, leu2-0/leu2-0; met15-0/MET15; LYS2/lys2-0; ura3-0/ura3-0) and deletion mutants isogenic with the BY4741 parent: *trp1Δ*, *alt1Δ*, *arg4Δ, his3Δ* (from Euroscarf, Germany). The *MSRA* and *MSRB* genes were overexpressed under the control of their native promoters in multicopy plasmids YEp351 and YEp352, respectively (2-micron replication system, expected copy number ~10–40 (Romanos et al., 1992, Wai et al., 2000)), as described previously (Sumner et al., 2005). Overexpression of FeS proteins under the control of the *tetO* promoter (with cultivation in the absence of doxycycline to derepress the promoter) was with the previously constructed plasmids pCM190-RLI1-HA (Alhebshi et al., 2012) and pCM190-YAH1-HA (Vallières et al., 2017). Strains expressing a fusion protein of mCherry and yeast enhanced GFP from the yEpRG-CGA plasmid (TDH3 GAP promoter, Appendix E, 6.5) (Altamura et al., 2016) and mutagenised versions were generated in the BY4741 background in this study as described below (3.2.2). Yeast strains were cultured at 30°C in either YEPD broth (see 2.2.1) or, where specified, YNB broth (0.69% yeast-nitrogen base without amino acids (Formedium, Norfolk, UK), 2% [w/v] D-glucose). Amino acids or uracil (Ura) were added to YNB as needed for strain auxotrophies or plasmid selection (20 mg L^{-1} histidine, 100 mg L^{-1} leucine, 30 mg L^{-1} lysine, 20 mg L^{-1} methionine, 20 mg L^{-1} uracil). Where necessary, media were solidified with 2% [w/v] agar (Sigma-Aldrich, St. Louis, MO, US).

3.2.2 Generating yEpRG constructs to assess Met misincorporation

3.2.2.1 Site-directed mutagenesis

The plasmid yEpRG harbours a construct encoding a fusion protein of yeast-optimised mCherry (yEmRFP) and yeast-enhanced GFP (yEGFP) (Altamura et al., 2016). The Met71 (ATG codon) in the mCherry protein encoded by yEpRG was replaced with Glu, Lys, Asp or Arg by site-directed mutagenesis, using the NEB® Q5® Site-Directed Mutagenesis Kit. The mutagenesis PCR (conditions in Table 3-1) was carried out with the primers in Table 3-2, using the NEB® Phusion® High-Fidelity DNA Polymerase instead of the Mutagenesis Kit's Q5® polymerase.

Table 3-1: Mutagenesis PCR conditions for the amplification of yEpRG.

Ingredient	**Final concentration in PCR reaction**	**Final amount (50 µL PCR reaction)**
0.5 µL plasmid DNA	0.5 ng μL^{-1}	25 ng
1 µL dNTPs	0.2 mM	10 nmol
2.5 µL primer forward	0.5 µM	0.025 nmol
2.5 µL primer reverse	0.5 µM	0.025 nmol
1.5 µL DMSO	3%	1.5 uL
10 µL 5X Phusion® HF reaction buffer	1X	1X
0.5 µL Phusion® HF DNA polymerase	0.02 U μL^{-1}	1 U
31.5 µL water	–	–

PCR programme	**Cycles**
98°C (5 min)	1x
98°C (0.5 min)	35x
60°C (0.5 min)	
72°C (3.33 min)	
72°C (5 min)	1x
10°C (hold)	1x

Table 3-2: Mutagenesis and sequencing primers for yEpRG.

Primer	**Sequence (3' → 5')**[a]
GAA forward (Glu)	ACCACAATTTgaaTATGGTTCAAAAGC
AAA forward (Lys)	ACCACAATTTaaaTATGGTTCAAAAGC
GAT forward (Asp)	ACCACAATTTgatTATGGTTCAAAAGCTTATGTTAAAC
AGA forward (Arg)	ACCACAATTTagaTATGGTTCAAAAGC
mutagenesis reverse	GACAAAATATCCCAAGCAAATG
sequencing forward	GGTGAAGGTGAAGGTAGA
sequencing reverse	TGAGTAACAGTAACAACACC

[a] The codon targeted by mutagenesis is specified by lower case letters.

Next, 1 µL PCR product was treated with 1 µL NEB® KLD Enzyme Mix (5' polynucleotide kinase, DNA ligase, DpnI) in a 10 µL reaction containing 1X KLD Reaction Buffer for 5 min at room temperature. The reaction mix was then added to 50 µL NEB® chemically competent *E. coli* DH5α and the cells were incubated on ice for 30 min, followed by 30 s at 42°C and another 5 min on ice. The cells were then suspended in 950 µL SOC medium (provided by the kit) and 100 µL of appropriate dilutions were plated onto LB-Amp (100 µg mL^{-1} Amp) agar plates, then incubated at 37°C. The original yEpRG plasmid was transformed by adding 1 µL plasmid (~500 ng) to 50 µL competent *E. coli* cells and following the steps as above. For each construct, five single colonies were selected from the transformation plates (2 for the original yEpRG plasmid) and grown overnight in LB-Amp broth. Plasmids were extracted and purified using the NucleoSpin® Plasmid Kit (Macherey-Nagel), following the manufacturer's instructions.

3.2.2.2 Plasmid verification

For transformation of *S. cerevisiae* BY4741 (modified protocol from Gietz and Woods (2002)) with the candidate plasmids (above), 5 mL of exponentially growing yeast cells were harvested (537*g*, 2 min), resuspended in 1 mL 0.1 M Li-Acetate and incubated at 30°C for 10 min. Cells were harvested by centrifugation (1150*g*, 4 min) and resuspended in the transformation mix: 240 µL 50% [w/v] PEG 4000 (final 33.7%), 36 µL 1 M Li-Ac (final 0.1 M), 52 µL DNA carrier (final 0.29 g L^{-1}), 28.5 µL water. The plasmid DNA was added (7.5 µL, equivalent to ~200–500 ng) and the mix was incubated at 30°C for 30 min, followed by 20 min at 42°C. Cells were centrifuged, resuspended in PBS and 100–200 µL of appropriate dilutions was plated onto selective YNB agar plates containing His, Leu and Met for incubation at 30°C (yEpRG encodes a *URA3* marker).

Yeast cells expressing mCherry from plasmid yEmRFP exhibit a red phenotype (Keppler-Ross et al., 2008), so only those transformations that resulted in white-

green colonies, indicating the loss of mCherry fluorescence (=successful replacement of the Met71 codon by mutagenesis) were selected for further experiments (a weak green colour stemming from the GFP expression). The corresponding plasmids (2–4 per construct) were sent for sequencing together with the relevant sequencing primers (Table 3-2) to Eurofins Genomics EU Sequencing GmbH (Cologne, Germany). The sequencing results obtained were analysed for the correct sequence of the mutagenesis region. Sequences were visualised using SnapGene® Viewer 5.1.7. The obtained strains are listed in Table 3-3. For some plasmids, the sequencing results obtained with the forward primer were ambiguous (see remarks in the table), although the results obtained with the reverse sequencing primer confirmed the correct sequence at the mutagenesis site. Strains transformed with plasmids that gave ambiguous sequencing results were not used in the experiments in this study. The sequences of the yEmRFP-GFP fusion protein and adjacent regions of the plasmid confirmed by sequencing in this study are available in Appendix E (6.5).

Table 3-3: Met misincorporation reporter constructs based on yEpRG.

Strain/plasmid ID	Amino acid at position 71 in mCherry	Used in this study?	Remarks
mCh-GAA-1	Glu	yes	/
mCh-GAA-2		yes	/
mCh-GAA-3		yes	/
mCh-GAA-4		yes	/
mCh-AAA-2	Lys	yes (plate reader only[a])	Seq. fw primer repeated[b], low quality in mutagenesis region[c]
mCh-AAA-4		yes	/
mCh-GAT-2	Asp	yes (plate reader only)	Seq. fw primer repeated, low quality in mutagenesis region
mCh-GAT-5		yes	/
mCh-AGA-1	Arg	yes	/
mCh-AGA-2		no	low quality in mutagenesis region
mCh-AGA-3		yes (plate reader only)	Seq. fw primer repeated, low quality in mutagenesis region
mCh-1	Met	yes	/
mCh-2		yes (plate reader only)	/

[a] See 3.2.3. No flow cytometry experiments were performed with this strain.
[b] The first sequencing result obtained with the forward primer displayed unexpected bases at the position of interest, so the sequencing was repeated. The result from the second sequencing displayed the expected bases with a low read quality, see [c].
[c] Background signal in the region of interest decreased the sequencing quality/reliability in reactions using the forward sequencing primer.

3.2.3 Fluorescence detection in a fluorescence microplate reader

To assess the mCherry and GFP fluorescence, a selection of the yeast strains expressing the generated yEpRG variants (Table 3-3) was incubated in black 96-well plates (CELLSTAR® 96-well plates with black wells and clear bottom) in selective YNB or non-selective YEPD (starting OD_{600}~0.1, 30°C, continuous linear shaking at 1096 rev min^{-1}). The OD_{600}, GFP fluorescence (excitation: 485/20 nm, emission: 528/20 nm) and mCherry fluorescence (excitation: 540/35 nm, emission: 600/40 nm) were measured every 2 h in a BioTek® microplate reader (Synergy HTX).

3.2.4 EW, NaOCl or ozonated water treatment of *S. cerevisiae*

Yeast cultures were inoculated to OD_{600}~0.5 from overnight starter cultures in broth (from single colonies) and cultured to exponential phase (OD_{600}~1.8) in YNB broth (10 mL in 50 mL shake flasks). For amino acid pre-culture experiments, different amino acids, S-adenosyl methionine chloride dihydrochloride (SAM, ≥75% purity) or N-acetyl cysteine (NAC) at up to 0.3 mM were included in the experimental cultures. All pre-culture conditions were in buffered YNB (0.1 M potassium phosphate pH 6.0), apart from experiments that included Met or Lys pre-culture only (Met addition did not affect the pH of YNB broth and Lys addition increased the pH minimally, from pH~5.45 without Lys addition to pH~5.7 with 0.3 mM Lys). Cells were harvested by centrifugation (1150*g*, 4 min), washed two times in equal volumes of HPLC grade water, and diluted to OD_{600}~2 in HPLC grade water. Aliquots of 10 µL cell suspension were transferred to 96-well plates, and treated for 5 min with 90 µL of either diluted EW (usually 0.03–0.05% [0.5–1 mg L^{-1} FAC], up to 0.5% [9–10 mg L^{-1} FAC]), NaOCl (0.6–0.7 mg L^{-1} FAC) or ozonated water (see 2.2.3 for sanitiser details). Treatments were stopped by adding 100 µL of 2X YEPD. For recovery in broth, aliquots (100 µL) were transferred to fresh 96-well plates and cultured at 30°C with continuous linear shaking (1096 rev min^{-1})

in a BioTek® microplate reader (Epoch2 or Synergy HTX). The OD_{600} was measured every 30 min and used to estimate survival as described below. Survival on agar plates was determined by plating 50 µL of appropriate dilutions onto YEPD agar plates and subsequent colony enumeration.

3.2.5 Arsenite and paromomycin treatment of *S. cerevisiae*

Yeast cultures in YNB medium supplemented with the appropriate amino acids were diluted to OD_{600}~0.5 for 3.5 h-treatments or to OD_{600}~0.01 for 20 h-treatments. Between 125–250 µM sodium arsenite or 25–200 µM paromomycin was added to cultures (control: stressor-free YNB). Suspensions were grown in 100 µL aliquots in 96-well plates at 30°C (continuous linear shaking; 1096 rev min^{-1}) in a BioTek® microplate reader (Epoch2). The OD_{600} was measured every 30 min and readings at either 3.5 h or 20 h were used to estimate the growth.

3.2.6 Heat treatment of *S. cerevisiae*

After EW treatment (0.01–0.5% EW [0.2–10 mg L^{-1} FAC]), cells suspended in YEPD (50 µL or 150 µL, as specified) were transferred to 0.2 mL reaction tubes and heat-treated for 5 min (actively cooling down to 22°C for a 1 min hold after the treatment) as described in 2.2.7. The gradient setting on the PCR cycler to achieve different temperatures was: temperature: 59°C, gradient: 20°C (as before) or temperature: 41°C, gradient: 28°C, resulting in 30.2°C (2^{nd} column from the left on the heating block), 45°C (8^{th} column) and 50.4°C (10^{th} column). Heat treated samples (40 µL or 100 µL) were brought to 100 µL with YEPD as necessary and recovery in broth was assessed in 96-well plates as described above (3.2.4).

3.2.7 Estimating yeast survival according to growth recovery in broth

Growth curves from broth cultures after treatments (described above) were analysed for the period of exponential growth using RStudio (code is available in Appendix F, 6.6). For every six consecutive OD_{600} values during this period (overlapping; i.e., every string of 3 hours within the exponential growth period), the exponential regression was determined. The 3-hour period with the highest slope was selected and extrapolation to the y-intercept of the regression was used as an estimate for density of viable cells at t = 0 h, similar to the methods described by Fernández-Niño et al. (2018) and Qiu et al. (2017). For validation of the method, *S. cerevisiae* BY4741 was diluted and aliquots (50 µL) spread plated to determine linearity of correlation between values for calculated starting cell density (measured OD_{600} divided by dilution factor), viability (colony forming units, cfu) and the y-intercept of growth in broth (see 3.3.1.2). Linearity of the correlation was also examined for cfu (agar) and y-intercept (broth) determinations with EW treated yeast cells. Survival estimates based on the y-intercept determination are referred to as recovery rates throughout.

3.2.8 Aconitase and fumarase assay in cell extracts

The method was as described previously (Lalève et al., 2016). Briefly, *S. cerevisiae* BY4741 was grown to exponential phase in 50 mL YEPD (250 mL shake flasks). Cells were washed, pooled and treated with EW (for *in-vivo* treatments but not for *in-vitro* EW treatments, described below) as outlined above, except that cell suspensions were concentrated to OD_{600}~200 in water and 1 mL suspension was treated with 19 mL EW (0.3% [v/v], equivalent to 5.4–6 mg L^{-1} FAC) with treatments inactivated using 20 mL of 2X YEPD (for survival analysis, samples were taken at this point, diluted and spread to YEPD agar for cfu determination, or used for recovery analysis in YEPD broth). Cells were harvested (2876*g*, 4°C, 10 min), transferred to a 4°C (aerobic) room and resuspended in

250 µL cold resuspension buffer (0.72 mM $MnCl_2$ in 10 mM MES [pH 6], Halt™ Protease Inhibitor Cocktail [1X], with oxygen depleted by pre-incubation in 10% CO_2, 10% H_2, 80% N_2 for at least 2 h). Cells were lysed with 500 µL cold glass beads (acid washed, 425–500 µm (Sigma Aldrich), pre-conditioned with resuspension buffer) in 7 vortexing cycles (one cycle comprised of 30 s at high speed followed by 30 s on ice), centrifuged (15,900*g*, 4°C, 5 min) and aliquots of the supernatants (50 µL) frozen in liquid nitrogen and stored at –80°C. Protein concentrations in the extracts were determined with the Bio-rad Protein Assay Kit according to the manufacturer's Microassay Procedure. For *in-vitro* EW treatments, 155 µg protein extracted from untreated cells was mixed with EW (final concentration 10% EW [v/v], 180–200 mg L^{-1} FAC) or primaquine (500 µM) for 20 min, in the absence or presence of 3 mM methionine or cysteine. Aliquots (~25 µL) from the *in-vitro* treatments comprising 140 µg protein or aliquots of 140 µg protein from *in-vivo* treatments (EW treated cells) were then mixed with aconitase buffer (50 mM potassium phosphate buffer [pH 7.4], 30 mM DL-isocitric acid trisodium, 0.6 mM $MnCl_2$) or fumarase buffer (50 mM potassium phosphate buffer [pH 7.4], 50 mM L-malic acid) to a total volume of 700 µL in quartz cuvettes. The absorbance at 240 nm was recorded every 30 s for 30 min (baseline correction at 340 nm, DeNovix DS-11 FX+ Spectrophotometer/Fluorometer). The enzyme activity was determined from the gradient of the linear portion of the absorbance curve with the extinction coefficients ε_{240}(cis-aconitate) = 3.6 mM^{-1} cm^{-1}; ε_{240}(fumarate) = 2.44 mM^{-1} cm^{-1} (Lalève et al., 2016), reaction volume v = 0.7 mL, protein mass m = 0.14 mg, optical path length d = 1 cm:

$$enzyme\ activity\ \left[\frac{\mu mol}{\min\ mg}\right] = \frac{absorbance\ gradient\ \left[\frac{1}{min}\right]\ v[mL]}{\varepsilon_{240nm}\left[\frac{mL}{\mu mol\ cm}\right]\ m[mg]\ d[cm]}$$

3.2.9 Reconstitution of aconitase FeS clusters

The reconstitution assay was adapted from previous protocols (Ollagnier-de-Choudens et al., 2001, Moulis and Meyer, 1982, Mons et al., 2018). The extraction buffer (MES) of crude protein extracts (3.2.8) was replaced by Tris buffer (0.1 M, pH 8) by applying 400 µg protein in 140 µL MES buffer to 2 Vivaspin® 500 columns (Sartorius, Surrey, UK) and adding 750 µL Tris buffer to each column across three rounds of centrifugation to concentrate the sample (15,000*g*, 30 min, 4°C, aerobic conditions). A final volume of ~70 µL per spin column with 1–2% residual MES was reached and samples from both columns were then pooled.

Half of the protein extract in Tris buffer (70 µL) was used for a "pre-reconstitution" assay of aconitase and fumarase activity as described above (31.5 µL sample used per assay). The other 70 µL were incubated with 5 mM DTT for 30 min before adding 100 mM NaCl, 100 µM Na_2S and 100 µM ammonium iron(II) sulphate ($(NH_4)_2Fe(SO_4)_2(H_2O)_6$; Mohr's salt) to a final volume of 100 µL and incubating for 2 h (the incubations were at ~25°C in oxygen-free conditions [10% CO_2, 10% H_2, 80% N_2]). Aconitase and fumarase activity were measured (as described above) in 40 µL aliquots after the reconstitution. Due to observed low stability of aconitase, a "quick reconstitution" protocol was adapted where the buffer exchange step was skipped and the protein extract in MES (150–160 µg protein) was incubated either in atmospheric or oxygen-free conditions with the reconstitution chemicals (DTT, NaCl, Na_2S, Fe^{2+}, concentrations as above, 40 µL total volume) for 20 min at room temperature before determining the aconitase activity for an aliquot of 140 µg protein. Protein extracts and reconstitution reactions were kept in plastic tubes which may have introduced oxygen into the samples.

3.2.10 Flow cytometric analysis of the Met misincorporation reporters

Samples from growing YNB cultures (either stressor-free YNB, arsenite or paromomycin treatments or Met pre-culture in YNB) were harvested by centrifugation (1150*g*, 4 min), washed and resuspended in PBS for analysis by flow cytometry as described below. For other experiments, EW treatments were carried out as described in 3.2.4, except that overnight cultures were diluted to OD_{600}~0.03–0.05 and cultivated overnight to reach exponential phase. After harvesting and washing cells in HPLC grade water, cells (100 µL) were treated with 900 µL EW (0.01–0.03% EW [v/v], 0.2–0.6 mg L^{-1} FAC) for 5 min, and treatments were stopped by adding 1 mL 2X YEPD (larger treatment volumes compared to 3.2.4 were needed to achieve sufficient cell numbers for flow cytometry). Recovery in broth was assessed as above (3.2.7). Aliquots (500 µL) of the YEPD-inactivated treatments were added to 10 mL YEPD and incubated for 0.5–2 h in shake flasks at 30°C, 120 rev min^{-1}. Cells were harvested by centrifugation (537*g*, 5 min), washed once with PBS (1150*g*, 4 min) and resuspended in PBS for flow cytometric analysis. Cells were analysed with a Sony ID7000™ Spectral flow cytometer. GFP fluorescence was recorded with 488 nm excitation and 493.9–530.3 nm emission filter and mCherry fluorescence with 561 nm excitation and 589.5–624 nm emission filter. Events were gated based on SSC-Area vs. FSC-Area plots and doublets/cell clumps were excluded based on FSC-Height vs. FSC-Area plots. In the resulting "single-cell" gate, data for ~10,000 cells were collected per sample.

3.2.11 Statistical analysis and software

Tests for statistical significance and linear regression were performed as described in 2.2.11. Flow cytometry data were analysed within the Beckman Coulter Kaluza 2.1 software.

3.3 Results

3.3.1 Yeast treatment with EW

3.3.1.1 Sensitivity of yeast to EW treatment

The effectiveness of EW on the yeast *S. cerevisiae* BY4741 was confirmed at low EW dilutions (0.03–0.1% [v/v], equivalent to 0.5–2 mg L^{-1} FAC, treatment of water-washed cells, Figure 3-3). Survival on agar plates (cfu) was strongly reduced (≥2.5 log) after 5 min treatment with EW dilutions of 0.1%. The survival was further assessed in suspension (growth in YEPD after EW treatment) and recovery rates were determined by y-intercept extrapolation as described below (3.3.1.2). Partial killing of the yeast cells was confirmed for the EW range between 0.02–0.1% (0.4–2 mg L^{-1} FAC, Figure 3-4). The survival rates estimated in broth were lower than those determined on agar (e.g., 0.05% EW resulted in ~70% survival on agar and ~8% recovery in broth), which could be related to any lag before resumption of exponential growth in broth, which would affect accuracy of the y-intercept extrapolation for estimating the surviving cell numbers (see 3.3.1.2). In addition, survival may have been affected by minor changes in the EW manufacturing (experiments were ~2 years apart) or the dilution of EW in sterile distilled water (SDW) or sterile tap water in Figure 3-3 (as opposed to HPLC grade water in Figure 3-4; see 3.3.1.3 for an assessment of EW dilution effects).

A

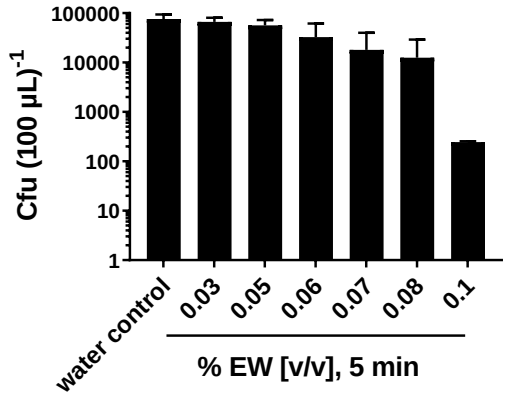

B

% EW [v/v]	Log reduction	Survival rate [%]
0.03	0.04 ± 0.16	97 ± 32
0.05	0.16 ± 0.09	71 ± 14
0.06	0.48 ± 0.59	56 ± 50
0.07	0.96 ± 0.70	19 ± 22
0.08	1.09 ± 1.16	27 ± 37
0.1	2.52 ± 0.09	0.3 ± 0.1

Figure 3-3: Yeast survival after EW treatment according to cfu on agar plates. *S. cerevisiae* BY4741 was treated with increasing concentrations of EW (5 min, 0.03–0.1% [v/v]; equivalent to ~0.5–2 mg L^{-1} FAC, EW dilutions were in SDW or sterile tap water). A) Survival was assessed by spread plating 50 µL of appropriate dilutions and subsequent enumeration of colony forming units (cfu) on YEPD agar, given as cfu per 100 µL undiluted suspension. Mean values ± SD are shown for at least 3 biological replicates (except 0.07%, 0.08% and 0.1%: n = 2). B) Log reductions were calculated based on data shown in A (reduction rates were calculated separately for each replicate and the values in B are mean ± SD of the reduction rates for the different replicates). The detection limit was ~3.2 log reduction.

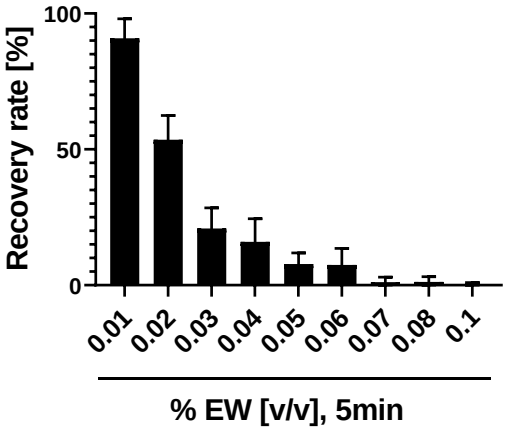

Figure 3-4: Yeast survival after EW treatment according to recovery in YEPD broth. *S. cerevisiae* BY4741 was treated with increasing concentrations of EW (5 min, 0.01–0.1% EW [v/v]; 0.2–2 mg L^{-1} FAC, dilutions in HPLC grade water) and survival was estimated by subsequent recovery in YEPD broth (see 3.3.1.2). Mean values ± SD are shown for 6 biological replicates.

3.3.1.2 Developing a higher throughput method to estimate yeast survival in broth

Spread plating for cfu counts to estimate numbers of viable cells is a laborious method, while simple optical density (OD) readings do not discriminate live from dead cells. In order to establish a more convenient method for estimating cell survival post stress, it was reasoned that the timing of detectable exponential growth in broth, starting from suspensions with low viable cell numbers, should reflect the starting number of viable cells. Accordingly, growth curves from broth cultures after EW and other treatments were analysed for the period of exponential growth, determining the y-intercept of the exponential regression of the exponential phase as an estimate for the density of viable cells at t = 0 h (see Methods 3.2.7). For validation of the method, *S. cerevisiae* BY4741 was diluted and aliquots (50 µL) spread plated to test linearity of correlation between values for calculated starting cell density (based on the OD_{600} of the undiluted suspension divided by the dilution factor), viability (colony forming units, cfu) and the y-intercept of growth in broth (Figure 3-5 A,B). Growth on agar was highly correlated with both the starting cell density (panel A) and the y-intercept (panel B). The y-intercept values were lower than the calculated starting OD_{600} values (~30–50% of the OD_{600} values; data in panels A and B are from the same experiments). This may suggest either limited viability of non-stressed cultures, or a lag-phase effect that underestimates the starting density as determined by y-intercept extrapolation. Therefore, y-intercept values should not be interpreted as real absolute starting densities, but comparing the y-intercepts of different (treatment) conditions should allow to estimate relative survival. For this reason, linearity of correlation was also examined for cfu (agar) and y-intercept (broth) determinations with EW treated yeast cells (Figure 3-5 C). Following EW treatment, the correlation between cfu (agar) and y-intercept (broth) was weaker than with non-stressed cell suspensions but still strong (R^2 = 0.74 vs. R^2 = 0.97). Some deviation may be caused by non-killing effects such as a growth delay of stressed cells (Lu et al., 2009) which cannot be easily detected by cfu

enumeration, resulting in lower survival estimates based on the y-intercept than based on cfu enumeration. Overexpression of certain genes was found to affect EW resistance in this study (see below, 3.3.4, 3.3.5.2) and it was tested in one comparative experiment whether such EW resistance (relative to empty-vector control strains) could be detected with both methods, i.e., cfu enumeration and y-intercept determination. The yeast strains were treated with EW and it was found that survival of EW treatment calculated from the y-intercept was generally lower than that based on cfu but very similar relative effects of the genetic manipulations were observed with both methods in the comparative experiment (Figure 3-5 D), e.g., higher survival of the *RLI1* overexpressing strain compared to its empty vector control (this result [EW resistance of the overexpression strain] is presented in more detail in 3.3.5.2). Overall, the results support the use of growth extrapolation to the y-intercept for estimating starting viable-cell density. Throughout, EW was diluted to give estimated survival between 5% and 50% (unless stated otherwise). The lower limit was to counter experimental variation observed at very low starting viable-cell densities. The upper limit (50%) was to minimise the relative influence of potential growth-delay effects (as opposed to cell death events) on the measurements: survival rates calculated with the present method are estimates as they may encompass a contribution from any lag phase extension, and will therefore be referred to as recovery rates after treatments.

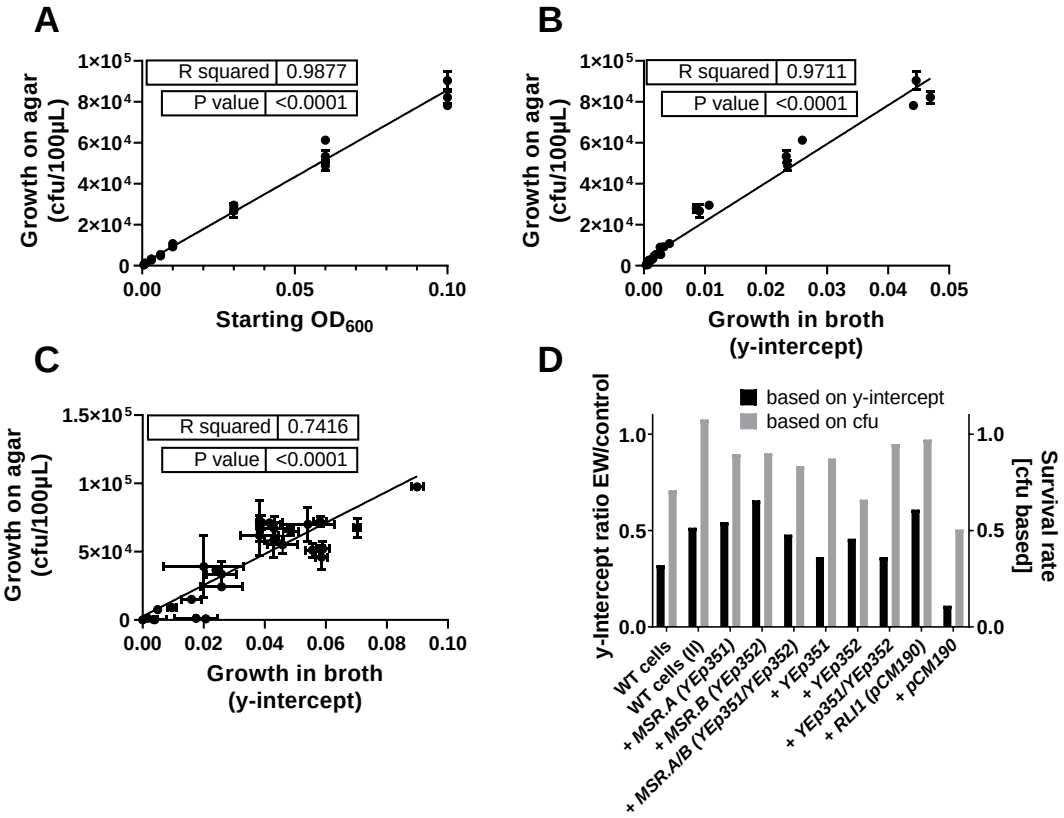

Figure 3-5: The y-intercept method for estimating survival in broth cultures as recovery. A,B,C) *S. cerevisiae* BY4741 was diluted in SDW to different starting densities (A,B) or treated with increasing concentrations of EW (C) (0.01–0.1% EW [v/v] in SDW or sterile tap water; 0.2–2 mg L^{-1} FAC). The starting OD_{600} was calculated by measuring the OD_{600} of an undiluted yeast suspension and dividing by the corresponding dilution factor. Survival on agar was determined after treating samples of equal cell densities with increasing EW concentrations and by spread plating appropriate dilutions and subsequent enumeration of colony forming units (cfu), given as cfu per 100 µL undiluted suspension. For growth in broth, 100 µL cells were cultured in 96-well plates in a BioTek® microplate reader (30°C, 1096 rev min^{-1}) and, for the period of highest growth rate (maximum slope in an exponential regression), the y-intercept was determined (see Methods 3.2.7). The correlation coefficient (R^2) and p-value of the linear regression are specified. Data are from at least 3 biological replicates, individual data points are shown ± SD of 2–3 technical replicates. Cfu values in C include the data presented in Figure 3-3. D) *S. cerevisiae* BY4741 transformed or not with the specified plasmids were treated with 0.03% [v/v] EW (0.5–0.6 mg L^{-1} FAC) for 5 min before survival was assessed on agar and in broth as described for A-C (data from 1 biological replicate). WT, wild type.

3.3.1.3 Diluting EW in water: effect of water purity on EW strength

As discussed in 1.6.3 and Chapter 2, the chlorine or oxidant demand of water used for diluting EW might negatively affect its sanitising ability. EW diluted in sterile tap water had a lower FAC and resulted in higher yeast recovery than EW diluted in sterile distilled water (SDW, Figure 3-6 A; a low EW dilution [0.05%] was

chosen to give partial survival and allow comparison of effects between water types), probably due to organic or inorganic constituents of the tap water. Treatment with EW diluted in HPLC grade water resulted in yeast recovery that appeared to be lower than recovery after treatment with SDW-diluted EW in one experiment (Figure 3-6 B). To avoid interference from the dilution water, and to ensure consistency, HPLC grade water was used when working with EW in most other experiments described in this chapter (for diluting EW, preparing yeast cell suspensions for treatments, and for water control treatments) unless stated otherwise. This may explain the lower recovery rate at EW dilutions around 0.03% [v/v] presented in most figures (including Figure 3-4; ~21% recovery at 0.03% EW; dilution in HPLC grade water) compared to the EW effect summarized in Figure 3-3 (~97% survival at 0.03% EW; dilution in SDW or sterile tap water). It should be noted that in addition to potential reactivity of EW with water constituents, the pH of different water samples as well as osmotic shock conditions of cells in purified water may influence the overall EW efficacy and survival.

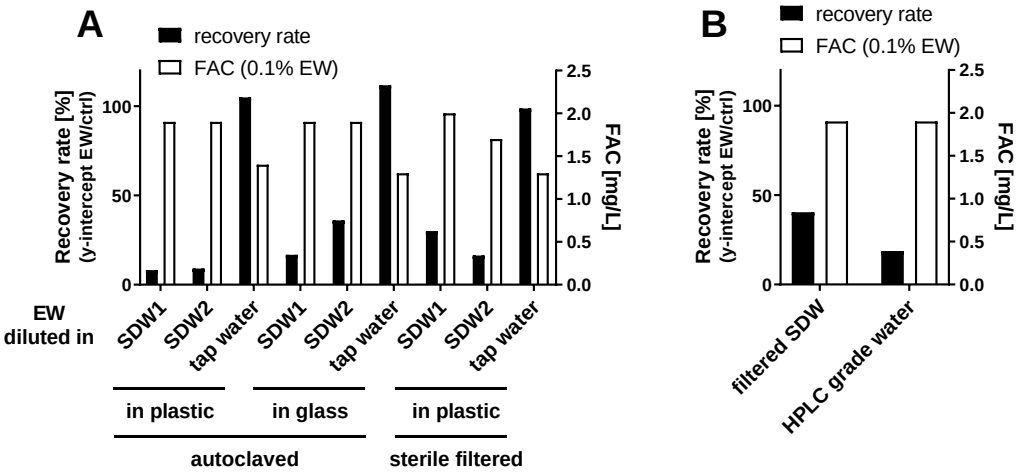

Figure 3-6: Recovery of yeast after treatment with EW diluted in water of different purities. *S. cerevisiae* BY4741 was treated with diluted EW (0.05% [v/v], 5 min). Cell suspensions and EW dilutions were prepared in SDW or tap water that was sterilized by autoclaving in plastic tubes or glass bottles or by filtration (0.22 µm filter pore size) (A) or in HPLC grade water or filtered SDW (B). SDW1 and SDW2 (A) are from two separate water purification units (both PURELAB® Option CV35 by ELGA Veolia, UK). Survival was estimated by subsequent recovery in YEPD broth (see 3.3.1.2), and recovery rates were calculated relative to a control treatment with the corresponding water type (filled bars). Data from 1 biological replicate. Free available chlorine (FAC) concentrations were measured in 0.1% EW dilutions and are plotted on the right y-axis (white bars).

3.3.2 Pre-culture with different amino acids before EW treatment reveals protective effect of Met

3.3.2.1 Met pre-culture exhibits protective effect, but no other tested amino acids

In the previous chapter, certain amino acids were noted to affect EW activity particularly strongly (2.3.4.1). It was hypothesised that the level of these amino acids within cells (accumulated free amino acids or protein-bound, influenced by uptake of exogeneous amino acids or biosynthesis) might influence cellular EW resistance (defined as recovery from EW treatment). This was tested first by supplying higher levels of these amino acids to cells for defined incubation periods followed by removal of any remaining extracellular amino acid before the EW treatment. This was to avoid chemical inactivation of EW by extracellular amino acids, allowing study of the effect of amino acid accumulated by cells. Lower EW concentrations (0.03–0.05% [v/v]; 0.5–1 mg L^{-1} FAC) than in the previous experiments on amino acids and *A. niger* spores (2.3.4.1) were needed with *S. cerevisiae* to avoid complete killing, so that the response to EW could be studied. Survival of *S. cerevisiae* was estimated as recovery by culturing cells in broth after EW treatment and determining the y-intercept of the exponential phase as described above (3.3.1.2). Exogenously supplied amino acids can be readily taken up by yeast cells. Pre-culture of yeast for 4–5 h in defined medium (amino-acid free YNB, supplemented with required amino acids for strain auxotrophies, see Figure 3-7) supplemented with different amino acids (0.3 mM), followed by EW treatment in the absence of amino acids, revealed a protective effect of methionine (Figure 3-7 A). Pre-culture with Met increased EW recovery by >1.5 fold (FDR adjusted p = 0.0158, comparing between control-YNB with 0.13 mM Met and pre-culture condition [0.3 mM Met]). Other amino acids chosen based on the EW inactivation results (2.3.4.1; Trp, Tyr, Arg, His and Asn) did not exhibit a protective effect (Arg and Tyr actually gave slight sensitization). Pre-culture with Cys inhibited yeast growth so it could not be tested. Pre-culture with N-acetyl-

cysteine (NAC), commonly used as a Cys precursor, did not inhibit yeast growth but did not protect against EW (Figure 3-7 B). Additionally, the amino acid lysine was tested because Lys pre-treatment had previously been reported to increase resistance against pro-oxidant treatment (Olin-Sandoval et al., 2019). However, no protective effect against EW treatment could be observed in the present study in either the Lys prototrophic (BY4741) or the Lys auxotrophic (BY4742) strain of *S. cerevisiae* (Figure 3-7 C).

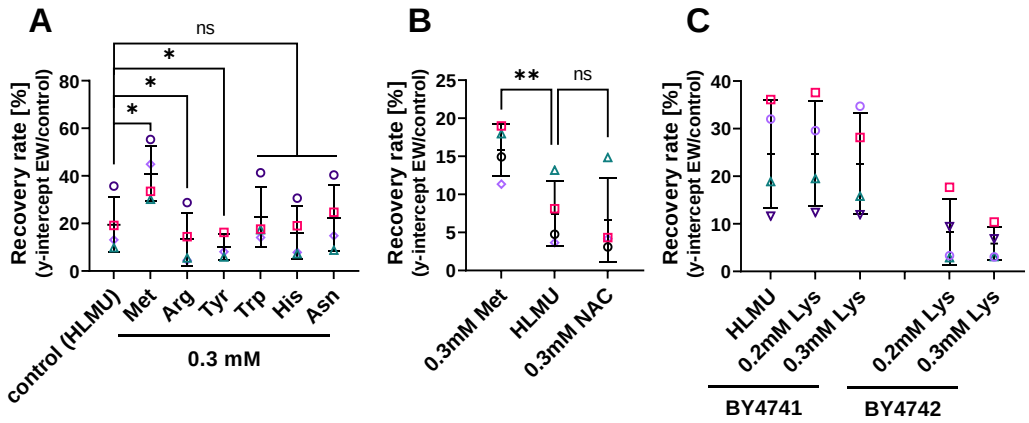

Figure 3-7: Influence of cellular methionine on recovery after EW treatment. Survival of yeasts after EW treatment (0.03–0.05% [v/v] in HPLC grade water; 0.5–1 mg L^{-1} FAC, 5 min) was estimated by subsequent recovery in YEPD broth (see 3.3.1.2). *S. cerevisiae* BY4741 (A,B,C) or BY4742 (C, as specified) were pre-cultured with amino acids at the specified total concentrations for 4–5 h prior to treatment; control growth and pre-culture were in YNB broth also containing 0.1338 mM Met, 0.129 mM His, 0.763 mM Leu, 0.178 mM Ura (HLMU, for BY4741), or without Met for BY4742 (C). Where amino acids were added to the control broth, the specified pre-culture concentration (0.2 mM or 0.3 mM) refers to the final total concentration (i.e., including the control-broth content). YNB was buffered (0.1 M potassium phosphate buffer pH 6) in A and B. Cells were washed in HPLC grade water before treatment. NAC, N-acetyl cysteine. All plots: mean values ± SD are shown for at least 3 biological replicates, with different replicate experiments distinguished by different symbols. Significant differences versus relevant controls are denoted by *p<0.05; **p<0.01; ns, not significant; according to paired *t*-test (two-tailed) with correction for multiple comparisons by controlling the false discovery rate at 5% FDR (Benjamini et al., 2006).

3.3.2.2 The protective effect is not related to yeast amino acid auxotrophies

The protective effect of Met was not dependant on the Met auxotrophy (biosynthetic defect demanding externally supplied Met) of the *S. cerevisiae* BY4741 laboratory strain used above, as the isogenic Met-prototrophic strain

S. cerevisiae BY4742 was also protected by Met pre-treatment (Figure 3-8 A). Furthermore, deletion strains auxotrophic for Trp (*trp1Δ*), Arg (*arg4Δ*) or His (BY4741: *met15Δ*, *his3Δ*), and the "partial" alanine auxotroph *alt1Δ* (which accumulates less (but not zero) intracellular Ala than the wild type (Peñalosa-Ruiz et al., 2012)); Ala did not have a particularly strong EW inactivation effect [2.3.4.1], and was used as a control amino acid), were not protected by their respective amino acid (Figure 3-7 A, Figure 3-8 B).

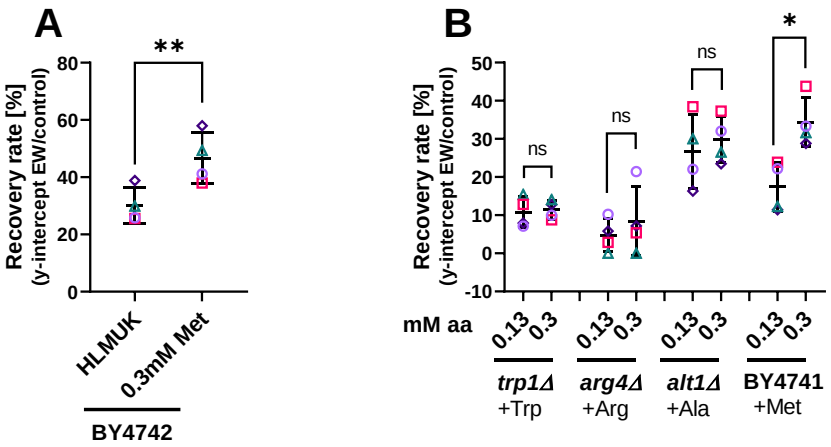

Figure 3-8: Influence of cellular methionine on yeast recovery after EW treatment is independent of amino acid auxotrophies. Survival of yeasts after EW treatment (0.03–0.05% [v/v], diluted in HPLC grade water; 0.5–1 mg L^{-1} FAC, 5 min) was estimated by subsequent recovery in YEPD broth (see 3.3.1.2). *S. cerevisiae* BY4742 (A) or BY4741 (a *met15Δ* methionine auxotroph) and deletion strains isogenic to BY4741 (*trp1Δ,* tryptophan auxotroph; *arg4Δ,* arginine auxotroph; *alt1Δ,* "partial" alanine auxotroph) (B) were pre-cultured with the specified amino acids at the specified total concentrations for 4–5 h prior to treatment; control growth and pre-culture were in YNB broth also containing 0.1338 mM Met, 0.129 mM His, 0.763 mM Leu, 0.178 mM Ura (B), plus 0.21 mM Lys for BY4742 (A, "HLMUK"). Where amino acids were added to the control broth, the pre-culture concentration (0.13 or 0.3 mM) refers to the final total concentration (i.e., including the control-broth content). YNB was buffered (0.1 M potassium phosphate buffer pH 6) in B. Cells were washed in HPLC grade water before treatment. Mean values ± SD are shown for at least 3 biological replicates, with different replicate experiments distinguished by different symbols. Significant differences versus relevant controls are denoted by *p<0.05; **p<0.01; ns, not significant; according to paired *t*-test (two-tailed) with correction for multiple comparisons by controlling the false discovery rate at 5% FDR (Benjamini et al., 2006).

3.3.2.3 Met also protects against NaOCl and ozonated water

Because EW is likely to contain different active species, it was tested whether the observed effect of Met pre-culture on resistance to EW (Figure 3-7, Figure 3-8) was mimicked with NaOCl treatment. Similar to EW, pre-culture with Met gave increased resistance to NaOCl treatment (Figure 3-9 A). To test non-FAC components, ozonated water was used. Like EW, ozonated water was produced using an electrolysis technology but, unlike EW, it does not contain FAC. In water, ozone reacts to form other reactive species such as highly reactive hydroxyl radicals (Wang et al., 2020). Recovery after ozonated water treatment was also increased after Met pre-culture (Figure 3-9 B). The results suggest that Met may protect against both chlorine and non-chlorine active species in EW.

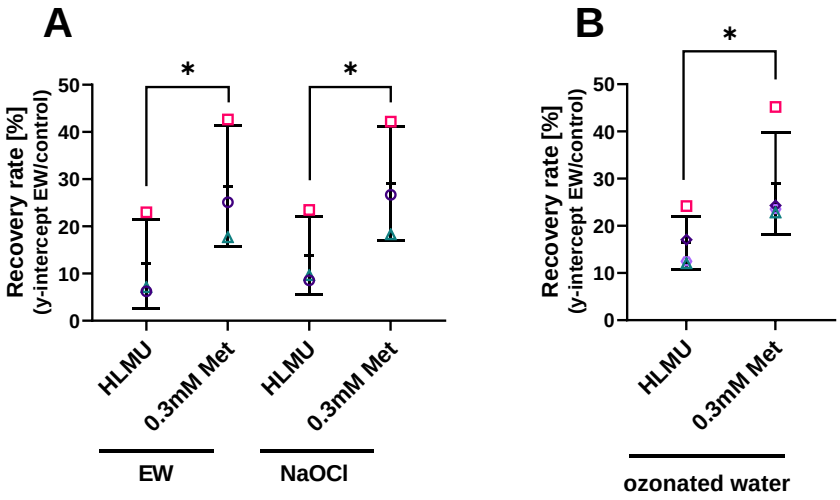

Figure 3-9: Influence of cellular methionine on recovery after NaOCl and ozonated water treatment. Survival of yeasts after treatment was estimated by subsequent recovery in YEPD broth (see 3.3.1.2). A) Treatment for 5 min either with EW or NaOCl, in parallel, both oxidants at 0.7 mg L^{-1} FAC (diluted in HPLC grade water). B) Treatment with ozonated water, used within 2 min of its generation for a 5 min treatment. Data are shown only for experiments where cell recovery was >10%, to minimise the influence of technical variation that was observed in response to ozonated water stress. A,B) *S. cerevisiae* BY4741 was pre-cultured with amino acids at the specified total concentrations for 4–5 h prior to treatment; control growth and pre-culture were in YNB broth also containing 0.1338 mM Met, 0.129 mM His, 0.763 mM Leu, 0.178 mM Ura (HLMU). The Met pre-culture concentration (0.3 mM) refers to the final total concentration (i.e., including the control-broth content). Cells were washed in HPLC grade water before treatment. Mean values ± SD are shown for at least 3 biological replicates, with different replicate experiments distinguished by different symbols. Significant differences versus relevant controls are denoted by *p<0.05; according to paired *t*-test (two-tailed) with correction for multiple comparisons by controlling the false discovery rate at 5% FDR (Benjamini et al., 2006).

3.3.3 Distinguishing a role for Met itself as opposed to a downstream metabolism product

3.3.3.1 The protective effect can be reproduced with D-Met but not SAM pre-treatment

All cellular life relies on L-isomers of amino acids, and it was confirmed that *S. cerevisiae* BY4741 is unable to grow on D-Met as the sole Met source, whereas growth in medium containing L-Met was not affected by D-Met addition (Figure 3-11). Adding D-Met to medium containing L-Met (0.13 mM) to a total of 0.3 mM Met (D+L) did not mimic the protective effect observed with 0.3 mM L-Met in the Met-auxotrophic strain BY4741 (Figure 3-10 A). In contrast, adding D-Met to medium free of L-Met for the pre-culture of the Met prototrophic strain BY4742 resulted in a protective effect; the effect of D-Met was actually larger than the effect of L-Met pre-culture (Figure 3-10 B). Increased D-Met uptake in medium free of L-Met may potentially be due to a lack of competition for the Met uptake systems (such as Mup1) in the absence of L-Met (Gits and Grenson, 1967, Isnard et al., 1996) and potentially due to a lack of feedback inhibition that would downregulate Met uptake systems in the presence of L-Met (downregulation relies on Cys and potentially SAM, products of enzymatic reactions of L-Met, see 3.1.3.2). This protective effect of the metabolically inactive D-Met suggests a direct role of the Met molecule itself in EW resistance.

The first metabolism product of methionine utilisation is S-adenosyl-methionine (SAM) (Ljungdahl and Daignan-Fornier, 2012). Pre-treatment with SAM did not improve resistance of the BY4741 strain to EW, further supporting a role of Met itself in protection, rather than a Met metabolic product (Figure 3-10 C). SAM uptake and utilization was confirmed by the restoration of growth of *S. cerevisiae* BY4741 in Met-free, SAM-supplemented medium (Figure 3-11; note that these assays are limited by the SAM-purity [≥75%]). The possibility that an effect of

the presence of L-Met on SAM uptake could explain the above lack of effect of SAM on EW resistance (similar to the suggested effect on D-Met above) was ruled out by pre-treating BY4742 with SAM in Met-free medium, which did not consistently protect the yeast against EW (Figure 3-10 D). Cysteine is a further metabolic product of Met (Figure 3-2) with important antioxidant activity (Ljungdahl and Daignan-Fornier, 2012, Tamura et al., 2010) but pre-treatment with the Cys precursor NAC (described above) did not protect against EW treatment (Figure 3-7 B).

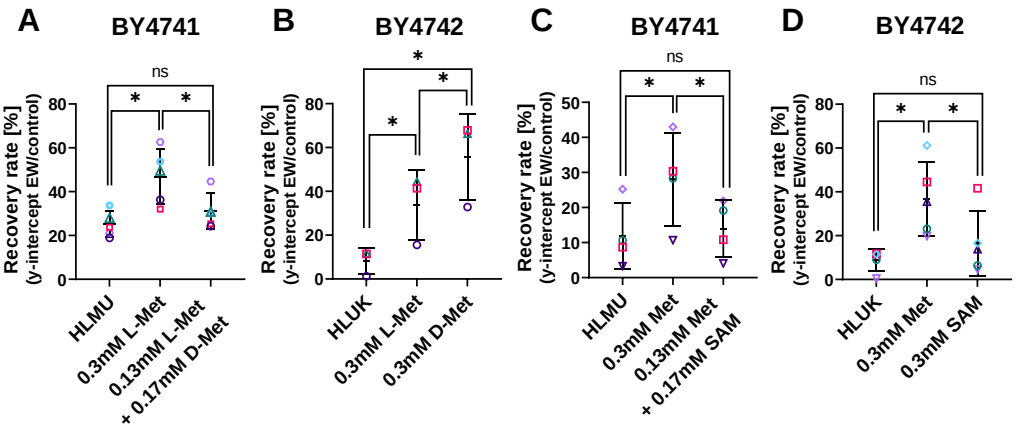

Figure 3-10: Influence of methionine isomers or SAM on yeast recovery from EW treatment. Survival of yeasts after EW treatment (0.03–0.05% [v/v], in HPLC grade water; 0.5–1 mg L^{-1} FAC, 5 min) was estimated by subsequent recovery in YEPD broth (see 3.3.1.2). Pre-culture of *S. cerevisiae* BY4741 (A,C) or BY4742 (B,D) with L-Met, D-Met or S-adenosyl-methionine (SAM) at the specified total concentrations for 4–5 h prior to EW treatment; control growth and pre-culture were in YNB broth also containing 0.1338 mM Met, 0.129 mM His, 0.763 mM Leu, 0.178 mM Ura (HLMU, A,C), or 0.21 mM Lys instead of Met for BY4742 (HLUK, B,D). Where amino acids were added to the control broth, the pre-culture concentration (0.3 mM) refers to the final total concentration (i.e., including the control-broth content). YNB was buffered (0.1 M potassium phosphate buffer pH 6) in C and D. Cells were washed in HPLC grade water before EW treatment. Mean values ± SD are shown for at least 3 biological replicates, with different replicate experiments distinguished by different symbols. Comparisons of interest were tested by paired *t*-tests (two-tailed) with correction for multiple comparisons by controlling the false discovery rate at 5% FDR (Benjamini et al., 2006); *p<0.05; ns, not significant.

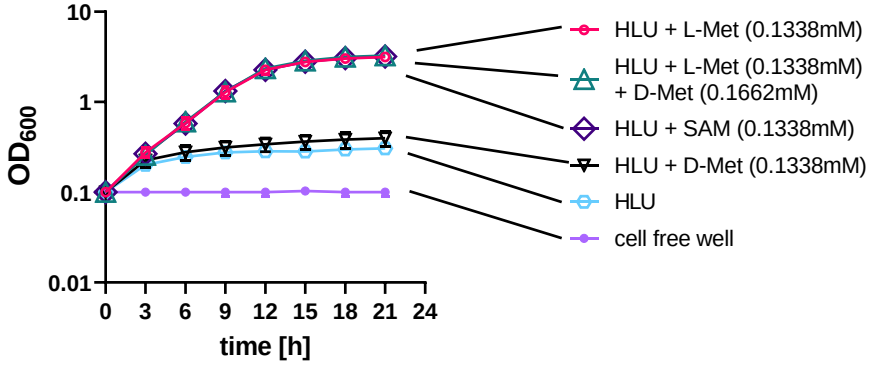

Figure 3-11: Yeast growth in minimal medium supplemented with different Met sources. Culture density of *S. cerevisiae* BY4741 was determined at 3 h intervals in a shaking plate reader (starting OD_{600}~0.1). The growth medium was YNB broth (buffered, 0.1 M phosphate buffer pH 6) supplemented with 0.129 mM His, 0.763 mM Leu, 0.178 mM Ura (HLU) plus Met or S-adenosyl-methionine (SAM) at the specified concentrations. Mean values ± SD are shown for 3 biological replicates.

3.3.3.2 The Met protective effect is already evident after only 10 min pre-treatment

Saturation of Met uptake is reported to occur within 10 min of Met addition to Met-free medium (Schwabe and Bruggeman, 2014), and regulation of the uptake systems in response to high Met levels, as evidenced by the elimination of the high-affinity transporter Mup1 from the membrane (see also 3.1.3.2), commences within 10 min (Menant et al., 2006). In the present study, 10 min L-Met pre-culture was sufficient to increase resistance of yeast to EW, and longer Met pre-treatments did not add further advantage; if anything, 10 min pre-culture resulted in the highest protective effect (Figure 3-12; t2).

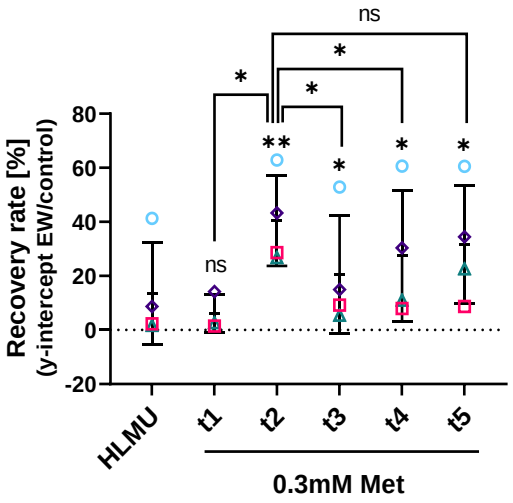

Figure 3-12: Influence of Met pre-culture of varying duration on recovery from subsequent EW treatment. Survival of yeasts after EW treatment (0.03–0.05% [v/v], in HPLC grade water; 0.5–1 mg L^{-1} FAC, 5 min) was estimated by subsequent recovery in YEPD broth (see 3.3.1.2). Pre-culture of *S. cerevisiae* BY4741 with Met at the specified concentration for varying durations during exponential growth: t1, <0.5 min; t2, 10 min; t3, 2–2.5 h; t4, 4–5 h; t5, 20 h (sub-cultured after ~16 h), before harvesting cells for EW treatments. Control growth (HLMU) was in YNB broth containing 0.1338 mM Met, 0.129 mM His, 0.763 mM Leu, 0.178 mM Ura, and Met was added to reach a total concentration of 0.3 mM for pre-culture conditions. Cells were washed in water before EW treatment. Mean values ± SD are shown for at least 3 biological replicates, with different replicate experiments distinguished by different symbols. *p<0.05; **p<0.01; ns, not significant; according to paired *t*-test (two-tailed), comparing between HLMU control and Met pre-culture unless shown by a connecting line, with correction for multiple comparisons by controlling the false discovery rate at 5% FDR (Benjamini et al., 2006).

3.3.4 Overexpression of methionine sulphoxide reductases protects against EW

Methionine residues can be naturally oxidised to methionine sulphoxide (MetO) but can be reduced back to methionine by cellular methionine sulphoxide reductases, encoded by *MSRA*, *MSRB* and *fRMSR* in yeast. It was hypothesised that Met oxidation by EW could explain the above protective effects on cells of adding Met in its reduced form, suggesting a potential role of accumulated Met as a direct ROS scavenger in EW stress. Accordingly, improved maintenance of reduced Met by MSR activity should also increase resistance to EW. The yeast MsrA and MsrB enzymes were overexpressed under the control of their native

promoters on multicopy plasmids (2-micron replication system, expected copy number ~10–40 (Romanos et al., 1992, Wai et al., 2000)) as characterised previously (Sumner et al., 2005), either alone or in combination. In all cases, resistance of yeast to EW was significantly increased by elevated *MSR* expression (Figure 3-13), suggesting that the level of reduced Met specifically is important for resistance to EW.

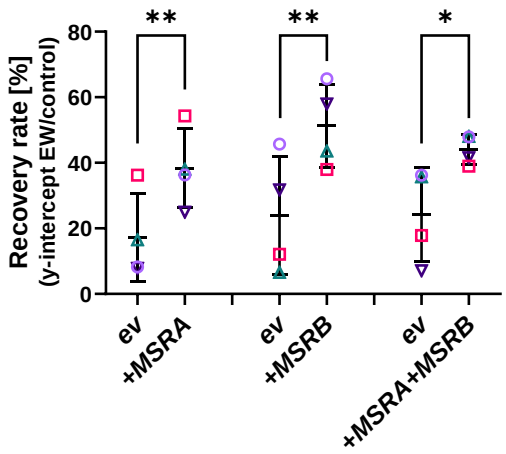

Figure 3-13: Influence of overexpressing MetO-reducing activities on recovery from EW treatment. *S. cerevisiae* BY4741 overexpressing *MSRA* and *MSRB* in multicopy vectors YEp351 and YEp352, respectively, encoding methionine sulphoxide reductases (ev, empty vector). Survival of yeasts after EW treatment (0.03–0.05% [v/v], in HPLC grade water; 0.5–1 mg L^{-1} FAC, 5 min) was estimated by subsequent recovery in YEPD broth (see 3.3.1.2). Cells were washed in HPLC grade water before treatment. Mean values ± SD are shown for at least 3 biological replicates, with different replicate experiments distinguished by different symbols. Comparisons of interest were tested by paired *t*-tests (two-tailed) with correction for multiple comparisons by controlling the false discovery rate at 5% FDR (Benjamini et al., 2006); *p<0.05; **p<0.01.

3.3.5 Damage to FeS cluster proteins

3.3.5.1 Activity of the FeS cluster protein aconitase is decreased after EW treatment

Methionine in its oxidised state (MetO) in cells has previously been reported to increase oxidative damage to iron-sulphur clusters (Sideri et al., 2009). We hypothesised that the protection against EW by methionine observed in the present study could be related to the maintenance of FeS protein function. Protein

extracts from yeast were exposed to EW (10% [v/v]; 180–200 mg L^{-1} FAC). Primaquine exposure served as a positive control as this drug is known to target FeS clusters (Lalève et al., 2016). Relative activity of the FeS cluster protein aconitase (normalised to fumarase activity) was decreased by ~70% in EW treated extracts (Figure 3-14 A; note that fumarase is also a citric acid cycle enzyme but does not contain an FeS cluster). The absolute enzyme activity (Figure 3-14 B) of fumarase was affected much less by EW compared to aconitase (absolute fumarase activity was decreased by ~20%, paired t-test (two-tailed) of EW-treated vs. untreated fumarase activity gives an FDR-adjusted p-value = 0.250; absolute aconitase activity was decreased by ~73%, FDR-adjusted p-value = 0.020). As fumarase activity was not strongly affected by EW treatments, aconitase only was assayed in further *in-vitro* experiments, at standardised protein-extract additions. Adding Met or Cys to the *in-vitro* EW treatments of protein extracts suppressed the strong inhibition of aconitase activity by EW (Figure 3-15).

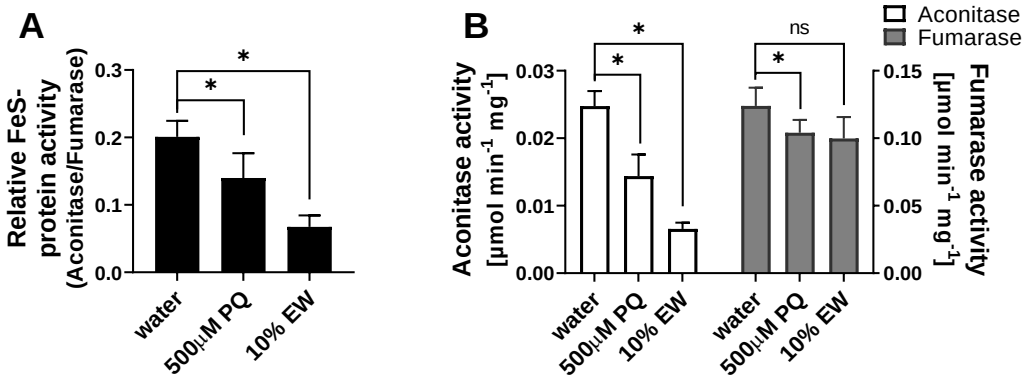

Figure 3-14: Decreased activity of the FeS protein aconitase after *in-vitro* EW treatment. Crude protein extracts from exponentially growing *S. cerevisiae* BY4741 cells were treated *in-vitro* with 500 µM primaquine (PQ), 10% [v/v] EW [180–200 mg L^{-1} FAC] or HPLC grade water (control) for 20 min, before determination of aconitase and fumarase activities. A) Aconitase activity is normalised to fumarase activity (a non-FeS protein). B) Absolute activities. Mean values ± SD are shown for at least 3 biological replicates. *p<0.05; ns, not significant; according to paired *t*-test (two-tailed) with correction for multiple comparisons by controlling the false discovery rate at 5% FDR (Benjamini et al., 2006).

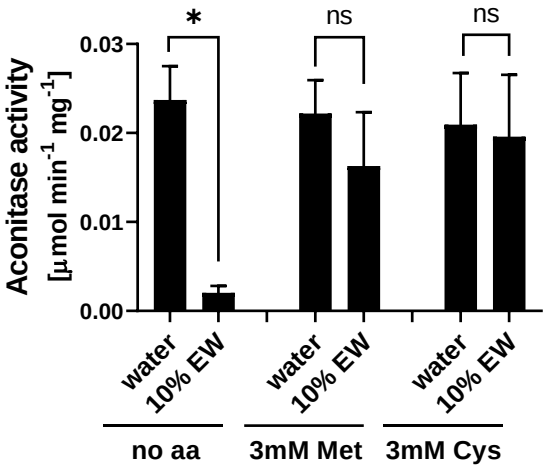

Figure 3-15: Met and Cys protect aconitase from inhibition by EW *in-vitro*. Crude protein extracts from exponentially growing *S. cerevisiae* BY4741 cells were treated *in-vitro* with 10% [v/v] EW [180–200 mg L^{-1} FAC] or HPLC grade water (control) for 20 min, before determination of aconitase activity. Met or Cys (3 mM) were added to protein extracts shortly before EW exposure. Mean values ± SD are shown for at least 3 biological replicates. *p<0.05; ns, not significant; according to paired *t*-test (two-tailed) with correction for multiple comparisons by controlling the false discovery rate at 5% FDR (Benjamini et al., 2006). aa, amino acid.

To test whether similar effects on aconitase activity could be detected during *in-vivo* EW treatment of yeast cells, a lower EW dilution (0.3% [v/v]; 5.4–6 mg L^{-1} FAC) was used for yeast cell treatments, to avoid non-specific effects due to lethality, yielding >80% cell viability according to cfu counts and >50% according to the y-intercept method (Figure 3-16 C; difference between the methods was not unexpected, see 3.3.1.2). Enzyme assays with protein extracts obtained from the EW-treated cells revealed a ~22% decrease in relative aconitase activity ($p = 0.0425$) (Figure 3-16 A,B; note that the decrease of absolute (as opposed to normalised) aconitase activity is not significant ($p = 0.056$) as it does not take into account the slight decrease in fumarase activity, as an internal control for general protein activity, in the EW treated samples). A protocol for FeS cluster reconstitution adapted from published protocols (Moulis and Meyer, 1982, Mons et al., 2018, Ollagnier-de-Choudens et al., 2001) was tested on protein extracts of EW treated yeast cells (0.3% EW, samples from Figure 3-16), however the FeS

cluster reconstitution was not successful in restoring aconitase activity (see Appendix G, 6.7), which may be due to observed low aconitase stability at room temperature during the reconstitution protocol, the need for further processing steps (e.g., purifying the enzyme from the crude protein extract), the presence of oxygen during the reconstitution (performed in plastic tubes) or due to additional damage to the aconitase enzyme by EW that cannot be repaired by reconstituting the FeS cluster, such as (potentially irreversible) damages to amino acid side chains (e.g., aconitase contains 18 Met-residues, 9 Cys, 9 Trp, 21 Tyr and these amino acids were highly reactive with EW in other experiments in this thesis).

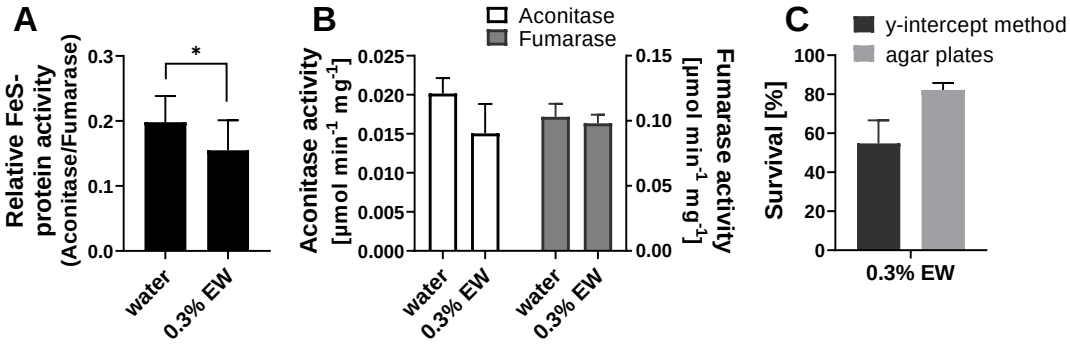

Figure 3-16: Decreased aconitase activity after EW treatment of yeast cells (*in-vivo*). *In-vivo* EW treatment (0.3% [v/v] EW; 5.4–6 mg L^{-1} FAC, 5 min) of exponentially growing *S. cerevisiae* BY4741 cells followed by protein extraction and determination of enzyme activities (the dense yeast suspensions needed for sufficient protein yield required a higher % EW in these experiments for comparable effect to other *in-vivo* treatments in this study). A) Aconitase activity is normalised against fumarase activity (a non-FeS protein). B) Absolute aconitase and fumarase activities. C) Survival of the yeast cells was determined by spread plating appropriate dilutions on agar plates and subsequent colony enumeration as well as by estimating recovery in YEPD broth (y-intercept method, see 3.3.1.2). Mean values ± SD are shown for at least 3 biological replicates. *p<0.05, according to paired *t*-test (two-tailed).

3.3.5.2 Overexpression of the FeS protein Rli1 increased yeast recovery from EW treatment

A different FeS protein, the essential Rli1 protein, has roles in critical cellular functions such as translation, ribosome biogenesis and recycling (Young et al., 2015). It is an important target of oxidative stress due to impaired supply of the

FeS-cofactor to the protein under such conditions, and Rli1 overexpression in yeast increases resistance to pro-oxidants (Alhebshi et al., 2012). Overexpression of Rli1 increased yeast resistance to EW (Figure 3-17). In contrast, overexpression of a different essential FeS-protein, the ferredoxin Yah1 involved in mitochondrial FeS cluster assembly, did not reproducibly increase resistance to EW, though Yah1 overexpression was previously associated with pro-oxidant sensitivity (Vallières et al., 2017). Taken together, the results in this section suggest that FeS cluster proteins are an important cellular target of EW action.

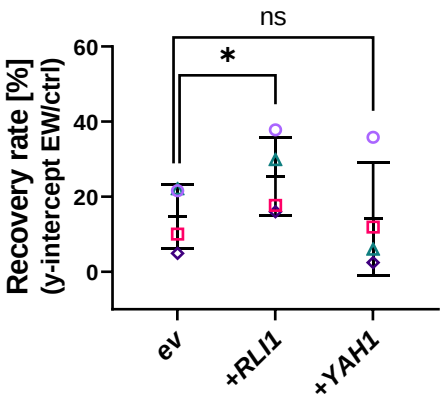

Figure 3-17: Effect of overexpression of FeS cluster proteins on yeast recovery from EW treatment. Overexpression of the essential FeS proteins *RLI1* or *YAH1* from vector pCM190 (ev, empty vector) in *S. cerevisiae* BY4741. Survival of yeasts after EW treatment (0.03–0.05%; 0.5–1 mg L^{-1} FAC, 5 min) was estimated by subsequent recovery in YEPD broth (see 3.3.1.2). Mean values ± SD are shown for at least 3 biological replicates, with different replicate experiments distinguished by different symbols. *p<0.05; ns, not significant; according to paired *t*-tests (two-tailed) with correction for multiple comparisons by controlling the false discovery rate at 5% FDR (Benjamini et al., 2006).

3.3.6 Investigating Met mistranslation in yeast in response to EW treatment

3.3.6.1 Fluorescent reporters for detecting Met misincorporation

In conditions of oxidative stress, Met misincorporation into proteins has been reported to increase in mammalian cells and this effect has been proposed to be

a protective response mechanism against ROS-induced protein damage (Netzer et al., 2009). Met misincorporation into proteins in unstressed conditions has been reported in *S. cerevisiae* for Arg/Lys to Met substitutions (Wiltrout et al., 2012). It was hypothesised that Met misincorporation may take place during/after EW stress conditions, and that this may contribute to the protective effect of Met pre-culture against EW treatment. A fluorescence-based reporter construct for Met misincorporation has been developed previously for mammalian cells, using a GFP-mCherry fusion protein (Gomes et al., 2016). The mCherry fluorophore is normally formed in an auto-catalysed reaction of three amino acids, one of which is Met. Replacing Met with a different amino acid will result in a non-fluorescent protein, as shown for substitutions with Lys, Asp and Glu (Gomes et al., 2016). In mCherry gene variants encoding for such substitutions, a gain-of-fluorescence represents the misincorporation of Met at the mutated position.

Similar constructs were generated for *S. cerevisiae* in this study. The starting plasmid was yEpRG which contains a fusion of yeast codon-optimised mCherry (yEmRFP) and yeast-enhanced GFP (yEGFP) (Altamura et al., 2016). The fluorophore of mCherry consists of Met-Tyr-Gly (Shaner et al., 2004) which are located at residues 71–73 in yEmRFP. The Met codon (ATG) was mutated to Glu (GAA), Lys (AAA), Asp (GAT) or Arg (AGA). The choice of amino acids was based on the constructs published previously (Gomes et al., 2016) and the reported Met misincorporation events in yeast (Wiltrout et al., 2012). For each amino acid, the yeast-optimal codon was chosen based on the same codon-optimisation that was employed to generate yEmRFP (Keppler-Ross et al., 2008).

The absence of mCherry fluorescence was confirmed for yeasts expressing the mutagenised constructs (Figure 3-18 D). The growth behaviour of the two clones independently transformed with the original yEpRG plasmid (strains "mCh-1" and "mCh-2") was very similar to strains transformed with the mutagenised constructs

(Figure 3-18 A). Regarding the GFP fluorescence, small differences in fluorescence intensity were detected between the strains (Figure 3-18 C). For mCh-1 and mCh-2, the GFP and mCherry fluorescences per unit volume of culture increased similarly with increasing cell density (Figure 3-18 B), as expected for the expression of a fusion protein.

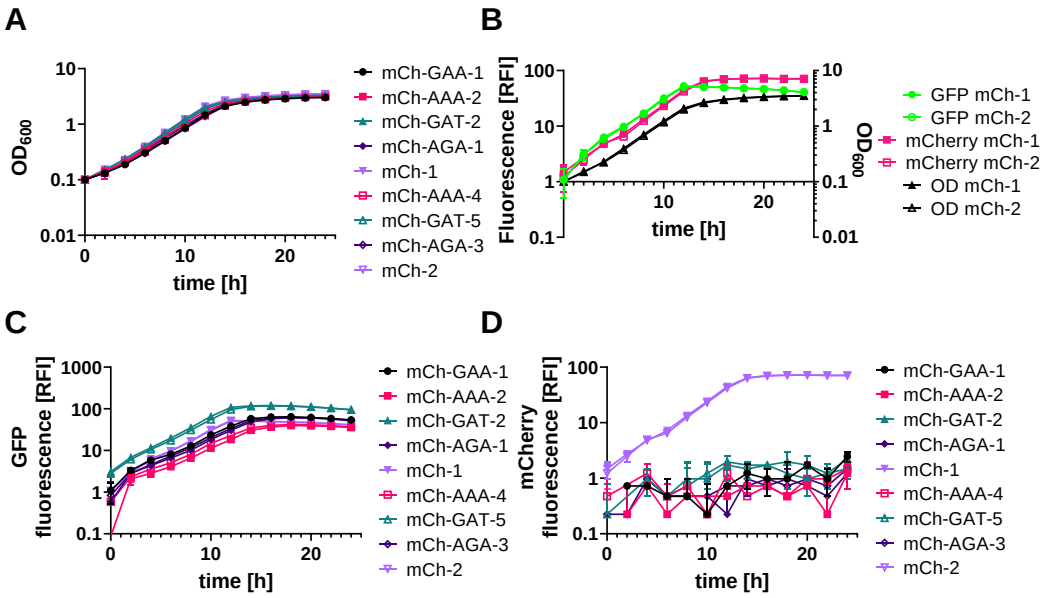

Figure 3-18: Growth and fluorescences of mistranslation reporter strains. *S. cerevisiae* BY4741 transformed with variants of yEpRG (depicted by different symbols and colours, see Table 3-3 for strain details) were grown in YNB broth supplemented with the appropriate amino acids. The OD_{600} (A), GFP (C) and mCherry (D) fluorescence (RFI, relative fluorescence intensity per unit culture volume) were recorded every 2 h in a BioTek® Synergy HTX microplate reader. The background reading for cell-free medium was subtracted from the fluorescence values. B) The GFP (green circles) and mCherry (red squares) fluorescences of the mCh-1 and mCh-2 strains expressing the non-mutagenised fusion protein increased proportionally with the OD_{600} (black triangles). Mean values ± SD are shown for 4 technical replicates (1 biological replicate).

The yEpRG plasmid carries the *URA3* gene as a selection marker, restoring the ability to synthesise uracil in yEpRG-transformed *ura3Δ*-mutant yeast strains (such as *S. cerevisiae* BY4741). Recovery after EW treatment was carried out in non-selective YEPD medium throughout this study which, containing uracil, does not positively select for yEpRG-expressing cells. However, the strains retained their GFP and (for the mCh-1 and mCh-2 strains) mCherry fluorescences in YEPD

throughout the exponential phase for at least 10 h (Figure 3-19 A–C). This supported use of a short-term recovery in YEPD after EW treatment prior to assessing the mistranslation. The 5 min-EW treatment is likely too short for mistranslation event to be detectable in newly synthesized protein, so a subsequent recovery phase allowed for some continued protein synthesis to address this. An alternative approach would have been to test prolonged EW treatments (>5 min), however relevant effects in this chapter (i.e., EW protective effect of Met pre-culture) were observed when treating yeast with EW for 5 min and, to maintain consistency, 5 min-EW treatments were therefore chosen for assessing Met misincorporation.

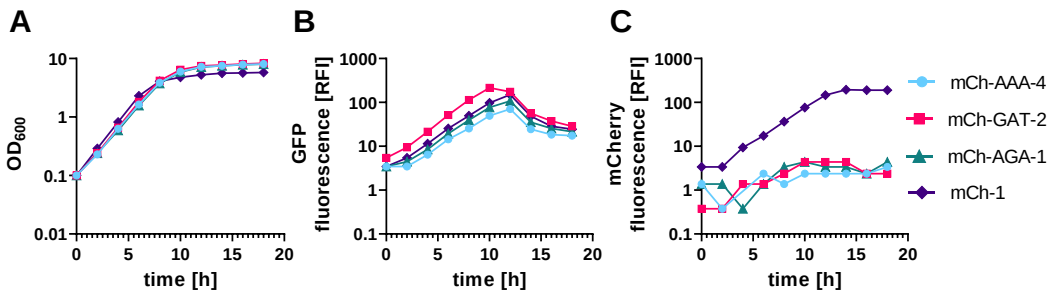

Figure 3-19: Growth and fluorescences of mistranslation reporter strains in non-selective YEPD. *S. cerevisiae* BY4741 strains transformed with variants of yEpRG were grown as described in Figure 3-18, using YEPD broth instead of selective YNB medium. A) OD_{600} reads of yeast growth. B) GFP fluorescence (RFI, relative fluorescence intensity per unit culture volume). C) mCherry fluorescence. Data from 1 biological replicate.

3.3.6.2 Detecting background Met misincorporation with the fluorescent reporter constructs

The strains expressing the different yEpRG variants were assessed by flow cytometry. The non-transformed control strain (BY4741) showed no mCherry or GFP fluorescence, and the mCh-1 strain showed a linear relationship between mCherry and GFP fluorescence of individual cells (Figure 3-20), as expected for the expression of a fusion protein. In the strains carrying the mutagenised constructs mCh-AGA-1, mCh-GAT-5 and mCh-AAA-4, most cells showed GFP

fluorescence but not mCherry. However, the mCh-GAA-1 strain showed low levels of mCherry fluorescence, especially in cells expressing high levels of the fusion protein as indicated by a high GFP signal (Figure 3-20). This gain of mCherry fluorescence suggested that Glu-to-Met misincorporation events may take place in non-stressed conditions in *S. cerevisiae*, similar to the results obtained previously for mammalian cells (Gomes et al., 2016).

Strain	YNB	YEPD
BY4741	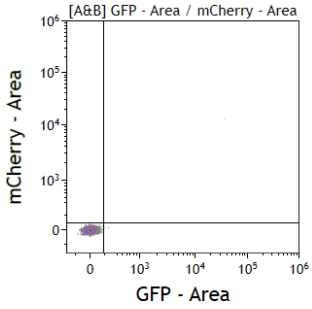	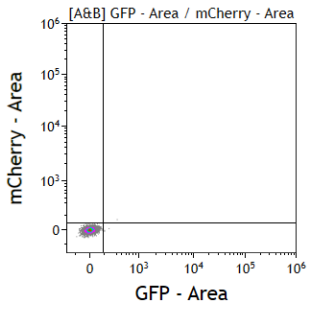
mCh-1	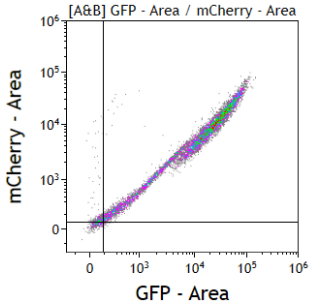	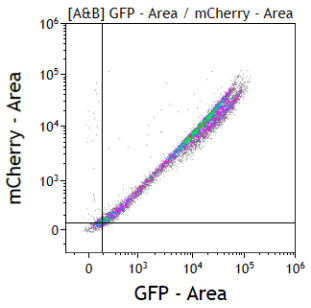
mCh-GAA-1	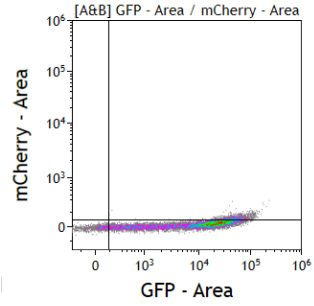	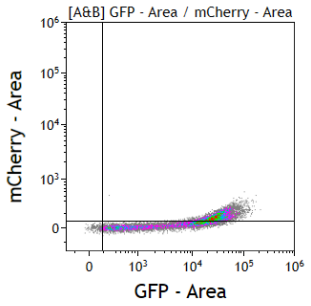

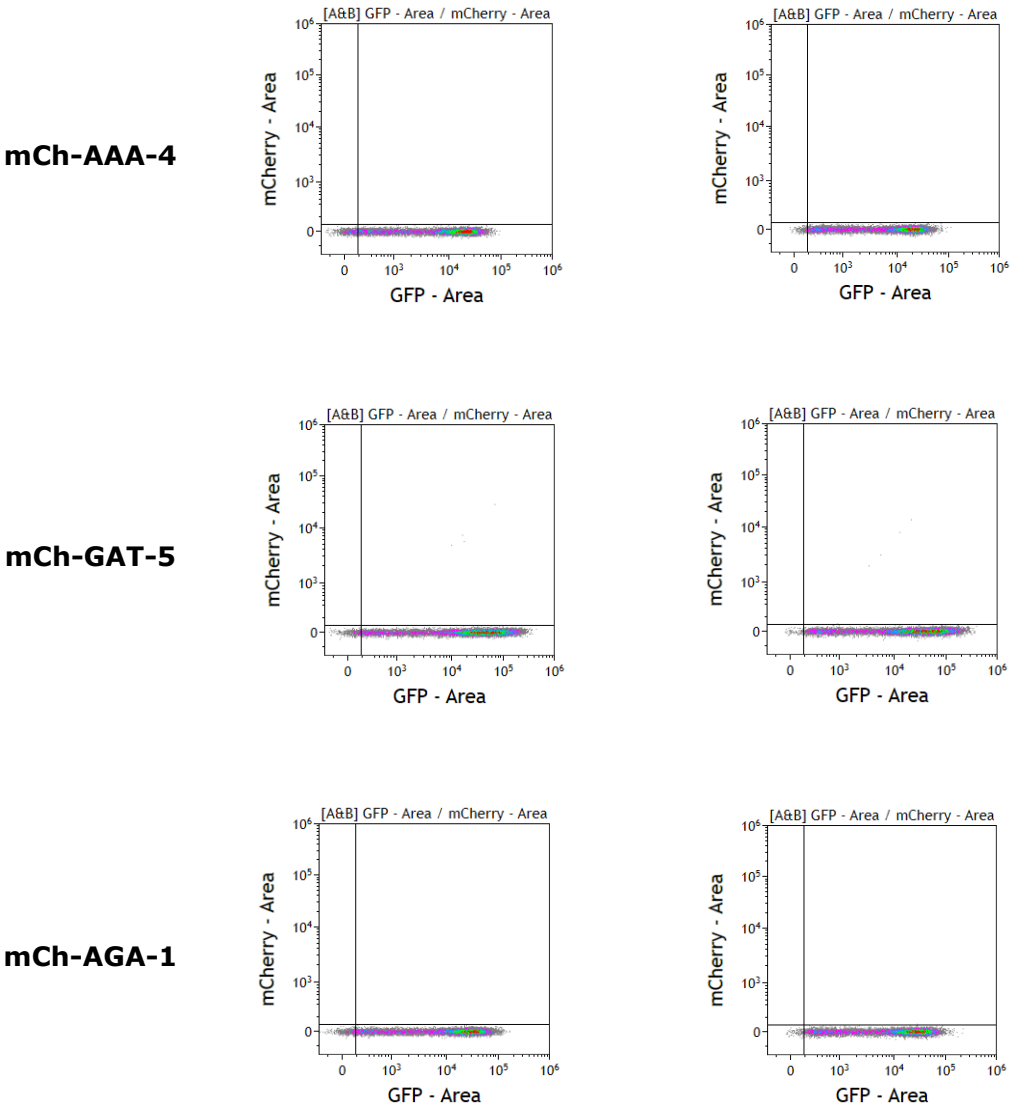

Figure 3-20: Dot plots of cellular mCherry and GFP fluorescences obtained by flow cytometry. *S. cerevisiae* BY4741 transformed or not with yEpRG variants (see Table 3-3) were grown in selective YNB medium or switched to YEPD for 1.5 h. Cell doublets were excluded based on the FSC area-to-height ratio of events (not shown). For each cell (represented by single points), the mCherry fluorescence is plotted on the y-axis against the GFP fluorescence on the x-axis. Data are from one representative from 2 biological replicates. ~10,000 cells were analysed per sample.

The median mCherry fluorescence was calculated to help illustrate the results observed in the dot plots. Compared to the other mutagenised constructs, the mCh-GAA-1 strain showed an increase in the median mCherry fluorescence (Figure 3-21 A; significant according to paired two-tailed *t*-tests with FDR-correction comparing mCh-GAA1 to the other strains). Notably, the mCherry

fluorescence was higher for cells grown in YEPD than in YNB, for all tested strains. The GFP fluorescence varied depending on the strain and was highest for the mCh-GAT-5 strain (Figure 3-21 B). In contrast to mCherry, the GFP fluorescence was lower in YEPD than in YNB for some of the strains.

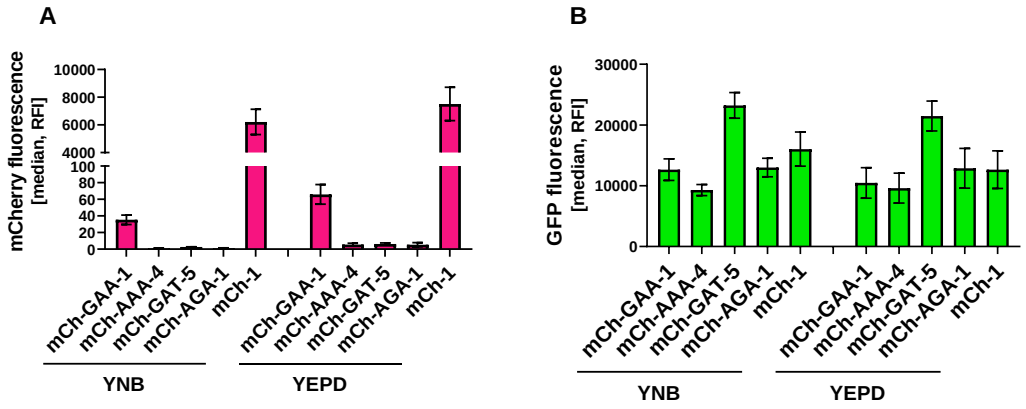

Figure 3-21: Median mCherry and GFP fluorescences of the yEpRG variant strains. *S. cerevisiae* BY4741 transformed with yEpRG variants (see Table 3-3) were grown in selective YNB medium or switched to YEPD for 1.5 h. The median fluorescence from all cells of a sample (excluding doublets) was determined by flow cytometry. A) mCherry fluorescence, B) GFP fluorescence. Mean values (of the medians) ± SD are shown for 2 biological replicates (mCh-AAA-4, mCh-GAT-5, mCh-AGA-1) or at least 6 biological replicates (mCh-GAA-1, mCh-1). RFI, relative fluorescence intensity.

The mCherry and GFP proteins are expressed as a fusion protein. The GFP fluorescence can therefore serve as a measure for the amount of fusion protein expressed. Consequently, the mCherry fluorescence was normalised against the GFP fluorescence. To avoid working with very low numbers, the resulting ratio was multiplied by the factor 1000 ([mCherry fluorescence / GFP fluorescence] * 1000). Different individual cells expressed the fusion protein to different extents, as shown by the cellular GFP fluorescence within samples which was detected over the wide range of 0–10^5 relative units (see x-axis in Figure 3-20). In the mCh-GAA-1 strain, the detected mCherry fluorescence remained low and relatively similar across cells with GFP levels ranging from ~0 up to ~10^4 relative units (Figure 3-22 A). This meant that the mCherry/GFP ratio was comparatively

high at the lowest cellular GFP levels (Figure 3-22 B). Therefore, these particular high values reflect large changes in the GFP fluorescence rather than in mCherry fluorescence, and so do not indicate mistranslation events. This trend to high ratios at low GFP values was observed for all the mutagenised strains but not for the mCh-1 strain due to the higher mCherry fluorescence in this strain.

A cut-off value was therefore chosen at <8000 RFI GFP fluorescence, represented by the vertical line in Figure 3-22 B, to exclude high ratios caused by low GFP fluorescence. For further experiments below, ratios of mCherry/GFP (termed "relative mCherry fluorescence") were only calculated for cells which had a GFP reading equal or larger than 8000, i.e., cells expressing amounts of the fusion protein deemed sufficient for any observed increases in the ratio to represent real relative increases in mCherry fluorescence (i.e., misincorporation events). Consistent with the above observations, the mCherry/GFP ratio was very low in the mCh-GAT-5, mCh-AAA-4 and mCh-AGA-1 strains and was increased in the mCh-GAA-1 strain (Figure 3-23). The low but detectable increase in the ratio for the mCh-GAA-1 strain in the control conditions supports the use of the ratio as a measure of Met misincorporation (consistent with the observed mCherry fluorescence in this particular strain, Figure 3-20, Figure 3-21). The ratio of the mCh-GAA-1 strain was between ~0.5–1% of the ratio calculated for the mCh-1 strain which expresses the unmodified mCherry protein. Methionine misincorporation at Lys and Arg positions was detected at a frequency of 0.66% in 9 yeast proteins (Wiltrout et al., 2012), but the % fluorescence ratio here may not directly translate into % misincorporation.

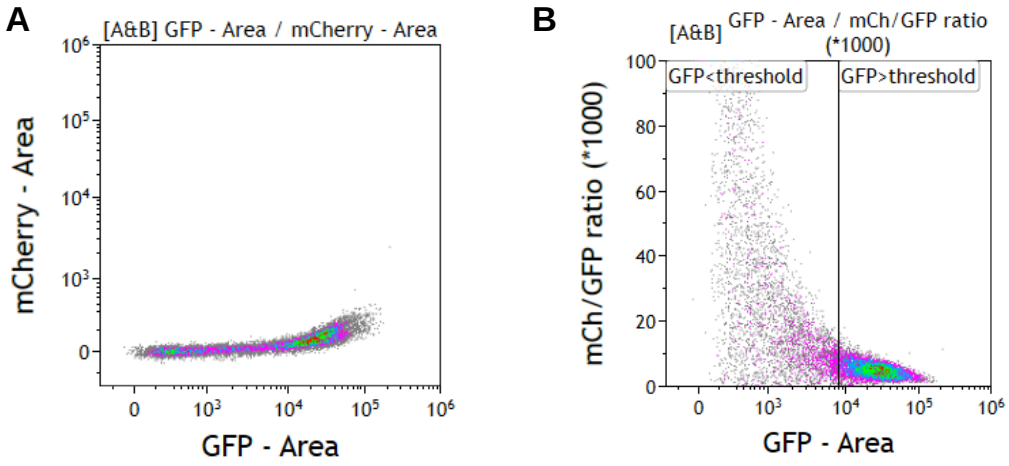

Figure 3-22: Relative mCherry expression: calculating the mCherry/GFP ratio. Data for the mCh-GAA-1 strain (cultivated in YNB) which expresses the mCherry(M71E)-GFP fusion protein. A) Dot plot of the cellular mCherry and GFP fluorescences (~12,500 analysed cells). B) The ratio of mCherry divided by GFP (multiplied by factor 1000 to avoid low decimal numbers) was calculated for each cell and plotted against the cell's GFP fluorescence. The y-axis was limited to 100 but ratios >100 were also detected (at low GFP values). The vertical line represents a cut-off at GFP = 8000 relative units, to exclude very high ratios caused by low GFP fluorescence (at low GFP, detected mCherry was not visibly increased, see A).

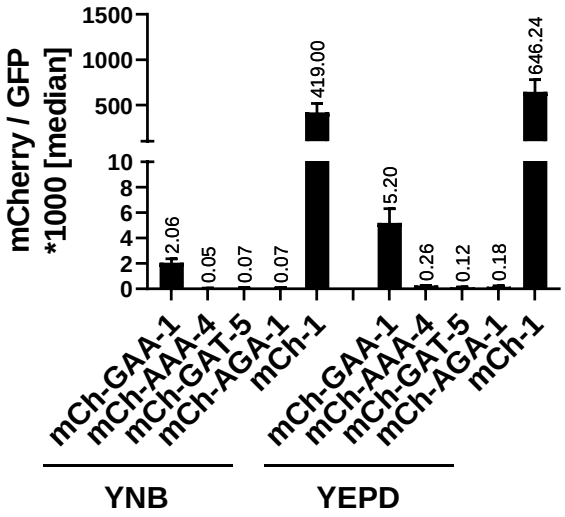

Figure 3-23: Relative mCherry fluorescence in the yEpRG variant strains. *S. cerevisiae* BY4741 transformed with yEpRG variants (see Table 3-3) were grown in selective YNB medium or switched to YEPD for 1.5 h. After excluding events with GFP fluorescence <8000 relative units, the ratio of mCherry to GFP fluorescence was calculated for each cell (multiplied by factor 1000, see Figure 3-22 for details), and the median ratio was determined for each replicate. The bars show the mean values ± SD of the median for 2 biological replicates (mCh-AAA-4, mCh-GAT-5, mCh-AGA-1) or at least 6 biological replicates (mCh-GAA-1, mCh-1). Each bar is labelled with its averaged median value.

3.3.6.3 Does EW treatment increase Met misincorporation?

To assess whether *S. cerevisiae* increases the Met misincorporation rate in response to EW treatment, in a first test the constructed strains were exposed to 0.02% EW (~0.4 mg L^{-1} FAC) and the fluorescence was determined immediately post-treatment or after a 2 h recovery period in rich YEPD medium. No increase in the mCherry/GFP ratio was detected compared to the untreated controls (Figure 3-24 A). The yeast recovery rate was around 70–80% (except mCh-1: 43%; note that recovery of mCh-1 was not consistently lower in other experiments, cf. Figure 3-26), indicating high survival (Figure 3-24 B).

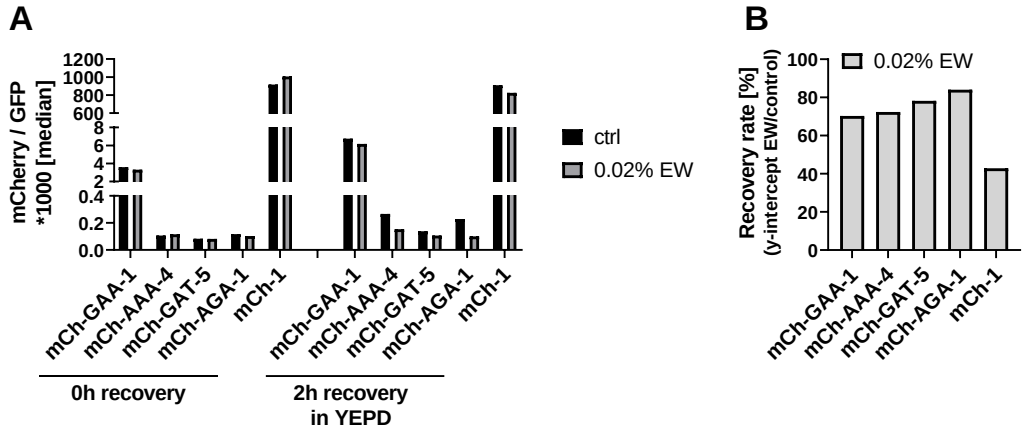

Figure 3-24: Relative mCherry fluorescence from the Met misincorporation constructs after 0.02% EW treatment. *S. cerevisiae* BY4741 transformed with yEpRG variants (see Table 3-3) were treated with 0.02% [v/v] EW [~0.4 mg L^{-1} FAC] for 5 min. Cells were analysed by flow cytometry immediately post-treatment (0h) or after 2 h recovery in YEPD (30°C, shaking). A) The mCherry and GFP fluorescences of cells were determined and the fluorescence ratio calculated for each event as described in the legend to Figure 3-22. ~9,000 cells per sample were analysed. For each condition, the median of the per-cell fluorescence ratios was determined. EW, grey bars; ctrl: no-treatment control, black bars. B) Survival of yeasts after EW treatment was estimated by subsequent recovery in YEPD broth (see 3.3.1.2). Data from 1 biological replicate.

Because no increase in Met misincorporation was detected after treatment with 0.02% EW and 2 h recovery in YEPD, recovery periods between 0.5 and 1.5 h were also tested in combination with different EW concentrations (0.01–0.03% EW; 0.2–0.6 mg L^{-1} FAC). The following experiments were performed using the

mCh-GAA-1 and mCh-1 strains only; the other mutagenised constructs (mCh-AAA-4, mCh-GAT-5, mCh-AGA-1) had shown no or only very low mCherry fluorescence, so mCh-GAA-1 was deemed more promising due to the detectable apparent levels of background Met misincorporation with this construct. The other constructs were tested in follow-up experiments using the "optimal" EW treatment conditions determined as described below. Strain mCh-1 was used as a control strain to assess any non-specific effects that EW treatment may have on the GFP or mCherry fluorescence, as fluorescence changes in this strain do not represent Met misincorporation events (the mCherry gene in this strain already encodes the correct Met71).

For an initial quality check, the GFP fluorescence of both the mCh-GAA-1 and mCh-1 strains was assessed post-EW treatment. A small trend towards lower median fluorescence with increasing % EW was observed for these strains (Figure 3-25 A,B), which may have been related to decreasing viability (<15% recovery at 0.03% EW, except mCh-1 in one experiment (83%), Figure 3-26 C). The differences between GFP fluorescence of EW-treated samples compared to control samples were not significant, indicating that reporter protein expression was not disrupted non-specifically by the treatment, so mistranslation could be assessed in these conditions, especially at 0.01% and 0.02% EW.

Unexpectedly, the median mCherry fluorescence was reduced after treatment with 0.01% EW (Figure 3-25 C,D), which was only significant for the mCh-GAA-1 strain after 1 h recovery, although FDR-adjusted p-values were close to significant ($p = 0.05–0.07$) for 1.5 h and 1 h in both strains. At 0.03% EW, the mCherry fluorescence in the mCh-1 (control) strain seemed somewhat increased, further suggesting that the low survival at this treatment condition may result in unspecific effects, making this high EW concentration less appropriate to assess mistranslation compared to the other two concentrations.

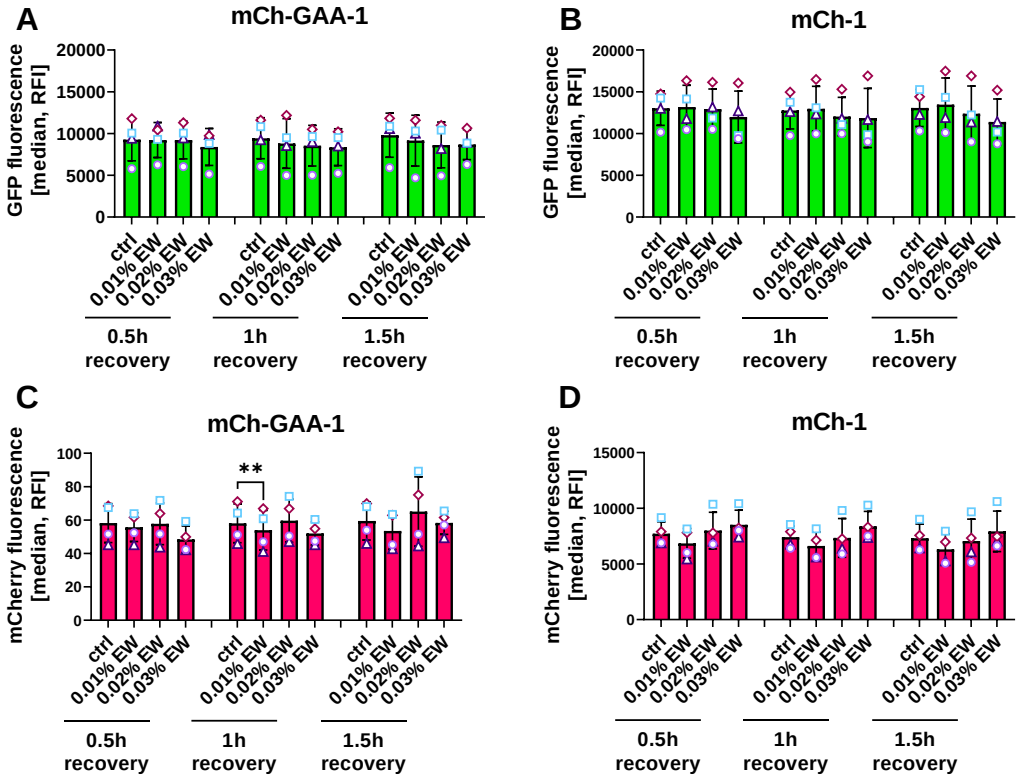

Figure 3-25: Effect of EW treatment on cellular GFP and mCherry fluorescence. *S. cerevisiae* expressing yEpRG variants (mCh-GAA-1 [A,C], mCh-1 [B,D]) were treated with EW (0.01–0.03% [v/v]; 0.2–0.6 mg L^{-1} FAC, 5 min) and recovered in YEPD for 0.5–1.5 h (ctrl, no-EW control). Cell samples were analysed by flow cytometry and the median GFP (A,B) and mCherry fluorescence (C,D) was measured. Mean values ± SD of the medians are shown for 4 biological replicates. Values of individual replicates are specified by different symbols and colours. Significance tests compared all treatments with the respective no-EW control; **p<0.01; according to paired *t*-test (two-tailed) with correction for multiple comparisons by controlling the false discovery rate at 5% FDR (Benjamini et al., 2006). RFI, relative fluorescence intensity.

To assess the Met misincorporation rate, the mCherry/GFP ratio was calculated in the mCh-GAA-1 strain. No significant increase in the ratio was detected at any of the EW concentrations tested (Figure 3-26 A). Small apparent increases (consistent across all four replicates) in the ratio after treating with 0.02% EW and recovering for either 1 or 1.5 h (compared to the untreated controls) were not significant and could not be reproduced in further experiments (see Figure 3-28, Figure 3-29 and Figure 3-30). In the mCh-1 strain, an increase in the mCherry/GFP ratio was detected in some replicates at 0.03% EW, further supporting that non-specific effects may take place at this treatment concentration

(Figure 3-26 B). Consistent with the observed decrease in median mCherry fluorescence for samples treated with 0.01% EW (Figure 3-25), the ratio for this condition was reduced compared to the control in most replicate experiments (non-significant in mCh-GAA-1, significant at the 0.5 h time point in mCh-1). It was observed that the recovery rate in 0.01% EW-treated samples was >100% in 3 out of 4 replicates (Figure 3-26 C).

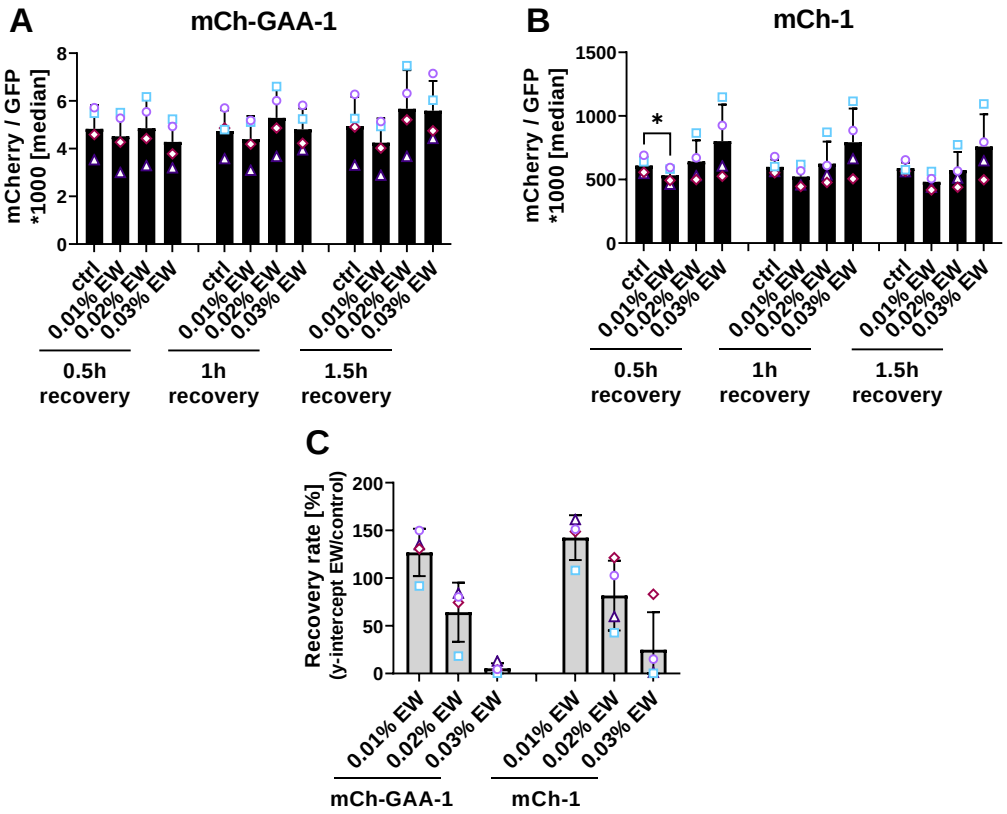

Figure 3-26: Relative mCherry fluorescence from the Met misincorporation constructs after EW treatment and recovery. *S. cerevisiae* expressing yEpRG variants (mCh-GAA-1 [A,C], mCh-1 [B,C]) were treated with EW (0.01–0.03% [v/v]; 0.2–0.6 mg L^{-1} FAC, 5 min) and recovered in YEPD for 0.5–1.5 h (ctrl, no EW-control). A,B) Samples were analysed by flow cytometry to determine the mCherry and GFP fluorescence of individual cells and the fluorescence ratio was calculated for each cell as described in Figure 3-22. For each condition and replicate, the median of the ratios was determined. C) Survival of yeasts after EW treatment was estimated by subsequent recovery in YEPD broth (see 3.3.1.2). Bars show means ± SD for 4 biological replicates. Values of individual replicates are specified by different symbols and colours. In A and B, significance tests compared all treatments with the respective no-EW control; *p<0.05; according to paired *t*-test (two-tailed) with correction for multiple comparisons by controlling the false discovery rate at 5% FDR (Benjamini et al., 2006).

Because a small, non-significant increase in the mCherry/GFP ratio was detected with the mCh-GAA-1 strain at 0.02% and 1.5 h, these conditions were also tested in other clones of mCh-GAA-strains generated in this study, named mCh-GAA-2, mCh-GAA-3 and mCh-GAA-4 (see Table 3-3). Strains mCh-GAA-1–3 showed comparable fluorescence intensities of both GFP and mCherry whereas these signals were much weaker in the mCh-GAA-4 strain (Figure 3-27 A,B). However, all four strains had detectable levels of mCherry fluorescence that were higher than the mCherry levels obtained with the other constructs (mCh-AGA-1, mCh-AAA-4, mCh-GAT-5; Figure 3-21), indicating background Glu-to-Met misincorporation events in all four mCh-GAA clones.

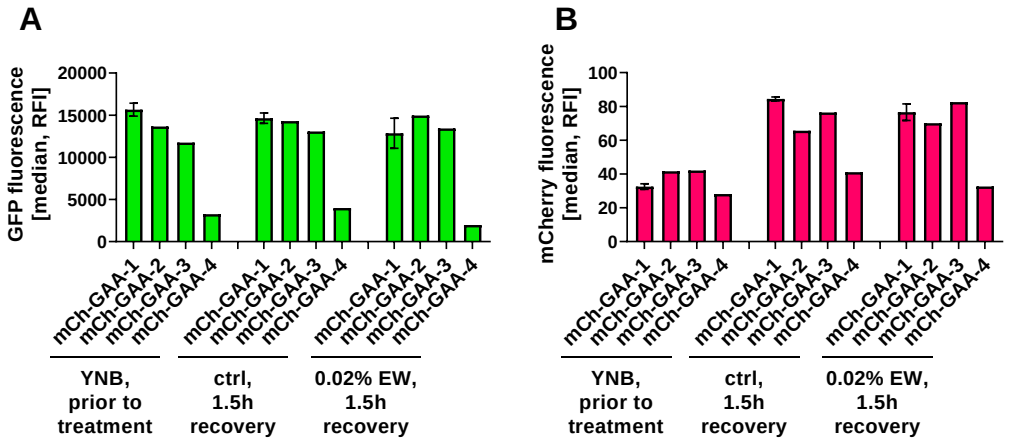

Figure 3-27: GFP and mCherry fluorescence in the strains mCh-GAA1–4. Exponentially growing *S. cerevisiae* expressing yEpRG variants with a M71E mCherry mutation (mCh-GAA-1–4) were harvested (YNB prior to treatment), and treated with 0.02% [v/v] EW [~0.4 mg L^{-1} FAC] for 5 min, followed by 1.5 h recovery in YEPD (ctrl, no EW-control). Fluorescence was determined by flow cytometry. A) Median GFP fluorescence. B) Median mCherry fluorescence. Data from 1 biological replicate (~11,000 cells were analysed per sample), except mCh-GAA-1: mean values (of the medians) ± SD are shown for 2 biological replicates both grown on the same day as the other strains. RFI, relative fluorescence intensity.

The mCherry/GFP ratio was calculated to assess the Met misincorporation rate after EW treatment in the different mCh-GAA-strains. This experiment consists of one biological replicate only and therefore does not allow the assessment of statistical significance, however comparing the results of the different mCh-GAA

clones to each other will indicate whether any observed effect is consistent across the clones. In contrast to the previous results (Figure 3-26 A), treatment with 0.02% EW combined with 1.5 h recovery in YEPD did not result in a higher mCherry/GFP ratio in the mCh-GAA-1 strain compared to the untreated control in this experiment (Figure 3-28 A). Similarly, the mCh-GAA-2 and mCh-GAA-4 strains showed no increase, however a small increase was detected in mCh-GAA-3. Potentially, this may be related to the yeast recovery rates in this experiment (≥100% for mCh-GAA-1, -2 and -4; Figure 3-28 B) which was higher than the recovery at the same treatment condition in the previous experiment (up to 84%; Figure 3-26 C), whereas the recovery of mCh-GAA-3 (70%) was more similar to the previous experiment.

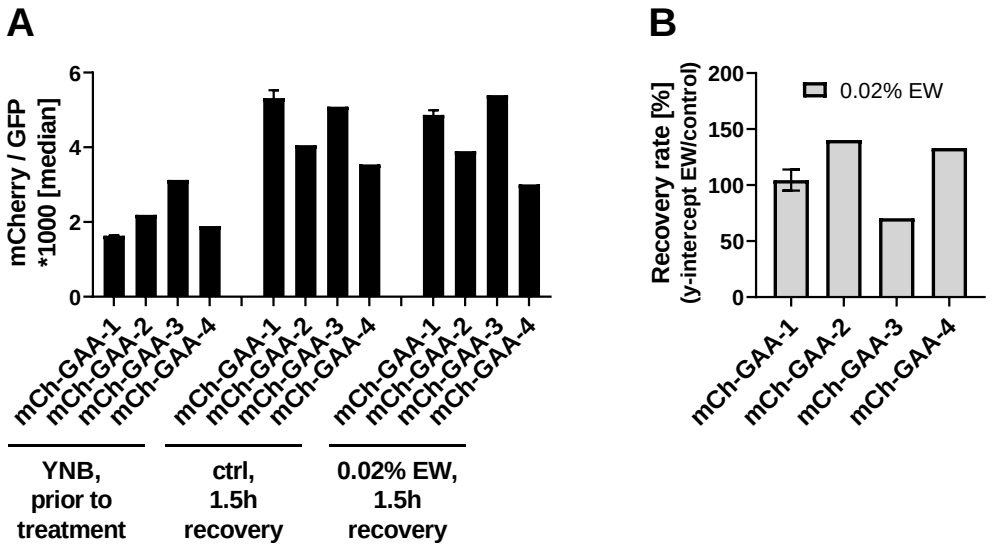

Figure 3-28: Relative mCherry fluorescence in the mCh-GAA-1–4 strains after EW treatment. *S. cerevisiae* expressing yEpRG variants with a M71E mCherry mutation (mCh-GAA-1–4) were harvested (YNB prior to treatment), and treated with 0.02% [v/v] EW [~0.4 mg L^{-1} FAC] for 5 min, followed by 1.5 h recovery in YEPD (ctrl, no EW-control). A) Samples were analysed by flow cytometry to determine the mCherry and GFP fluorescences of individual cells and the fluorescence ratio was calculated for each event as described in Figure 3-22. For each condition and replicate, the median of the ratios was determined. B) Survival of yeasts after EW treatment was estimated by subsequent recovery in YEPD broth (see 3.3.1.2). Data from 1 biological replicate (~11,000 cells were analysed per sample), except mCh-GAA-1: mean values (of the medians) ± SD are shown for 2 biological replicates both grown on the same day as the other strains.

Finally, the condition that resulted in a small, non-significant increase of the mCherry/GFP ratio in the mCh-GAA-1 strain in the first experiment (Figure 3-26 A) was applied to the other mutagenised strains. The ratio was not increased after EW treatment compared to the control for any of the strains, including the mCh-GAA-1 strain in this experiment (Figure 3-29 A). The yeast survival was in the expected range (~70–80% recovery) and slightly higher in the mCh-GAA-1 strain (2 replicates, 83 and 99%, Figure 3-29 B). This experiment consisted of one biological replicate only and was not repeated due to the apparent lack of effect of EW treatment on the relative mCherry fluorescence. Taken together, the data do not support the hypothesis that 5 min EW treatments induce Met misincorporation in yeast.

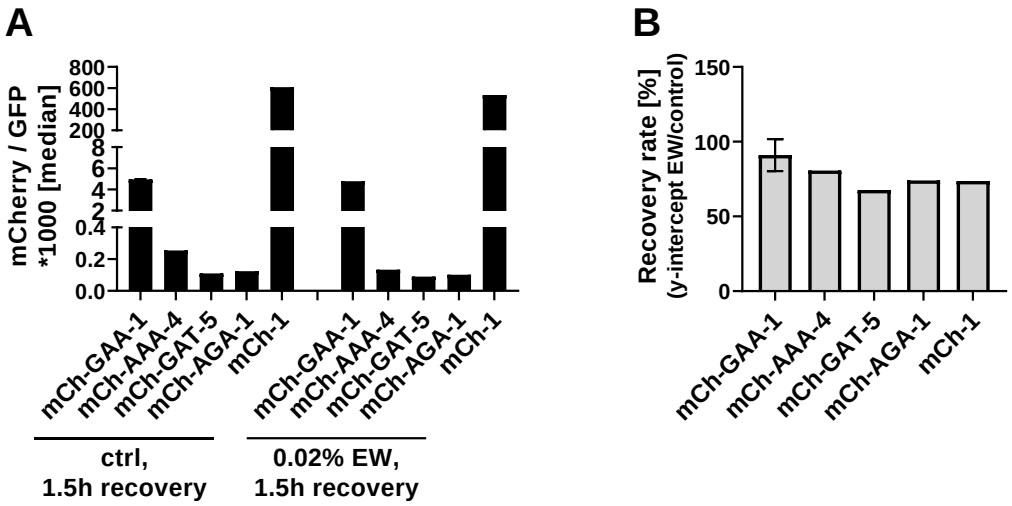

Figure 3-29: Relative mCherry fluorescence from different yEpRG variants after 0.02% EW treatment and 1.5 h recovery. *S. cerevisiae* BY4741 transformed with yEpRG variants (see Table 3-3) were treated with 0.02% [v/v] EW [~0.4 mg L^{-1} FAC] for 5 min, and recovered in YEPD for 1.5 h. A) The mCherry and GFP fluorescences of cells were determined by flow cytometry and the fluorescence ratio was calculated for each event as described in Figure 3-22. For each condition and replicate, the median of the ratios was determined. B) Survival of yeasts after EW treatment was estimated by subsequent recovery in YEPD broth (see 3.3.1.2). Data from 1 biological replicate (~12,000 cells were analysed per sample), except mCh-GAA-1: mean values (of the medians) ± SD are shown for 2 biological replicates both grown on the same day as the other strains.

3.3.6.4 Does Met pre-culture affect the Met misincorporation?

Growing *S. cerevisiae* in medium with increased Met concentrations (0.3 mM instead of 0.13 mM) prior to EW treatment increased the yeast survival after the treatment (see 3.3.2). One possible explanation could be that increased Met levels lead to higher levels of Met misincorporation into proteins, which would then protect other residues in the proteins against oxidative damage, as proposed previously (Netzer et al., 2009, Lee et al., 2014a). In a first set of experiments, the mCh-GAA-1 and mCh-1 strains were exposed to increased Met levels (0.3 mM) in YNB for 4 h before sampling for flow cytometry. No difference in the mCherry/GFP ratio was recorded when comparing the 0.13 mM Met condition with the 0.3 mM Met condition (Figure 3-30 A). In a second experiment, mCh-GAA-1 was cultured with high Met levels for 17 h, cells were harvested and washed to remove extracellular Met and subsequently treated with EW and recovered for 1.5 h in YEPD. The cells pre-exposed to 0.3 mM Met actually showed decreased mCherry/GFP ratios compared to the 0.13 mM Met condition, both after 0.02% EW treatment and in the untreated control (Figure 3-30 C). Observed differences between the control in panel C (decreased ratio at 0.3 mM Met), and similar samples in panel A (no decrease), may relate either to the differences in Met pre-culture duration (4 h in A vs. 17 h in C), sampling from different media (sampling directly from the pre-culture YNB medium in A vs. sampling from the YEPD recovery medium in C) and/or the growth phase at which cells from the Met pre-culture were harvested from YNB for assay (for flow cytometry assay in A and for EW treatment/recovery, followed by flow cytometry, in C), which was at higher OD_{600} values for the samples in panel C than in A (Figure 3-30 B,D). The decrease in the mCherry/GFP ratio does not support the hypothesis that Met pre-culture protects yeast cells against EW by increasing the Met misincorporation rate. In this experiment, the initially suggested increase in mCherry/GFP ratio compared to the control after 0.02% EW treatment (Figure 3-26) could not be reproduced, similar to a lack of increase in Figure 3-28. The yeast recovery at this

concentration was higher (83–111% recovery, Figure 3-30 E) than in Figure 3-26 (≤84%) and more similar to Figure 3-28 (≥100%). Taken together, the present data do not support a strong effect of Met pre-culture and EW treatment on the Met misincorporation rate in yeast.

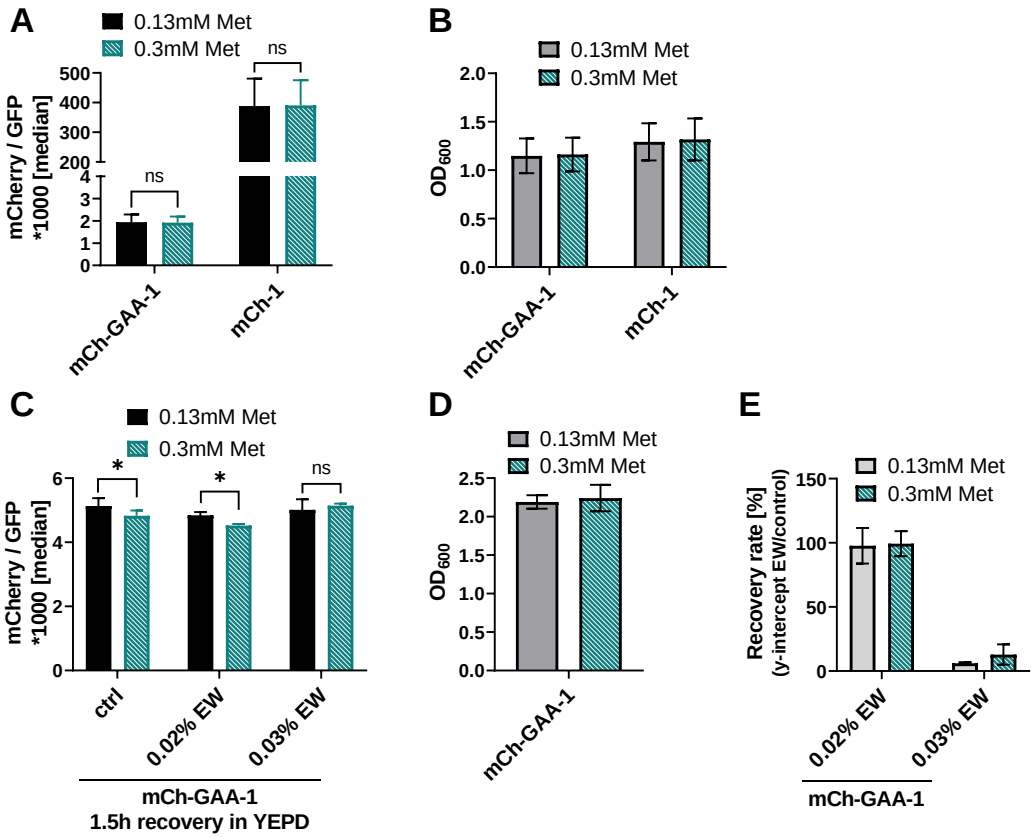

Figure 3-30: Relative mCherry fluorescence from the Met misincorporation constructs after Met pre-culture and EW treatment. A,B) *S. cerevisiae* expressing yEpRG variants (mCh-GAA-1, mCh-1) were grown in YNB in the presence of 0.13 or 0.3 mM Met for 4 h. C–E) Met pre-culture with mCh-GAA-1 as in A, except that the pre-culture period was 17 h, and samples were treated with EW dilutions (0.02–0.03% [v/v]; 0.4–0.6 mg L^{-1} FAC, 5 min) and recovered in YEPD for 1.5 h (ctrl, no-EW control). Note that the data from the 0.13 mM condition of 2 of the replicates in this dataset is the same mCh-GAA-1-data as shown in Figure 3-29. A,C) Samples were analysed by flow cytometry to determine the mCherry and GFP fluorescences of individual cells and the fluorescence ratio was calculated for each cell as described in Figure 3-22. For each condition and replicate, the median of the ratios was determined. B,D) The OD_{600} of the YNB cultures was recorded after 4 h (B) or 17 h (D) prior to harvesting cells from the pre-culture media. E) Survival of yeasts after EW treatment was estimated by subsequent recovery in YEPD broth (see 3.3.1.2). Bars show mean values ± SD for at least 3 biological replicates. *p<0.05; ns, not significant; according to paired *t*-test (two-tailed) with correction for multiple comparisons by controlling the false discovery rate at 5% FDR (Benjamini et al., 2006).

3.3.6.5 Testing the constructs with reported inducers of mistranslation: arsenite and paromomycin

The study that developed the fluorescent reporter for mammalian cells used arsenite treatment to induce an oxidative stress-dependent increase in Met misincorporation (Gomes et al., 2016). Paromomycin at 8.1–40 µM is known to increase mistranslation events in yeast including stop-codon readthrough, Arg-to-His and His-to-Tyr misincorporation (Vallières et al., 2020). The EW treatment in yeast did not have a strong effect on the Met misincorporation rate, as described in the preceding sections, so control treatments with other reported misincorporation-inducers (arsenite, paromomycin) might help to determine whether the lack of effect is specific to the EW treatment, or extends to other treatments, potentially suggesting general differences between yeast and mammalian cells regarding Met misincorporation.

Treating yeast with 125 µM arsenite for 3.5 h in this study did not lead to a significant increase of the relative mCherry fluorescence in the mCh-GAA-1 strain (FDR-adjusted p = 0.126, paired two-tailed *t*-test), although the ratio was slightly increased compared to the untreated control in all 5 biological replicates, and no such increase could be observed in the mCh-1 strain (Figure 3-31 A). No increase in the mCherry/GFP ratio was observed after treatment with 100 µM or 200 µM paromomycin (Figure 3-31 A,B). These treatment concentrations were sub-lethal (Figure 3-31 C,D; OD_{600} values are given for culture in the presence of arsenite or paromomycin (continuous stress exposure) in these experiments instead of recovery rates which apply only for post-treatment growth analysis). A two-fold higher concentration of arsenite (250 µM) seemed to increase the relative mCherry fluorescence more strongly (Figure 3-31 B; 1.2-fold increase, non-significant; FDR-adjusted p = 0.055). At this concentration, the growth was reduced by ~32% compared to the control growth (Figure 3-31 D). It cannot be ruled out that higher arsenite concentrations than used here may result in a

stronger and significant increase in relative mCherry fluorescence, indicative of Met misincorporation. However, higher concentrations would be expected to also reduce the yeast growth more strongly and mistranslation events in such conditions might be non-specific side-effects of high stress of cell death.

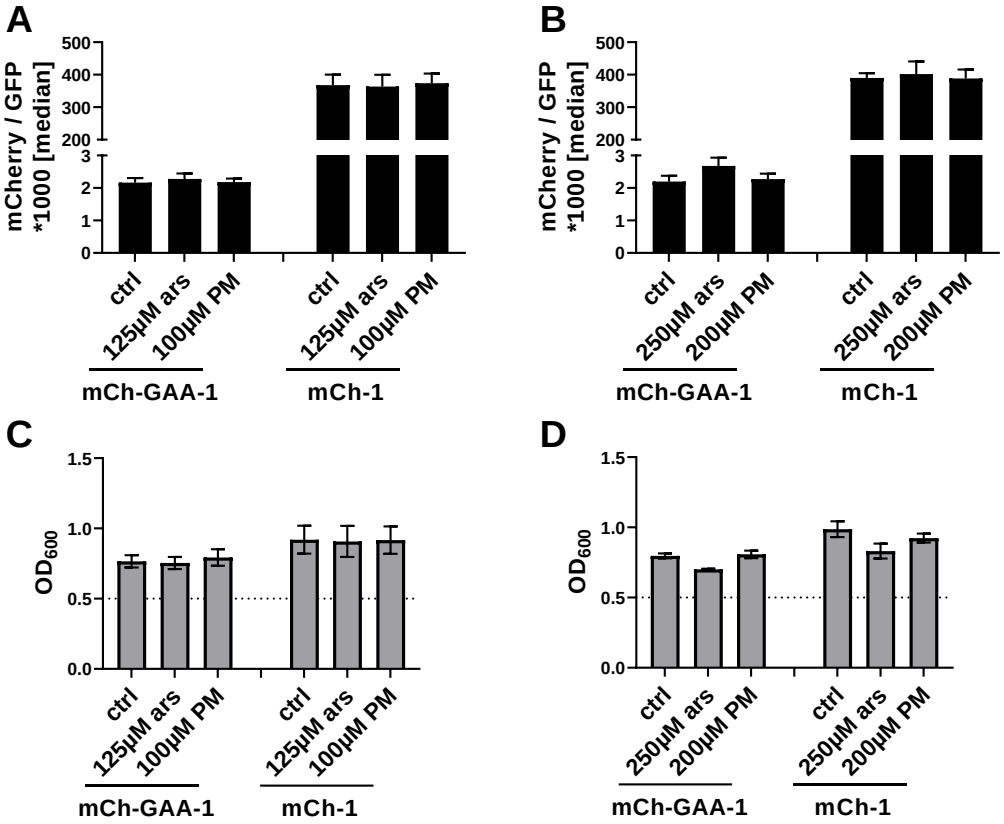

Figure 3-31: Relative mCherry fluorescence from the Met misincorporation constructs after arsenite or paromomycin exposure for 3.5 h. *S. cerevisiae* expressing yEpRG variants (mCh-GAA-1, mCh-1) were exposed to arsenite (ars) or paromomycin (PM) at the specified concentrations for 3.5 h in selective YNB broth in shaking conditions in a BioTek® microplate reader (ctrl: stressor-free YNB). A,B) The mCherry and GFP fluorescence of cells was determined by flow cytometry and the fluorescence ratio was calculated for each cell as described in Figure 3-22. For each condition and replicate, the median of the ratios was determined. C,D) Cells were inoculated to OD_{600}~0.5 (dotted line) and the OD_{600} was determined after 3.5 h before sampling cells for flow cytometry analysis. Data are mean values ± SD for at least 3 biological replicates.

Treatments with arsenite and paromomycin were additionally carried out overnight (20 h exposure). No increase in the mCherry/GFP ratio was observed with either 125 µM arsenite overnight or 25 µM paromomycin (Figure 3-32 A,B). Neither of these treatments reduced the yeast growth (Figure 3-32 D,E). Increasing the paromomycin concentration to 50 µM overnight increased the

mCherry/GFP ratio, however the ratio was also increased in the mCh-1 control strain (Figure 3-32 C), which suggests non-specific effects as this strain does not report on mistranslation. The growth was barely and non-significantly reduced when treating with 50 µM paromomycin (Figure 3-32 E). Higher paromomycin concentrations were tested (100 µM) but reduced the overnight growth of the strains (to ~50–60% of the control) and were therefore not analysed further. Taken together, the results suggest that Met misincorporation may not be strongly induced as a specific effect of arsenite or paromomycin in *S. cerevisiae*. Without a positive control, it cannot be said for sure whether the presented constructs are suitable for Met misincorporation detection during stress conditions in yeast.

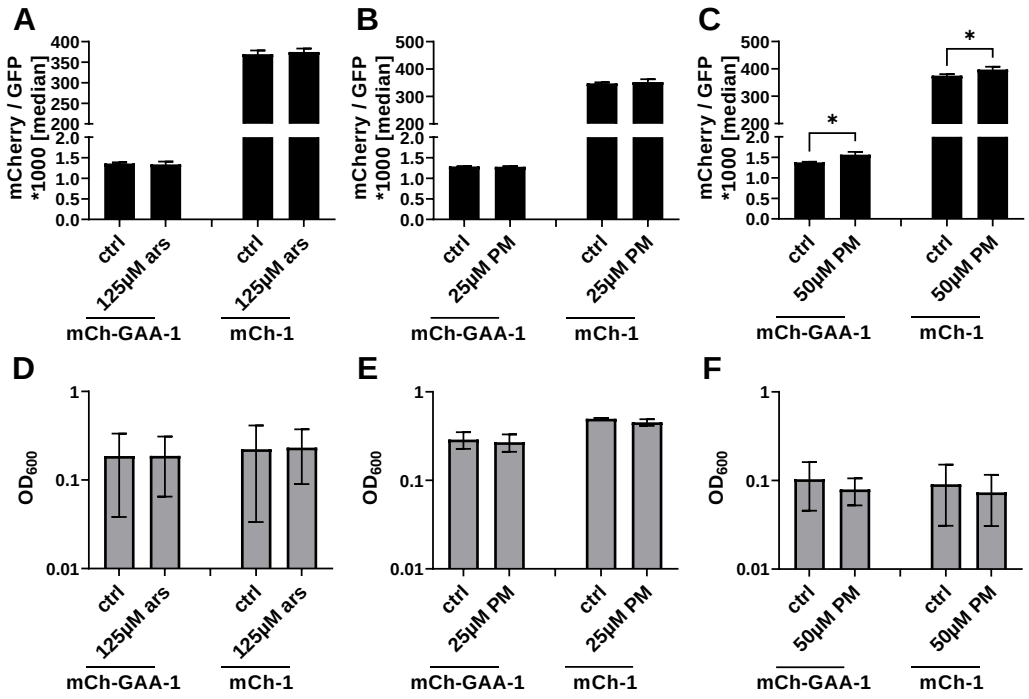

Figure 3-32: Relative mCherry fluorescence from the Met misincorporation constructs after arsenite or paromomycin exposure for 20 h. *S. cerevisiae* expressing yEpRG variants (mCh-GAA-1, mCh-1) were exposed to arsenite (ars; A,D) or paromomycin (PM; B,C,E,F) at the specified concentrations for 20 h in selective YNB broth in shaking conditions in a BioTek® microplate reader (ctrl: stressor-free YNB). A–C) The mCherry and GFP fluorescence of cells was determined by flow cytometry and the fluorescence ratio was calculated for each cell as described in Figure 3-22. For each condition and replicate, the median of the ratios was determined. C–E) Cells were inoculated to OD_{600}~0.01 and the OD_{600} was determined after 20 h before sampling cells for flow cytometry analysis. Data are mean values ± SD for at least 3 biological replicates, except B,E where n = 2. *p<0.05; according to paired *t*-test (two-tailed) with correction for multiple comparisons by controlling the false discovery rate at 5% FDR (Benjamini et al., 2006).

3.3.7 EW combined with heat treatment

The effect of EW treatment combined with subsequent heat treatment on *A. niger* was studied in Chapter 2 (2.3.6). Here, combining 0.03% EW (0.54–0.60 mg L^{-1} FAC) with subsequent 45°C heat treatment (both 5 min) of yeast resulted in lower recovery (11%) than expected from (the product of the fractional growth obtained for) each individual treatment (relative growth 0.248 [0.03% EW alone] x 0.69 [heat treatment (45°C) alone] = 0.17, corresponding to 17%) (Figure 3-33). However, this difference was within one standard deviation of the mean of the observed recovery. Tests were repeated in two separate biological replicates with higher temperatures and an increased range and/or number of EW dilutions (Figure 3-34 A,B). Again, the growth in combination appeared to be lower than expected (panel A: combination of 0.03% EW and 54.6°C: 0.472 x 0.105 = 0.050, versus 0.013 measured; panel B: combination of 0.03% EW and 52.5°C: 0.259 x 0.348 = 0.090, versus 0.019 measured). Based on these results, a short heat treatment (~50–55°C) after treatment with diluted EW (0.03%) may increase the inactivation of yeast, although the presented data alone are not sufficient to determine whether the effect size is sufficient to provide benefits in EW applications. The measured survival after combined EW + heat treatment in yeast was ~1.5–5 x lower than the expected survival (see above calculations), and this effect was smaller than the effect observed when exposing *A. niger* to EW and subsequent heat treatment (measured survival was ~5–8 x lower than the expected survival in *A. niger*, 2.3.6).

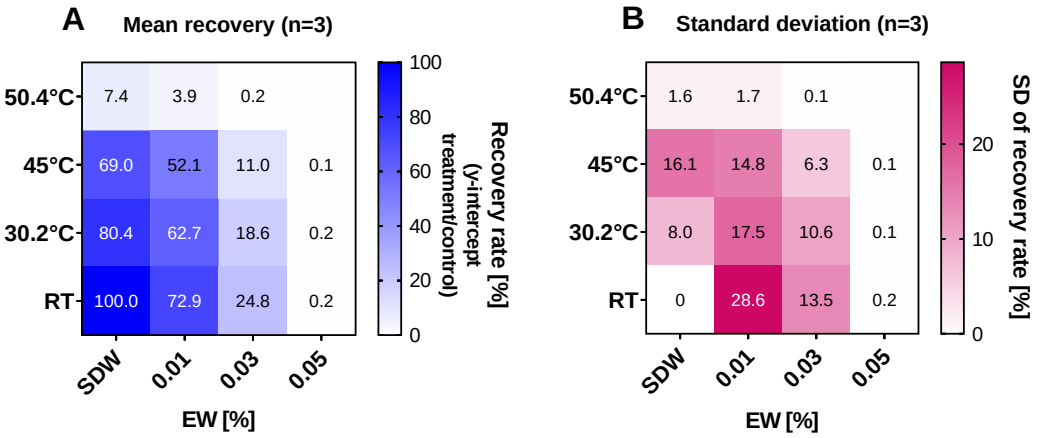

Figure 3-33: Yeast treatment with EW followed by heat treatment. Exponentially growing *S. cerevisiae* BY4741 were treated with EW (0.01–0.05% [v/v]; 0.2–1 mg L^{-1} FAC, dilutions in SDW, 5 min). Treatments were stopped by adding equal volumes of 2X YEPD and 50 µL aliquots were heat treated (30.2°C, 45°C or 50.4°C) for 5 min (Prime Thermal Cycler, Techne). Survival of yeasts was estimated by subsequent recovery in YEPD broth (see 3.3.1.2). Mean values (A) and standard deviation (B) are shown for 3 biological replicates, fields are labelled with the numerical value (missing values are <0.1 but >0). RT, room temperature. SDW, sterile distilled water.

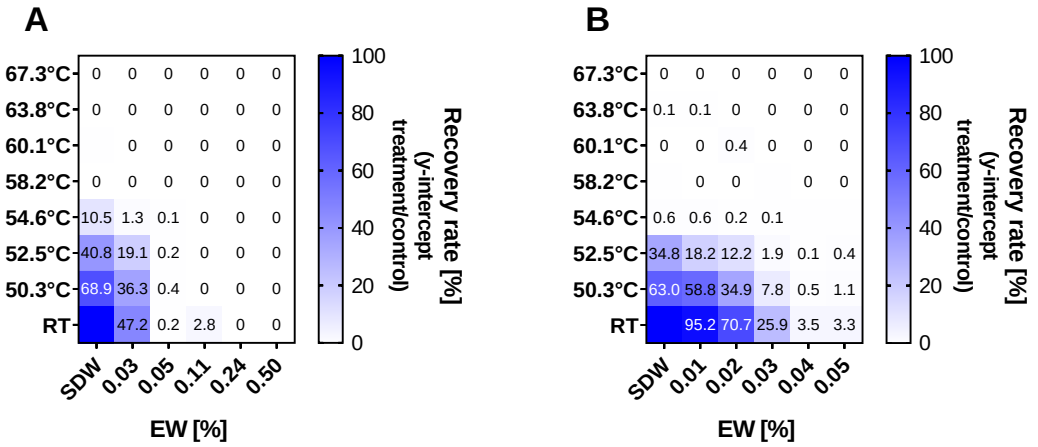

Figure 3-34: Yeast treatment with EW followed by heat treatment, refined ranges. Exponentially growing *S. cerevisiae* BY4741 were treated with EW (0.01–0.05% [v/v]; 0.2–1 mg L^{-1} FAC, diluted in SDW, 5 min). Treatments were stopped by adding equal volumes of 2X YEPD and 150 µL aliquots were heat treated (50.3°C–67.3°C) for 5 min (Prime Thermal Cycler, Techne). Survival of yeasts was estimated by subsequent recovery in YEPD broth (see 3.3.1.2). Data from 1 biological replicate each are shown in A and B, fields are labelled with their numerical value (missing values are <0.1 but >0, except SDW/RT control: 100%). RT, room temperature. SDW, sterile distilled water.

3.4 Discussion

This chapter built on the reactivity of EW with amino acids identified in Chapter 2. It was observed here that supplying yeast cells with increased levels of Met prior to EW treatment results in higher yeast survival. This effect was unique to Met among the tested amino acids and was not linked to downstream metabolism products of Met, suggesting a protective role of Met itself. EW treatment also inactivated FeS cluster proteins, which have previously been reported to be susceptible to conditions where high levels of oxidised Met were present (Sideri et al., 2009). A potential role for Met misincorporation as a cellular response to EW in yeast was not supported by the results of this study. These results identify important targets of EW in yeast.

3.4.1 Methionine as a scavenger of reactive species

The data presented in this study suggest a potential protective system against EW-induced damage *in-vivo,* involving methionine. Pre-culture with methionine, to allow accumulation of the amino acid, specifically (compared to other amino acids) increased recovery from EW treatment. The effect could be mimicked by the D-Met isomer but not by the first metabolic product of Met utilisation (SAM), and occurred rapidly (within 10 min incubation with elevated Met). This suggested a role of the methionine molecule itself in protection against EW. Furthermore, the Met protective effect appeared to extend to a more general form of oxidative stress protection, as it could be reproduced with both NaOCl and ozonated water. One possible explanation is that free or protein-incorporated Met acts as a ROS scavenger during EW treatment, protecting other targets from EW-induced damage. Methionine can readily be oxidised by different ROS and FAC (Bin et al., 2017, Storkey et al., 2014), and was demonstrated to react with EW in Chapter 2. Methionine residues in proteins are considered to confer a ROS scavenging action

that may protect other residues from oxidative damage (Schindeldecker and Moosmann, 2015). The proposed role of Met in ROS scavenging is supported by the Met/MetO recycling system, where methionine sulphoxide reductases (MSRs) re-reduce oxidised methionine (Lowther et al., 2000, Kim et al., 2014). The potential formation of toxic by-products from secondary oxidation of MetO was discussed in the previous chapter (2.3.4.2), and the risk of by-product formation when MetO accumulates would further necessitate continuous reduction of the MetO pool. The present data show that *MSR* overexpressing yeast cells had increased resistance to EW. This study also shows several parallels between EW and NaOCl. Elsewhere, HOCl produced by neutrophils as part of the immune response increased Met oxidation in *E. coli*, while elevated *MSR* expression gave increased bacterial survival of HOCl (Rosen et al., 2009). Replacing Met residues with norleucine residues in *E. coli* proteins increased the bacterium's sensitivity to NaOCl, supporting the hypothesis that Met residues protect proteins from FAC stress (Luo and Levine, 2009). In yeast, deletion of *MSRA* or double deletion of *MSRA*/*MSRB* increased NaOCl sensitivity, and overexpression of *MSRA* or Met-rich proteins protected against NaOCl (Tarrago et al., 2012), similar to the protective effect of *MSR* overexpression against EW presented here. In the previous chapter, other amino acids (Trp, Tyr) were as or more effective at inactivating the fungicidal activity of EW than Met (when treating *A. niger* spores with the amino acid + EW mix, 2.3.4.1), although Met was more reactive with EW than Trp when assessing *in-vitro* activity (by assessing the oxidising activity of the amino acid + EW mix with the fluorescent probe APF, 2.3.5.1). Interestingly, Trp and Tyr did not provide protection when supplied to yeast prior to EW treatments. The lack of a specific oxidation repair system for these amino acids (such as the MSR system for Met) may explain why accumulation of non-Met amino acids does not improve yeast resistance to EW. The role of Met in the cellular response to oxidative stress is further reflected by the upregulation of genes of oxidation-reduction and oxidative stress categories, including MsrA, in Met starvation conditions (Petti et al., 2011).

3.4.2 Met mistranslation: making use of the scavenging action

3.4.2.1 Concept of Met misincorporation as a protective strategy of cells against ROS stress

Methionine occurs naturally in cellular proteins but is not distributed equally. For instance, mitochondrial proteins (especially proteins of the inner mitochondrial matrix and respiratory chain) contain higher Met levels than the cellular average (Schindeldecker and Moosmann, 2015). In addition to genetically encoded Met residues, it has been shown in mammalian and yeast cells using tRNA-microarrays that Met can be aminoacylated to non-Met tRNAs, leading to misincorporation of Met into proteins (Netzer et al., 2009, Wiltrout et al., 2012), while mitochondrial tRNAs were found not to be misacylated with Met (Wiltrout et al., 2012). Many of the reported Met-misacylations replace charged or polar amino acids. Such hydrophilic amino acids tend to be located at the protein-water interface (Malleshappa Gowder et al., 2014) which means that the misincorporated Met residues are likely to be exposed to the aqueous environment. During oxidative stress conditions, the rate of Met-misacylation increases up to 10-fold in mammalian cells, suggesting a potential short-term protection due to elevated Met misincorporation that would shield other protein residues from oxidation (Netzer et al., 2009). Another effect of Met misincorporation may be the formation of protein variants with distinct (and potentially beneficial) activities and cellular localisation, shown for Ca^{2+}/calmodulin dependent kinase in Ca^{2+} stress conditions (Wang and Pan, 2016).

An increase of Met incorporation into fluorescent reporter proteins under oxidative stress conditions has previously been used as a measure of Met mistranslation events at the protein level (Lee et al., 2014a, Gomes et al., 2016), i.e., an alternative approach to using tRNA-microarrays. In these assays, a Met residue in the fluorophore was mutated to yield a non-fluorescent protein and

misincorporation restores fluorescence. This led to indirect indication of Met misacylation of $tRNA^{Glu}$ (Gomes et al., 2016), $tRNA^{Lys}$, $tRNA^{His}$ and $tRNA^{Gly}$ (Lee et al., 2014a) and the misincorporation of such (misacylated) Met into the fluorescent reporter proteins in response to arsenite. In yeast, basal misincorporation in non-stressed conditions has also been demonstrated: Several cytosolic tRNAs were shown to be misacylated with Met in a microarray, and incorporation into proteins was confirmed in trypsin-digested peptides, where substitution of Arg and Lys by Met resulted in longer cleavage products (Wiltrout et al., 2012).

3.4.2.2 Oxidative stress treatments did not increase Met misincorporation in yeast

It was hypothesised that during or after EW stress, Met misincorporation into proteins may occur as a cellular stress response. Increased Met supply through the growth medium may increase the availability of Met for misacylation reactions and increase the chance of misincorporation. Overexpression of MSR enzymes should then also make the misincorporation strategy more successful by increasing the MetO reduction activity, consistent with the observed increased survival of such overexpression strains. The mCherry-GFP fusion protein reporter plasmids in this study were constructed following the previously published reporter plasmids for human cells (Gomes et al., 2016) and, consistent with the previously reported results, Met misincorporation events at a Glu codon could be detected in unstressed conditions in *S. cerevisiae* in this study. Fluorescence of the mCherry variant with the Met-to-Glu substitution (mCherry-Glu) could theoretically also be caused by fluorescence of this variant (through fluorophore formation involving Glu), however this has been addressed previously by showing that a recombinantly expressed mCherry-Glu variant is not fluorescent, and that Glu does not undergo fluorophore formation, suggesting that observed fluorescence in strains expressing mCherry-Glu variants (such as mCh-GAA in this study) is indeed caused by Glu-to-Met misincorporation events (Gomes et al., 2016). In

yeast, the Met-tRNA-synthetase forms a complex with Arc1p, a general tRNA-binding protein, and the Glu-tRNA-synthetase, and it has been shown that this AME complex misacylates $tRNA^{Glu}$ with Met *in-vitro* whereas misacylations of $tRNA^{Met}$ with Glu are very rare (Wiltrout et al., 2012). The present study indicates that, consistent with such misacylation events, incorporation of Met at Glu codons (GAA) into proteins occurs in yeast cells. It should be noted that the mCherry sequence contains 24 GAA codons and it is not known how Met misincorporation at these other positions would affect the fluorescence.

It could not be shown that EW treatment increases the Met misincorporation rate. A small, non-significant increase was recorded in one experiment but was not reproducible across experiments, potentially due to differences in the extent of EW effect (reflected in yeast survival) between the experiments. Even if the observed effect in the first experiment were a real effect, it is very small and would not suggest that Met misincorporation into proteins is a major part of the yeast response to EW. Paromomycin, a known inducer of mistranslation, also did not increase the Met misincorporation at concentrations between 25–100 µM, whereas previously, an increase in stop-codon read-through and Arg-to-His misincorporation was reported after 8.1 µM paromomycin treatment (16 h), and His-to-Tyr misincorporation at 40 µM (Vallières et al., 2020). Additionally, it could not be conclusively shown that arsenite treatment increased Met misincorporation in yeast, in contrast to the previous studies in mammalian cells (Gomes et al., 2016, Lee et al., 2014a, Netzer et al., 2009). However, only one of the previous studies states the use of sub-lethal arsenite levels (Netzer et al., 2009), as used here, whereas the other relevant studies either did not comment on survival (Gomes et al., 2016) or used arsenite concentrations that reduced cell viability to ~60% in similar experiments within the same paper (Lee et al., 2014a); this makes it difficult to rule out unspecific effects. Additionally, it is possible that the described short-term protective strategy of mammalian cells against oxidative

stress by Met misincorporation into proteins does not occur in yeast. For mammalian cells, it is known that the extracellular signal-related kinase ERK1/2 phosphorylates two Ser residues (Ser209 and Ser825) in the Met-tRNA-synthetase (MetRS), reducing the accuracy and inducing misacylation events (Lee et al., 2014a), but it is not known whether a similar mechanism exists in yeast: sequence alignments do not support a similar regulatory mechanism in yeast (application of the the NCBI BLAST® blastp tool during the course of this study showed that the yeast MetRS sequence aligns to residues 250–821 of the human sequence [51% identity], excluding the relevant Ser residues).

Stress exposure may affect the fluorescence of the reporter proteins. Unexpected fluorescence phenotypes were observed in several experiments (decreased mCherry fluorescence after treatment of mCh-GAA-1 and mCh-1 with 0.01% EW, increased mCherry/GFP ratio in the mCh-1 strain after overnight treatment with paromomycin, increased GFP fluorescence but decreased mCherry fluorescence when switching from YNB to YEPD medium). Importantly, if the mCherry fluorescence is more strongly reduced than GFP fluorescence in a specific condition, this may hide increases due to mistranslation events in the GAA1 strain, potentially decreasing the sensitivity of the reporter.

In this study, pre-treatment with D-Met resulted in increased recovery after EW treatment in the Met-prototrophic yeast strain (*S. cerevisiae* BY4742). Tight regulation prevents incorporation of D-amino acids into proteins (Kuncha et al., 2019). This suggests that the observed protective effect of L-Met against EW treatment is at least partly due to free Met, consistent with the observed absence of a connection between EW and Met misincorporation into proteins, although it is also possible that the different Met isomers exert distinct protective mechanisms.

3.4.3 Methionine oxidation: potential regulatory roles

In addition to a protective ROS scavenging effect, Met oxidation has been proposed as a posttranslational protein modification that regulates protein activity. A reported minor (potentially regulated) oxidase activity of MSR enzymes (catalysing the oxidation of Met to MetO) supports the idea of Met oxidation as a controlled regulatory mechanism (Lim et al., 2011, Cao et al., 2018). A new database (MetOSite, https://metosite.uma.es/) collates methionine sulphoxidation sites identified in proteins from different species where the Met oxidation state affects activity, protein-protein interaction, stability or protein localisation (Valverde et al., 2019). Inactivation of proteins by Met oxidation has been reported, for instance in the bacterial chaperone GroEL and the antioxidant enzyme catalase, two proteins important in the oxidative stress response (Khor et al., 2004a, Mahawar et al., 2011). One relevant example is the bacterial transcription factor HypT (also named YjiE) that is activated by HOCl mediated oxidation of three methionine residues and increases HOCl resistance upon activation (Drazic et al., 2013). It has been suggested that the oxidation results in a conformational change that enables DNA binding of HypT (Jo et al., 2019). So far, MetOSite lists three studies that discovered protein regulation by Met oxidation in *S. cerevisiae*. During oxidative stress such as from NaOCl, a co-chaperone (Fes1) of a class of heat shock proteins (Hsp70s) is oxidised at three Met residues (potentially more), resulting in decreased activity of Fes1 and in consequence decreased activity of the Hsp70 proteins (Nicklow and Sevier, 2020). This was speculated to have one or several benefits during stress conditions, such as prolonged binding of misfolded peptides to Hsp70, enabling other binding partners to interact with Hsp70 which may favour degradation over re-folding, or activation of other stress responses. A different co-chaperone of Hsp70s, Mge1, important for protein import into the mitochondrial matrix, protein folding and FeS cluster biogenesis, loses activity upon Met oxidation, reversible by (mitochondrial)

MsrB activity (Allu et al., 2015). A strain expressing an oxidation resistant variant (M155L) of Mge1 survived better in oxidative stress conditions (Marada et al., 2013). In enolase 1, oxidation of methionine 171 reduces the enzyme activity and an oxidation-resistant M171L protein conferred increased NaOCl resistance of the yeast, consistent with a regulatory role for the protein's Met oxidation state (Lin et al., 2017). Therefore, whereas loss of activity after Met oxidation may be a form of incidental damage during oxidative stress, it could also improve stress resistance by triggering alternative processes or pathways. In future studies, it would be interesting to test whether Met oxidations in Fes1, Mge1 and enolase 1 also play a role during EW stress. Another example of regulation mediated by Met-oxidation is the nitrate-specific transcription factor NirA in *Aspergillus nidulans* which is inactivated when methionine 169 is oxidised but is activated and accumulates in the nucleus upon exposure to nitrate, correlated with reduction of the MetO residue (Gallmetzer et al., 2015). Interestingly, the Met reduction was independent of MsrA and MsrB in this case, while the oxidation was catalysed (maybe indirectly) by a flavin-containing monooxygenase (FmoB). Future efforts to identify further Met-oxidation regulatory effects will be helped by recent methodological advances, such as: isotopic labelling of unoxidised Met residues or probes specific for exposed Met residues on proteins allowing identification of reactive Met residues using LC-MS/MS (Lin et al., 2017, Bettinger et al., 2020), the computational prediction of MetO sites (Veredas et al., 2020) and the synthesis of MetO containing peptides (Cai et al., 2020).

3.4.4 Effects of methionine on the cell wall

It is possible that increased supply of Met via the medium induces cellular processes that in turn increase cellular resistance to EW. It has been reported that Met supplementation (10 mM) increased the susceptibility of the yeast cell wall to enzymatic degradation, potentially due to lower glucan and mannan

concentrations, but also increased protein concentrations in the cell wall (Killick, 1971). In the case of EW treatment, such increased protein levels in the wall might be beneficial: EW is inactivated by proteins (2.3.3), therefore if EW encounters increased protein levels before entering the cell, the active EW species may become inactivated before they cause intracellular damage. Yeast resistance to the cell-wall damage from calcofluor white was increased after deleting the genes encoding the Met uptake protein Mup1 or the SAM synthetase Sam1 (Zhao et al., 2019), suggesting a potential connection between Met metabolism and cell wall stability or composition. Other possible Met effects may include ROS scavenging in the periplasmic space to protect the cell membrane from oxidation, in line with reported bacterial methionine-rich periplasmic peptides and periplasmic MetO reductases (Tarrago et al., 2020, Melnyk et al., 2015).

3.4.5 FeS cluster proteins are EW targets

Increased oxidant resistance has recently been described after pre-culture of yeast cells with high lysine, similar to the methionine pre-culture in this study (Olin-Sandoval et al., 2019). However, lysine pre-culture did not improve EW recovery in this study. The lysine effect was explained by potential regulatory effects of excess Lys entering polyamine metabolism, and by increased production of the ROS scavenger glutathione. The protective effect of Met pre-culture against EW may also, at least partly, be more indirect than purely ROS scavenging, and some possibilities have been discussed above. Furthermore, it has been shown previously that elevated MetO levels or decreased reduced-Met lead to increased oxidative targeting and turnover of FeS clusters (Sideri et al., 2009). Accordingly, increasing the level (via pre-culture) or maintenance (*MSR* overexpression) of reduced Met should help to keep FeS clusters intact in oxidising cellular environments. Oxidative stress in general is well known to target surface-exposed FeS clusters in proteins (Imlay et al., 2019). Superoxide and hydrogen peroxide

oxidise $[4Fe\text{-}4S]^{2+}$ clusters to $[4Fe\text{-}4S]^{3+}$, followed by release of iron yielding $[3Fe\text{-}3S]^{1+}$, rendering FeS enzymes inactive (Imlay, 2006). FeS proteins such as ferredoxins are highly reactive with FAC (Albrich et al., 1981) although the reactivity depends on the protein, and some FeS clusters are more stable than others upon FAC exposure (Hurst et al., 1991). NaOCl may, potentially via ROS generation in cells, damage the clusters in bacterial FeS proteins (Romsang et al., 2018). Damage to the mitochondrial FeS assembly machinery (ISC) in *S. cerevisiae* induces iron release and increases ROS formation, consistent with observed sensitisation to oxidants (Gomez et al., 2014). The present study shows that EW impairs activity of the FeS cluster protein aconitase, a known key target of pro-oxidant agents (Lalève et al., 2016). It should be noted that aconitase is mainly localised in the mitochondrial matrix and damage to aconitase is therefore likely an indirect/secondary effect of EW action, as chemical EW species will first encounter the cell wall, membrane and cytoplasm. The reconstitution of the FeS cluster was not successful. This may suggest shortcomings of the method due to technical constraints arising from the limited stability of the aconitase enzyme. The reconstitution was carried out in plastic tubes, which may introduce oxygen into otherwise oxygen-free conditions, potentially affecting the aconitase stability and reconstitution. Previously, chemical reconstitution of the FeS cluster in human ferredoxin was reported to be unsuccessful and successful reconstitution required the FeS transfer protein mNT (Mons et al., 2018), however the same group reported successful chemical reconstitution of (purified) aconitase [% restored activity not reported] (Ferecatu et al., 2014) (in the present study, aconitase reconstitution was attempted in crude protein extracts). Chemical reconstitution alone is generally only sufficient to repair clusters that have only lost their first ("labile") iron. The unsuccessful reconstitution could mean three things: (i) EW-induced FeS cluster damage was limited to the labile iron, but the method needed optimisation (e.g., true oxygen-free conditions); (ii) FeS cluster damage was more

extensive/irreversible; (iii) damage to the aconitase protein (e.g., amino acid oxidation) by EW contributed to the loss of enzymatic activity.

3.4.6 The FeS protein Rli1 may be a target of EW treatment

Rli1 overexpression protected against EW, similar to a reported protective effect against several pro-oxidants (Alhebshi et al., 2012). Rli1 is required for the nuclear export of ribosomes, initiation and termination of translation and ribosome recycling (Schuller and Green, 2017, Kispal et al., 2005). Rli1 function is highly conserved and essential for cells, requiring the mitochondrial and cytosolic FeS assembly machinery to assemble its two [4Fe-4S] clusters, pathways that are ROS hyper-sensitive (Gomez et al., 2014, Paul et al., 2015). Considering its essentiality for cell viability, this study suggests that Rli1 could be a key target of EW. EW was shown in Chapter 2 (2.3.3) to react strongly with proteins, potentially necessitating increased protein synthesis (to replace damaged proteins) during or after EW treatments. Rli1 has important roles for protein synthesis, so targeting of Rli1 by EW may also impact the cellular recovery from EW damage. Decreased Rli1 activity has been shown to increase mistranslation in the form of stop-codon readthrough, related to the role of Rli1 in translation termination (Khoshnevis et al., 2010). Rli1 overexpression was shown to reduce mistranslation (stop-codon read-through) events during mistranslation inducing treatments (Alhebshi, 2014). Therefore, if Rli1 function is decreased during EW treatment (e.g., by decreased FeS cluster assembly due to oxidative perturbation of FeS assembly pathways) this may additionally provoke mRNA mistranslation and protein misfolding events, offering another explanation for the protective effect of Rli1 overexpression. However, Rli1-dependent protection against the pro-oxidant paraquat was not linked to decreased mistranslation (Alhebshi, 2014). Accordingly, this study suggested that EW treatment does not induce Met misincorporation (3.4.2.2), although other types of mistranslation events are possible and were not

investigated here. Interestingly, Met has been reported to influence translation, including by increasing ribosome synthesis via the TORC1 pathway, resulting in increased translation capacity (Walvekar and Laxman, 2019) and suggesting a possible link between cellular Met and Rli1 function in ribosome export and recycling.

3.4.7 The connection between methionine and FeS clusters

As mentioned above, the reported contribution of reduced-Met to FeS cluster maintenance (Sideri et al., 2009) offers (partial) explanations for the protection by Met against EW. It is likely that FeS cluster proteins are EW targets that may be protected by the Met scavenging activity. Furthermore, connections between the regulation of methionine metabolism and iron homeostasis have been reported, e.g., transcriptional regulators of Met biosynthesis affect certain iron homeostasis genes (Petti et al., 2011) suggesting some connection between these pathways. Cbf1, one of the regulators of the sulphur metabolic genes involved in Met biosynthesis (see 3.1.3.2), also (potentially indirectly) binds to Aft1, a transcription factor for iron metabolism genes (Measday et al., 2005). Furthermore, other regulators of the *MET* regulon (such as Met4 and Met31) can directly or indirectly repress iron homeostasis genes, including Isu2, a gene of the FeS cluster biosynthesis pathway, repressed by Met31 and/or Met32 (McIsaac et al., 2012, Petti et al., 2012). Addition of Met might then result in the de-repression of these iron homeostasis genes by suppressing the activity of the Met-regulated transcription factors (Ouni et al., 2010).

In a different study, iron utilisation was shown to be upregulated in Met restricted conditions in *S. cerevisiae* (Zou et al., 2017). Deletion of the *MSRA* and *MSRB* genes resulted in upregulation of Fe-regulon genes (Sideri et al., 2009). When two transcriptional regulators that regulate iron uptake and use (Aft1 and Aft2)

are deleted, yeast strains are Met auxotrophic in aerobic (but not anaerobic) conditions, rescued by addition of methionine or homocysteine (Blaiseau et al., 2001). The cytosolic iron-sulphur protein assembly (CIA) component Met18 (Mms19) is required for methionine biosynthesis (Stehling et al., 2012). The bacterial transcription factor HypT, activated by Met oxidation during HOCl stress, downregulates iron acquisition genes, resulting in lower intracellular iron levels (Drazic et al., 2013), which offers a concept by which the Met oxidation state could regulate iron metabolism, although such a regulatory mechanism may not be present in fungi. As mentioned above, Met oxidation in the yeast Mge1 protein inactivates its function (Allu et al., 2015), and Mge1 is involved in the transfer of assembled [2Fe-2S] clusters from Isu1/2 to Grx5, an essential step of FeS cluster assembly in mitochondria (Lill et al., 2015).

Therefore, there are many potential connections between Met and iron homeostasis/FeS metabolism. As discussed earlier, the present data indicated a protective effect of Met, but not its downstream metabolic products. It is noteworthy nevertheless that the sulphide used for FeS biogenesis stems from cysteine (Stemmler et al., 2010), which is a downstream product of methionine (Ljungdahl and Daignan-Fornier, 2012), and FeS clusters are in most cases coordinated by cysteine residues of the protein (Imlay, 2006). However, pre-treatment with the cysteine pre-cursor NAC did not protect against EW in this study. Finally, the SAM in radical SAM enzymes has been proposed to protect their [4Fe-4S] cluster from the attack of oxygen (Imlay et al., 2019), but again, SAM pre-treatment, although responded to by the yeast (allowing growth of the Met auxotrophic strain in Met-free medium, assuming SAM was not chemically degraded in the medium or that samples did not contain sufficient Met due to limited SAM purity [≥75%]), did not provide protection against EW treatment in this study.

3.4.8 Potential interactions between EW and heat treatments

EW treatment followed by heat treatment resulted in lower fungal survival than expected based on an additive effect, when tested against *A. niger* (2.3.6) or *S. cerevisiae* (3.3.7), potentially suggesting a synergistic effect. Similarly, previous studies found significantly higher killing of bacteria when EW treatment was followed by heat treatment (51°C, on its own non-lethal) (Han et al., 2018), or of bacteria and fungi when EW treatment and heat treatment (up to 65°C) were applied simultaneously (Rahman et al., 2011, Liu et al., 2017, Ovissipour et al., 2018). Future studies could also investigate heat treatment prior to EW treatment and the effect on proteins. Heat treatment leads to protein denaturation and unfolding, which may make amino acid side chains more accessible for subsequent reaction with EW and result in more complete protein inactivation.

3.4.9 Conclusions

Taken together, the data suggest a mode of action of EW that includes Met oxidation and FeS cluster damage. Other ROS targets and antioxidant systems described in 3.1.1 and 3.1.2 may be additionally involved in EW damage/repair. Met likely functions as a ROS scavenger that protects other cellular targets against EW induced damage, as well as NaOCl damage and (FAC-independent damage after) ozonated water treatment. Increasing the available Met levels, or shifting the equilibrium of Met/MetO towards the reduced form, could then increase the ROS scavenging capacity. The scavenging effect may be carried out by free Met (as suggested by D-Met induced protection) or protein-bound Met, however Met misincorporation into proteins was not found to be increased during the EW response. Nevertheless, this study produced some evidence at the protein level for Glu-to-Met misincorporation events in yeast in stress and non-stress conditions. Met oxidation in proteins may also regulate protein activity, triggering downstream effects that may be identified in future studies. The ROS scavenging

activity of Met may protect FeS cluster proteins from damage which have been indicated by the present study to be a target of EW treatment. This is another piece of evidence linking Met oxidation and iron metabolism, a connection that has been reported but is not fully understood yet. Additional effects of EW treatment cannot be ruled out. While the presented data do not suggest a protective role of Met metabolism products, it is noteworthy that one downstream product (via cysteine) is the ROS scavenger glutathione (Ljungdahl and Daignan-Fornier, 2012). The first downstream metabolism product (SAM) is important for methylation reactions, for instance during the synthesis of phosphatidylcholine, an important component of biological membranes (Sadhu et al., 2014). Furthermore, Met-independent regulatory effects in response to EW treatment are likely, as for instance HOCl-responsive chaperones have been reported in bacteria (e.g., regulated by Cys oxidation or N-chlorination) (Goemans and Collet, 2019, Voth and Jakob, 2017). Chaperones activated by oxidative stress (H_2O_2 or H_2O_2+Cu^{2+}) have also been reported in yeast (Jang et al., 2004, Voth et al., 2014).

Regarding applications of EW in the food industry, the present results suggest that the growth substrate of food spoilage fungi has the potential to affect their survival of subsequent treatment. This could be relevant in the case of protein-rich foods or protein contamination of the process, even if the protein contaminant is not present during the EW treatment itself (similar to the pre-treatment conditions that were used in this study). The oxidative targeting of Met and FeS clusters may inform the rational combination of EW with other sanitising treatments (referred to as "hurdle technology" in the food industry, see 1.5.1). Importantly, the results obtained in the present chapter on the mode of action were informed by the results in Chapter 2, representing a top-down strategy where data on chemical reactivity of the sanitiser with likely industrial contaminants, via narrowing down the reactivity to specific molecules, led to the characterisation of cellular targets. This strategy may be useful to characterise other sanitisers or antimicrobials as well.

4 Response of *Aspergillus niger* to EW: growth delays and heterogeneity of outgrowth from individual spores

4.1 Introduction

4.1.1 Phenotypic heterogeneity in the microbiological stress response

Within a population of genetically identical cells, variation between single cells can often be observed, and this phenomenon has been termed phenotypic (or non-genotypic) heterogeneity (Ackermann, 2015). Such variation can be beneficial for a population because individual cells may survive stressful or fluctuating environments and because cellular tasks may be divided between cells within the population which can increase the growth rate and performance (Ackermann, 2015, Holland et al., 2014). For instance, populations of the food spoilage yeast *Zygosaccharomyces bailii* were shown to contain a small sub-population with high resistance against the preservative sorbic acid (Stratford et al., 2014). Phenotypic heterogeneity can be caused by stochastic fluctuations in molecular processes (such as "noisy" gene expression or molecule distribution during cell division), differential activation of regulatory processes in different cells, periodic oscillations (such as cell cycle progression), cellular age, cell-cell interactions (through direct physical contact or signalling molecules) or epigenetic modifications (Ackermann, 2015, Avery, 2006). Phenotypic heterogeneity commonly occurs at a frequency that cannot be explained by spontaneous genetic mutation, and phenotypic variation can be distinguished from genetic variation by assessing the inheritance of the phenotype of a sub-population (Smith et al., 2007, Avery, 2005).

Methods for assessing phenotypic heterogeneity include gradients of dose-response curves for stressor treatments, fluorescent probes for individual metabolic functions, single-cell -omics or sequencing, microfluidic single-cell analysis and the analysis of micro- or macro-colony size (Hewitt et al., 2016, Dusny and Schmid, 2015). The growth rate of a cell is an indicator for the global physiological status of the cell. Colony formation rates depend partly on the growth rate of the starting cell(s) but, especially at the macro-colony level, the growth can be further influenced by heterogeneous divergence of single cells within colonies (Hewitt et al., 2016). Decreased mean colony-size and increased colony-to-colony size variation was demonstrated in *Z. bailii* growing under sorbic acid stress (Stratford et al., 2014). Factors like the proximity of competitor colonies and the accumulation of toxic by-products also influence variation in microbial colony size (Chacón et al., 2018). When assessing phenotypic heterogeneity, one challenge is ruling out environmental fluctuations, as cells can respond rapidly to small changes in extracellular conditions (Dusny and Schmid, 2015).

4.1.2 Phenotypic heterogeneity in filamentous fungi

As filamentous fungi grow into complex hyphal networks, in contrast to unicellular cell populations, heterogeneity can be assessed either at the level of individual fungal spores, in individual hyphae or zones of the same mycelium or in different isogenic mycelia (Hewitt et al., 2016). For *Aspergillus* spp., variation in transcript and protein levels and protein secretion has been found between hyphae of the same mycelium and between individual colonies. Hyphae of *Aspergillus* species are divided into cells by septa which contain pores to allow cytosolic transfer and mixing, but these pores can be plugged by Woronin bodies and this process can maintain hyphal heterogeneity by creating distinct hyphal zones (Bleichrodt et al., 2012). Gene expression in *A. niger* colonies is differentially regulated between the

periphery and the centre of a colony, and between different peripheral hyphae (Vinck et al., 2011, Levin et al., 2007), and such differential regulation occurs e.g., in response to local changes in the available nutrient sources (Daly et al., 2020). At the level of individual conidia, it was shown that the cell wall composition of *A. fumigatus* conidia is phenotypically heterogeneous and the level of heterogeneity undergoes changes throughout germination (Bleichrodt et al., 2020). In the cited study, increased chitin levels in the cell wall of a conidial sub-population was correlated with a higher tolerance to the antifungal drug caspofungin and higher numbers of 'persister' conidia that can evade host immune responses; thus providing a potential example of an adaptive advantage conferred to *Aspergillus* species through phenotypic heterogeneity. The temperature during *A. fumigatus* conidia formation impacts their properties, including sensitivity to stress treatment (heat, H_2O_2, UV), levels of accumulated compatible solutes, pigments and secondary metabolites (Hagiwara et al., 2017). Heterogeneous responses to heat stress were also demonstrated in *A. niger* conidia (some variation was due to uneven heating patterns but heterogeneity [biphasic killing curve] was still observed when all conidia were heated uniformly) (Fujikawa et al., 2000). In addition, the lag time before germination of individual *A. niger* conidia (and other fungi) is heterogeneous, and both the lag time and its variability can increase in stressful conditions (Dagnas et al., 2017). The formation of conidia in conidiophores can also be a source of variation, as the age of conidia within one colony, as well as the position within a chain of formed conidia, can influence the properties of the single conidia (Dijksterhuis, 2019, Teertstra et al., 2017).

4.1.3 Stress response of filamentous fungi

As mentioned above, the growth of filamentous-fungal colonies differs in some important ways from that of single celled microorganisms (the latter forming through single-cell division events), as the former consist of an interconnected

hyphal network, and properties such as the hyphal branching frequency affect the radial growth rate of colonies (Pazouki and Panda, 2000, Fricker et al., 2017). Fungal spores also have some markedly different properties to vegetatively growing cells. Conidia are easily dispersed, show increased stress resistance compared to vegetative growth structures and can form during adverse conditions, e.g., during food processing and storage, therefore representing an important food spoilage risk (Dijksterhuis, 2017). While such fungal spores have low metabolic activity, examples of active repair mechanisms in ungerminated *Penicillium* spores in water have been reported (Dijksterhuis, 2019). Recently, it has been shown that fully developed *Aspergillus* conidia (before dehydration, which induces dormancy) exhibit transcriptional activity and modulate their transcription in response to environmental stress conditions (Wang et al., 2021). Furthermore, the fungal spore coat consists of a thick, pigmented cell wall, and molecules such as trehalose and polyols (especially mannitol in the case of *A. niger*) accumulate in the cytosol (Dijksterhuis, 2019, Teertstra et al., 2017). This is likely to impact the reactivity of incoming stressors (such as EW) with molecules within spores. For instance, mannitol is a hydroxyl radical scavenger, and whereas it has been reported that mannitol does not react notably with FAC directly (Arnhold et al., 1993), mannitol was shown to protect *A. niger* against NaOCl-induced oxidative stress (Ruijter et al., 2003). Filamentous fungi also tend to have a more diverse range of antioxidant enzymes than unicellular fungi, as well as secondary metabolites with antioxidant function (Aguirre et al., 2006, Kawasaki and Aguirre, 2001). It has previously been reported that stress responses in *S. cerevisiae* and other fungi can be similar yet differ in specific aspects (Milisavljevic and Kojic, 2020), serving as a reminder that mechanisms in model organisms can differ somewhat from other organisms of interest and that key results from model organisms should be experimentally validated in other organisms, too.

4.1.4 Aims

Variability in the fungal stress response can represent a problem for food safety and spoilage modelling (Stratford et al., 2014, Dijksterhuis, 2017). This chapter addressed the possibility of EW inducing phenotypic variation in treated *A. niger* spores. Macro-colony area analysis after spore treatment and outgrowth was chosen to assess variation between individual colonies, because colony size analysis can be performed easily even with filamentous fungi. Sub-lethal EW levels were chosen to allow the study of cellular response mechanisms that may be hidden by more general cell death events at higher EW doses, and because the inactivation of active species in EW by organic substances (described in Chapter 2) may result in low effective EW doses in application settings where organic substances are present. Furthermore, the EW response of *A. niger* spores may differ in certain aspects to the EW response of *S. cerevisiae*, studied in Chapter 3. Specifically, it was tested whether the protective effect of Met pre-culture (observed in yeast) could be observed in *A. niger*, and the EW response of *A. niger* was studied more broadly by assessing transcriptome changes induced by EW treatment.

4.2 Materials and methods

4.2.1 Colony size analysis

Cultivation of *A. niger* and treatment with EW, NaOCl and ozonated water were as described in 2.2.1 and 2.2.6. EW was diluted to 0.03–0.4% [v/v] (0.5–8 mg L^{-1} FAC) in HPLC grade water for experiments assaying colony size. NaOCl was diluted in HPLC grade water as specified (2–7.5 mg L^{-1}) and ozonated water was used as described in 2.2.3. Chloramines were produced by mixing equal volumes of 40 µM amino acids solution (equimolar mix of alanine, arginine, asparagine, aspartate, glutamate, glutamine, glycine, histidine, isoleucine, leucine, lysine, methionine, phenylalanine, serine, threonine, tyrosine, valine, tryptophan) and 0.1% EW (1.8–2 mg L^{-1} FAC, equivalent to 34–38 µM HOCl; resulting in the final mixed concentrations: 20 µM amino acids, 0.05% EW). The mix was held for 5 min before it was used for spore treatments. After 5 min treatments with EW, NaOCl, ozonated water or chloramines (500 µL treatment volume), treatments were stopped by mixing with an equal volume of 2X YEPD followed by 1:125 dilution in 1X YEPD. Where specified, treatments were stopped by diluting 1:250 in HPLC grade water, or alternatively by adding equal volumes of L-ascorbic acid (40 or 400 µM), 5 min incubation and subsequent 1:125 dilution in HPLC grade water. Appropriate dilutions (100 µL) were plated onto YEPD agar in order to achieve ~20 colonies per plate. At least 5 plates were prepared as technical replicates per condition. Where specified, 7.5 mM ascorbic acid was included in the YEPD agar. After defined growth periods (44–51 h) at defined growth temperatures (28°C unless specified), colonies on plates were imaged using the auto setting of a Nikon D3200 digital camera with a Nikon DX AF-S NIKKOR 35 mm 1:1.8G lens. Images were then analysed in ImageJ 1.49k using a custom-build macro (see Appendix H, 6.8). Colonies that were touching other colonies or the side of the agar plate were

excluded from the analysis, resulting in an average of ~40–60 analysed colonies per control condition in each experiment.

4.2.2 Flow cytometric analysis of *A. niger* conidia and germlings

Untreated or EW-treated spores were cultivated in YEPD (20 mL, 5 x 10^4 spores mL^{-1}) for germination periods as specified (up to 2.5 h, 28°C, 150 rev min^{-1}). Cultures were harvested (537*g*, 15 min), resuspended in 1 mL PBS, centrifuged (9000*g*, 4 min) and resuspended in 0.5 mL PBS. Analysis of germinated and non-germinated spores in PBS was carried out in a BD FACS Canto™ A flow cytometer. Single spore events were gated based on light scatter properties (SSC-A/FSC-A) and doublet exclusion (SSC-H/SSC-A). The FSC-A was analysed as a measure of relative spore size to measure the swelling of spores during early germination (Hayer et al., 2013). 5000–10,000 single spore events were analysed per condition.

4.2.3 *In-vitro* assays with fluorescent dyes and ascorbic or formic acid

The *in-vitro* assay was performed as described in 2.2.10. Briefly, formic acid or ascorbic acid at 3.5–70 µM (final concentration) was mixed with 0.016% EW and incubated for 1–15 min as specified, before mixing with APF dye (5 µM). Fluorescence was recorded within 2 min of mixing with dye, with excitation at 485/20 nm and emission at 528/20 nm (BioTek® microplate reader Synergy HTX).

4.2.4 Amino acid pre-culture with *A. niger*

4.2.4.1 Methionine pre-culture on YNB agar

A. niger N402 was grown on YNB agar (0.69% yeast-nitrogen base without amino acids (Formedium, Norfolk, UK), 2% [w/v] D-glucose, 2% [w/v] agar) supplemented or not with 0.13–3 mM Met. Culture conditions, harvest of conidia

and EW treatment were as described in 2.2.1 and 2.2.6. EW was diluted to 0.4–1% [v/v] (7.2–20 mg L^{-1} FAC) in HPLC grade water for spore treatments and survival was assessed by plating onto YEPD agar and subsequent colony enumeration.

4.2.4.2 Amino acid pre-culture in AMM broth

Aspergillus minimal medium (AMM) contained 6 g L^{-1} $NaNO_3$, 2% [v/v] salt solution, 0.02% [v/v] trace elements and 10 g L^{-1} glucose, adjusted to pH 6.5 (salt solution: 26 g L^{-1} KCl, 26 g L^{-1} $MgSO_4.7\ H_2O$, 76 g L^{-1} KH_2PO_4; trace elements: 40 mg L^{-1} $Na_2B_4O_7.10\ H_2O$, 80 mg L^{-1} $CuSO_4.5\ H_2O$, 800 mg L^{-1} $FeSO_4.H_2O$, 800 mg L^{-1} $MnSO_4.4\ H_2O$, 800 mg L^{-1} $NaMoO_4.2\ H_2O$, 8 g L^{-1} $ZnSO_4$). Amino acids (methionine, arginine, histidine, asparagine, alanine) were added at 0.3 mM (control: no amino acid added). Germination cultures (20 mL AMM) were inoculated to 10^6 spores mL^{-1} (28°C, 150 rev min^{-1}, 4 h). Cultures were harvested by three rounds of centrifugation to remove any extracellular amino acids (537*g*, 10 min and 2 x 3,381*g*, 4 min) and resuspended in 0.1% Tween 80. At least 100 conidia were inspected visually under the microscope and swollen spores were counted to assess the beginning of germination. Suspensions were adjusted to 10^6 spores mL^{-1} and treated with EW (0.1–1% [v/v]; 1.8–20 mg L^{-1} FAC) as described in 2.2.6. After addition of 2X YEPD to stop the treatment, 100 µL samples were incubated statically in 96-well plates at 28°C for OD_{600} determination over time, as described in 2.2.6.

4.2.5 Transcriptome analysis

4.2.5.1 EW treatment of germinating conidia

Suspensions of conidia (*A. niger* N402) were prepared as described in 2.2.1. Conidia were germinated in 1 L cultures (10^5 spores mL^{-1}, 28°C, 150 rev min^{-1}, 6 h, medium: 67% [v/v] YEPD, 33% [v/v] Tween 80 0.1% (final 0.033% [v/v]))

and harvested by filtration using 500 mL filter systems (0.22 µm PES, Sterilizing, Low Protein Binding, Corning Inc. Life Sciences, NY, US). Conidia were recovered from the filter by adding 2 x 10 mL Tween 80 (0.1% [v/v]) and gently dislodging conidia from the filter using a cotton swab, followed by centrifugation (537*g*, 3 min), resuspension in 1 mL Tween 80 (0.1%) and filtering through a 40 µm cell strainer. Aliquots (500 µL) of the suspension were treated with either 50 mL EW (0.04% [v/v] diluted in sterile tap water; full strength EW pre-dilution for these experiments had ~1600–1700 mg L^{-1} FAC) or sterile tap water. At intervals, treatments were stopped by centrifugation (2876*g*, 10 min, 4°C) and resuspension in 10 mL YEPD. After appropriate dilution in YEPD, 100 µL samples were plated onto YEPD-agar and incubated for 2 days at 28°C before colony enumeration to assess the strength of the EW effect in the experiments. The remaining volume (of the YEPD-resuspended treatments) was centrifuged (2876*g*, 10 min, 4°C), resuspended in 500 µL Tween 80 (0.1%), centrifuged (9000*g*, 5 min, 4°C), resuspended in RNA extraction buffer (0.6 M NaCl, 0.1 M EDTA, 0.2 M $Na^+CH_3COO^-$, 4% [w/v] SDS), frozen in liquid nitrogen and stored at –80°C.

4.2.5.2 RNA extraction

Tubes with the EW-treated samples were placed into liquid nitrogen and the frozen samples were transferred into lysis chambers (pre-cooled at –20°C) together with 0.5 mL glass lysis beads (150 µm, BDH Chemicals Limited, Poole, UK or Sigma-Aldrich). Spore lysis was performed at 2000 rev min^{-1} for 4 min in a laboratory ball mill (Mikro U Dismembrator, Sartorius Stedim Biotech, Germany). The lysate was mixed on ice with 600 µL Lysis Buffer (Plant/Fungi Total RNA Purification Kit, Norgen Biotek, Thorold, Canada) and 6 µL β-mercaptoethanol, then centrifuged twice (9000*g*, 5 min, 4°C) to obtain the clear aqueous phase free of debris. The solution was incubated at 55°C for 5 min to dissociate RNA-protein complexes. The following steps were according to the RNA Purification Kit's manufacturer's instructions, with samples kept on ice. The sample was applied to the kit's filter

column, centrifuged (12,000*g*, 2 min) and the flow-through mixed 1:1 with pure ethanol. It was then applied to the kit's spin column and washed three times with ~500 µL Washing Buffer (20,000*g*, 2 min). The column was dried by centrifugation (2000*g*, 4 min) and air-dried for 10 min. RNA was eluted with 40 µL RNase free water (treated with 0.1% diethyl pyrocarbonate (DEPC) for 1 h and autoclaved twice) by centrifugation (200*g*, 2 min, then 12,000*g*, 2 min) and stored at –80°C.

4.2.5.3 RNA quality control

The RNA purity was assessed using a DeNovix Nanodrop by checking for A260/A280 and A260/A230 ratios ≥1.8. The RNA was quantified at the DeepSeq Facility at the QMC (Medical School, University of Nottingham) using the Qubit RNA BR Kit (following the manufacturer's instructions). The RNA integrity was assessed by gel electrophoresis after mixing 100–200 ng RNA with 2X RNA loading dye (NEB), to confirm the presence of the 18S and 28S rRNA bands. Agarose gels (1.25% agarose, 0.2 µg mL^{-1} ethidium bromide) were prepared in TBE buffer (10.8 g L^{-1} tris, 5.5 g L^{-1} boric acid, 0.93 g L^{-1} EDTA).

4.2.5.4 RNA-sequencing

Further sample processing and transcriptome analysis were performed by the Centre for Genomic Research (CGR) at the University of Liverpool. RNA samples were depleted of DNA by treatment with Turbo DNase (Thermo Fisher). Ribosomal RNA was removed with the Human/Mouse/Rat RiboZero Magnetic Kit from Illumina. RNA-sequencing libraries were prepared using the NEBNext® Ultra™ Directional RNA Library Prep Kit for Illumina® #E7420 with 15 amplification cycles and purified using AMPure XP beads. The quantity and quality of the generated cDNA were checked using Qubit, the Agilent 2100 Bioanalyser and by qPCR using the Illumina Library Quantification Kit from Kapa (KK4854) on a Roche Light Cycler LC480II. Sequencing was performed on 50 µL denatured cDNA (300 pM) using an

Illumina® HiSeq 4000 platform with version 1 chemistry using sequencing by synthesis (SBS) technology to generate 2 x 150 bp paired-end reads.

4.2.5.5 Bioinformatic analysis

The bioinformatic analysis and significance tests were also performed by the CGR (Liverpool). Base calling and de-multiplexing of indexed reads (assigning barcoded reads to separate samples after sequencing of pooled samples) were performed by CASAVA version 1.8.2 (Illumina) and trimming of Illumina adapter sequences was performed using Cutadapt version 1.2.1 with the option "–O3" to trim 3' ends that matched the adapter sequence by at least 3 bp (Martin, 2011). Low quality bases were removed by trimming with Sickle version 1.200 with a minimum window quality score of 20. Reads shorter than 20 bp were also removed after trimming. The reads were mapped using Tophat version 2.1.0 (read mat orientation: "--library type fr firststrand", number of hits to be reported: "-g 1") (Langmead and Salzberg, 2012) to the reference genome of *Aspergillus niger* CBS 513.88 available on the *Aspergillus* genome database (N402 reference genome was not available at the time of analysis, see also discussion section):

http://www.aspergillusgenome.org/download/sequence/A_niger_CBS_513_88/current/A_niger_CBS_513_88_current_chromosomes.fasta.gz and http://www.aspergillusgenome.org/download/gff/A_niger_CBS_513_88/A_niger_CBS_513_88_current_features.gtf

Gene expression was calculated using htseq count (Anders et al., 2015) and raw count data were converted into FPKM (fragments per kilobase per million reads). The analysis of differentially expressed (DE) genes was performed in R (version 3.3.3) using the EdgeR package (Robinson et al., 2010). A generalized linear model (GLM) (Nelder and Wedderburn, 1972) was used for data modelling, data were normalised using the Trimmed Mean M-value method to correct for

differences in library size among different samples and log2 fold change (logFC) values were calculated using tagwise dispersion. Significance was tested using a Likelihood Ratios (LR) test (Wilks, 1938) and p-values were adjusted for multiple testing using the false discovery rate (FDR) approach (Benjamini and Hochberg, 1995). FDR-adjusted p-values <0.05 were defined as significant.

4.2.6 Statistical analysis and software

Tests for statistical significance, linear regression and flow cytometry analysis were performed as described in 2.2.11 and 3.2.11. RStudio (version 1.1.463) was used to generate histograms using the hist function (break width = 15, x-axis range = 0, 255) and heatmaps of logFC values using the gplots::heatmap.2 function. The *Aspergillus* genome database, AspGD (Cerqueira et al., 2014) was used to obtain gene annotations and to analyse gene ontology (GO) terms among DE genes by using the GO Slim Mapper (http://www.aspergillusgenome.org/cgi-bin/GO/goTermMapper).

4.3 Results

4.3.1 Effect of sub-lethal and partially lethal EW treatment on *A. niger* conidia and their outgrowth

4.3.1.1 Sub-lethal EW treatment delays the formation of *A. niger* colonies post-treatment

In sanitising and disinfecting treatments, EW needs to be applied at a concentration that is sufficient to fully inactivate fungal spores. However, in practice that may not always be possible. One concern is the quenching of active species in EW by the presence of organic matter (see Chapter 2). This may lead to lower effective EW concentrations in an application, resulting in some survival of target fungi. In order to understand such risks, effects of low EW levels on spore outgrowth of *A. niger* were tested. Suspensions of *A. niger* conidia were treated with diluted EW (≤0.4%, equal to ≤8 mg L^{-1} FAC, allowing partial or full survival, cf. Figure 2-1). After the treatment, spores were diluted in YEPD and plated on YEPD agar. The colony areas arising from samples treated with 0.06–0.4% EW (1–8 mg L^{-1} FAC) were decreased by 14–60% compared to the no-EW control (boxplot of colony areas for one representative replicate shown in Figure 4-1 A). There was a significant negative correlation between the mean colony area and the EW dose (Figure 4-1 B). The survival was ~100% for EW doses up to 0.3% (Figure 4-1 C; note that survival was ≥100% in 2 replicates and below 100% for 1 replicate). This indicates that the observed growth delay post-treatment occurs independent of a killing effect, and even sub-lethal concentrations of EW can delay subsequent spore outgrowth of *A. niger*. The decreased colony area arising from EW-treated spores may be related to slow outgrowth, increased lag time before outgrowth or a combination of these and other potential mechanisms, and the term 'growth delay' will be used throughout to encompass such processes (except where slow growth specifically was tested, cf. 4.3.2).

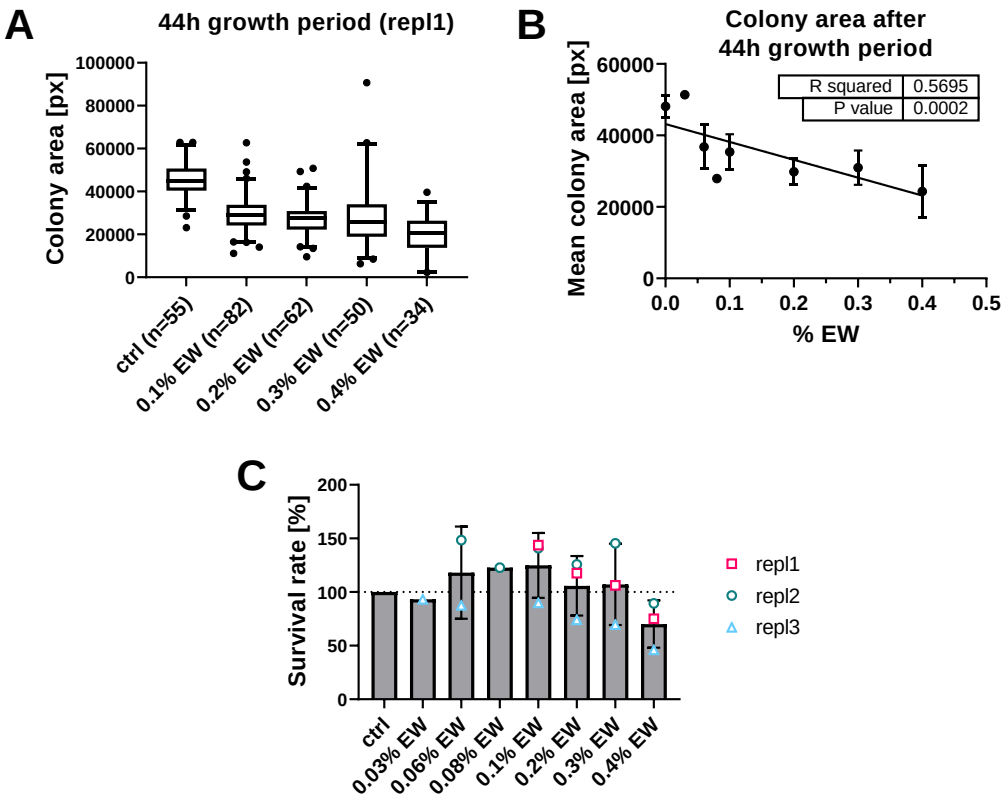

Figure 4-1: Low concentrations of EW delay subsequent spore outgrowth of *A. niger*. Spores were treated with EW dilutions (0.03–0.4% [v/v] in HPLC grade water; 0.5–8 mg L^{-1} FAC) for 5 min. 100 µL of appropriate dilutions were plated onto YEPD agar and the size (area) of colonies was measured after 44 h by imaging (see 4.2.1). A) The distribution of colony areas in pixels is shown for 1 replicate. The boxes extend from the 25th to the 75th percentiles (the line within the boxes is the median) and the whiskers show the 5th and 95th percentiles, with values above and below the whiskers shown as individual points. n, number of analysed colonies (colonies that were touching another colony or the edge of the plate were excluded for colony area analysis [but included for survival rate determination in C]). B) The average ± SD of the mean colony area at different EW concentrations is shown for 3 replicates together with the linear regression. C) Survival was determined by colony enumeration and calculated relative to the untreated control (ctrl). The survival of the individual biological replicates is shown with superimposed symbols. repl, biological replicate. Mean values ± SD are shown for 3 biological replicates, except 0.03% and 0.08%: n = 1 and 0.06%: n = 2.

4.3.1.2 Sub-lethal EW treatment increases the colony size variation

It was further studied whether all colonies were affected by low level EW treatments in the same way, or whether single spores would react differently to the treatment, resulting in a larger range of colony sizes (= areas) after the recovery period. Such differences may occur when different spores accumulate different levels of damage (e.g., protein damage), which may also be related to

intrinsic differences between single spores (e.g., protein composition differences). To study such variation, the coefficient of variation (CV = standard deviation divided by the sample mean) of the colony areas was calculated. In the untreated control samples, the CV was lower at later time points (48 h, higher mean colony area) than at the earlier time point (44 h, lower mean colony area, Figure 4-2 A). Therefore, there could be a risk of overestimating CV values for EW treated samples at the 44 h time point due to the growth delay in these samples. To account for such effects, the CV of EW-treated samples was assessed at a time point at which the mean colony size of the EW treated sample was similar to the mean colony size of the control at 44 h, and these CVs were compared to the 44h control CV value. The variation in colony area (CV) was generally higher in EW-treated samples than in the control (Figure 4-2 A). The CV increased with increasing EW dose, and this correlation was statistically significant (Figure 4-2 B).

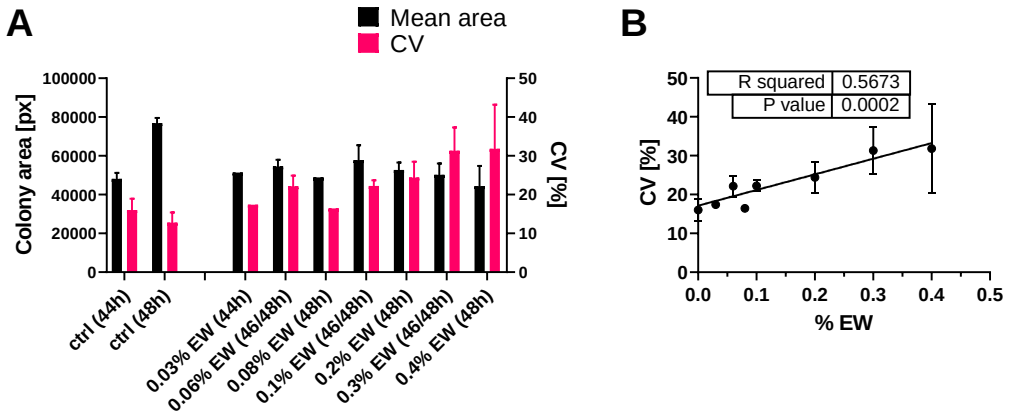

Figure 4-2: Low concentrations of EW increase the colony size variation in *A. niger*. Spores were treated as described in the Figure 4-1 legend (data from same experiments). A) The mean colony area (in pixels, black bars) and the coefficient of variation (CV, %, pink) were determined after defined growth periods (44–48 h, as specified) that resulted in a similar mean colony area in the treated samples as in the untreated control at 44 h. 46/48 h refers to cases where different time points were chosen for the different biological replicates, reflecting day-to-day variation in the absolute effect size of the growth delay. B) The linear regression of the CV values at the different EW concentrations displayed in A. Mean values ± SD are shown for 3 biological replicates, except 0.03% and 0.08%: n = 1 and 0.06%: n = 2.

4.3.2 The increase in variation is not caused by slow growth alone

The observed increase in colony size variation could have several explanations. One hypothesis was that slowed outgrowth of spores (such as after EW treatment) non-specifically pronounces differences in subsequent colony size, e.g., by exacerbating differences between slow and fast growing/germinating spores. The slowed outgrowth was mimicked by recovery of control and EW treated samples at lower temperatures. For control (no-EW treatment) samples, reducing the recovery temperature from the standard 28°C to 23°C did not increase the colony size variation (CV) and even slightly decreased the CV (Figure 4-3 A; FDR-corrected p-value of the paired two-tailed *t*-test between 28°C (46 h) and 23°C (66 h) = 0.0246). In contrast, the CV was increased in 2 out of 3 control replicates when the recovery growth took place at room temperature (20°C ± 2°C). It is possible that the observed differences in CV at the different temperatures are actually related to fluctuations in the set temperature conditions (temperature control is not perfect), which are expected to be greater in the room temperature condition than in the 23°C (incubator, recently purchased) and 28°C (temperature controlled room) conditions. Another explanation for the higher CV observed at room temperature in some experiments is addressed in 4.4.2. Overall, lowering the temperature alone (for outgrowth of no-EW control samples) did not consistently increase the CV, suggesting that slow outgrowth alone is not responsible for the increase in variation. In contrast, when EW treated samples were grown at lower temperatures, the CV (already higher than the CV of the no-treatment control, consistent with Figure 4-2) was further increased (Figure 4-3 A; FDR-corrected p-value of the paired two-tailed *t*-test between 0.1% at 28°C and 0.1% at 23°C was p = 0.0254). The overall number of colonies and survival was not significantly affected by the recovery temperature (Figure 4-3 B; according to paired two-tailed *t*-tests between all control outgrowth temperature conditions (cfu) and all EW-treatment outgrowth temperatures (cfu and survival rates), with

FDR-correction for multiple testing). As before, survival >100% for 0.1% EW treatments was recorded in some experiments. Overall, it should be noted that lowered temperatures not only slow down growth, but can also induce cold stress responses which may influence the observed phenotypes.

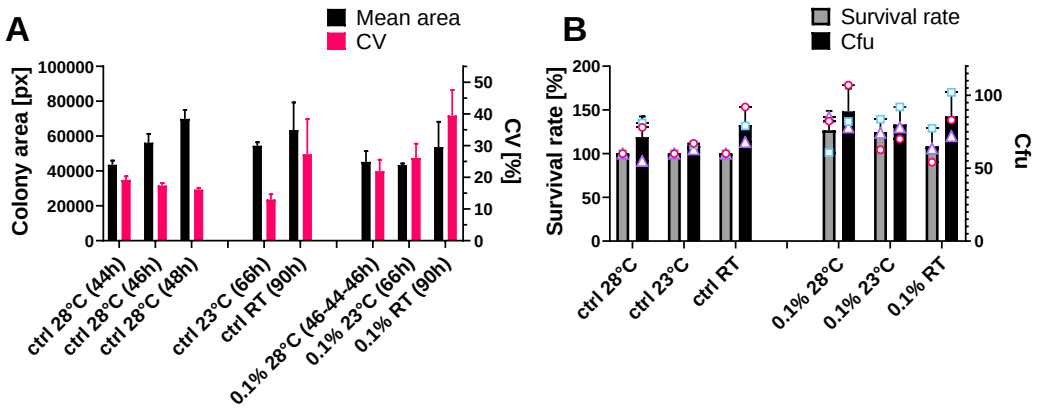

Figure 4-3: Colony size variation and survival at lower recovery temperatures. Spores were treated or not with 0.1% EW (% [v/v] in HPLC grade water; 1.8–2 mg L^{-1} FAC) for 5 min. 100 µL of appropriate dilutions were plated onto YEPD agar and incubated at 28°C, 23°C or room temperature (RT, 20 ± 2°C). A) The area (in pixels, black bars) and coefficient of variation (CV, %, pink) of the colonies was measured after the specified growth periods by imaging (see 4.2.1). "46-44-46h" refers to different time points that were chosen for the different biological replicates, reflecting day-to-day variation in the absolute effect size of the growth delay. B) Survival (%, grey bars) was determined by colony enumeration (cfu, colony forming units, total from 5 technical replicate plates, black bars) and calculated relative to the untreated controls (ctrl). The values of the individual biological replicates are shown with superimposed symbols. Mean values ± SD are shown for 3 biological replicates.

The above data showed that slow growth at low temperatures alone was not sufficient to increase the colony size variation, but that EW treatment combined with outgrowth at low temperatures increased the variation more than EW treatment alone. One hypothesis to explain this observation was that the repair of EW-induced damage might be slowed down during slow growth at low temperatures. Because there will already be some heterogeneity between single spores (e.g., some may accumulate more damage arising from the treatment), such differences could be amplified when the repair processes are slowed down: Whereas relatively intact spores would only be slowed down in their growth,

damaged spores would be slowed down in their growth *and* in their repair processes. If that is correct, the slow+damaged sub-population should produce a left skewed distribution of the colony areas. The data distribution was assessed by plotting histograms of the colony areas. First, the absolute colony area measurements were transformed into % of the mean for each replicate experiment in order to be able to pool comparable data from these biological replicates (i.e., normalised for variation in the mean colony area between replicates). Comparing the histograms of EW-treated samples grown at 23°C or at room temperature with the 28°C condition, no left skew at lower temperatures could be observed (Figure 4-4). It is additionally possible that spores that accumulate less damage than the population average are favoured at lower temperature because they need to perform less repair than the population average. That might add a right skew to the distribution which, combined with the processes described (left skew), could give a net wider distribution of colony areas in both directions. Such a wider distribution was evident for EW-treated spores incubated at 23°C and at room temperature (Figure 4-4). This is consistent with interactions between repair processes and growth rates as proposed above, although it does not rule out alternative explanations for the increased variation seen after EW combined with lower temperature recovery.

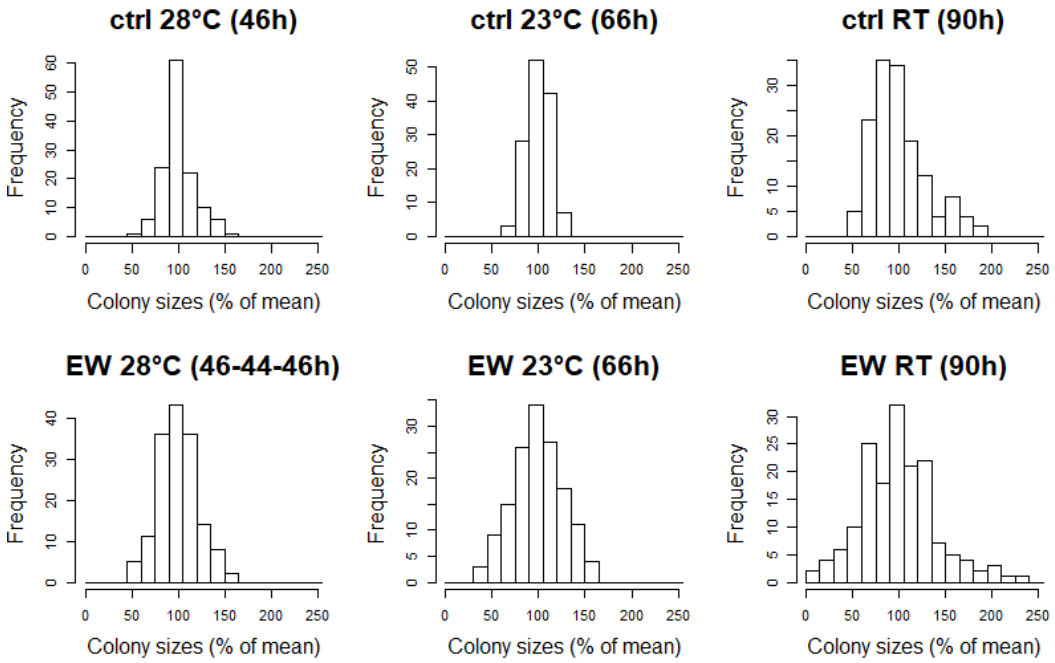

Figure 4-4: Distribution of the colony areas after treatment with low EW concentrations and low temperature recovery. Spores were treated or not with 0.1% EW (% [v/v] in HPLC grade water; 1.8–2 mg L^{-1} FAC) for 5 min. 100 µL of appropriate dilutions were plated onto YEPD agar and incubated at 28°C, 23°C or room temperature (RT, 20 ± 2°C). The area of the colonies was measured after the specified growth periods by imaging (see 4.2.1). Mean values and CV of the datasets are plotted in Figure 4-3. The colony area values were transformed into % of the mean for each replicate, the data were then pooled for 3 biological replicates and histograms were plotted with 15%-bar width.

4.3.3 Ruling out genetic variation

Within a population, individuals may also acquire spontaneous mutations that can affect the phenotype. To test for a possible genotypic component to the heterogeneity described above, first *A. niger* spores were treated with 0.3% EW (5.4–6 mg L^{-1} FAC; a dose reducing colony size by 26–29% after recovery on YEPD agar and giving 71–99% survival; Figure 4-5 A,B), and then two small, medium and large colonies were selected by eye from each biological replicate. For the no-EW controls, two colonies of average size were selected. The mean area of these colonies is given in Figure 4-5 C. Colonies were then streaked onto PDA slopes and re-grown for one week. Spores from these PDA slopes were harvested and treated (or not) again with 0.3% EW. The resultant colony areas

and variation for the different sub-cultures, with or without EW treatment, did not correlate with the original colony sizes from which they were derived after the first treatment (Figure 4-5 D; linear regression analysis for the two measures (mean colony area or CV) of EW-treatments or controls *after* sub-culture plotted against the different colony sizes *before* sub-culture showed no significant correlations [R^2<0.02, p>0.05, not shown]). Similarly, the germination efficiency (number of cfu) in controls and EW-survival in treatments were not different for any of the sub-cultures stemming from the isolated colonies of different sizes (Figure 4-5 E). These results suggested that the observed differences in colony size post EW-treatment were not heritable traits and so were not due to genetic differences. This supports the inference that the observed variation arises from non-heritable phenotypic heterogeneity of spore damage and/or responses to EW within a population.

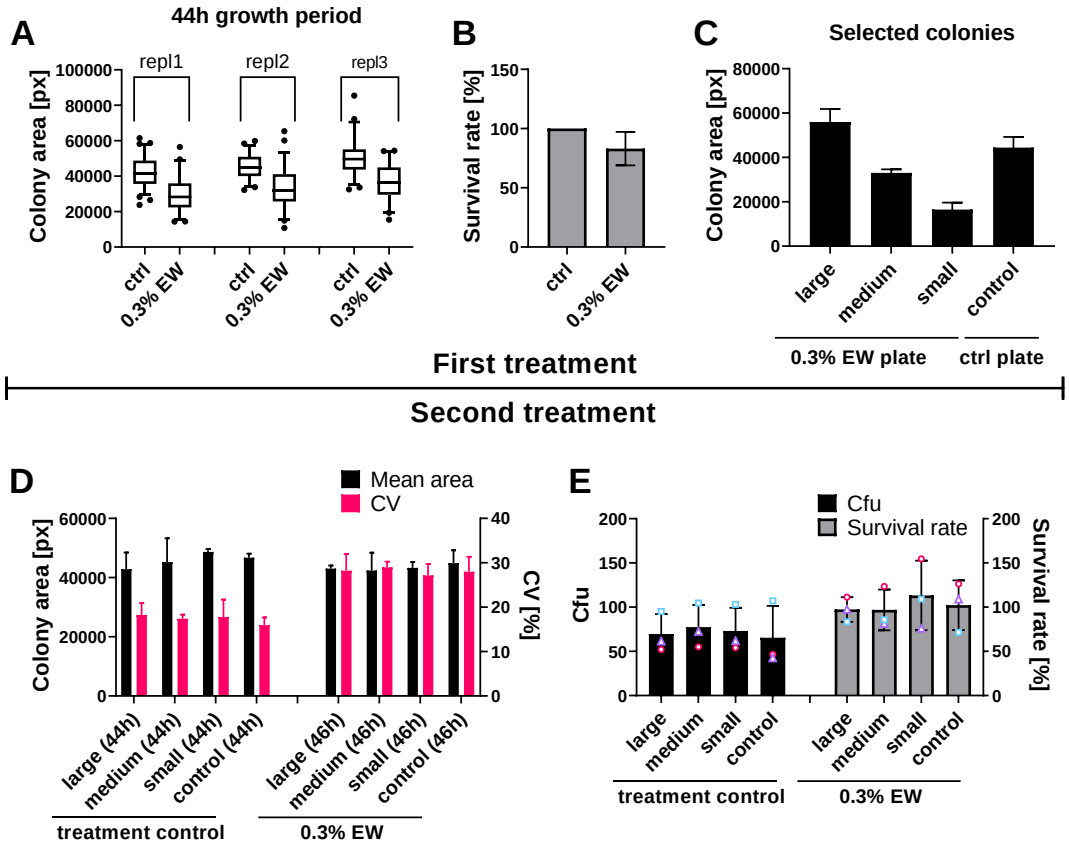

Figure 4-5: Assessing a potential genetic component to colony size variation following EW treatment. Spores were treated or not with 0.3% EW (% [v/v] in HPLC grade water; 5.4–6 mg L^{-1} FAC) for 5 min. 100 µL of appropriate dilutions were plated onto YEPD agar and incubated for 44 h. A) The areas of the colonies (in pixels) was measured by imaging (see 4.2.1). The boxes extend from the 25th to the 75th percentiles (the line within the boxes is the median) and the whiskers show the 5th and 95th percentiles, with values above and below the whiskers shown as individual points. repl, biological replicate. B) Survival was determined by colony enumeration and calculated relative to the untreated control (ctrl). C) Large, medium and small colonies from the EW-treated plates were selected by eye and chosen for re-growth on PDA slopes. Average-size control colonies were chosen. Two colonies were chosen per size as technical replicates (resulting in six total colonies that were analysed per size across 3 biological replicates). D) Spores obtained from the re-grown colonies were treated again ('second treatment') as described in A), and the colony area (in pixels, black bars) and coefficient of variation (CV, %, pink) determined. E) Growth after the second treatment was determined by colony enumeration (colony forming units, cfu, total from 5 technical replicate plates, black bars) and the survival (grey) calculated relative to the untreated controls. Cfu and survival values of the individual biological replicates are shown as superimposed symbols. Mean values ± SD are shown for 3 biological replicates.

4.3.4 Testing the effect of sub-lethal or partially lethal NaOCl and ozonated water on *A. niger*

Above, it was shown that low levels of EW delayed colony growth and increased colony size variation. The increased variation was not caused by slow growth alone, and the effects on colony size and variation were non-heritable. To further understand the causes of the observed effects, specifically regarding the FAC and/or chlorine-free components of EW, similar experiments were carried out with diluted NaOCl and ozonated water. The highest EW dose used in the experiments above was 0.4% which equals 7–8 mg L^{-1} FAC. NaOCl was used at concentrations up to 7.5 mg L^{-1} (= 7.5 ppm). The colony size variation (CV) was increased after NaOCl treatments (Figure 4-6 A,B) and the colony area was decreased in a concentration-dependent manner (Figure 4-6 C). The applied NaOCl concentrations were sub-lethal (Figure 4-6 D; survival was ≥100% for all treatments; survival at 7.5 ppm was very high for one biological replicate due to very dense growth on one of 5 agar plates (technical replicates), a possible artefact from spore clumping or similar).

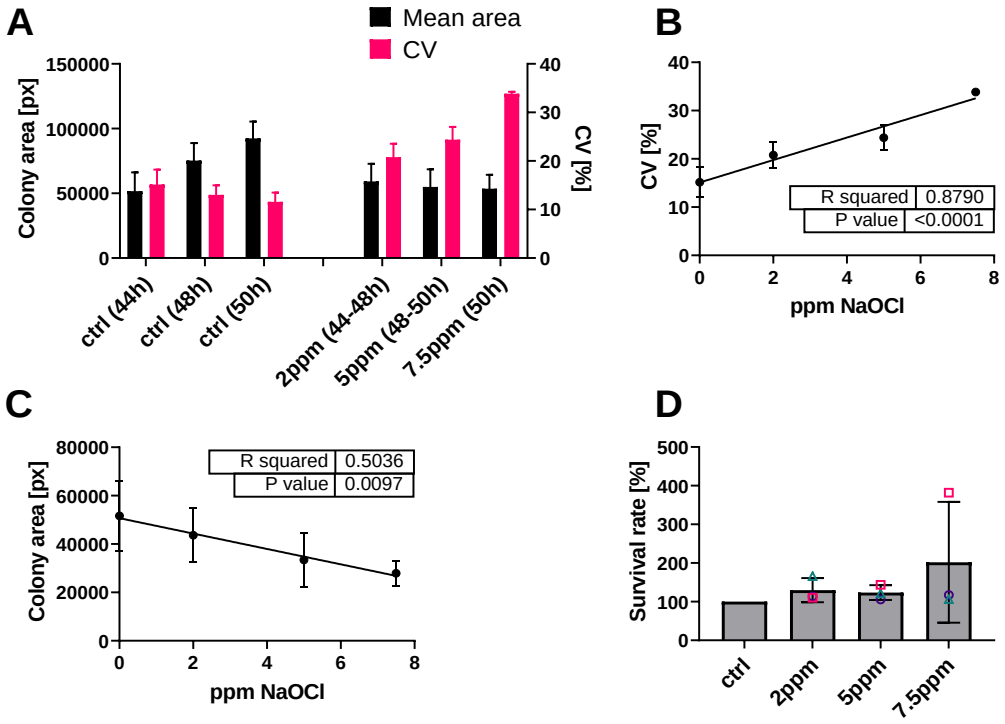

Figure 4-6: Effect of low concentrations of NaOCl on colony growth and colony size variation. Spores were treated or not with NaOCl dilutions (ppm = mg L^{-1} FAC, in HPLC grade water) for 5 min. 100 µL of appropriate dilutions were plated onto YEPD agar and incubated for the specified periods. A) The area of the colonies (in pixels, black bars) and coefficient of variation (CV, %, pink) were measured by imaging (see 4.2.1). B,C) The linear regression was determined for the CV at the time points given in A (B) and for the colony area at 44 h (C) at different NaOCl concentrations. D) Survival was determined by colony enumeration and calculated relative to the untreated control (ctrl). Survival of individual biological replicates is shown with superimposed symbols. Mean values ± SD are shown for 3 biological replicates.

In contrast to NaOCl and EW, treatment with ozonated water did not delay the colony growth (Figure 4-7 A; the mean colony area after 44 h in treated samples was ~99% of the mean control sample area). This was despite a relatively strong reduction in viability (Figure 4-7 B; survival was 18–60%). Different (sub-lethal) concentrations of ozonated water were not tested because the low shelf life (minutes) and the strong batch-to-batch variation make it difficult to control or predict the survival rate in these experiments. However, above, the strongest EW concentration (0.4%, resulting in 46–89% survival) did show a clear growth delay (Figure 4-1; mean colony size was reduced by ~50% compared to no-EW controls). The occurrence of a growth delay and increase in variation were further

confirmed for lower survival rates after 1% EW treatment (8–66% survival; mean colony size reduced by ~60% compared to no-EW controls) in an experiment presented below (Figure 4-8). The results of 0.4–1% EW treatments collectively contrasted with those for ozonated water.

The variation in colony size (CV) after ozonated water treatment was slightly increased in two out of three replicates (increase by +0.5% and +4% CV) and decreased in one replicate (by –4%; overall difference in the mean CV between control and treatment was non-significant according to a paired two-tailed *t*-test). The observed (non-signficant) effects on the CV after ozonated water treatment were much smaller than the increase in CV observed with the highest EW doses (0.3–0.4% EW leading to an increase of up to + ~20% CV, and 1% EW leading to an increase between +22 and +43% CV, Figure 4-1 and Figure 4-8). In conclusion, the effects observed with low concentrated EW could be reproduced with NaOCl but not with the chlorine-free oxidant ozonated water.

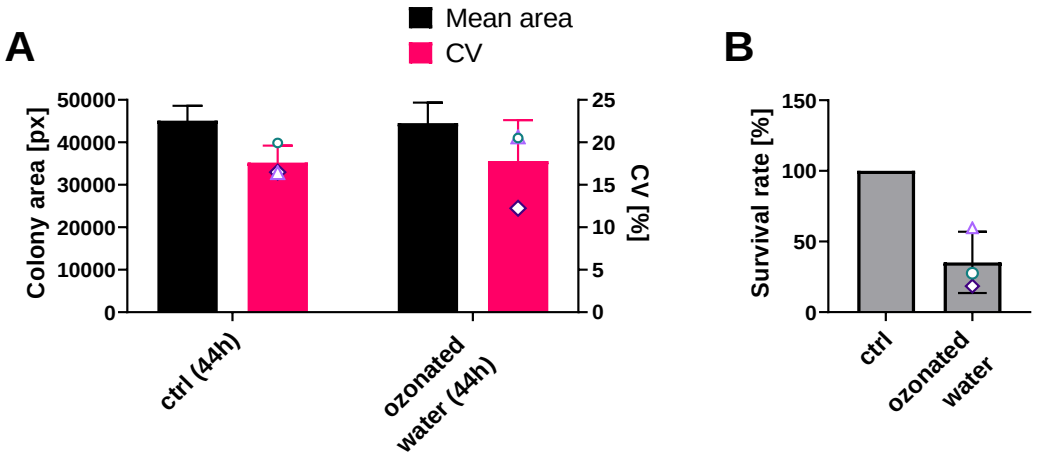

Figure 4-7: Effect of ozonated water on colony growth and colony size variation. Spores were treated or not with ozonated warer for 5 min. 100 µL of appropriate dilutions were plated onto YEPD agar and incubated for the specified periods. A) The area of the colonies (in pixels, black bars) and coefficient of variation (CV, %, pink) were measured by imaging (see 4.2.1). B) Survival was determined by colony enumeration and calculated relative to the untreated control (ctrl). Survival of individual biological replicates is shown with superimposed symbols. Mean values ± SD are shown for 3 biological replicates.

4.3.5 Delay and variation are evident in the first 2 h of germination post-treatment

Because the colony area measurements performed here represent an endpoint measurement, the observed growth delay and increased colony-colony variation after EW treatment could occur at any point throughout the ≥44 h growth period on YEPD agar. To test whether early germination events showed effects similar to the ones observed at the macro-colony level, spores were recovered for 2 h in YEPD after treatment with low concentrated EW and swelling of spores was assessed by flow cytometry. First it was confirmed that the normal delays in colony growth and increased colony-colony variation on agar, described above, were still evident for the spores treated at different EW doses in these particular experiments (Figure 4-8 A,B; samples of the treated spores were incubated on YEPD agar for ~2 days as above).

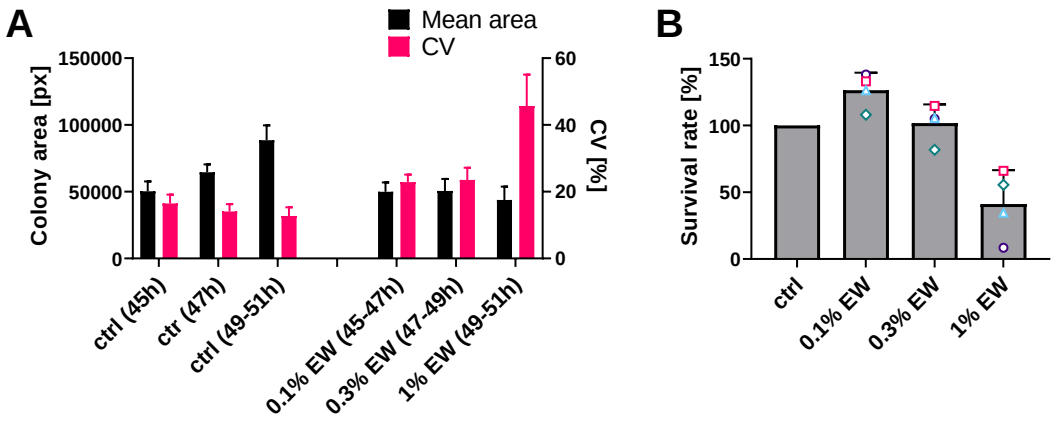

Figure 4-8: Colony area, variation and survival rate data for samples used below (Figure 4-10, Figure 4-11) for flow cytometry assessment. Spores were treated or not with EW dilutions (% [v/v] in HPLC grade water; 1.8–20 mg L^{-1} FAC) for 5 min. 100 µL of appropriate dilutions were plated onto YEPD agar and incubated for the specified periods. A) The area of the colonies (in pixels, black bars) and coefficient of variation (CV, %, pink) were measured by imaging (see 4.2.1). B) Survival was determined by colony enumeration and calculated relative to the untreated control (ctrl). Survival for individual biological replicates is shown with superimposed symbols. Mean values ± SD are shown for 4 biological replicates.

Before assessing the germination of the EW-treated spores by flow cytometry, the germination in untreated control conditions was assessed to validate the method. Spores were germinated in YEPD for up to 2.5 h, with samples taken every 0.5 h. Swelling of spores is expected during early germination (Hayer et al., 2013) and the forward scatter (FSC) in flow cytometry can be used as a measure of particle size distribution (van den Brule et al., 2020), so the FSC can be used to assess such early germination events (Hayer et al., 2013). As expected, the FSC increased steadily over 2.5 h (Figure 4-9 A, representative histograms for one biological replicate; B, mean values). Based on the FSC distribution of non-germinated spores, a 'germination-positive' gate was defined (Figure 4-9 C; note that this gate may contain any spore doublets that were not successfully excluded by the gating strategy [4.2.2]). Most spores moved into this gate within 1 h of triggering germination (Figure 4-9 D).

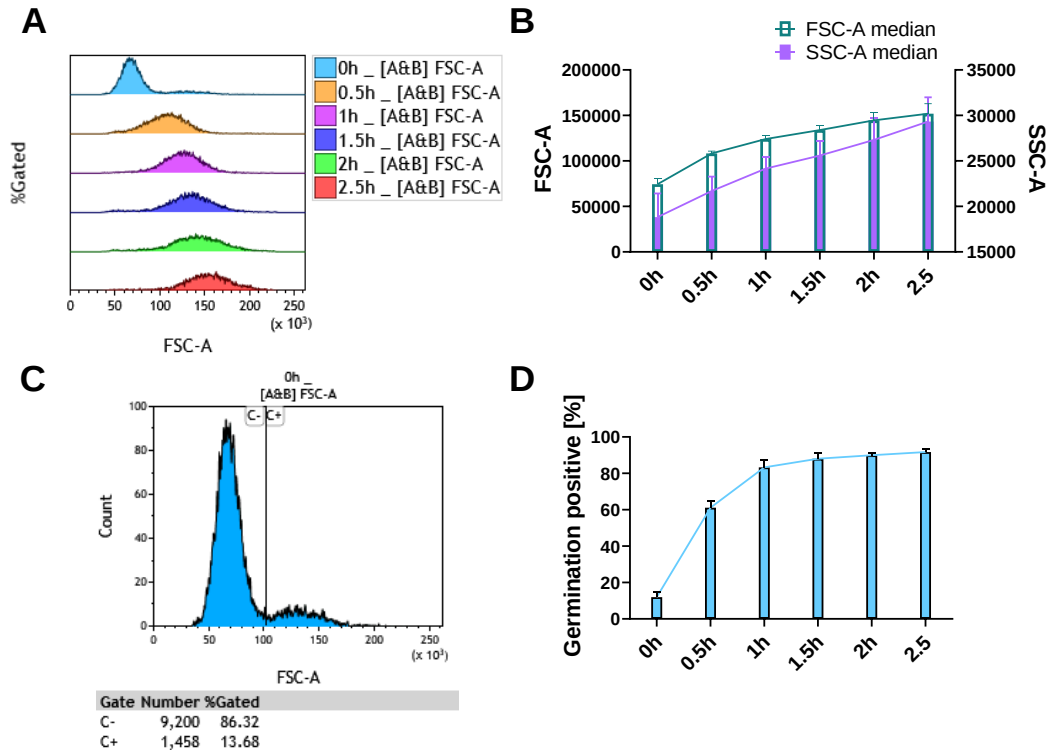

Figure 4-9: Flow cytometric analysis of germinating *A. niger* spores. Spores were germinated in YEPD for 0–2.5 h and harvested at the specified time points. The forward scatter (FSC-A; flow cytometry signal area) and sideward scatter (SSC-A) were measured in a BD FACS Canto™ A flow cytometer. A) Histograms of the FSC distribution at different time points in one representative biological replicate ([A&B] in the mini-legend refers to the gating strategy to exclude cell clumps and debris). B) Average of the population median across 3 biological replicates for the FSC and SSC median. C) FSC distribution of non-germinated spores (0 h) and gate definition. Germination positive events were defined as events on the right of the vertical line. D) Events (%) in the germination-positive gate. Mean values ± SD are shown for 3 biological replicates.

After validating the above measures for tracking early germination events (FSC increase and % events in the germination-positive gate), the germination after treatment with low EW concentrations (Figure 4-8) followed by 2 h YEPD germination post-treatment was assessed. The FSC was significantly decreased after EW treatment + 2 h germination compared to the untreated control (Figure 4-10 A). Similarly, fewer events were found in the germination-positive gate in EW treated samples than in the control (Figure 4-10 B). This suggested that the early germination events in the first 2 h after the EW treatment were delayed when using either sub-lethal (0.1, 0.3% EW) or partially lethal (1%)

concentrations. It was noted that the SSC of 0.1% EW treated cells was increased (Figure 4-10 A), suggesting an effect of EW treatment on the optical properties related to granularity and surface topography of the spores (Jaroszeski and Radcliff, 1999).

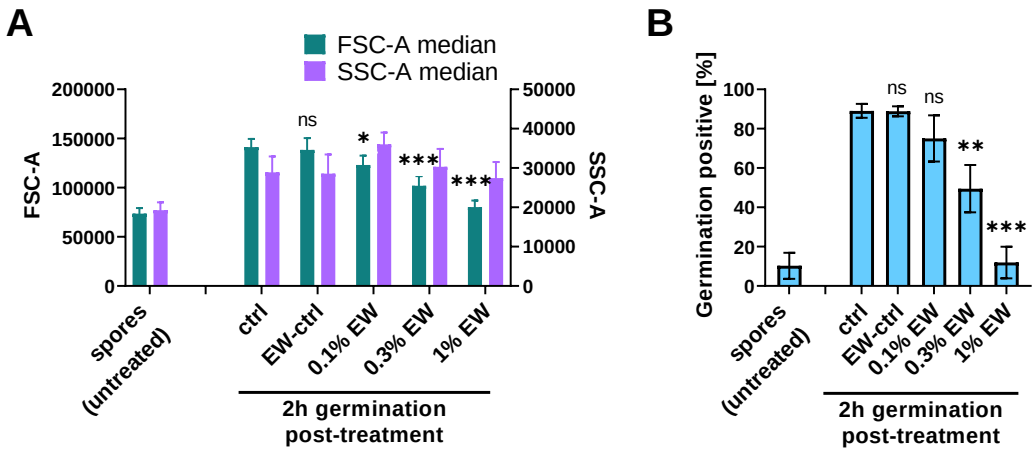

Figure 4-10: Germination after treatment with low concentrations of EW assessed by flow cytometry. Spores were treated or not with diluted EW; see Figure 4-8 legend for details. Immediately after treatment, spores were transferred into YEPD broth and germinated for 2 h. 'EW-ctrl' refers to a condition where 1% EW was mixed with YEPD and spores were added subsequently (instead of exposing spores to active EW). This served as a control for potential reaction products between EW and YEPD that may affect the germination (no such effects were observed). 'Spores' were untreated, ungerminated spore samples. A) The forward scatter (FSC-A) and sideward scatter (SSC-A) were measured in a BD FACS Canto™ A flow cytometer. B) Events (%) in the germination-positive gate (see Figure 4-9). Mean values ± SD are shown for 4 biological replicates. *p<0.05; **p<0.01; ***p<0.001; ns, not significant; according to paired *t*-test (two-tailed) with correction for multiple comparisons by controlling the false discovery rate at 5% FDR (Benjamini et al., 2006), comparing between 2 h-germinated ctrl and treatments.

The germination of untreated spores over 2.5 h was characterised by a shift of the whole population to higher FSC values and, from 0.5 h, without obvious changes to the shape of the population distribution between the germination time points (Figure 4-11 A). Consequently, the variation of the FSC measure (coefficient of variation, CV) was relatively consistent at all time points after 0 h (Figure 4-11 C). In contrast, the FSC distributions after 0.1% and 0.3% EW treatment + 2 h germination in YEPD were widened compared to the control (Figure 4-11 B). The CV of the FSC was increased significantly for 0.3% EW (FDR-corrected p-value of

the paired *t*-test = 0.009). As this increased variation occurred at sub-lethal EW treatment (cf. Figure 4-8), it cannot be caused by a proportion of dead (non-germinating) spores. Only one replicate (out of 4 biological replicates) treated with 0.3% resulted in survival slightly below 100% (81%) but the CV was increased in all 4 replicates. The histograms in Figure 4-11 B show the results for one representative replicate where 0.3% EW did not decrease survival. Taken together, the flow cytometry results suggested that the growth delay and increase in variation that could be observed at the colony level (after 2 days of growth) could already be observed after 2 h of germination. The presented results do not rule out further effects also after 2h germination, but they do provide evidence for the effect in the first 2 h of germination.

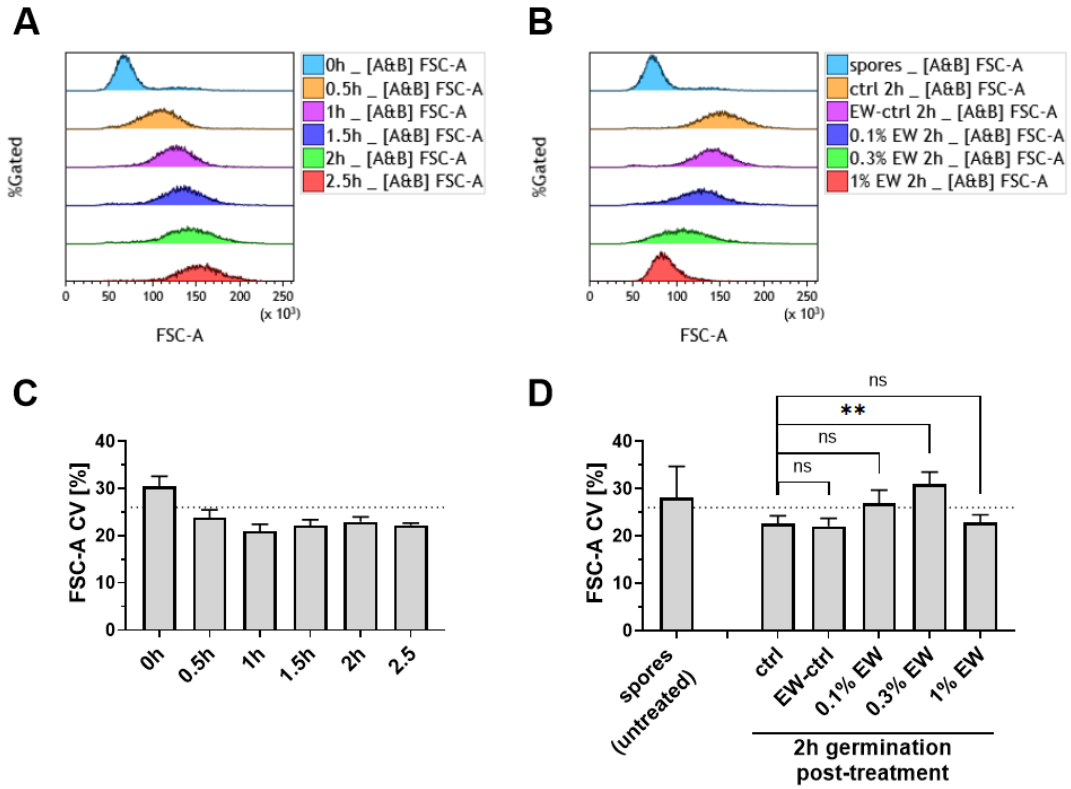

Figure 4-11: Heterogeneity of spore germination assessed by flow cytometry. Spores were germinated in YEPD for 0.5–2.5 h (A,C, see Figure 4-9 for details) or treated or not with diluted EW and transferred into YEPD for 2 h germination (B,D, see Figure 4-8 for details). 'EW-ctrl' refers to a condition where 1% EW was mixed with YEPD and spores were added subsequently (instead of exposing spores to active EW). This served as a control for potential reaction products between EW and YEPD that may affect the germination (no such effects were observed). 'Spores' were untreated, ungerminated spore samples. A,B) Histograms of the forward scatter (FSC-A) distribution at different time points (A) and different treatment conditions (B) in 1 representative biological replicate each ([A&B] in the legend refers to the gating strategy to exclude cell clumps and debris). C,D) The coefficient of variation (CV, %) of the FSC was determined. The dotted line at 26% in both graphs represents the highest measured CV value (among the individual values from the biological replicates) in the untreated germinating samples (0.5–2.5 h) in panel C. Mean values ± SD are shown for at least 3 biological replicates. **p<0.01; ns, not significant; according to paired *t*-test (two-tailed) with correction for multiple comparisons by controlling the false discovery rate at 5% FDR (Benjamini et al., 2006).

4.3.6 Investigating survival above 100%

In several experiments above, survival >100% (up to ~150%) was unexpectedly recorded after treatment with EW or NaOCl at low concentrations. All experiments assessing low EW or NaOCl concentrations up to this section combined (sections 4.3.1 to 4.3.5) consisted of 19 biological replicates, i.e., 19 independent experiments. In 12 out of 19 experiments, survival >100% was recorded (Figure

4-1, Figure 4-3, Figure 4-5, Figure 4-6, Figure 4-8; experiments were counted if at least one EW concentration in the experiment resulted in survival >110% [increases of less than 10% were deemed too low to represent an interesting effect]), although for 3 out of the 19, outgrowth of the same samples was performed at three different temperatures per experiment, and survival >110% was recorded only in one (1 experiment out of the 3) or two (2 experiments) of these temperatures. The most frequently used EW doses in the above experiments were 0.1% and 0.3% EW (10 and 13 experiments each), and the survival was significantly different from 100% for 0.1% EW (according to a one-sample two-tailed *t*-test ($p = 0.002$); not significant for 0.3% EW). It is possible that survival >100% was caused by (technical) variation in the colony forming numbers between individual plates within the same experiment, i.e., that higher numbers on EW-treated plates were obtained by chance. To assess the variability of colony forming numbers, a control sample (no treatment) was plated onto two separate sets of agar plates (each set consisting of 5 plates as technical replicates) in 3 separate experiments. For each set, the sum of colonies from all 5 plates was calculated. One of the sets was randomly selected as 'ctrl 1' and the "survival" of the 'ctrl 2'-set was calculated relative to ctrl 1. A "survival" rate of >100% was calculated in 2 out of 3 experiments (121% and 133%, Figure 4-12), suggesting that technical variation between experiments could have contributed to some instances of survival rates >100%. Such technical variation may be due to clumping of spores, where two (or more) clumped spores would lead to only one colony in some samples, resulting in less colonies despite plating the same number of spores. Increasing the Tween 80 concentration in spore suspensions (0.1% in the present work) may have helped to reduce clumping events. It is further possible that EW treatment impacted such spore clumping: if two clumped spores were separated during EW treatment (e.g., due to reactivity of the EW with the spore coat), they could then form two colonies instead of one, thereby increasing the number of colonies on recovery plates. EW treated spores showed increased

sideward scatter properties in flow cytometry analysis, potentially indicating changes to the spore surface (see 4.3.5, Figure 4-10) which may impact adhesion/clumping behaviour.

On the other hand, if the colony formation efficacy in control conditions was <100% (i.e., not all spores were successfully forming colonies), then a real increase in survival (i.e., colony formation efficacy) after EW treatment would be possible [reported survival rates are % of control colonies], albeit not the most likely explanation. Observations of growth induction at low stressor concentrations (with inhibition at higher concentrations) are known as hormesis (Pradhan et al., 2017), see 4.4.4. In some experiments, the survival rates followed a consistent trend across replicates (see Figure 4-8 B: in 3 out of 4 replicates, survival >110% was recorded after treatment with 0.1% EW and survival was between 105–115% with 0.3% EW, and in all 4 replicates the survival was higher at 0.1% EW than at 0.3% [significant according to paired two-tailed *t*-test, p = 0.005]), potentially suggesting an effect specific to a narrow range of EW concentrations before partial lethality occurs at higher levels. Consistent trends would not be expected in the case of purely statistical variation between colony numbers in non-lethal conditions and may potentially be explained by the processes outlined above (reduced clumping and/or increased colony formation efficacy). However, the inherent variability of colony numbers obtained with the agar plating method as shown here (Figure 4-12) limits the conclusions from this method.

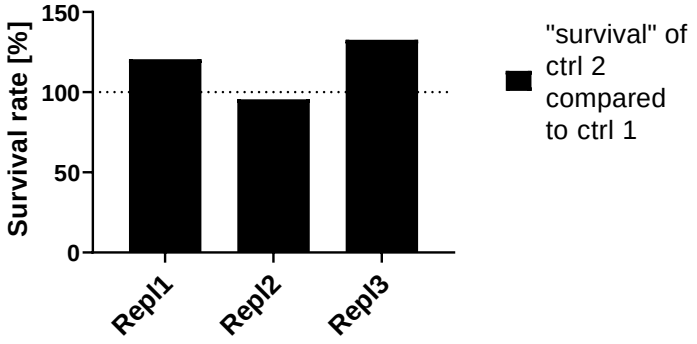

Figure 4-12: Variability of germination efficiency of *A. niger* between replicate assays. Spores were treated with HPLC grade water for 5 min (control conditions of EW treatment experiments described above). 100 µL of appropriate dilutions in YEPD were plated onto two sets of YEPD agar (each set consisting of 5 technical replicate plates) and incubated for 2 days. "Survival" was determined by colony enumeration (sum of 5 plates) and calculated for set 2 ('ctrl 2') relative to set 1 ('ctrl 1'). Repl1–3, biological replicates.

4.3.7 Investigating the role of potential chloramine formation for the growth delay and increased heterogeneity in response to EW

4.3.7.1 The growth delay and increased variation in colony size do not depend on the YEPD addition post EW treatment

Treatment of *A. niger* spores with low EW concentrations delayed the subsequent outgrowth of colonies in the absence of EW, and growth delays of *A. niger* had been observed in earlier experiments where EW treatment was in the presence of added free amino acids or protein-rich substances (Figure 2-8, Figure 2-9, Figure 2-10, Figure 2-11, Figure 2-12). For instance, in certain experiments (Figure 2-12), the EW was allowed to react with oxidised-Met (MetO), followed by inactivation of the FAC, before spores were added to the (inactivated) mix, and growth inhibition was observed. This indicated a potential inhibitory role of non-FAC components, formed from the reaction between FAC and available organic compounds such as MetO (EW-free MetO treatments did not inhibit fungal growth). The reaction between amino acids and FAC can yield different oxidation products including organic chloramines (chlorinated at the amino group) which

can have antimicrobial activity (see 4.4.3.1) (Szabó et al., 2019, Panasenko et al., 2013). It was hypothesised that the growth delays in those earlier experiments may have been due to the formation of inhibitory compounds such as chloramines (2.3.4.2, 2.4.4.2, see 4.4.3.2 for a detailed discussion) and that organic chloramines possibly form from reactions between active EW species and amino acids within fungal spores. Additionally, the EW treatment protocol in this study added YEPD to EW treatments at the end of the treatment period to inactivate the EW. It is possible that chloramines were formed during this inactivation step when proteins and amino acids in rich YEPD react with the FAC of EW. These chloramines could then potentially have entered the fungal spores and resulted in a growth delay effect.

To investigate whether the YEPD inactivation step might be the source of the observed growth delay, an alternative EW treatment protocol was employed where the YEPD inactivation step post-treatment was replaced by a 1:250 dilution step in water (2X YEPD is normally added to dilute the treatment 1:2, followed by a 1:125 dilution in 1X YEPD). If the addition of YEPD was the source of the hypothesised chloramines, the growth delay effect should disappear when treatments were diluted in water instead of YEPD. However, as before (Figure 4-1, Figure 4-2), a significant negative linear correlation between colony size and EW dose ($R^2>0.85$, $p<0.001$), and positive correlation between CV and EW dose ($R^2>0.5$, $p<0.05$) were observed for both the YEPD and the water dilution protocol (correlation graphs not shown), and no significant differences in the mean colony size or variation (CV) post EW-treatment could be observed between both protocols (Figure 4-13 A,B; differences were non-significant according to paired *t*-tests). No differences in survival were evident between the YEPD and the water protocols (Figure 4-13 C), indicating that the 1:250 dilution in water was sufficient to stop effective action of EW after the 5 min treatment period. Taken together, the data suggest that the growth delay and increase in variation observed after

low-level EW treatment are not related to the YEPD inactivation step and are rather caused by effects of the EW treatment itself (e.g., by intracellular chloramine formation as hypothesised above).

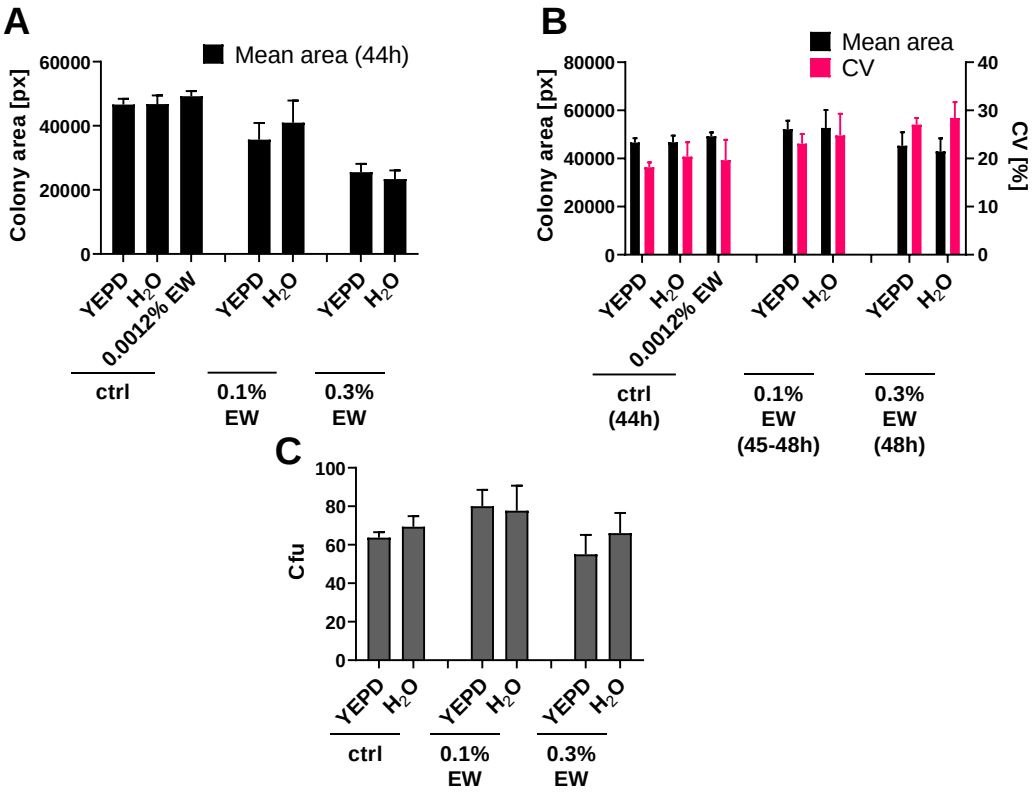

Figure 4-13: Growth delay and increased colony size variation in *A. niger* after low-level EW treatment stopped by water dilution versus YEPD addition. Spores were treated or not with 0.1–0.3% EW (% [v/v] in HPLC grade water; 1.8–6 mg L^{-1} FAC) for 5 min. Treatments were stopped by adding equal volumes of 2X YEPD followed by 1:125 dilution in 1X YEPD ("YEPD") or by diluting 1:250 in HPLC-grade water ("H_2O"). In addition, control treatments were diluted in 0.0012% EW (equal to 0.3% diluted 1:250) to rule out residual EW activity after the water dilution step. 100 µL of appropriate dilutions were plated onto YEPD agar and incubated for 44–48 h. A) The mean colony area was determined after 44 h. B) The mean colony area (in pixels, black bars) and the coefficient of variation (CV, %, pink) were determined after defined growth periods (44–48 h, as specified) that resulted in a similar mean colony area in the treated samples as in the untreated control (44 h). "45–48h" refers to cases where different time points were chosen for the different biological replicates, reflecting day-to-day variation in the absolute effect size of the growth delay (the same time points were chosen for YEPD and H_2O samples within the same experiment to allow comparison of the two protocols). C) Survival was determined by colony enumeration (Cfu, colony forming units, total from 5 technical replicate plates). Data are mean values ± SD for 3 biological replicates, except 0.0012% EW: n = 2.

4.3.7.2 Stopping EW treatments by adding ascorbic acid, a scavenger of ROS and chloramines

Previous studies on different antimicrobials and EW have shown that oxidative damage can continue post-treatment, after removal of the stressor (Hong et al., 2019, Mokudai et al., 2015). Both cited studies showed that providing antioxidants post-treatment increased the survival of microorganisms. To test for a similar 'rescuing' effect here on the growth delay and increased variation after EW treatment, the antioxidant ascorbic acid was selected because this compound also reduces (and thereby inactivates) chloramines (Raftery, 2007, Carr et al., 2000). To reduce one mole of HOCl to chloride (Cl^-), one mole of ascorbic acid is needed (Carr et al., 2000), and the fast inactivation of EW (~5.5–6.1 µM HOCl) by near-equimolar levels of ascorbic acid (7 µM) was confirmed here by the loss of EW-induced APF fluorescence (Figure 4-14; the loss of APF fluorescence at less than equimolar ascorbic acid levels (3.5 µM) may suggest further reactivities between EW and the oxidised dehydroascorbic acid). Therefore, equimolar levels of ascorbic acid were used to inactivate EW after 5 min of *A. niger* treatment. It should be noted that reactivity of ascorbic acid is lower with chloramines than with free chlorine (Peskin and Winterbourn, 2001, Folkes et al., 1995) and that the reactivity varies depending on the type of chloramine (Carr et al., 2000). However, the level and type of (hypothesised) chloramine formation within the fungal spores is unknown, making it difficult to estimate the required ascorbic acid dose for chloramine inactivation. It is likely that intracellular chloramine levels resulting from EW treatment would be lower than the free chlorine levels introduced by the EW, due to reactivities of the free chlorine with other (non-amine) spore components.

Ascorbic acid (at 40 µM) was used to inactivate EW after spore treatments (at 0.1% [v/v] EW, equal to 34–38 µM HOCl [assuming the FAC is HOCl]), instead of the usual YEPD inactivation step. After 5 min EW treatment, ascorbic acid or YEPD

were added and the mixture was incubated for 5 min, followed by dilution (1:125) in water. The spore survival, mean colony size and colony size variation were no different between EW treated samples inactivated with either 40 µM ascorbic acid or YEPD (Figure 4-15 A–C; non-significant according to paired two-tailed *t*-tests). Therefore, a higher ascorbic acid dose (400 µM) was employed in two biological replicates. Whereas the usual decrease in colony outgrowth was observed in EW treated samples inactivated with 400 µM ascorbic acid, similar to YEPD-inactivated samples (Figure 4-15 A; difference was non-significant according to *t*-test between EW treatments inactivated with YEPD or 400 µM ascorbic acid), the variation in colony size (CV) appeared to be lower in the EW samples inactivated with 400 µM ascorbic acid, compared to YEPD inactivation (Figure 4-15 B; non-significant, note that this is based on two biological replicates which limits the statistical power, see also comment below). The colony formation (survival) of EW treated or control spores was not impacted by the 400 µM ascorbic acid inactivation step (Figure 4-15 C; differences were non-significant according to paired two-tailed *t*-tests). The results may suggest that inactivation by ascorbic acid of certain active species (e.g., ROS, chloramines) formed during the EW treatment may partly suppress the normal variation in outgrowth of EW-treated spores. Repetition of these experiments also at higher levels of ascorbic acid and/or EW might help to support this effect in future work (these could not be carried out here due to time constraints at the end of the project).

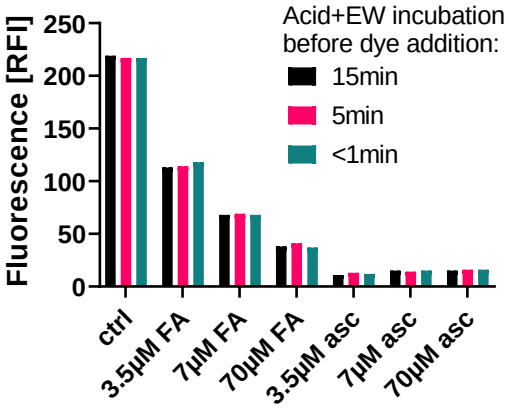

Figure 4-14: Influence of ascorbic and formic acid on the oxidising properties of EW. EW (0.016% [v/v], equal to ~5.5–6.1 µM HOCl [assuming the FAC is HOCl]) was mixed with 3.5–70 µM ascorbic acid (asc) or formic acid (FA) and incubated for 15 min (black bars, left), 5 min (pink bars, centre) or less than 1 min (green) before mixing with the fluorescent ROS probe APF (5 µM). Fluorescence (RFI, relative fluorescence intensity) was recorded within two minutes of mixing. ctrl, no acid was added to the EW.

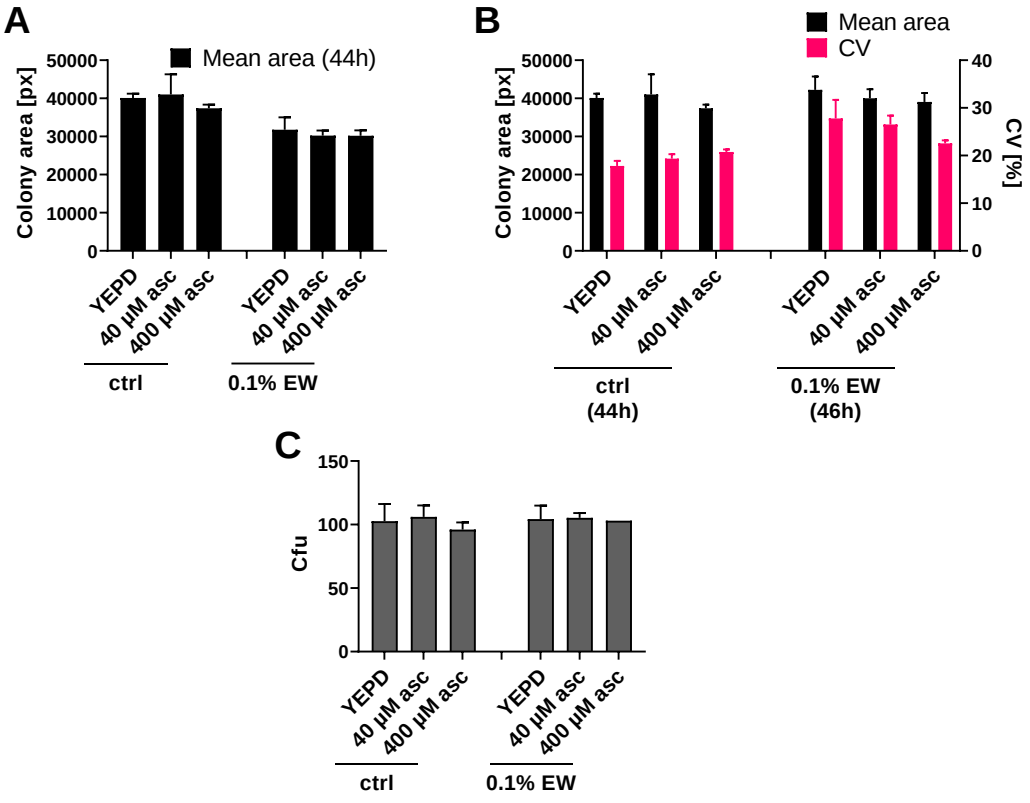

Figure 4-15: Effects of inactivating EW with ascorbic acid or YEPD on *A. niger* colony size and its variation. Spores were treated or not with 0.1% EW (% [v/v] in HPLC grade water; 1.8–2 mg L^{-1} FAC) for 5 min. Treatments were stopped by adding equal volumes of 2X YEPD or ascorbic acid (asc, 40 µM or 400 µM as specified) and incubating for 5 min before diluting 1:125 in HPLC grade water. 100 µL of appropriate dilutions were plated onto YEPD agar and incubated for 44–46 h. A) The mean colony area was determined after 44 h. B) The mean colony area (in pixels, black bars) and the coefficient of variation (CV, %, pink) were determined after defined growth periods (44–46 h, as specified) that resulted in a similar mean colony area in the treated samples as in the untreated control (44 h). C) Survival was determined by colony enumeration (Cfu, colony forming units, total from 5 technical replicate plates). Data are mean values ± SD for 3 biological replicates, except inactivation with 400 µM ascorbic acid: n = 2.

4.3.7.3 Outgrowth of EW-treated spores on YEPD agar containing ascorbic acid

The studies on post-treatment stress cited above provided antioxidants in the outgrowth media (broth or agar) following short-term treatments (Hong et al., 2019, Mokudai et al., 2015). *A. niger* spores treated or not with EW were therefore plated onto YEPD agar containing ascorbic acid. A higher ascorbic acid concentration (7.5 mM, in YEPD agar [pH not determined]) than in the above experiments (up to 0.4 mM, in water) was chosen because reactivities between ascorbic acid and YEPD components are likely (Pischetsrieder et al., 1998), reducing the availability of ascorbic acid for reaction with potential EW-induced species (initial tests showed no effect of 2.5 mM ascorbic acid in agar on the EW-induced colony size effects, not shown). Notably, untreated spores produced larger colonies on the ascorbic acid-containing agar than on the standard YEPD agar (Figure 4-16 A). As before, the colony size of EW-treated spores was decreased on YEPD agar, and also appeared to be decreased on ascorbic acid-containing agar (Figure 4-16 A). The decrease relative to the respective controls was calculated to indicate a comparison of the effect size. The colony size of EW-treated spores appeared to be less strongly decreased on the ascorbic acid-containing agar than on the standard agar (86% of the control for ascorbic acid-agar vs. 79% for standard agar) however this was based on two biological replicates only (the difference in percentage values was non-significant according to a paired two-tailed *t*-test and would require repetition to increase the statistical power). This proposed effect suggested that 7.5 mM ascorbic acid in the YEPD agar could partially rescue the growth delay effect. Reactivities aside from the proposed reactivity of ascorbic acid with chloramines may take place, e.g., ascorbic acid can also reduce Fe^{3+} ions in the media to Fe^{2+}, which in the presence of ROS from EW-treatments can further increase ROS levels (Fenton-chemistry) (Stadtman, 1991), complicating the interpretation of the ascorbic acid effect in agar.

The variation (CV) of colony size for samples grown on ascorbic acid-containing YEPD agar was compared with the CV on normal YEPD agar at time points where the mean colony size was similar. Inclusion of ascorbic acid in the agar did not suppress the increased variation in colony size post-EW treatment (Figure 4-16 B; non-significant according to a paired two-tailed *t*-test between EW-treated samples on YEPD agar [46 h] and ascorbic acid-containing agar [44 h]). In these experiments, growth on ascorbic acid containing agar did not significantly affect the number of colony forming units after EW treatment (Figure 4-16 C; non-significant according to a paired two-tailed *t*-test).

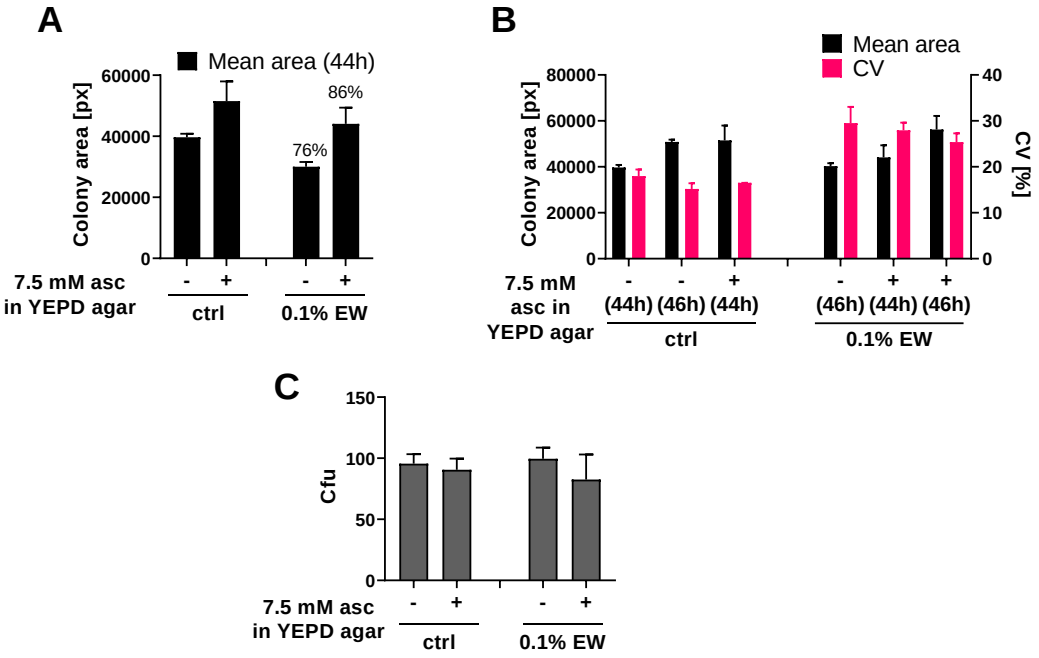

Figure 4-16: Outgrowth of EW-treated *A. niger* spores on YEPD agar containing ascorbic acid. Spores were treated or not with 0.1% EW (% [v/v] in HPLC grade water; 1.8–2 mg L^{-1} FAC) for 5 min. Treatments were stopped by adding equal volumes of 2X YEPD. 100 µL of appropriate dilutions were plated onto YEPD agar with (+) or without (–) added 7.5 mM ascorbic acid (asc) and incubated for 44–46 h. A) The mean colony area was determined after 44 h. The bars of EW treated samples are labelled with the mean percent value of the colony area relative to the respective control. B) The mean colony area (in pixels, black bars) and the coefficient of variation (CV, %, pink) were determined after defined growth periods (44–46 h, as specified) that resulted in a similar mean colony area in the treated samples compared to each other and to the controls. C) Survival was determined by colony enumeration (Cfu, colony forming units, total from 5 technical replicate plates). Data are mean values ± SD for 2 biological replicates.

4.3.7.4 Chloramine treatment of *A. niger* spores and ascorbic acid inactivation

Above, it was hypothesised that organic chloramines may form within fungal spores during EW treatment and that these might contribute to the observed effects on colony size and its variation. However, the use of ascorbic acid does not distinguish between effects of chloramines or ROS. Therefore, spores were treated with chloramines to see whether these could mimic the observed effects on colony growth. Organic chloramines are typically generated by mixing organic amines, such as amino acids, with HOCl (Szabó et al., 2019, How et al., 2016, Amiri et al., 2010). An excess of amino acids is often used to prevent the accumulation of free chlorine or the formation of side products other than monochloramines. In the present study, a mix of 18 amino acids (exluding Pro and Cys for solubility reasons) was mixed with EW. In Chapter 2 of this study, high reactivities between EW and amino acid solutions were shown (mixing equimolar levels of EW [6.9–7.6 mM HOCl] and amino acids [5–7 mM] resulted in full loss of EW fungicidal activity for most amino acids, Figure 2-10). In most amino acids, the α-amino group is the group in the molecule that is the most reactive with HOCl, except Met and Cys, in which the side chain reactivity is at least two orders of magnitude higher than the amino group reactivity, and His, in which the side chain has similar reactivity as the amino group (Pattison and Davies, 2001). It can therefore be assumed that reactions between most amino acids and the HOCl in EW yield monochloramines (amino acids chlorinated at the α-amino group). The Met in the amino acid mix used here is expected to inactivate a part of the FAC due to its side-chain reactivity that does not produce chloramines (yielding MetO). Previous studies reported no chloramine formation when 5 x excess levels of Cys, Met or Trp were mixed with HOCl (How et al., 2016). Therefore, it was decided to mix approximately equimolar levels of amino acids (40 µM) and EW (34–38 µM HOCl) to avoid full inactivation of the FAC by Met and to enable chloramine formation (Met concentration in the amino acid mix was 40 µM divided by 18 [number of amino acids in the mix] = 2.2 µM). It should be kept in mind that the use of

equimolar levels (as opposed to an excess of amino acids) carries the risk of free chlorine accumulation (although this should be low based on the observed high reactivity of amino acids and EW in this study) or side product formation. One solution could have been to exclude Met from the mixture. However, Met is present within fungal cells and (based on several results in this study) likely to react with EW during treatments. In addition, EW reaction with oxidised-Met (MetO) might even lead to the formation of an inhibitory product (cf. Figure 2-11, Figure 2-12), so excluding Met when trying to recreate a potential chloramine-effect in spores did not seem sensible here.

Equal volumes of the amino acid solution and diluted EW were mixed to give 20 µM amino acids (or chloramines) and 0.05% EW (17–19 µM HOCl) and allowed to react for 5 min. As explained above, there is a risk of residual FAC accumulation in the amino-acid/EW mix. If there was no reactivity between the EW and the amino acids, the mix would contain 0.05% EW, and based on Figure 4-2, as little as 0.05% EW could delay colony formation and increase the variation in colony size. However, such a scenario is unlikely, instead the FAC level is expected to be lowered due to reactions between FAC and amino acids. A slightly lower EW concentration (0.03% EW) in Figure 4-2 did not seem to affect the colony size or its variation (note that data for this particular EW concentration are from one biological replicate only). Based on these considerations, it is unlikely that any remaining FAC levels in the mix will be sufficient to affect the colony size or its variation. The mix will therefore be referred to as "chloramines" in the following text.

Treatment of *A. niger* spores with the chloramines gave a small decrease in mean colony size (Figure 4-17 A) that was consistent across replicates but was non-significant (paired two-tailed *t*-test, $p = 0.085$). The treatment was stopped by diluting in HPLC-grade water (similar to the protocol in Figure 4-13) instead of

YEPD addition to avoid potential reactivities of the chloramines with YEPD. Alternatively, the treatment was stopped by adding 40 µM ascorbic acid. In contrast to the water-diluted samples, the chloramine-treated, ascorbic acid-inactivated samples did not show a consistent decrease in colony size (*t*-test of the comparison between the asc-'inactivated' control sample and asc-'inactivated' chloramine sample: $p = 0.458$; Figure 4-17 A). The colony size variation was increased in the chloramine treated condition ($p = 0.045$) and no significant difference between both chloramine treated conditions (diluted and ascorbic-acid inactivated) was observed ($p = 0.089$; the CV values in ascorbic-acid inactivated samples were slightly higher than in water-diluted samples across all three replicates) (Figure 4-17 B). The number of colony forming units was not negatively affected by the chloramine treatment or by ascorbic-acid inactivation after the chloramine treatment (Figure 4-17 C; non-significant according to paired two-tailed *t*-tests). Taken together, these results show that sub-lethal chloramine treatments can increase the colony size variation (assuming that the EW+amino acid mix yielded chloramines). Higher chloramine concentrations should be tested in the future to see if significant colony growth delays can be achieved. Ascorbic acid had no significant effect in these assay conditions, but it cannot be ruled out that higher levels of ascorbic acid would not suppress the chloramine effects, as was suggested above for EW and 400 µM ascorbic acid.

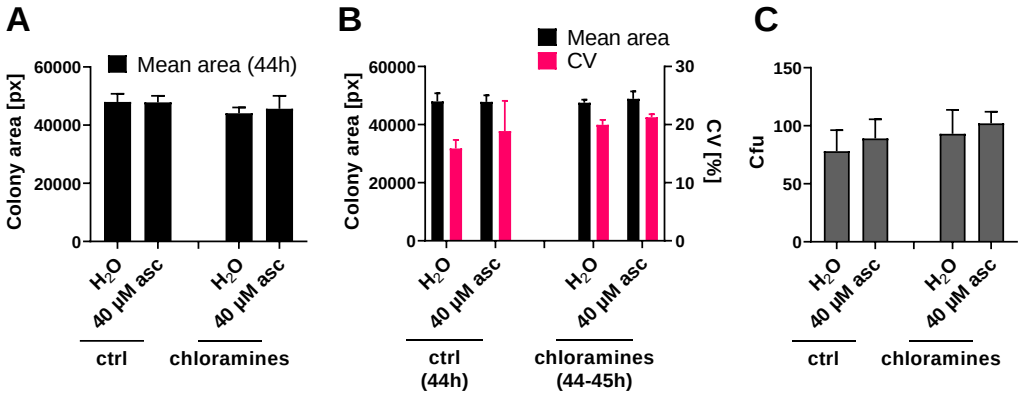

Figure 4-17: Effects of chloramine treatments and inactivation with ascorbic acid on *A. niger* colony size and its variation. A mix of 18 amino acids (excluding Pro and Cys, see 4.2.1) at 40 µM was mixed with equal volumes of 0.1% EW [v/v] (34–38 µM HOCl) resulting in 20 µM amino acids (or chloramines) and 0.05% EW in the mix, incubated for 5 min to allow chloramine formation and subsequently used to treat *A. niger* spores (ctrl, amino acids were mixed with HPLC grade water instead of EW). Treatments were stopped by diluting 1:250 in HPLC grade water ("H_2O") or by adding equal volumes of 40 µM ascorbic acid ("asc") and 5 min incubation, followed by 1:125 dilution in HPLC grade water. 100 µL of appropriate dilutions were plated onto YEPD agar and incubated for 44–46 h. A) The mean colony area was determined after 44 h. B) The mean colony area (in pixels, black bars) and the coefficient of variation (CV, %, pink) were determined after defined growth periods (44–46 h, as specified) that resulted in a similar mean colony area in the treated samples as in the untreated control (44 h). "44–45h" refers to cases where different time points were chosen for the different biological replicates (the same time points were chosen for H_2O and asc samples within the same experiment to allow comparison of the two protocols). C) Survival was determined by colony enumeration (Cfu, colony forming units, total from 5 technical replicate plates). Data are mean values ± SD for 3 biological replicates.

4.3.7.5 Chloramine treatment and outgrowth on YEPD agar containing ascorbic acid

Similar to the experiments with EW in 4.3.7.3, chloramine treated spores were subsequently cultivated on YEPD agar containing 7.5 mM ascorbic acid (2 biological replicates). No difference in colony size was observed between chloramine-treated spores plated on ascorbic-acid containing and standard YEPD agar (non-significant according to a paired two-tailed *t*-test between the relative decreases [in %] compared to the relevant untreated controls obtained with both outgrowth agars; Figure 4-18 A). The colony size variation after chloramine treatment was not decreased on the ascorbic acid-containing agar compared to standard agar (Figure 4-18 B; the CV was actually non-significantly increased on ascorbic-acid agar). No significant effects of outgrowth on ascorbic acid-containing

agar after chloramine treatment on the number of colony forming units was observed (Figure 4-18 C; non-significant according to paired two-tailed *t*-test). In summary, growth on ascorbic acid-containing agar did not rescue the (suggested) growth delay or the increased variation observed after chloramine treatment.

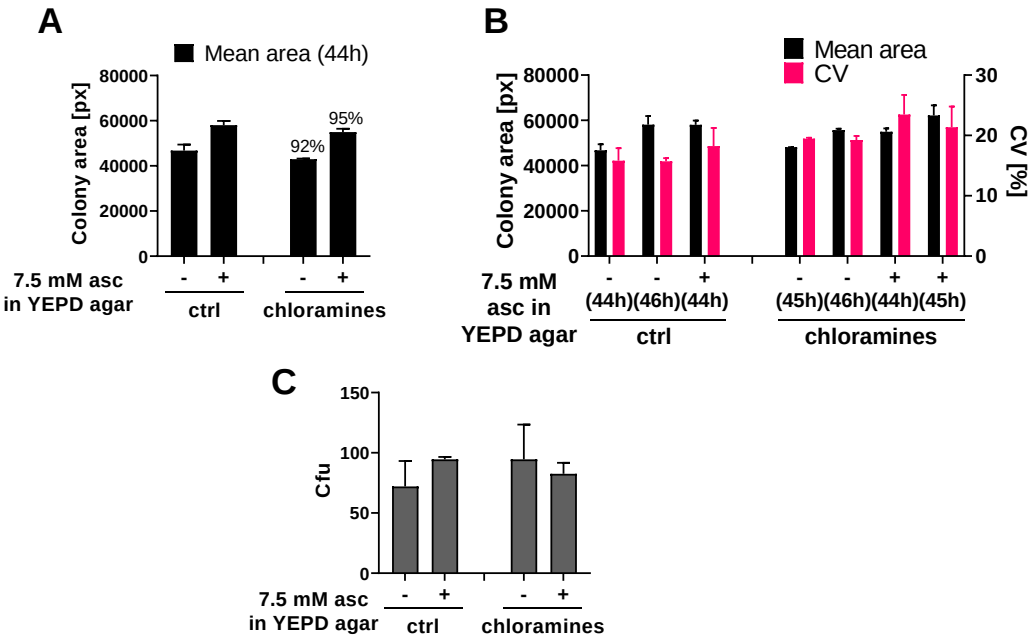

Figure 4-18: Outgrowth of chloramine-treated *A. niger* spores on YEPD agar containing ascorbic acid. A mix of 18 amino acids (excluding Pro and Cys, see 4.2.1) at 40 µM was mixed with equal volumes of 0.1% EW [v/v] (34–38 µM HOCl), resulting in 20 µM amino acids (or chloramines) and 0.05% EW in the mix, incubated for 5 min to allow chloramine formation and subsequently used to treat *A. niger* spores (ctrl, amino acids were mixed with HPLC grade water instead of EW). Treatments were stopped by diluting 1:250 in HPLC grade water ("H_2O") and 100 µL of appropriate dilutions were plated onto YEPD agar with (+) or without (–) added 7.5 mM ascorbic acid (asc) and incubated for 44–46 h. A) The mean colony area was determined after 44 h. The bars of EW treated samples are labelled with the percent value of the colony area relative to the respective control (the individual values did not support a higher apparent percentage on asc-agar; replicate 1: (–) 96%, (+) 94%, replicate 2: (–) 88%, (+) 95%). B) The mean colony area (in pixels, black bars) and the coefficient of variation (CV, %, pink) were determined after defined growth periods (44–46 h, as specified) that resulted in a similar mean colony area in the treated samples compared to each other and compared to the controls. C) Survival was determined by colony enumeration (Cfu, colony forming units, total from 5 technical replicate plates). Data are mean values ± SD for 2 biological replicates.

4.3.8 Effect of Met pre-treatment on survival of *A. niger* after EW treatment

4.3.8.1 Effect of Met pre-culture on YNB agar

This study revealed a protective effect of methionine pre-culture on the recovery of yeast cells after EW treatment (see 3.3.2). It was tested whether growth in the presence of Met would also protect *A. niger* against subsequent EW treatment. It has been shown that the conditions in which conidia are formed can influence their properties and stress resistance (Hagiwara et al., 2017, Bleichrodt et al., 2020, Ruijter et al., 2003, Wang et al., 2021). Therefore, *A. niger* conidia were grown on YNB slopes supplemented or not with different Met levels. YNB was the minimal medium used in the yeast Met pre-culture experiments and resulted in good growth of *A. niger* as well. In three out of five biological replicates, the conidia pre-grown on YNB slopes containing 1 mM Met survived subsequent EW treatment better than the 0 mM Met-controls (Figure 4-19). However, this result was not consistent across all five replicates and there was no significant difference in the combined data. The instances of increased survival (at 1 mM Met) were apparent in replicates where the control (0 mM Met) survival was below 20%, but the effect even for these three replicates was not significant (p-value of paired two-tailed *t*-test of the comparison between 0 mM and 1 mM for those three replicates was 0.0602). There was no evidence for increased survival of Met pre-grown cultures in replicates where survival of the 0 mM-control was >20%. It is possible that any protective effect of Met pre-culture depends on the dose and killing effect of an EW treatment. No protective effect was evident for *A. niger* pre-grown with other Met concentrations (Figure 4-19). Overall, the results do not clearly support a protective effect of Met in *A. niger*. Caveats of the method are discussed in 4.4.5.

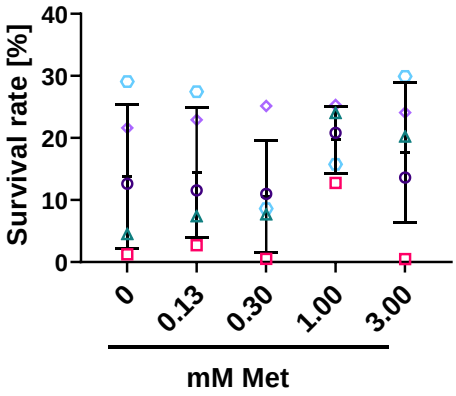

Figure 4-19: Influence of methionine pre-culture on YNB agar on the survival of *A. niger* conidia after EW treatment. Conidia were grown on YNB slopes supplemented with the specified methionine concentrations and harvested after 1 week. After EW treatment (5 min, 0.4–1% [v/v]; 7.2–20 mg L^{-1} FAC), survival was assessed by plating appropriate dilutions (100 µL) on YEPD agar and subsequent colony enumeration. Mean values ± SD (black lines and error bars) are shown for 5 biological replicates, with different biological replicates distinguished by different symbols.

4.3.8.2 Effect of Met pre-culture in AMM broth

Because the Met pre-culture in yeast had been in broth, conidia of *A. niger* were also cultured for 4 h with different amino acids in AMM minimal broth prior to EW treatment. Amino acids were supplied at 0.3 mM, consistent with the yeast experiments. The amino acids were a selection of those tested in the yeast pre-treatment experiment (Figure 3-7), plus Ala as a control that did not show particularly strong reactivity with EW (Figure 2-10). Conidia were recovered in YEPD broth in 96-well plates after the EW treatment and the relative growth compared to a no-EW control was calculated at two time points: the first time point (15 h) was chosen within the period of strongest initial outgrowth of the EW treated samples (Figure 4-20 B,C; control growth shown in panel A) and the second (24 h) when growth slowed down, consistent with other experiments in this study that also assessed the growth after 24 h (cf. Figure 2-10). Samples that were pre-cultured with different amino acids did not show differences in outgrowth following EW treatment when assessing the mean OD_{600} values across replicates (Figure 4-20 A–C). Averaging the OD_{600} values may hide small effects if there are

systematic differences in growth between replicates (e.g., due to day-to-day variation in the exact initial spore concentration). For this reason, the relative growth (OD_{600} of EW treated samples divided by OD_{600} of the respective control) was calculated for each replicate separately, as relative effects should be consistent across replicates even if the absolute OD_{600} values may vary. The relative growth of the different pre-culture conditions was assessed at two levels of EW treatment strength that resulted in ~50% and ~5–10% growth relative to the control at the 15 h time point (Figure 4-20 D,E). No significant increase in relative growth was observed for any of the pre-culture conditions compared to the no-amino acid control (non-significant according to paired two-tailed *t*-tests with FDR correction). Overall, no increased survival of Met (or other amino acid) pre-treated *A. niger* could be observed following pre-culture in broth, similar to the outcome after Met pre-culture on agar (Figure 4-19). It should be noted that the 4 h incubation in AMM medium resulted in only very low levels of visible swelling of the conidia (Figure 4-20 F), meaning that this experiment does not assess vegetative cells that may be more comparable to yeast cells in their behaviour in response to EW.

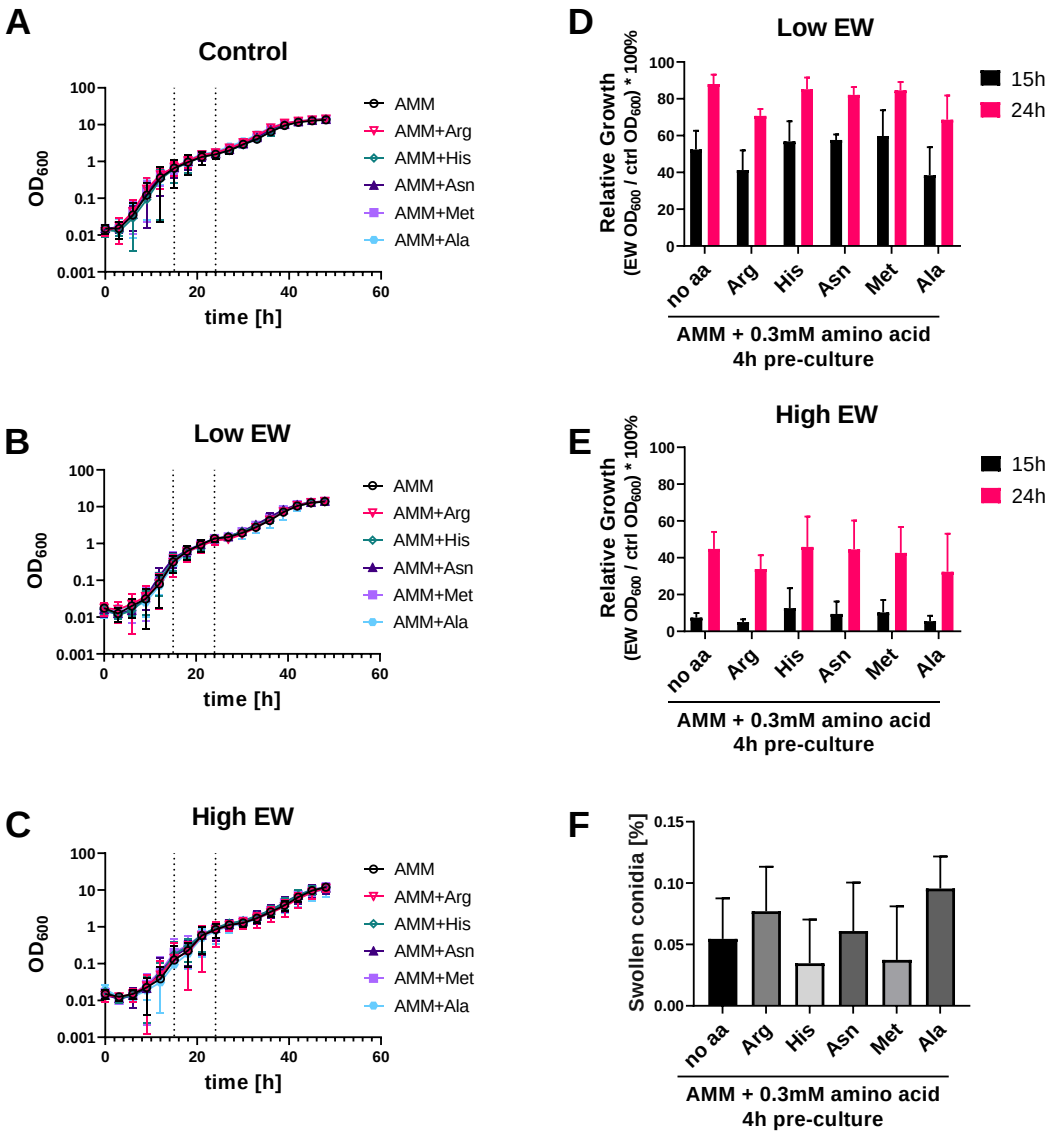

Figure 4-20: Influence of pre-culture with methionine and other amino acids in AMM broth on the survival of *A. niger* conidia after EW treatment. Conidia were incubated in AMM minimal medium supplemented or not with the specified amino acids at 0.3 mM for 4 h at 28°C. After harvesting and washing to remove extracellular amino acids, conidia were treated with EW (5 min) and the growth of the surviving conidia was detected by OD_{600} readings at appropriate time points. Low EW: 0.1–0.6% EW [v/v] (1.8–12 mg L^{-1} FAC), resulting in ~50% growth relative to the control growth at 15 h (B,D). High EW: 0.3–1% EW [v/v] (5.4–20 mg L^{-1} FAC), resulting in ~5–10% growth at 15 h (C,E). Note that the overlap in EW concentrations between 'low EW' and 'high EW' conditions was related to day-to-day variation in EW effect strength. A–C) Growth curves of control (A) and EW treated samples (B,C). The dotted lines indicate the 15 h and 24 h time points. D,E) Relative growth in EW treated samples compared to the no-EW control at 15 h (black bars) and 24 h (pink). F) After the 4 h incubation in AMM, the percentage of swollen conidia (indicating the beginning of germination) was determined by visual inspection of at least 100 spores per condition under the microscope. Data show mean ± SD for 4 biological replicates.

4.3.9 Transcriptome analysis of the *A. niger* response to EW

4.3.9.1 EW treatment of *A. niger* conidia and sample preparation

Some results in this chapter highlighted certain differences between the EW response of *A. niger* and *S. cerevisiae*, potentially related to differences between fungal spores and vegetative cells. Furthermore, interesting effects of EW on the outgrowth of *A. niger* spores after EW treatment were found but the availability of appropriate strains (e.g., deletion mutant libraries) to study such effects in detail is more limited in filamentous fungi compared to the model organism *S. cerevisiae*. To shed more light on the response of *A. niger* spores to EW, its transcriptome response was studied, because the analysis of changes in mRNA levels during stress treatments can reveal information about the stress response of organisms. *A. niger* was treated or not with EW and the transcript levels of treatment and control samples were compared. Dormant *A. niger* conidia have only low metabolic activity (Novodvorska et al., 2016) and undergo extensive transcriptome changes in the first hours of germination (Novodvorska et al., 2013, van Leeuwen et al., 2013). It was deemed beneficial to analyse the EW response of metabolically active (i.e., germinating) conidia because it was thought that dormant conidia might not show strong regulation of their transcriptome in response to stress. However, a recent study demonstrated that fully developed conidia (before dehydration) exhibit transcriptional activity and that this activity is modulated in response to stress, even in spores suspended in water after detachment from the conidiophore (Wang et al., 2021). The presented transcriptomics experiment was designed before the information from the cited study became available and so here, conidia were allowed to germinate for 6 h in YEPD before EW treatment to induce metabolic activity. Another option would have been to treat dormant conidia, followed by YEPD recovery, as was performed in different experiments throughout this thesis. However, the extensive transcriptional changes in the first hours of *A. niger* germination (Novodvorska et

al., 2013, van Leeuwen et al., 2013) may have complicated the analysis and identification of EW-specific transcriptional changes during those processes, e.g., in the case of EW-induced delays in germination.

Germinated conidia (6 h after transfer of dormant conidia to YEPD) were treated with EW for at least 10 min, and also 30 min, 1 h and 2 h, to allow sufficient time for transcriptional changes to occur. To avoid reactivities of the EW with YEPD components, conidia were first transferred into 0.1% Tween 80. Control treatments were with sterile tap water (EW for treatments was diluted in sterile tap water). These conditions represent starvation conditions with nutrient and osmotic stresses which will induce a range of transcriptome changes. This will make it more difficult to identify EW-specific transcriptome changes. The impact of this and other limitations of the protocol will be discussed in 4.4.6, and the presented data in this results section should be viewed with caution.

RNA was extracted from treated and control samples at these time points in four separate biological experiments. The survival of treated conidia was assessed by plating appropriate dilutions onto YEPD agar and subsequent colony enumeration. Survival decreased with increasing treatment time (Figure 4-21) and was very low after 2 h (on average 10%). Therefore, samples from the first 3 time points (10 min – 1 h) only were selected initially for downstream transcriptome analysis, as adaptive-type responses are expected to be dampened or non-existent where there is substantial killing. Nevertheless, one 2 h sample was analysed as a replacement for RNA from the 10 min time point of replicate 4, which was lost during the extraction procedure; the samples analysed further by transcriptomics are highlighted with white boxes in Figure 4-21. The transcriptome sequencing and analysis were performed by the Centre for Genomic Research (CGR) at the University of Liverpool. Pairwise comparisons were made between treatment and

control samples of each replicate to then identify differentially expressed (DE) genes at the different time points (Table 4-1).

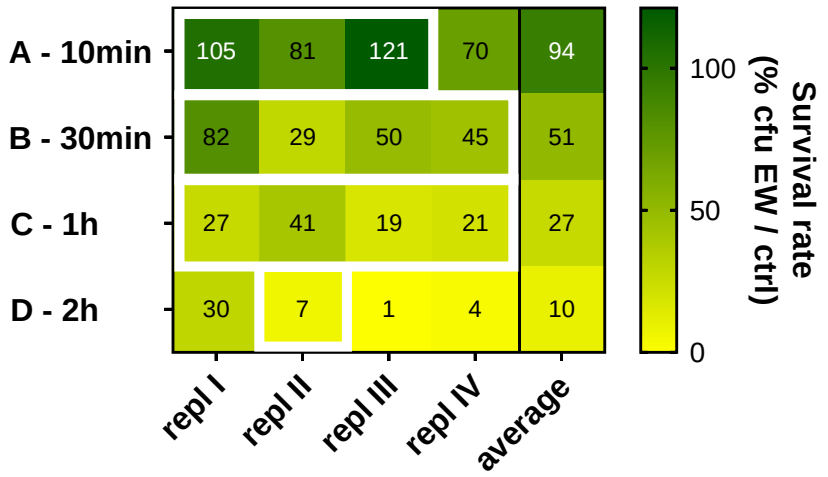

Figure 4-21: Survival rates of EW treated *A. niger* for transcriptome analysis. Conidia were germinated in YEPD for 6 h before EW treatment (0.04% [v/v], diluted in sterile tap water, FAC of undiluted EW: 1600–1700 mg L^{-1} FAC) for 10 min, 30 min, 1 h or 2 h. Control: sterile tap water. Treatments were stopped by centrifugation followed by resuspension in YEPD. 100 µL of appropriate sample dilutions were plated onto YEPD agar and incubated for subsequent colony enumeration. Survival was calculated relative to the untreated controls. Repl I–IV: independent biological replicates. Fields are labelled with their corresponding survival rate. White boxes highlight samples that were analysed by transcriptomics.

Table 4-1: Experimental design for the transcriptome analysis. Details of samples are given in Figure 4-21.

Pairwise comparisons				Time point
Treatment samples (EW treated spores)		Control samples (untreated spores)		
Sample number	Replicate	Sample number	Replicate	
25	repl I	26	repl I	A – 10 min
31	repl II	32	repl II	
37	repl III	38	repl III	
27	repl I	28	repl I	B – 30 min
33	repl II	34	repl II	
39	repl III	40	repl III	
45	repl IV	47	repl IV	
29	repl I	30	repl I	C – 1 h
35	repl II	36	repl II	
41	repl III	42	repl III	
47	repl IV	48	repl IV	
49	repl II	50	repl II	D – 2 h

4.3.9.2 Bioinformatics analysis and identification of differentially expressed genes

The bioinformatics analysis was performed by the CGR. Reads were mapped to the reference genome of *A. niger* CBS 513.88. The reference genome was chosen because its mapped genes were available on the *Aspergillus* genome database, however this industrial strain differs from the laboratory strain N402 (used for the transcriptomics experiment). Furthermore, *Aspergillus niger* N402 was originally generated from a N400 wild type using UV mutagenesis, inducing several mutations (Demirci et al., 2021). The choice of strain will be critically discussed in 4.4.6. Mapping efficiencies were between 41.91% and 65.08%, which was lower than expected based on the CGR's experience with the mapping tool (TopHat2), possibly suggesting limited quality of the RNA samples, although newer mapping tools have since been reported to outperform TopHat2 (Musich et al., 2021). The low mapping efficiency is also likely due to the mismatch between the experimental and reference genome strains. A total of 12,243 genes were detected, equivalent to 87% of the known ORFs of the reference genome. Correlation analysis revealed poor correlation of samples from the same conditions across biological replicates (the correlation between samples from the same control or treatment times across replicate experiments was not higher than the correlation between samples from other conditions; Figure 4-22), indicating that the technical and/or biological variation between the replicate experiments is as high as, or higher than the treatment-induced differences between the EW treatment and control samples at the different time points. It should be noted that this high variation between replicate experiments limits the strength of the analysis of transcriptome changes in this study. It is not entirely clear what caused the high variation but potential explanations include day-to-day variation in conidia preparations and in EW effect strength (resulting in variable survival rates, Figure 4-21) and the dilution of EW in sterile tap water for the transcriptome experiment with potential day-to-day variation in tap water constituents (EW was diluted in HPLC grade water for most experiments in this thesis but the effect of

water purity on EW strength [cf. 3.3.1.3] was investigated only after the transcriptome analysis was completed). The log10 count data of the samples were also analysed by principal component analysis (PCA). This did not reveal a very clear clustering of the different treatment vs. control samples (Figure 4-23; note that the PCA components only explain a small amount [~1.5–2%] of the sample variation, again suggesting limited data quality). However, all control samples (with two exceptions) were located towards the right of the PCA plot and all treatment samples to the left (Figure 4-23 A). For the first two time points (10 min and 30 min treatments, shown in Figure 4-23 B,C), the treatment and control samples were not well separated, and treatment and control samples from the same replicate experiment clustered relatively closely together, suggesting that the variation between replicate experiments was greater than the EW treatment effect size in these samples (Figure 4-23 B,C; treatment and control samples from the same replicate experiment are labelled with consecutive numbers, cf. Table 4-1). On the other hand, the samples from the later time points (1 h and 2 h) showed a clear separation of the treatment and control samples (Figure 4-23 D), suggesting that data from these samples may show a stronger EW-treatment dependent effect.

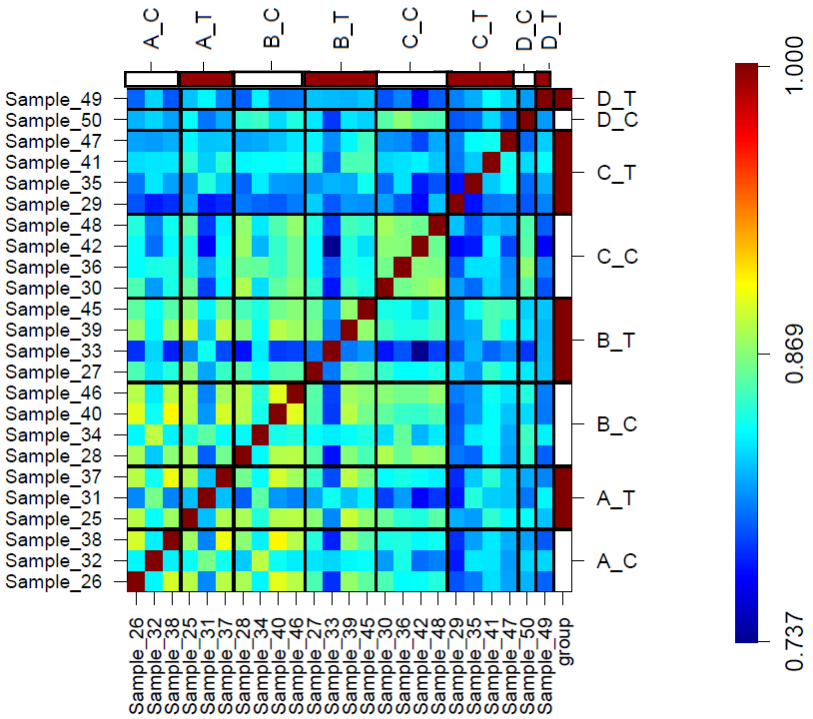

Figure 4-22: Correlation heatmap of transcriptomics samples. Samples were extracted RNA from *A. niger* treated or not with EW (details see Table 4-1). The Pearson correlation coefficients (scale shown on bar to the right) were calculated based on the log10 count data of the samples. Blocks along the diagonal from bottom left to top right show the within-group correlations. A,B,C,D, treatment times 10 min, 30 min, 1 h, 2 h. _T, treatment (burgundy group labels), _C, control (white). This figure was provided by the Centre for Genomic Research, University of Liverpool.

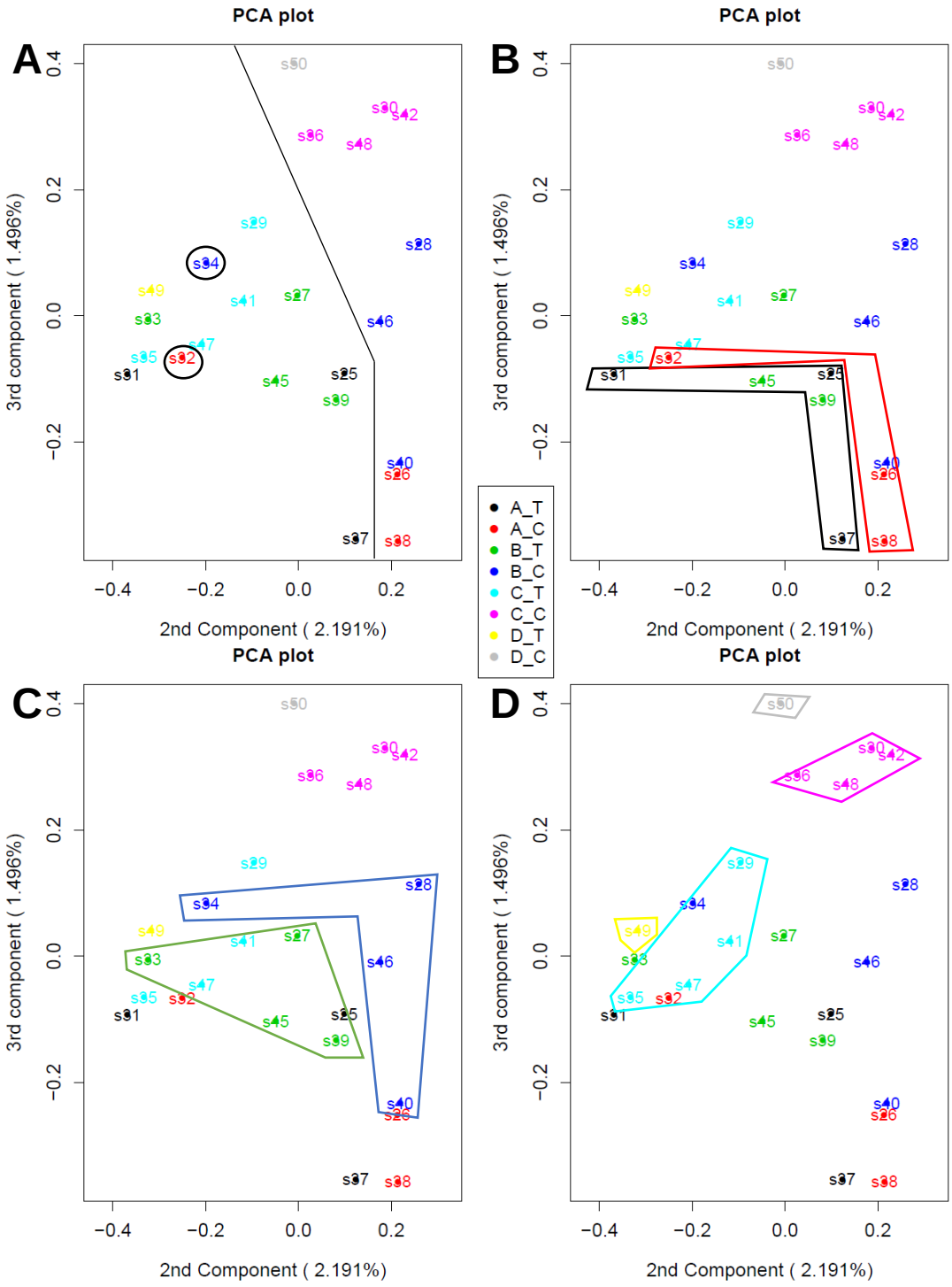

Figure 4-23: Principal component analysis (PCA) of the transcriptomics samples to analyse the variation between treatment- and control-group samples. Samples were extracted RNA from *A. niger* treated or not with EW (details see Table 4-1). The PCA was calculated using all the log10 read count data from each sample and determining the principal component scores 2 and 3 for each sample within EdgeR (in brackets: % variance explained by the principal component). Panel A) Control samples are all located to the right of the line and within the black circles. Panels B-D) Control and treatment samples from the different time points are highlighted separately in boxes; B) 10 min time point, treatment samples in black, control in red; C) 30 min time point, treatment in green, control in blue; D) 1 h time point, treatment in turquoise, control in pink, and 2 h time point, treatment in yellow, control in grey. Mini-legend for colour scheme (centre): A,B,C,D, treatment times 10 min, 30 min, 1 h, 2 h. _T, treatment, _C, control. This figure was provided by the Centre for Genomic Research, University of Liverpool.

The EdgeR analysis for finding differentially expressed (DE) genes in response to EW treatment revealed 660 DE genes between treatment and control conditions (total of all DE genes found for one or more time point(s)), with 251 upregulated genes and 409 downregulated genes. Most DE genes were found for the 1 h-time point samples (Table 4-2, Figure 4-24), consistent with the clearer separation between treatment and control samples that was evident for this time point in the PCA above. There was little overlap between the different time points: 103 DE genes were found for more than one time point, and 16 DE genes found in three out of the four time points (Figure 4-25). Very few DE genes (4) were found for the 10 min-time point samples which may indicate little response of *A. niger* to the EW dose within 10 min (note also the high survival of the 10 min-treatment samples, Figure 4-21). It is also possible that transcriptome changes in response to the transfer to water (nutrient/osmotic stress) masked most EW-induced changes at this early time point.

Table 4-2: Differentially expressed genes between EW treatments and controls.

Treatment times	**10 min**	**30 min**	**1 h**	**2 h**
DE[a]	4	98	612	65
DE_up	3	32	240	10
DE_down	1	66	372	55

[a] DE, differentially expressed genes. Up, upregulated, down, downregulated.

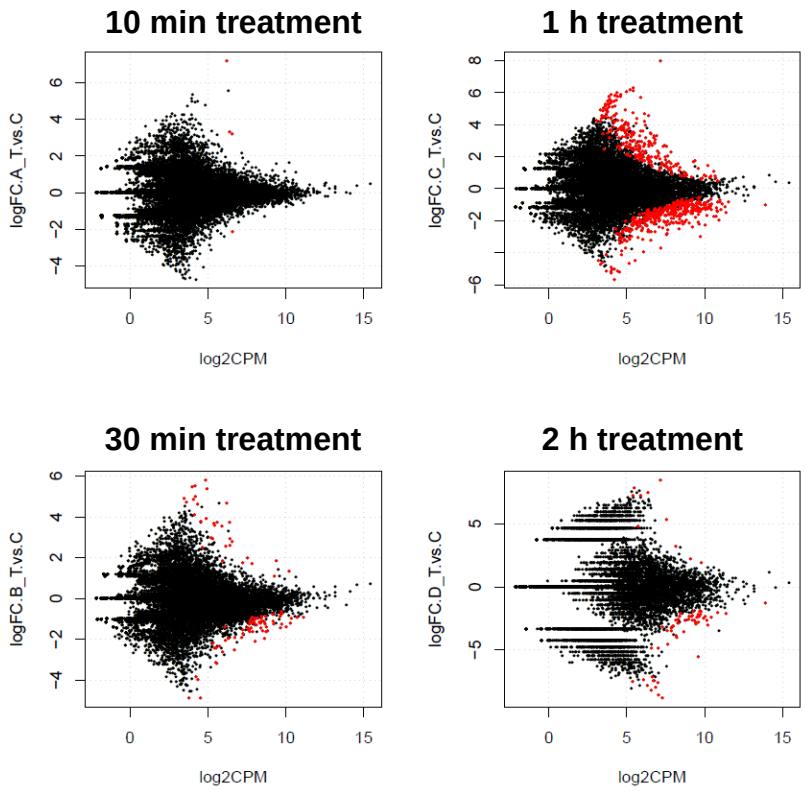

Figure 4-24: Fold change of gene expression in the transcriptome data sets. The log2 fold change (logFC) was plotted against the log2 counts per million (log2CPM) separately for each treatment time. The significance of the logFC was calculated within EdgeR and p-values were adjusted for multiple testing using the false discovery rate (FDR) approach (Benjamini and Hochberg, 1995). Hits with a FDR-adjusted p-value <0.05 were defined as significant and are coloured in red. This figure was provided by the Centre for Genomic Research, University of Liverpool.

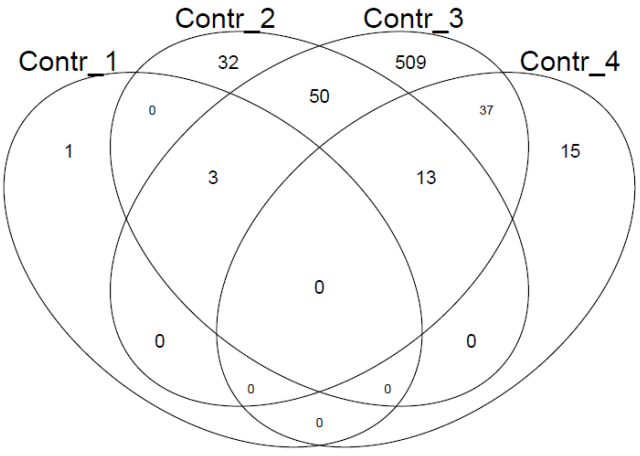

Contr_1: control vs. treatment 10 min
Contr_2: control vs. treatment 30 min
Contr_3: control vs. treatment 1 h
Contr_4: control vs. treatment 2 h

Figure 4-25: Venn-diagram of the DE genes. See Table 4-1 and Table 4-2 for details on the treatment times and DE gene numbers. This figure was provided by the Centre for Genomic Research, University of Liverpool.

4.3.9.3 Analysis of DE genes: GO terms

The DE genes were ordered by the sum of their logFC (log2 fold change) values for the four treatment time points. A visual analysis showed that the greatest fold-change values occurred in the 1 h and 2 h treatment times, and upregulation (or downregulation) of the separate genes was relatively consistent across the time points (Figure 4-26). The 2 h time point consisted of only one replicate (one control and one treatment sample), so idenfication of DE genes in this condition used estimated dispersion (variability) in the EdgeR analysis, making the results for the 2 h condition statistically less reliable. There were cases where a gene was upregulated by EW at one time point but downregulated at another. However, many of the plotted genes were significantly differentially expressed at only one time point, so such differences between time points might not represent a significant change from down- to up-regulation (or vice versa) in regulation over time, i.e., only the upregulated (or only the downregulated) effect may be significant. A more detailed analysis of DE genes that were significant at more than one time point is provided further below (4.3.9.4).

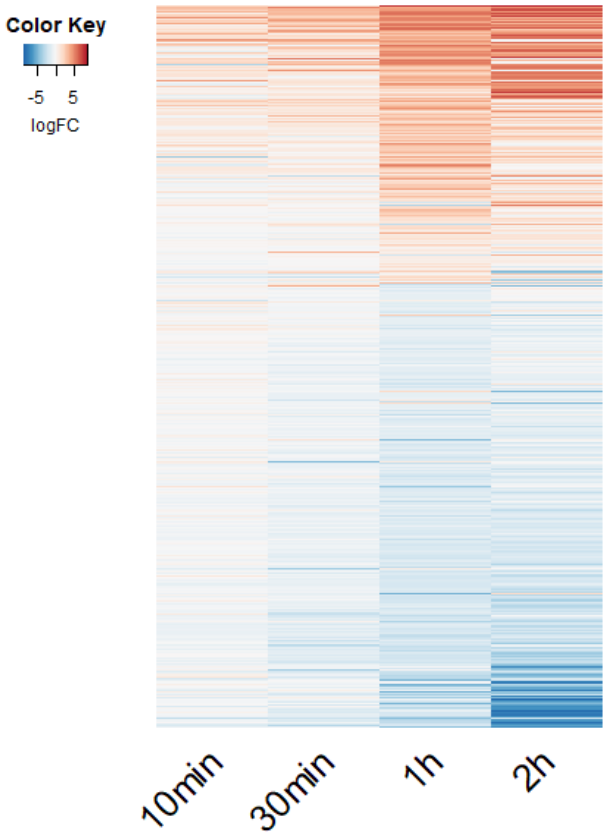

Figure 4-26: Heatmap of logFC (log2 fold change) of all DE genes in response to EW. The DE genes found in the transcriptome dataset (Table 4-2) are ordered from top to bottom by the sum (not shown) of their logFC across the different sampling times (10 min to 2 h). logFC values for each gene at the different times are presented, with positive values shown in red and negative values in blue.

Next, the biological processes, molecular functions and cellular components of the EW-responsive DE genes were analysed using the AspGD GO Slim Mapper (see 4.2.6). For all DE genes and separately for the upregulated DE genes and the downregulated DE genes, the relative numbers of genes clustered into the different functional GO groups within each of the three sets (all DE, upregulated, downregulated) was compared to relative gene numbers falling into each GO category from the full gene set (all detected genes across all samples). The results for all GO terms are listed in Appendix I (6.9.1). Results for the most represented GO terms within the all-DE set are visualised below (Figure 4-27, Figure 4-28; to limit the size of the figure, GO terms that had less than 15 gene matches within

the all-DE dataset were excluded from Figure 4-27, and additionally GO terms with less than 10 gene matches within the all-DE dataset were excluded from both figures because relative changes based on <10 genes are less meaningful). Most GO terms were represented within the DE gene sets at similar relative percentages (of the total-gene counts in the relevant set; % genes) as in all detected genes (Figure 4-27, Figure 4-28). Certain GO terms were overrepresented in the upregulated DE genes compared to the full dataset (defined by ≥1.25-fold increase in the % genes in the upregulated dataset); namely the processes: transport (1.36 x increase), RNA metabolic process (1.29 x), organelle organisation (1.57 x), response to stress (1.68 x), cellular protein modification (1.30 x), developmental process (1.76 x), cell cycle (2.00 x), DNA metabolic process (2.10 x) (Figure 4-27); the molecular functions: hydrolase activity (1.27 x), DNA binding (1.39 x), RNA binding (1.45 x), peptidase activity (1.87 x), protein kinase activity (1.71 x) and ligase activity (1.67 x) (Figure 4-28 A); the cellular components: membrane (1.43 x), nucleus (1.31 x), mitochondrion (1.40 x), endomembrane system (1.44 x), plasma membrane (1.54 x), chromosome (1.44 x), extracellular region (1.45 x), cytosol (2.48 x) and vacuole (2.00 x) (Figure 4-28 B). Interestingly, the downregulated subset of DE genes contained a higher percentage of genes with unknown processes, functions and components (Figure 4-27, Figure 4-28) which may explain why most GO terms were underrepresented in this subset (unknown genes might, upon characterisation, fall into some of the GO term classes). GO terms that were overrepresented in the upregulated subset were generally underrepresented in the downregulated subset (defined by ≤0.75-fold change), except some that were underrepresented in the downregulated but not overrepresented in the upregulated subset: response to chemical (0.64 x in the downregulated subset), carbohydrate metabolic process (0.50 x), filamentous growth (0.73 x), transcription (0.59 x), oxidoreductase activity (0.51 x), transporter activity (0.68 x), protein binding (0.52 x); and others that were overrepresented in the

upregulated (see above) but not underrepresented in the downregulated subset: cellular protein modification process (0.80 x in the downregulated subset), DNA metabolic process (1.14 x), protein kinase activity (0.86 x), ligase activity (1.25 x), mitochondrion (0.80 x), vacuole (1.25 x). Regulation of biological processes was underrepresented in both subsets of DE genes (0.84 x in the upregulated subset; 0.59 x in the downregulated subset). Four genes (*An03g05140*, *An12g02840*, *An15g07530*, *ppoC*) within the DE dataset matched to the GO process term "toxin metabolic process" (excluded from the figure due to the low number of gene matches as stated above), and these were all upregulated (Appendix I, 6.9.1; in the all-genes dataset, 96 genes matched to this GO process). Note again that the matching to GO terms was likely limited by the low mapping efficiency of the obtained sequences to the (mismatched) reference genome.

Because the GO term "response to stress" was enriched within the upregulated DE genes, and this fits the expectations during stress treatments, the 21 upregulated genes in this GO process were further investigated. Among the 21 genes, there were genes involved in DNA repair processes (*An02g08730, An01g07220, An02g02970, An12g07910, An15g01140, An17g01760*), oxidative stress response (*An11g10080, An08g03240, ppoC*), protein and/or translation activity regulation (*An05g00530, An01g14160*), protein-ubiquitin degradation (*An01g11160*) and amino acid transport (*An07g03690*). Notably, *An03g05080* was upregulated (significant for the 1 h time point), logFC = 3.14, non-significantly upregulated at the other time points), which is a computationally mapped ortholog to the *S. cerevisiae* methionine-R-sulphoxide reductase *fRMsr.* This suggested a parallel with the involvement of MSR-enzymes in the EW response of *S. cerevisiae* observed in this study (see 3.3.4). The other MSR orthologs, *An07g07560* (ortholog to *MSRA*) and *An11g02640* (ortholog to *MSRB*), were not significantly differentially expressed.

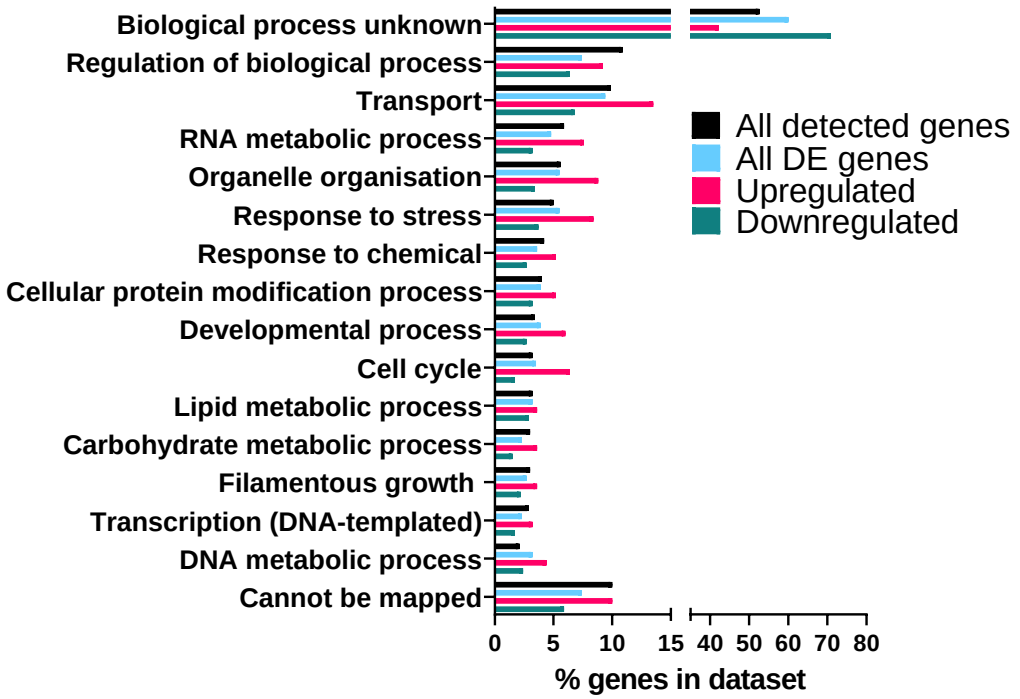

Figure 4-27: GO Slim terms for biological processes in the transcriptome dataset for *A. niger* response to EW. All detected genes (black bars, 12243 total genes), all DE genes (blue, 660 genes) or the up- and down-regulated subsets (pink [251 genes] and green [409]) of the DE genes were analysed using the AspGD GO Slim Mapper. GO terms with less than 15 gene matches in the DE dataset are not shown. Full data are available in Appendix I, 6.9.1.

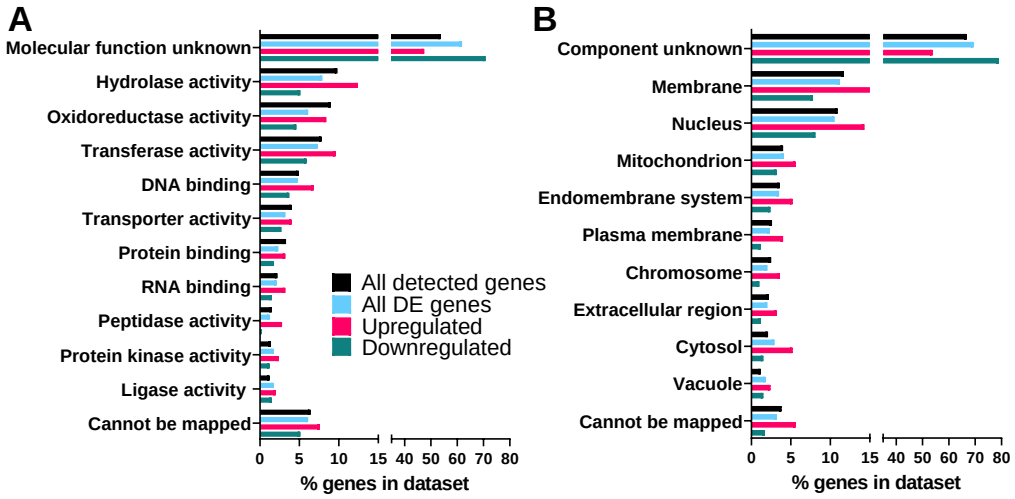

Figure 4-28: GO Slim terms for metabolic functions and cellular components in the transcriptome dataset for *A. niger* response to EW. All detected genes (black bars, 12243 total genes), all DE genes (blue, 660 genes) or the up- and down-regulated subsets (pink [251 genes] and green [409]) of the DE genes were analysed using the AspGD GO Slim Mapper. A) Molecular functions. B) Cellular components. GO terms with less than 10 gene matches in the DE dataset are not shown. Full data are available in Appendix I, 6.9.1.

4.3.9.4 Analysis of DE genes: functions of selected genes

To further interrogate the DE gene data in the EW-treated samples, two separate strategies were employed to select the most strongly differentially expressed genes. In the first approach, genes that were differentially expressed at more than one time point were selected (103 genes, see Figure 4-25) and separated into genes with known or predicted function, and genes without a known function. For the second strategy, the maximum absolute fold change across the 10 min, 30 min or 1 h time points was determined for each DE gene and the 40 genes with the highest (significant) fold changes were selected for further consideration (the 2 h time point was excluded for ordering by maximum fold change [but included for the analysis] as it had several high fold change values [cf. Figure 4-26] but consisted of only one replicate, and while the EdgeR analysis allows the identification of significant DE genes even for one replicate by estimating the dispersion (variability) of the counts, DE genes obtained from this time point and their fold change values are statistically less reliable than DE genes from time points with 3–4 replicates). The first strategy revealed that most genes with a significant change in gene expression at more than one time point showed consistent up- or down-regulation across all time points (consistency was observed across all significant time points of a DE gene and often also for non-significant time points; Figure 4-29, Figure 4-30). Among those DE genes (found at more than one time point) that had unknown functions, a larger number were downregulated (Figure 4-30 B), consistent with the similar earlier observation in the GO term analysis (Figure 4-27, Figure 4-28).

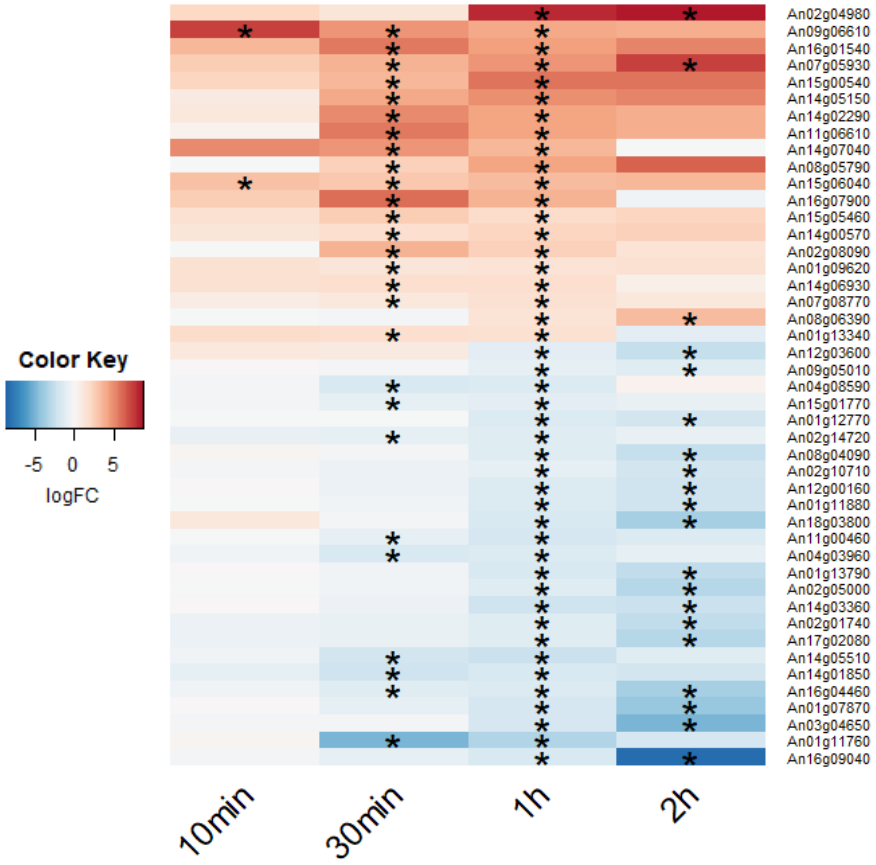

Figure 4-29: Log fold changes of EW-responsive DE genes found at more than one time point and with known or predicted function. The heatmap shows the logFC of upregulated genes in red (from the top) and downregulated genes in blue for the four EW-sampling times. Genes that showed a significant change in gene expression (logFC) are labelled with an asterisk. The significance of the logFC was calculated within EdgeR and p-values were adjusted for multiple testing using the false discovery rate (FDR) approach (Benjamini and Hochberg, 1995). The functions of the plotted genes are listed in Table 4-3.

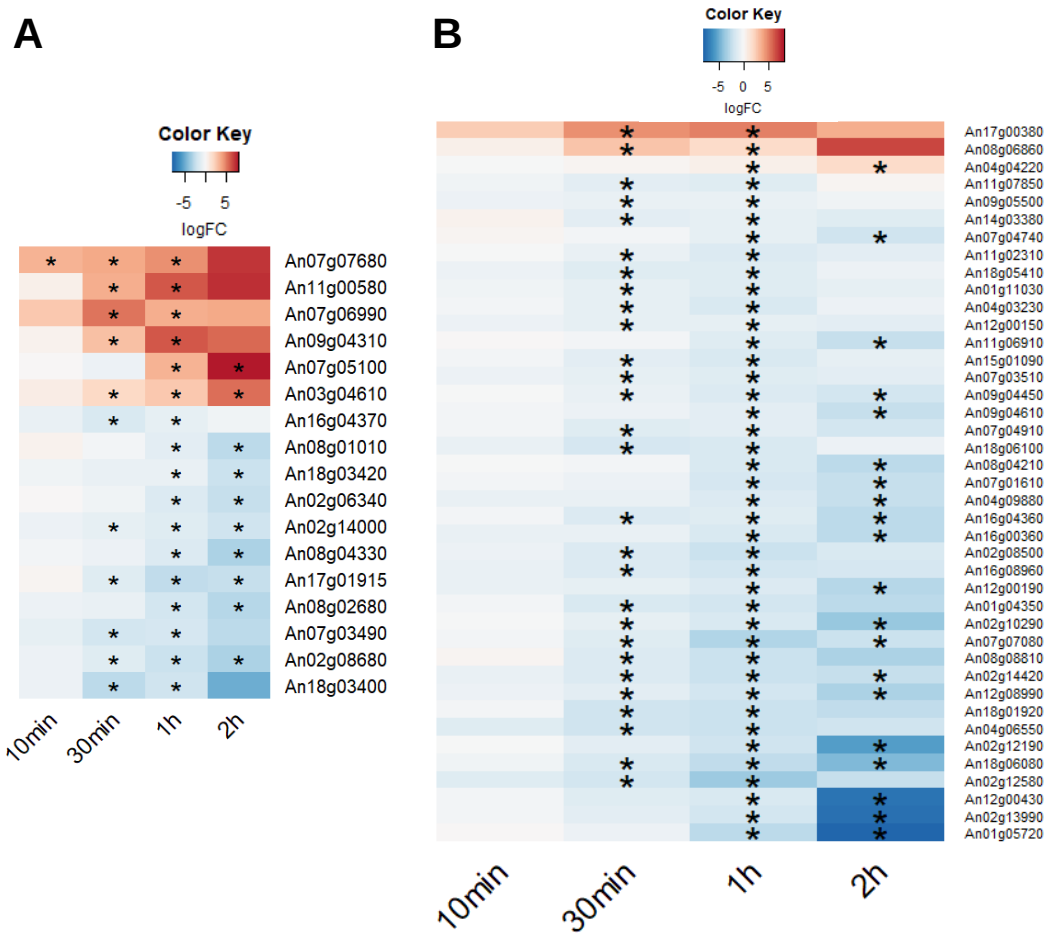

Figure 4-30: Log fold changes of EW-responsive DE genes found at more than one time points and with unknown function. The heatmaps show the logFC of upregulated genes in red (from the top) and downregulated genes in blue for the four EW-sampling times. A) Genes with reported orthologs in other *Aspergillus* species, but unknown function. B) Genes with unknown function. Genes that showed a significant change in gene expression (logFC) are labelled with an asterisk. The significance of the logFC was calculated within EdgeR and p-values were adjusted for multiple testing using the false discovery rate (FDR) approach (Benjamini and Hochberg, 1995). A searchable list of the genes and the orthologs reported for the genes in A) are available in Appendix I, 6.9.2.

For those DE genes (found at more than one time point) with known or predicted functions (shown in Figure 4-29), the functions annotated in the AspGD are listed in Table 4-3. Both the up- and down-regulated subsets contained genes involved in DNA binding and regulation, transcription, transport and tRNA metabolism (Table 4-3), but these encompass the most common GO processes among the annotated *A. niger* genes (Cerqueira et al., 2014). The upregulated subset also contained *An14g05150* with predicted ubiquitin-specific protease activity, and

genes involved in redox metabolism: *An11g06610* with a role in the biosynthesis of the redox cofactor NAD^+ and *An01g09620*, *An08g06390* and *An01g13340* with predicted oxidoreductase domains. The downregulated subset contained several genes involved (or predicted to be involved) in lipid metabolism (*An12g03600*, *An08g04090*, *An18g03800*, *An02g05000*, *An14g03360*, *An01g07870*), NADP specific malate dehydrogenase (*An12g00160*, reported to be involved in storage lipid accumulation (Wynn et al., 1999, Wynn and Ratledge, 1997)), one gene with a predicted oxidoreductase domain (*An01g11880*) and two genes with predicted roles in cell division and hyphal/filamentous growth (*An02g10710*, *An16g09040*).

Table 4-3: List of DE genes found at more than one time point and known or predicted functions. LogFC values are plotted in Figure 4-29.

Gene ID[a]	Function
Upregulated	
An02g04980	Ortholog(s) have… Activity: DNA helicase, DNA/RNA helicase, RNA helicase, ATP binding, nucleic acid binding activity Role in: maturation of LSU-rRNA from tricistronic rRNA transcript (SSU-rRNA, 5.8S rRNA, LSU-rRNA) Localisation: nucleolus
An09g06610	Has domain(s) with… Activity: predicted ATP binding, DNA binding, GTP binding activity Role in: cell cycle, cell division, chromosome segregation Localisation: integral component of membrane
An16g01540	Has domain(s) with predicted… Localisation: membrane
An07g05930	Ortholog(s) have… Activity: D-leucyl-tRNA(Leu) deacylase activity, D-tyrosyl-tRNA(Tyr) deacylase activity Role in: D-leucine catabolic process, D-tyrosine catabolic process, tRNA metabolic process Localisation: cytoplasm
An15g00540	Ortholog(s) have… Role in: late endosome to vacuole transport via multivesicular body sorting pathway Localisation: Vps55/Vps68 complex, fungal-type vacuole membrane
An14g05150	Ortholog(s) have… Activity: thiol-dependent ubiquitin-specific protease activity Role in: protein deubiquitination Localisation: cytoplasm, endoplasmic reticulum
An14g02290	Has domain(s) with predicted… Activity: ATPase-coupled cation transmembrane transporter activity, metal ion binding, nucleotide binding activity Role in: cation transport Localisation: integral component of membrane
An11g06610	Nicotinamide-nucleotide adenylyltransferase
An14g07040	Has domain(s) with predicted… Activity: DNA-binding transcription factor activity (RNA polymerase II-specific), zinc ion binding activity Role in: regulation of transcription (DNA-templated) Localisation: nucleus

Table 4-3 (cont.)	
An08g05790	Ortholog(s) have… Activity: glycogen phosphorylase activity, pyridoxal phosphate binding Role in: glycogen catabolic process, response to heat Localisation: cell surface, cytoplasm, hyphal cell wall
An15g06040	Has domain(s) with predicted… Activity: ATP transmembrane transporter activity, calcium ion binding activity Role in: transmembrane transport
An16g07900	Has domain(s) with predicted… Activity: amino acid transmembrane transporter activity Role in: amino acid transmembrane transport Localisation: membrane
An15g05460	Has domain(s) with predicted… Role in: transmembrane transport Localisation: integral component of membrane
An14g00570	Thymidylate synthase
An02g08090	Ortholog(s) have… Role in: mRNA splicing (via spliceosome), regulation of DNA methylation Localisation: spliceosomal complex, U4/U6 x U5 tri-snRNP complex, U5 snRNP
An01g09620	Has domain(s) with predicted… Activity: flavin adenine dinucleotide binding, long-chain-alcohol oxidase activity, oxidoreductase activity (acting on CH-OH group of donors) Role in: oxidation-reduction process
An14g06930	Has domain(s) with predicted… Activity: catalytic activity, coenzyme binding activity Role in: cellular metabolic process
An07g08770	Has domain(s) with predicted… Role in: transmembrane transport Localisation: integral component of membrane
An08g06390	Has domain(s) with predicted… Activity: NADP binding, coenzyme binding, oxidoreductase activity (acting on the CH-OH group of donors, NAD or NADP as acceptor), phosphogluconate dehydrogenase (decarboxylating) activity Role in: oxidation-reduction process, pentose-phosphate shunt
An01g13340	Has domain(s) with predicted… Activity: hydrolase activity (acting on carbon-nitrogen (but not peptide) bonds), oxidoreductase activity Role in: carbohydrate metabolic process, metabolic process
Downregulated	
An12g03600	1-acylglycerol-3-phosphate acyltransferase
An09g05010	Ortholog(s) have… Activity: (R)-carnitine transmembrane transporter activity, choline transmembrane transporter activity, ethanolamine transmembrane transporter activity, amino acid transmembrane transporter activity Role in: glycine betaine transport Localisation: membrane
An04g08590	Ortholog(s) have… Activity: deoxyribodipyrimidine photo-lyase activity, mRNA binding activity
An15g01770	Ortholog(s) have… Activity: DNA binding activity, methyltransferase activity Role in: ascospore formation and DNA methylation
An01g12770	Ortholog(s) have… Activity: TBP-class protein binding, transcription coregulator activity Role in: RNA polymerase II preinitiation complex assembly, transcription initiation from RNA polymerase II promoter Localisation: transcription factor TFIIA complex

Table 4-3 (cont.)	
An02g14720	Has domain(s) with predicted… Role in: transmembrane transport Localisation: integral component of membrane
An08g04090	Has domain(s) with predicted… Activity: acetoacetate-CoA ligase activity, catalytic activity Role in: lipid metabolic process, metabolic process
An02g10710	Ortholog(s) have… Activity: protein kinase activity, ATP binding, transferase activity (transferring phosphorus containing groups) Role in: ascospore formation, conidiophore development, conidium formation, hyphal growth, protein phosphorylation, regulation of mitotic cytokinesis and regulation of protein localization to mitotic spindle pole body, septation initiation signalling, sporocarp development involved in sexual reproduction Localisation: mitotic spindle pole body
An12g00160	Malate dehydrogenase (NADP-specific)
An01g11880	Has domain(s) with predicted… Activity: electron transfer activity, heme binding, iron ion binding, oxidoreductase activity (acting on paired donors, with incorporation or reduction of molecular oxygen activity) Role in: oxidation-reduction process
An18g03800	Acyl-CoA synthetase
An11g00460	Has domain(s) with predicted… Activity: ubiquitin-like modifier activating enzyme activity
An04g03960	Has domain(s) with predicted… Activity: transferase activity (transferring phosphorus-containing groups) Localisation: membrane
An01g13790	Has domain(s) with predicted… Activity: DNA binding, DNA-binding transcription factor activity, sequence-specific DNA binding activity Role in: regulation of transcription (DNA-templated)
An02g05000	Ortholog(s) have… Activity: 1-acylglycerophosphocholine O-acyltransferase activity
An14g03360	Ortholog(s) have… Activity: glycerol-3-phosphate O-acyltransferase activity, glycerone-phosphate O-acyltransferase activity Role in: phospholipid biosynthetic process, regulation of triglyceride metabolic process Localisation: endoplasmatic reticulum, lipid droplet
An02g01740	Ortholog(s) have… Activity: phenylalanine-tRNA ligase activity Role in: mitochondrial phenylalanyl-tRNA aminoacylation and tRNA processing Localisation: mitochondrion
An17g02080	Has domain(s) with predicted… Activity: metal ion transmembrane transporter activity Role in: metal ion transport, transmembrane transport Localisation: membrane
An14g05510	Has domain(s) with predicted… Activity: catalytic activity Localisation: membrane
An14g01850	Ortholog(s) have… Activity: gamma-aminobutyric acid:proton symporter activity, putrescine transmembrane transporter activity Role in: amino acid transmembrane transport, gamma-aminobutyric acid transport, putrescine transport, transmembrane transport Localisation: fungal-type vacuole membrane

Table 4-3 (cont.)	
An16g04460	Ortholog(s) have predicted… Activity: ATP binding, protein kinase activity, protein serine/threonine kinase activity, transferase activity (transferring phosphorus-containing groups) Role in: protein phosphorylation; localisation: nucleus
An01g07870	Has domain(s) with predicted… Activity: phospholipid binding activity
An03g04650	Has domain(s) with predicted… Activity: nucleic acid binding, nucleotide binding activity
An01g11760	Has domain(s) with predicted… Role in: transmembrane transport Localisation: integral component of membrane
An16g09040	Ortholog(s) have… Activity: N-acetylglucosamine-6-phosphate deacetylase activity, Role in: in N-acetylglucosamine catabolic process, cellular response to N-acetyl-D-glucosamine, cellular response to biotic stimulus, cellular response to starvation, filamentous growth, filamentous growth of a population of unicellular organisms in response to biotic stimulus, filamentous growth of a population of unicellular organisms in response to chemical stimulus

[a] Genes in bold were significantly differentially expressed at three time points (all other genes were significantly expressed at two time points).

Next, the 40 DE genes with the greatest (significant) fold change at any time point (10 min, 30 min or 1 h) were assessed, as described above. Most genes in this subset were upregulated, and all were significantly differentially expressed at the 1 h time point (Figure 4-31). Similar to the DE gene subsets above, the high-logFC subset contained genes involved (or predicted to be involved) in DNA binding, RNA binding, transcription, translation and transport (Table 4-4). Other upregulated genes had (predicted) domains or orthologs with oxidoreductase activity (*An01g12390*, *An08g08060*), a role in the biosynthesis of the antioxidant and electron transport chain component ubiquinone (*An04g06490*), DNA repair (*An15g01140*), fatty acid metabolism (*An18g01620*) and genes encoding different degradative enzymes; phytase *phyB* (*An08g11030*) which releases phosphate from the storage compound phytate (Mullaney et al., 2000), tannin acyl hydrolase (*An17g00830*), nicotinamide-nucleotide adenylyltransferase (*An11g06610*, involved in NAD^+ biosynthesis, also present in the above DE gene subset [DE genes found at more than one time point, Table 4-3]) and a putative amidase/acetamidase (*An16g07500*). The only downregulated gene with an

annotated function in this subset of DE genes had predicted oxidoreductase activity (*An18g05210*). Overall, the transcriptomics results suggested effects of EW treatment (combined with nutrient/osmotic stress) on central metabolic processes (DNA, RNA, proteins, transport) and stress response (including oxidative stress response), and connections to other sections of this chapter (regarding Met oxidation and hyphal/filamentous (out)growth) were observed (see discussion in 4.4.5 and 4.4.6).

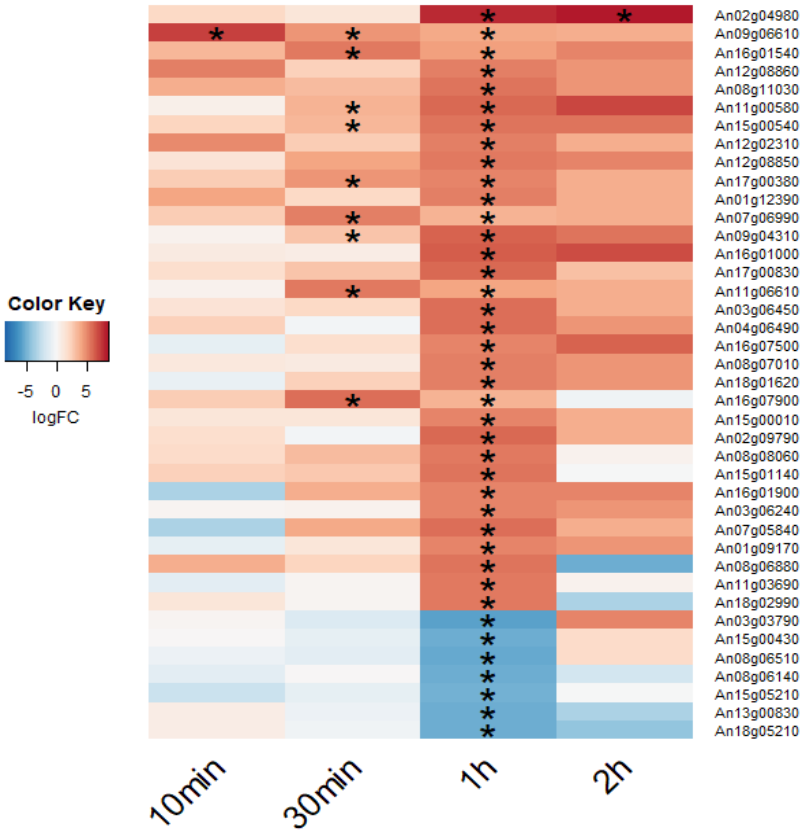

Figure 4-31: Log fold changes of the 40 most strongly differentially expressed genes induced by EW. The heatmap shows the logFC of upregulated genes in red (from the top) and downregulated genes in blue for the four EW-sampling times. Genes that showed a significant change in gene expression (logFC) are labelled with an asterisk. The significance of the logFC was calculated within EdgeR and p-values were adjusted for multiple testing using the false discovery rate (FDR) approach (Benjamini and Hochberg, 1995). The functions of the genes are listed in Table 4-4.

Table 4-4: List of the 40 most strongly differentially expressed genes and their known or predicted functions. LogFC values are plotted in Figure 4-31.

Gene ID[a]	Function or orthologs
Upregulated	
An02g04980	Ortholog(s) have… Activity:DNA helicase activity, DNA/RNA helicase activity, RNA helicase activity, ATP binding, nucleic acid binding Role in: maturation of LSU-rRNA from tricistronic rRNA transcript (SSU-rRNA, 5.8S rRNA, LSU-rRNA) Localisation: nucleolus
An09g06610	Has domain(s) with predicted… Activity: ATP binding, DNA binding, GTP binding activity Role in: cell cycle, cell division, chromosome segregation Localisation: integral component of membrane
An16g01540	Has domain(s) with predicted… Localisation: membrane
An12g08860	Protein of unknown function
An08g11030	Phytase (myo-inositol-hexakisphosphate phosphohydrolase); narrow pH optimum at around 2.5, very little activity at pH 5.0 Predicted role in cellular response to phosphate starvation
An11g00580	Ortholog of *A. oryzae* RIB40 : AO090023000204, *Neosartorya fischeri* NRRL 181 : NFIA_056440, *Aspergillus wentii* : Aspwe1_0171161 and *Aspergillus versicolor* : Aspve1_0147930
An15g00540	Ortholog(s) have… Role in: late endosome to vacuole transport via multivesicular body sorting pathway Localisation: Vps55/Vps68 complex, fungal-type vacuole membrane
An12g02310	Ortholog of *A. niger* CBS 513.88 : An01g11470, An12g02300, A. oryzae RIB40 : AO090701000387, AO090005000910, AO090010000602 and *Neosartorya fischeri* NRRL 181 : NFIA_011690, NFIA_052050
An12g08850	Protein of unknown function
An17g00380	Protein of unknown function
An01g12390	Has domain(s) with predicted… Activity: oxidoreductase activity Role in: oxidation-reduction process
An07g06990	Ortholog of *A. nidulans* FGSC A4 : AN4556, *A. fumigatus* Af293 : Afu2g02670, *A. oryzae* RIB40 : AO090026000612, *Aspergillus wentii* : Aspwe1_0036732 and *Aspergillus sydowii* : Aspsy1_0154947
An09g04310	Ortholog of *Aspergillus brasiliensis* : Aspbr1_0057159 and *Aspergillus acidus* : Aspfo1_0084546
An16g01000	Has domain(s) with predicted… Role in: transmembrane transport Localisation: integral component of membrane
An17g00830	Tannin acyl hydrolase with a predicted role in tannic acid degradation
An11g06610	Nicotinamide-nucleotide adenylyltransferase
An03g06450	Has domain(s) with predicted… Localisation: cell outer membrane, integral component of membrane
An04g06490	Ortholog(s) have… Activity: 2-polyprenyl-6-methoxy-1,4-benzoquinone methyltransferase activity, 3-demethylubiquinone-6 3-O-methyltransferase activity, hexaprenyldihydroxybenzoate methyltransferase activity Role in: ubiquinone biosynthetic process Localisation: extrinsic component of membrane, mitochondrial inner membrane, mitochondrion
An16g07500	Putative amidase/acetamidase
An08g07010	Ortholog of *A. nidulans* FGSC A4 : AN4122, AN2881, AN10123, AN0867, *A. fumigatus* Af293 : Afu1g13860, Afu1g15180, Afu3g11650 and *A. niger* CBS 513.88 : An02g07440, An01g13480

Table 4-4 (cont.)	
An18g01620	Has domain(s) with predicted… Activity: FAD binding, oleate hydratase activity Role in: fatty acid metabolic process
An16g07900	Has domain(s) with predicted… Activity: amino acid transmembrane transporter activity Role in: amino acid transmembrane transport Localisation: membrane
An15g00010	Has domain(s) with predicted… Role in: vesicle docking involved in exocytosis Localisation: exocyst
An02g09790	Ortholog(s) have… Activitiy: high-affinity thiamine:proton symporter activity Role in: thiamine import across plasma membrane Localisation: medial membrane band, plasma membrane, plasma membrane of cell tip
An08g08060	Has domain(s) with predicted… Activitiy: N,N-dimethylaniline monooxygenase activity, NADP binding, flavin adenine dinucleotide binding, oxidoreductase activity Role in: oxidation-reduction process Localisation: intrinsic component of endoplasmic reticulum membrane
An15g01140	Has domain(s) with predicted… Activity: phosphoric diester hydrolase activity, role in DNA repair Localisation: nucleus
An16g01900	Ortholog of *A. nidulans* FGSC A4 : AN3303, AN3346, AN3348, AN2044, AN8727 and *A. fumigatus* Af293 : Afu4g10080, Afu7g00420, Afu8g06100, Afu4g01242
An03g06240	Has domain(s) with predicted… Activity: ATP binding, DNA binding, helicase activity, nucleic acid binding, zinc ion binding activity
An07g05840	Has domain(s) with predicted… Role in: transmembrane transport Localisation: integral component of membrane
An01g09170	Ortholog(s) have… Activity: RNA binding activity, rRNA (guanine-N1-)-methyltransferase activity Role in: rRNA modification Localisation: mitochondrion
An08g06880	Protein of unknown function
An11g03690	Has domain(s) with predicted… Activity: DNA binding, DNA-binding transcription factor activity (RNA polymerase II-specific), zinc ion binding activity Role in: regulation of transcription (DNA-templated), transcription (DNA-templated) Localisation: nucleus
An18g02990	Ortholog(s) have… Activity: nucleotide binding activity, structural constituent of ribosome activity Role in: translation Localisation: mitochondrial large ribosomal subunit, mitochondrial ribosome
Downregulated	
An03g03790	Protein of unknown function
An15g00430	Protein of unknown function
An08g06510	Protein of unknown function
An08g06140	Protein of unknown function
An15g05210	Protein of unknown function
An13g00830	Protein of unknown function
An18g05210	Putative peroxisomal dehydratase; induced by fenpropimorph Predicted oxidoreductase activity Localisation: glyoxysome

[a] Bold genes were also found in the DE subset presented in Table 4-3.

4.4 Discussion

When organic matter is present during EW treatments, reactivities between organic compounds and EW active species result in the inactivation of EW species (see Chapter 2), resulting in low effective EW doses, which underlines the relevance of studies at such low EW doses. The present study showed that when *A. niger* spores were exposed to low doses of EW in short-term treatments, this delayed the subsequent fungal outgrowth and led to increased growth variation (colony-colony size variation). Specifically, both the growth delay and the increased heterogeneity were observed at the macro-colony level (assessing colony area variation among colonies) and during early germination (conidial swelling after 2 h). Both effects were non-heritable and were observed with chlorine-containing sanitisers (EW, NaOCl) but not with the chlorine-free oxidant ozonated water, suggesting a role for FAC in triggering the growth delay and increased variation. It was hypothesised that this FAC role may be mediated by chloramine formation. On the other hand, a protective effect of methionine pre-treatment on the EW survival of *A. niger* spores (similar to the protective effect observed in yeast, Chapter 3) could not be conclusively shown. Nevertheless, methionine sulphoxide reductase was one (of a number of) functions revealed by transcriptome analysis to be differentially upregulated during EW exposure of *A. niger*, so the RNA-sequencing dataset provided here might help to rationalise certain aspects of this organism's EW response.

4.4.1 Stress-induced heterogeneity in *A. niger*

Several stages of the EW treatment and spore recovery may contribute to the observed colony size heterogeneity. Damage induced by EW may vary from spore to spore due to stochastic differences, e.g., some spores may encounter more active EW species by chance, or EW species may encounter and inactivate different proteins in different spores, resulting in different severities of damage. In addition,

spores within a population may already be heterogeneous (e.g., in their gene expression/protein accumulation levels, see text below), so that some spores may be better protected against EW while others accumulate more damage. Furthermore, this intrinsic phenotypic heterogeneity might mean that some spores are better equipped to repair EW-induced damage.

Colonies of fungi such as *A. niger* were previously reported to grow heterogeneously, as measured by colony diameter, with the variation increasing at stressful (low and high) temperatures (Gougouli and Koutsoumanis, 2013, Dagnas et al., 2017). This is consistent with the observations in the present study, where colony area variation was visible in control conditions but increased after EW treatment. Increased variation post EW treatment was not only visible at the macro-colony level but also when spore size distribution was assessed by flow cytometry after 2 h of conidial swelling in YEPD, consistent with a potential dependence of colony size variation on spore-spore variation during early germination. The distributions of colony formation lag times and single spore germination times (in unstressed conditions) were previously shown to be similar for *A. niger*, suggesting that the variability in colony formation stems from the spore and/or early germination stages (Gougouli and Koutsoumanis, 2013). Heteroresistance against sorbic acid in *A. niger* has been reported for conidia (spread-plated onto sorbic acid-containing YEPD agar) but the stress response of germinating conidia (pregerminated [6 h] prior to plating) was more homogeneous (Geoghegan et al., 2020), suggesting that differences at the spore stage might be the determining factor for downstream stages, e.g., colony size heterogeneity, also in stress conditions. However, at stressful temperatures, colony formation of *A. niger* was found to be more variable than the germination time variation (Gougouli and Koutsoumanis, 2013). The authors attributed this effect to measurement and model fitting uncertainty but did not experimentally rule out the possibility that variability of post-germination processes (under

stressful conditions) may further increase the variation at the colony level. To assess the possibility that additional events between the 2 h time point (assessed by flow cytometry) and macro-colony assessment (44 h and later) may also influence the colony-size variation, it would be useful to study the growth variation post-EW treatment using a microfluidics system; this would allow tight control of the environment while enabling monitoring of germination, hyphal growth and early mycelium formation from single conidia (Dusny and Schmid, 2015, Grünberger et al., 2017).

Phenotypic heterogeneity can arise from diverse sources, such as gene expression noise, stochastic distribution of molecules, cell cycle progression, cellular ageing or epigenetic modifications, and these processes may also be interdependent (Ackermann, 2015, Guerreiro et al., 2021, Avery, 2006). Some or all of these processes may be involved in the observed variation in colony growth post EW treatment, in addition to a potential "chemical" or stochastic heterogeneity in EW-induced damage to spore components (described above). For instance, a gene whose expression contributes to phenotypic heterogeneity in *A. niger* has been reported in the context of sorbic acid stress resistance (Geoghegan et al., 2020). Colonies of filamentous fungi are made up of hyphae which grow only at their apices while transporting cytoplasmic material from the inner colony zones to the periphery (Trinci, 1971, Fricker et al., 2017). The colony growth depends on the hyphal growth rate but also on the amount of hyphal branching (Pazouki and Panda, 2000). Whereas the germ tube formation and early hyphal growth follow an exponential growth pattern, later stages of radial colony growth progress more linearly, potentially due to the depletion of storage compounds and the need for biosynthesis and transport through the hyphae (Gougouli and Koutsoumanis, 2013). The growth rate of single hyphae of *A. oryzae* differed depending on the age of the hyphae which can partially explain inter-hyphal variation (Foster, 2019). Hyphal heterogeneity of the cytoplasmic composition in *A. oryzae* and

A. niger is maintained by (reversible) plugging of septa by Woronin bodies (Bleichrodt et al., 2012, Bleichrodt et al., 2015). Many examples of heterogeneity in *A. niger* mycelium have been reported, including between different hyphae, different structural elements in mycelium, and between micro-colonies (Bleichrodt et al., 2013, Wösten et al., 2013, Levin et al., 2007, Daly et al., 2020, Tegelaar et al., 2020). Additionally, conidial spores are phenotypically heterogeneous which can affect their germination and outgrowth, including during stress conditions (Teertstra et al., 2017, Bleichrodt et al., 2020). While the underlying processes for spore- and mycelium-heterogeneity are not yet thoroughly understood, similar mechanisms may also influence the observed colony area variation in this study and also the observed decrease in such variation with increasing incubation time (under the same condition).

4.4.2 Stress-induced growth delay may be related to sub-lethal damage accumulation and/or spore-spore heterogeneity

A growth delay could be a sign of cellular damage caused by EW treatment that is insufficient to result in cell death but slows post-treatment growth (Nanba et al., 2013). Additionally, colony growth in control conditions (no EW treatment) was observed to be heterogeneous, and it is possible that EW treatment also selects for slow growing spores at partially lethal doses. This would be consistent with previous studies supporting the idea of beneficial effects from heterogeneity in an isogenic population due to harbouring of different sub-populations with distinct stress resistance profiles (Bleichrodt et al., 2020, Hagiwara et al., 2017). It was also hypothesised previously that slow growth or germination delays may enable spores to better react to stressful conditions (Bleichrodt et al., 2020). In addition, non-growing phenotypic sub-populations known as persister cells (e.g., in *Candida* biofilms) are able to survive high stressor levels and show increased ROS resistance (Wuyts et al., 2018). In *A. oryzae* colonies, 'persister-type' hyphae

with low transcriptional and translational activity were associated with increased stress resistance (Tegelaar et al., 2020). However, the presented experiments did not distinguish between a potential bet hedging hypothesis of sub-populations and an alternative hypothesis of (sub-lethal) damage accumulation during EW treatments, accounting for the observed growth effects across the whole population.

Increased colony size variation has previously been reported when the lag phase of colony formation by filamentous fungi was increased by several days or weeks, by growing at stressful temperatures or decreased water activity (Gougouli and Koutsoumanis, 2013, Dagnas et al., 2017). However the lag phase difference between EW-treated and control samples was small in the present study (up to 6 h) and conditions that delayed the growth by approx. 1 day (growth at 23°C, Figure 4-3) did not increase the variation. Interestingly, growth at room temperature in the present study increased variation (compared to higher growth temperatures [23°C or 28°C]) in 2 out of 3 replicates, suggesting that there may be a "threshold" growth delay (~2 days may be suggested from the present results) above which variation starts to increase. However, as the growth delay induced by EW treatments in this study was generally below such a threshold, the increase in variation must mostly be caused by factors other than the growth delay. It was recently shown that spore size and shape is correlated with the stress resistance of conidia of heat-resistant *Paecilomyces variotii* strains (van den Brule et al., 2020), and a possible explanation for the variation in colony size after EW treatment may be related to similar spore-spore heterogeneity: spores of different properties (such as different sizes, ages or solute contents) may differ in their EW response and/or levels of accumulated damage, resulting in different extents of growth delay and hence increased variation, similar to differential heat resistance or virulence reported for spores of different ages, solute levels or sizes (Li et al.,

2011, Dijksterhuis, 2007, Punt et al., 2020), although further tests would be needed to link EW resistance to potential subpopulations of *A. niger* conidia.

4.4.3 Potential role for chloramines in EW actions

4.4.3.1 Reported effects of chloramines

The increase in colony size variation and also the growth delay of colonies post treatment were observed with FAC-containing sanitisers (EW, NaOCl) and not ozonated water (chlorine-free). FAC is well known to react with amino acids, and it is highly reactive with the amino group of all amino acids and with the side chain of some amino acids, including Cys, Met, His, Trp (see 2.4.4.2) (Pattison and Davies, 2001, Storkey et al., 2014). These reactions with amino acids result in the formation of products such as chloramines (Pattison et al., 2007). High reactivity of EW with amino acids was also confirmed in this study (2.3.4.1). In biological systems, it is mainly mono-chloramines that are formed in this way, due to the large excess of proteins and amino acids over the FAC levels in most conditions (Szabó et al., 2019). Antibacterial effects (e.g., inhibition of DNA repair, mutagenesis, killing) have been reported for some chloramines, e.g., for chlorinated Pro, Gly, Arg, Cys, His, Met and others (Donnermair and Blatchley, 2003, Amiri et al., 2010, How et al., 2017). The side chains of Met and Cys are more reactive with FAC than their amino groups, and the first reactions between these amino acids and FAC are side chain oxidations (Pattison and Davies, 2001, Storkey et al., 2014), but subsequent chlorination of cystine (two oxidised cysteine molecules cross-linked by a disulphide bridge) and further oxidation of MetO (oxidised Met) have also been reported (Nagy and Ashby, 2005, Pattison et al., 2007). A study on the reactivity of natural organic matter from rivers with EW (5 mg L^{-1} FAC) showed that at 0.04 g L^{-1} added organic matter, the FAC was fully inactivated but partial bactericidal activity was retained, potentially indicating the formation of toxic products such as chloramine species (Ogunniyi et al., 2019).

Chlorine transfer reactions have been shown to mediate secondary damage of proteins during FAC treatment. For example, His residues in proteins become chlorinated at the imidazole side chain and then transfer the chlorine to other substrates, including other amino acids within the same protein (Pattison et al., 2007, Pattison and Davies, 2005). Oxidation of MetO to methionine sulphone has been proposed to be mediated by chloramines (Pattison et al., 2007). Chloramine formation can also lead to the generation of nitrogen-centred radicals which further contribute to protein and DNA oxidation (Hawkins and Davies, 1999, Hawkins et al., 2002). Such secondary effects may result in post-treatment stress, such as might (partially) explain the observed growth delay in FAC-treated *A. niger* spores. Post treatment oxidative stress has been reported to increase microbial killing (Hong et al., 2019, Mokudai et al., 2015). However, as the growth delay effects in the present study were not observed after treatment with ozonated water, it is suggested that mechanisms other than ROS accumulation are involved in the growth delay; such as mechanisms related to the formation of chloramines. Because chloramines are less reactive than FAC (Peskin and Winterbourn, 2001, Pattison and Davies, 2005), they might persist longer in the EW-treated spores than FAC species and this persistence may facilitate post FAC-stress effects.

4.4.3.2 Other observations across this thesis are consistent with chloramine formation

Generally, reactivity between EW and proteins or amino acids resulted in inactivation of EW fungicidal activity in this study, especially at molar excess of the amino compounds. However, several results across this thesis are also consistent with the formation of inhibitory protein- or amino acid-derived products during EW treatment. While the formation of such products was not the focus of the previous chapters, it is worth revisiting those observation and how they may connect to the hypothesised involvement of chloramines in the colony size effects (growth delay/variation) in this chapter. When MetO was mixed with EW,

subsequent treatment of *A. niger* spores with this mix resulted in growth inhibition only at high levels of MetO (2.3.4.2; MetO alone [not exposed to EW] did not inhibit growth). This inhibition was observed even when active species of EW were inactivated by YEPD addition prior to the spore treatment (but after an incubation period of the active EW with MetO), and the inhibitory effect disappeared when treated spores were diluted post treatment, consistent with the formation of an inhibitory product from the reaction between EW and MetO (potentially methionine sulphone (Pattison et al., 2007)) and extracellular accumulation. Furthermore, when EW was mixed with either Arg, His, Asn or Met and subsequently used to treat *A. niger* spores (in experiments to test whether the amino acids would inactivate the active EW species and allow fungal growth), full growth was observed at relatively high amino acid concentrations (~2.5–7 mM, depending on the amino acid), whereas growth at low and intermediate added amino acid concentrations was observed with a time delay compared to the control growth (2.3.4.1). With other amino acids, such a delay was not observed, e.g., Ala inactivated EW at high levels of added amino acid, allowing 100% relative growth compared to the control, but growth was fully inhibited below a threshold concentration. The growth delay observed with specific amino acids may therefore be due to the formation of inhibitory products, especially at low to intermediate (0.6–5 mM) amino acid concentrations (where there was a molar excess of FAC [20% EW was mixed with the amino acid, equivalent to ~7 mM HOCl]). The growth delays in these experiments were observed in broth, so they could indicate a growth delay in all spores or else partial killing of a subpopulation of the spores.

Discrepancies between the *in-vitro* and *in-vivo* reactivity tests in Chapter 2 also suggested the formation of inhibitory products: for the *in-vitro* tests (assessing EW oxidising activity with the fluorescent probe APF), Cys and Met were found to be the most reactive with EW (2.3.5.1), consistent with the reported highest reactivity of these two amino acids with FAC (Pattison and Davies, 2001, Storkey

et al., 2014). However, when amino acids and EW were mixed and subsequently used to treat *A. niger* spores, Trp and Tyr inactivated the EW more strongly (allowing fungal growth at lower levels of added amino acid than Cys or Met). This may suggest that whereas Cys and Met strongly react with EW, the products of such reactions have inhibitory activity, preventing fungal growth. At higher Cys and Met additions to EW, such effects were not visible, potentially indicating that the first oxidation products of Cys and Met (oxidised once at their respective side chains) were non-toxic (consistent with an observed lack of inhibition of *A. niger* growth in the presence of MetO, see 2.3.4.2), but further reactivities at a molar excess of FAC may yield inhibitory secondary products. Such further reactivities at molar excess of FAC have been shown for MetO residues in lysozyme (MetO was formed upon exposure of the protein to up to 10 x molar excess of HOCl, but was consumed again at 25 x molar excess HOCl) (Pattison et al., 2007) and for cystine (already oxidised cysteine) exposed to a further equimolar HOCl dose (yielding one-half molar equivalent of dichlorocysteine, at high pH) (Nagy and Ashby, 2005).

The above experiments are consistent with the formation of chloramines or other amino acid oxidation products that form extracellularly and that are present in the growth medium post-treatment (EW treatment mixes were diluted 1:2 only in YEPD before outgrowth, so that such proposed products would still be present at relatively high levels in the medium). However, growth delays were also observed in a different experiment involving potential chloramine formation and higher dilution post-treatment (2.3.3): EW was mixed with peptone or yeast extract (protein-rich substances) and subsequently used to treat *A. niger* spores, followed by 1:50 dilution in YEPD and plating onto YEPD agar. The formation of colonies on the agar was delayed compared to control colonies, and also compared to colonies of spores treated with EW+lysozyme or EW+BSA. The growth delay was observed despite the dilution step post-treatment, suggesting that proposed chloramines

(or other products) from the reaction between EW and peptone or yeast extract may have entered the fungal spores before the dilution took place (usually 5–10 min after the 5 min treatment).

Whether chloramines with toxic/inhibitory properties form will likely depend on the concentrations and properties of the amino compound reacting with EW, e.g., the reaction products of EW and some amino acids may not be inhibitory while other amino acids form toxic products when reacting with EW. Within cells or spores, many different amino compounds are available for a potential reaction with EW, so it is possible that some reaction products (such as chloramines) with inhibitory activity may form.

4.4.3.3 Hypothesis of chloramine formation leading to growth delay and increased colony size variation after EW treatments

Because the described experiments suggested that amino acid products such as chloramines inhibited or delayed the fungal growth, and chloramines have been reported to have antimicrobial activity (see above), it was hypothesised that the observed *A. niger* colony growth delay after EW treatment may also be related to chloramine formation. When EW enters fungal spores, it would encounter proteins and amino acids, and chlorination products (chloramines) may accumulate. If these have inhibitory effects, this may explain the growth delay of the spores into macro-colonies. As mentioned above, post-treatment oxidative stress after short-term treatments has been reported to contribute to the killing effect of antibiotic compounds in bacteria (Hong et al., 2019) and of EW treatments in *Candida albicans* (Mokudai et al., 2015). The latter study also observed smaller colonies after partially lethal EW treatments, consistent with the decreased colony size from EW-treated spores in the present study. Both cited studies observed increased survival when microorganisms were exposed to antioxidants post-treatment. When *A. niger* spores were exposed to the antioxidant ascorbic acid in

this study (either for 5 min post-treatment or by growing on ascorbic acid-containing agar), a decrease in the colony size variation and a slight increase in colony size (relative to the no-EW control) were observed, although these results were from biological duplicates so statistical significance was not established. One important future experiment would be to repeat such experiments at a range of ascorbic acid concentrations, to determine whether post-treatment stress contributes to the growth delay and increased colony-size variation. These experiments were not carried out in this project due to time constraints.

In the case of post-stress effects of antibiotics in bacteria, the authors suggested a role of (stressor-independent) self-amplifying ROS (Hong et al., 2019). Initial tests with fluorescent ROS probes in this study suggested ROS formation after EW treatments (see Appendix J, 6.10), but the absence of a growth delay or (significantly) increased variation after ozonated water treatment suggested a specific role of the FAC in EW (or NaOCl) for the effects described in this chapter, as opposed to ROS formation alone. A non-significant (but consistent across 3 biological replicates) growth delay and a statistically significant increase in variation were observed after chloramine treatment in this study. More experiments at higher chloramine concentrations would be necessary to confirm such proposed chloramine-induced effects and to contribute to the understanding whether chloramines may be the source of post-treatment stress in *A. niger* after EW treatments. Other explanations cannot be ruled out based on the presented data, e.g., other sub-lethal damage to fungal spores that slows down or halts fungal growth while it is being repaired. Chloramine accumulation in spores might result in variation through a variety of mechanisms, such as cell-cell differences in uptake, chloramine-responsive induction of intracellular processes or regulatory networks that are inherently 'noisy' and lead to increased variation, and/or by affecting single spores differently due to the inherent heterogeneity of formed conidia (Dijksterhuis, 2019, Teertstra et al., 2017), e.g., due to different size or

protein level and composition within single spores. Heterogeneous responses to chloramine treatments have been reported within bacterial biofilms (Huang et al., 1995) and between bacterial populations grown at optimal vs. sub-optimal temperatures (Berry et al., 2009).

4.4.4 Stress-induced increase in survival

In some experiments with sub-lethal EW treatments, survival >100% was recorded (survival between ~110% and ~150% was recorded in 12 out of 19 assessed independent experiments and survival after 0.1% EW treatment [10 experiments] was significantly different from, and higher than, 100%), although this may be partly related to technical variation of the agar plating method (see 4.3.6). As described above (4.3.6), the most likely explanation (apart from random technical variation) is that EW treatment may reduce spore clumping, and that those separated (previously clumped) spores result in additional colonies compared to the untreated control. Interestingly, recovery rates >100% were also recorded when yeast was treated with sub-lethal EW concentrations (Figure 3-26, Figure 3-28), and the recovery in those experiments was assessed in broth (as opposed to colony counting). Treatments with EW or NaOCl have been reported to increase germination of *Tilletia indica* spores (Bonde et al., 1999), and similarly exposure to low ozone levels also sometimes increased germination in different fungi (Hibben and Stotzky, 1969, Beare et al., 1999) although such effects do not always affect the colony size (Beare et al., 1999). Such phenomena of induction at low concentrations but inhibition at high concentrations of a stressor (or stimulant) are known as hormesis, although the underlying mechanisms are not well understood and such observations are often interpreted as technical variation (Pradhan et al., 2017), and technical variation or alternative explanations (i.e., reduced spore clumping) cannot be ruled out in the present study. A proposed increase in germination (in line with hormesis)

would only result in higher colony numbers if not all spores in the control condition successfully germinate and form colonies, in which case the hormesis effect might manifest in an increased rate of successful colony formation.

Future studies could aim to distinguish clearly between technical variation, reduced spore clumping and hormesis, e.g., by assessing large numbers of biological and technical replicates. In this study, flow cytometry experiments that assessed early germination events (2 h post-treatment) did not show an increase in germination (Figure 4-10), which does not support the hormesis hypothesis. In future experiments, spore samples could be analysed by flow cytometry directly after the EW treatment, as ungerminated samples that were not EW-treated showed a small subpopulation of high-FSC (=larger) events, potentially corresponding to clumped spores. This subpopulation may decrease or disappear in EW-treated samples if EW reduces spore clumping.

4.4.5 Potential involvement of methionine in the response of *A. niger* to EW treatment

While *A. niger* spores grown on YNB agar containing Met survived EW treatment better than those grown without Met in some experiments, the effect was not consistent or significant across all replicates. Therefore, it is possible that the EW response of *A. niger* spores differs somewhat from *S. cerevisiae*, where a clear protective effect of Met pre-treatment was evident (3.3.2). This might be related to additional antioxidant enzymes or accumulated compounds that are present in filamentous fungi and especially in spores, see 4.1.3. Most notably, mannitol, a storage compound that makes up 10–15% of the dry weight in *A. niger* conidia, was implicated in the conidial resistance to NaOCl (Ruijter et al., 2003), and fungal melanins have been reported to protect against oxidative stress including NaOCl (Butler and Day, 1998). During some experiments in the present study, conidial

pellets after EW treatments were observed to be of a lighter colour, potentially suggesting bleaching of melanins (not shown). It is also possible that the pre-treatment methods applied in the presented experiments did not allow sufficient Met accumulation within *A. niger* spores. The conditions of conidiospore formation (such as medium or temperature) have been shown to affect the properties of the conidia (stress resistance, cell wall properties, transcriptome, pigmentation) of *Aspergillus* species in several studies (Bleichrodt et al., 2020, Wang et al., 2021, Hagiwara et al., 2017); most notably (for comparing with the present experiments), growth on mannitol-containing medium of an *A. niger* mutant deficient for mannitol biosynthesis directly increased the conidial mannitol levels and increased the mutant's resistance to NaOCl and heat stress (Ruijter et al., 2003). This suggests that conidia formation in the presence of Met should be a valid method for studying the effects of Met levels on the EW resistance of spores. However, while uptake and accumulation of exogeneous Met have been demonstrated in *Aspergillus* germinating conidia and mycelium (Tazebay et al., 1995, Amich et al., 2013), it is not clear whether accumulation in conidia formed on Met-supplemented agar occurs and reaches sufficient levels to result in a protective effect. In AMM, cultivation without an additional nitrogen source may have been beneficial to ensure amino acid uptake, as the amino acids in the pre-culture experiment [Ala, Arg, Asn, His, Met] can all serve as a sole nitrogen source to support growth in the presence of germination-triggering and -sustaining sugars (Hayer et al., 2014). It is emphasised that the yeast cells in Met pre-treatment experiments were vegetative cells, whereas the *A. niger* experiment used conidia. As stated above, fungal spores differ from vegetative cells in properties such as metabolic rate, cell wall composition, intracellular metabolite concentrations, cytoplasm viscosity and stress resistance (Dijksterhuis, 2019), and germinating conidia undergo extensive metabolic changes as evidenced by gene and protein expression levels (Novodvorska et al., 2016, Novodvorska et al., 2013). Such differences between spores and vegetative cells could extend to a

weaker, or absent, phenotypic effect of Met pre-culture in *A. niger* (conidia) than in yeast (vegetative cells) here. It is difficult to analyse germinating conidia with certain conventional methods after the first few hours of germination (e.g., due to clumping issues during centrifugation, routinely observed in this study). However, recent microfluidic systems are suited to tracking single cell (or germling) growth and allow tight control of the environment (e.g., enabling the comparison between Met pre-treatment and control conditions) and microscopic observation of germination and hyphal growth (Grünberger et al., 2017). It was originally intended to study the EW response of *A. niger* in a microfluidic system in the present study. However this was not possible due to a combination of time constraints and limited access to facilities due to Covid restrictions. The upregulation of a predicted methionine sulphoxide reductase (*fRMSR* ortholog *An03g05080*) after EW treatment in the transcriptome dataset described in this chapter suggested that, while Met may not be the only or main scavenger of active EW species in *A. niger*, Met oxidation (and MetO reduction by MSR enzymes) may still be involved in the EW response of this species of filamentous fungus (note that 6 h germlings were sampled for the transcriptomics experiment, as opposed to (mostly) ungerminated spores in the pre-treatment experiments).

4.4.6 Transcriptome analysis after EW treatment of *A. niger*

As mentioned above, the use of certain conventional microbiological and genetic methods is limited in filamentous fungi. Analysing the transcriptome changes induced by stress treatment can be a powerful tool to assess the microbial stress response. The transcriptome of *A. niger* germlings (6 h germinated spores) treated (or not) with EW was analysed to identify genes that were differentially expressed between control and treatment samples, to gain further insight into how *A. niger* responds to EW stress. Several limitations affect the presented transcriptome analysis. First, the protocol included shifting germinating *A. niger*

conidia from rich YEPD media to 0.1% Tween followed by suspension in sterile tap water or water-diluted EW. This shift from a nutrient-rich media to starvation and osmotic stress conditions requires adaption and stress responses by the fungal spores, and this may hinder the identification of any specific EW-stress reactions in the transcriptome dataset, as certain detected changes may be related to the nutrient/osmotic stress and because already-stressed conidia may react differently to EW than non-stressed conidia. Alternative approaches would have been to shift conidia to diluted nutrient media (e.g., 0.1% peptone), incubate to allow adaption and then add an appropriate sub-lethal EW dose (however this approach might lead to chloramine formation from reactions between the EW and peptone, and transcriptome changes may be responses to EW, chloramines, or both), or else to treat conidia for shorter periods (with higher EW doses than in the presented 30 min to 2 h treatments) and recover in YEPD before harvesting for transcriptome analysis. It may have been beneficial to test different strategies in a small number of samples before choosing to most suitable experimental approach. For the approach used in this study, an additional control condition of conidia harvested before shifting from rich YEPD medium to nutrient-free conditions may have helped to identify general (non-EW-induced) transcriptome changes in response to the nutrient/osmotic stress. A second issue was the low survival in the 1 h and 2 h samples (~10–30%), so that unspecific killing effects may be detected in those samples. A third issue was the 30 min-processing time between the end of EW treatments and freezing the samples for RNA extraction, because fast, transient transcriptome changes may be missed. Furthermore, the choice of *A. niger* N402 was problematic, as this strain was obtained by UV mutagenesis (inducing several genetic changes compared to the wild strain N400) (Demirci et al., 2021) and a sequenced N402 reference genome was not available at the time of the analysis. Differences between N402 and the chosen reference genome of *A. niger* CBS 513.88 may explain the low mapping efficiency of the sequenced reads and limit the obtained information. It would have been better to

use a strain with a sequenced genome or at least the non-mutagenised N400 strain. Sequenced genomes of N402 have since been made available on https://fungidb.org (Laothanachareon et al., 2018) and in the NCBI Sequence Read Archive (Demirci et al., 2021), so repeating the bioinformatic analysis using the N402 reference genome might reveal new information from the present dataset (funding for re-analysis was not available as part of this study). The biological and technical variation between replicate RNA samples was relatively high compared to differences between control and EW-treated samples, probably due to the technical shortcomings described above and potentially also suggesting limited RNA quality in the samples. Overall, these issues limit the information that can be obtained from the dataset.

In line with the above considerations, some results in the transcriptome dataset were consistent with general metabolic repair and extensive transcriptional changes in conidia exposed to multiple stressors (EW+nutrient+osmotic), such as a high relative number (compared to all detected genes) of differentially expressed genes involved in key metabolic processes (transport, cellular organisation and development, protein metabolism and nucleic acid processes) and upregulation of hydrolases, ligases and stress response genes in EW-treated samples.

For some findings, it can be speculated that they may indicate EW-specific effects, but this would need to be re-tested in improved transcriptome analysis approaches, as the presented data is insufficient for substantiated claims. For instance, four upregulated genes involved in toxin metabolism (*An03g05140*, *An12g02840*, *An15g07530*, *ppoC*), encoding for proteins involved in the synthesis of secondary metabolites (polyketides, nonribosomal peptides) and proteins with (predicted) oxidoreductase activity, may be consistent with oxidative stress during and after EW treatments which may necessitate ROS scavenging proteins and molecules. Upregulation of DNA repair genes may indicate DNA damage caused

by EW, e.g., through DNA chlorination (Hawkins et al., 2007) or chloramine-mediated double strand breaks (Hawkins et al., 2002). Upregulation of protein ubiquitinylation genes would be consistent with EW-induced protein damage. Certain findings could be viewed as parallels to the observed delays in germination and colony growth after EW treatment observed in other parts of this chapter, including DE genes suggesting damage (repair) of DNA or proteins (damage may slow down fungal outgrowth) and the downregulation of two genes involved in cell division and hyphal/filamentous growth (*An02g10710*, *An16g09040*). Again, such speculations would need to be investigated in follow-up studies with improved experimental procedures.

To the best of my knowledge, there are no published studies on the effects of EW on a microbial transcriptome. This study highlighted parallels between EW and sodium hypochlorite, and the bacterial transcriptome response to sodium hypochlorite has been extensively studied, revealing upregulated DE genes related to general stress response, oxidative stress response, protein metabolism, energy metabolism (upregulated in two studies), virulence (one study), multidrug resistance/efflux, sulphur uptake and metabolism, cysteine and methionine biosynthesis, and downregulated genes involved in lipid metabolism, energy metabolism (three studies), virulence genes (one study) (Wang et al., 2009, Jang et al., 2009, Loi et al., 2018, Ceragioli et al., 2010, Bodet et al., 2012, Small et al., 2007, Lipus et al., 2019). Specific findings include the upregulation of FeS cluster assembly and repair and heat shock proteins in *E. coli* (Wang et al., 2009), upregulation of amino acid biosynthesis in *Staphylococcus aureus* (Loi et al., 2018), upregulation of inorganic ion transport/metabolism in *Bacillus cereus* (Ceragioli et al., 2010); upregulation of membrane transporters and downregulation of transport of molecules related to amino acid synthesis in *P. fluorescens* biofilms (Lipus et al., 2019). Parallels to the results presented here are the induction of genes involved in general and oxidative stress response,

protein metabolism, transport, replenishing of Met (via methionine sulphoxide reductase upregulation (Lipus et al., 2019), as shown here, or Met biosynthesis upregulation (Ceragioli et al., 2010)) and the downregulation of lipid metabolism genes.

Furthermore, several transcriptome studies have studied the oxidative stress response in *Aspergillus* species in response to a range of stressors. In *A. flavus* treated with H_2O_2, genes involved in transport, carbon metabolism, stress signalling, antioxidant mechanisms, secondary metabolite production and fungal development were differentially regulated (Fountain et al., 2016b, Fountain et al., 2016a), and a different group reported enrichment of genes related to translation, transport, secondary metabolites, cell wall proteins, fatty acid metabolism, transcription, respiration and drug resistance (Tian et al., 2021). In *A. fumigatus* treated with H_2O_2, secondary metabolism genes were enriched in the DE gene set (Kurucz et al., 2018). In oxidatively stressed *A. nidulans*, genes of the cell cycle, ribosome biogenesis and sterol metabolic processes were down-regulated and secondary metabolism genes were upregulated (Emri et al., 2015). In *A. niger* treated with H_2O_2, increased expression of the cysteine-motif antimicrobial peptide AnAFP (*An07g01320*) with proposed important metabolic signalling, sensing or effector roles, has been reported (Paege et al., 2016), but this gene was not among the DE genes in the present dataset. Some parallels between these studies and the results here include effects on transport, (oxidative) stress response, secondary metabolites, fungal development, translation and lipid metabolism. To allow a reliable comparison with these published studies, and to better understand the transcriptome response of *A. niger* to EW treatment, a refined experimental protocol according to the above considerations should be employed. Special attention should be paid to transcriptomics results that, if they can be confirmed, would be consistent with other results in this thesis, such as

the observed induction of methionine sulphoxide reductase relating to the wider evidence for Met roles in EW resistance.

4.4.7 Conclusions

Elucidating response mechanisms of food spoilage fungi to sanitisers can help to understand and predict the efficacy of treatments and can inform the rational development of the sanitiser technologies. In the present study, the early germination as well as the growth of *A. niger* spores into colonies were shown to be delayed by sub-lethal EW concentrations, and the spore-to-spore variation in germination and growth was increased. This has important implications for the validation of sanitising treatments, as the time of detectable growth may be shifted in treatment conditions relative to control conditions. In food surface sanitisation, for example, such effects may alter the time windows when it is most appropriate to sample and inspect produce for spoilage in assessing the success (or otherwise) of a treatment. The proposed accumulation of chloramines or other factors which result in the growth delay may help extend the shelf life of treated produce, and this is an important consideration when assessing alternative, non-chlorine sanitisers (such as ozonated water). The risk of by-product formation stemming from chlorine sanitisers motivates a move towards chlorine-free sanitisers, but the lack of chlorine species could affect and reduce the post-treatment inhibitory effect and reduce the shelf life of a product. The hypothesis of chloramine formation should be further investigated, e.g., by additional studies of the effect of chloramine treatments on the colony growth of *A. niger*, or by assessing the formation of chloramines using mass spectrometry (How et al., 2017). Experiments with filamentous fungi present technical challenges (e.g., regarding centrifugation issues) compared to unicellular organisms. To study the EW response of *A. niger* hyphae, microfluidic protocols should be adapted to help assess, for example, whether germ tube formation and hyphal growth (in addition

to early germination) are delayed and/or more variable after EW treatment, and whether vegetatively growing *A. niger* profits from Met pre-treatment prior to EW treatment, similar to vegetatively growing yeast.

5 Concluding remarks and future directions

Sanitisers and disinfectants are vital for reducing or removing the microbial load on food surfaces and food contact surfaces, to reduce both food spoilage and disease transmission through food, and the importance of effective sanitising and disinfecting has been brought into sharp focus by the Covid-19 pandemic (Fraser et al., 2021). This thesis focuses on applications of the sanitiser electrolysed water in the food industry, but many other industrial and household applications of sanitisers and disinfectants exist, underlining the importance of better understanding their efficacy and mode of action. The main advantage of EW compared to other products is that it can be produced on-site from simple ingredients, eliminating the need for transporting and storing concentrated solutions. One disadvantage of any chlorine-based sanitiser, besides potential regulatory restrictions, is the risk of inactivation by incidental organic matter or other non-target substances. Therefore, it is crucial to understand such inactivation mechanisms and the consequences for antimicrobial efficacy.

The results in Chapter 2 of this thesis demonstrated the benefits of a top-down approach to identify quenchers of EW fungicidal activity by studying chemical reactions partners of EW, starting from complex chemical matrices and narrowing down EW reactivity to specific organic molecules (proteins and amino acids). Interestingly, two separate assays showed differences in the reactivity of EW with specific amino acids (assays (i) and (ii): after mixing EW and amino acids, (i) the fungicidal activity of the mix was tested and (ii) the oxidising properties of EW were measured using the fluorescent probe APF). Cys and Met were the most efficient in inactivating the EW oxidising properties among the tested amino acids (assay ii) but Trp and Tyr were the most efficient at inactivating the fungicidal activity of EW (assay i). Reactions between certain amino acids and EW may yield inhibitory products, and this highlights the importance of antimicrobial efficacy

testing when assessing the consequences of EW reactivity with organic materials. For instance, methionine sulphone (MSO, a secondary oxidation product of Met) has antibacterial effects and whereas the formation of MSO in cells is not well studied, the presence of bacterial MSO-detoxifying proteins demonstrates the *in-vivo* relevance of this compound (Hentchel et al., 2015). Future work could focus on chemically identifying such proposed inhibitory products, e.g., by mass spectrometry (How et al., 2017) or NMR (Nagy and Ashby, 2005). All living organisms and many food products contain proteins (Slavin and Lloyd, 2012, Hoffman and Falvo, 2004), so the reactivity of EW with such compounds and potential by-product formation are important considerations for EW applications. Future work could aim to assess the reactivity of EW with other classes of biomolecules, e.g., lipids. Notably, the transcriptome analysis of EW-treated *A. niger* spores revealed the downregulation of lipid-metabolism genes, and whereas the mechanisms behind this observation are unclear, reactivity of certain lipids with EW cannot be ruled out. FAC reacts with unsaturated bonds in acyl chains of lipids and amino residues in polar head groups in certain phospholipids (Panasenko et al., 2013). Fatty acid oxidation products can cause off-flavours in food (Barden and Decker, 2016), which could be a concern for EW applications in the food industry. Moreover, the reactivity of FAC with amino sugars can result in the fragmentation of polysaccharides (Panasenko et al., 2013) and such reactivity (of EW) may be another interesting field of study and may also be relevant for the reactivity of EW with the fungal cell wall. Finally, the presence of antioxidants in different food products, e.g., in fruits and vegetables (Benzie and Choi, 2014) may represent a risk of EW inactivation, depending on the application process.

Because proteins and amino acids are abundant in all biological cells, reactivity of EW with such compounds is likely to affect the antimicrobial mode of action. The finding in Chapter 3 that increased cellular reduced-Met levels increased EW resistance of *S. cerevisiae*, potentially due to ROS and/or FAC scavenging by

accumulated Met molecules within cells, highlights the importance of understanding the chemical reactivities of EW for elucidating its antimicrobial mode of action. In future studies, the proposed intracellular Met oxidation should be further assessed, e.g., by measuring the accumulation and fate of Met within cells during EW treatments which may also help to further understand the link between oxidised-Met levels and FeS cluster protein damage, a link that has been published before and could also be observed for EW-induced damage in this thesis. Methods to address these questions could include measuring the cellular Met level and feeding labelled Met to allow microscopic or metabolic tracking, or making use of computational models that predict Met oxidation within molecules (Delmar et al., 2021). Recent advances in the identification of oxidised Met residues in the proteome of cells (Bettinger et al., 2020) could help to identify oxidation of protein-bound Met, thereby addressing the question whether EW-induced oxidation involves free or protein-bound Met, or both. Met-rich scavenger peptides for ROS or active chlorine species inactivation have been reported and can be analysed by polyacrylamide gel electrophoresis due to shifts in migration upon oxidation (Melnyk et al., 2015). Oxidation of Met residues can further regulate protein function in diverse species (Valverde et al., 2019) and potential EW-induced, Met-oxidation-mediated regulatory events could be the subject of future studies. The protective effect of Met pre-treatment could not be reproduced in *A. niger* spores in this thesis (tested in Chapter 4), but the methionine sulphoxide reduction system is widely conserved across fungi (Hage et al., 2021), suggesting that the proposed targeting of Met by EW may play a role in a range of food spoilage and other fungi. Importantly, a putative methionine sulphoxide reductase was upregulated in EW-treated *A. niger* (Chapter 4), suggesting that EW action in this fungus may also include Met oxidation. It would be interesting to study relevant enzymes in *A. niger*, e.g., by overexpression of Msr enzymes or also potential Rli1 orthologs (for some *Aspergillus* species including *A. fumigatus*,

A. oryzae and *A. flavus*, potential Rli1 orthologs are listed on FungiDB https://fungidb.org).

Chapter 4 also addressed an important aspect of microbial stress resistance, namely variability in the stress response. The finding that EW treatment can increase spore-spore heterogeneity and delay fungal outgrowth has important implications for the food industry and other potential EW applications, as such EW-induced effects might shift the time of detectable growth on food or other products post treatment. Therefore, growth delays and variation post-treatment are important considerations for risk assessments and probability-based spoilage modelling (Dagnas et al., 2017). Future studies could test whether growth delays and increased variation are induced by EW also in other relevant spoilage fungi, including wild isolates. Conidia on food (or other) surfaces are likely to originate from variable environments, so it would be beneficial to also test whether the conditions of spore formation (e.g., temperature, nutrients, conidial age) influence the described effects. The formation of inhibitory products from reactions between EW and organic substances, e.g., amino acids, was hypothesised in Chapter 2, and it was hypothesised further that such products, e.g., organic chloramines, may accumulate within spores during EW treatments and may result in the growth delay and increased variation. Initial experiments somewhat supported this hypothesis, but more work would be needed to identify such proposed organic chloramines and their effects. Fungicidal activity of organic chloramines or chloramides, e.g., chloramine T and N-chlorotaurine, against *Aspergillus* species has been demonstrated (Arnitz et al., 2009, Sheehan et al., 2019), but more research would be needed to link growth delays and increased phenotypic heterogeneity in fungi to such compounds. Understanding of these proposed post-treatment processes is important, as demonstrated by a study that reported chlorine treatment of outer fruit surfaces and subsequent exposure of the (diced) fruits to ascorbic acid (Moreira et al., 2017). Based on the data presented here,

such protocols may risk the (partial) inactivation of a post-treatment effect, and therefore may increase the risk of microbial survival.

Better understanding the reactivity of EW with organic compounds, the EW mode of action and the fungal response to EW can help to rationally develop EW applications and to improve EW formulations or treatment combinations, e.g., for hurdle treatment approaches (Oh et al., 2019). For instance, EW was successfully used to remove proteins from knife blades (Brasil et al., 2020), consistent with the high reactivity between EW and proteins shown here. A finding that EW treatment resulted in sub-lethally injured bacterial cells prompted the combination of EW with subsequent stress treatments and successfully increased the bacterial reduction (Han et al., 2018). Similarly, the growth delays in *A. niger* observed after EW treatment in the present study may suggest sub-lethal damage and subsequent treatments may increase the killing. Indeed, EW treatment followed by heat treatment resulted in lower growth than expected based on the product of the fractional growth from both individual stressors in *A. niger* (Chapter 2) and *S. cerevisiae* (Chapter 3). Many proteins are heat-sensitive and it is an intriguing possibility that EW-induced protein damage in spores or cells may increase protein heat sensitivity, but further studies would be needed to investigate such speculations, and testing heat treatment followed by EW treatment and the effect on protein stability may additionally be beneficial.

The results presented here can further contribute to predicting the antimicrobial efficacy of EW, including in the presence of organic substances. Such knowledge is especially relevant for application in parts of the world that lack widespread access to clean water resources, and such water scarcity is currently at risk of being exacerbated by factors like population growth and climate change (FAO, 2020). To further elucidate the fungal response to EW, especially with regards to filamentous fungi, novel techniques such as microfluidic systems should be further

developed, e.g., to study the hyphal development (and its delay/variation) after EW treatment. High-throughput studies such as transcriptomics could offer valuable insights, e.g., transcriptome studies in different fungal organisms with relevance to food applications, including wild isolates (Ellison et al., 2014), would allow the comparison of effects, for instance to investigate a potential conserved role of methionine sulphoxide reductases in the fungal EW response as hypothesised above.

Finally, it would be beneficial to test key effects of EW treatment in other fungal strains and species in addition to *A. niger* N402. This strain was obtained by UV mutagenesis and shows several genetic and phenotypic differences to its parent strain (wild type) N400, including reduced radial colony growth and conidiophore stalk length and differences in the production of certain degradative enzymes (Demirci et al., 2021). Especially the transcriptome analysis in Chapter 4 would have benefitted from using an *Aspergillus niger* strain with a reference genome available at the time of analysis. Other *Aspergilli* such as *A. flavus* and additional species such as *Penicillium* or *Fusarium* cause severe food losses and mycotoxin contaminations (1.2.3), so studying the effect of EW on such species would be of particular interest.

Bibliography

Abrashev, R. I., Pashova, S. B., Stefanova, L. N., Vassilev, S. V., Dolashka-Angelova, P. A. & Angelova, M. B. 2008. Heat-shock-induced oxidative stress and antioxidant response in *Aspergillus niger* 26. *Can. J. Microbiol.,* 54**,** 977-83.

Accensi, F., Cano, J., Figuera, L., Abarca, M. L. & Cabañes, F. J. 1999. New PCR method to differentiate species in the *Aspergillus niger* aggregate. *FEMS Microbiol. Lett.,* 180**,** 191-196.

Ackermann, M. 2015. A functional perspective on phenotypic heterogeneity in microorganisms. *Nat. Rev. Microbiol.,* 13**,** 497-508.

Afari, G. K. & Hung, Y.-C. 2018. A meta-analysis on the effectiveness of electrolyzed water treatments in reducing foodborne pathogens on different foods. *Food Control,* 93**,** 150-164.

Afshari, R. & Hosseini, H. 2013. Non-thermal plasma as a new food preservation method, its present and future prospect. *J. Paramed. Sci.,* 5**,** 116-120.

Aguirre, J., Hansberg, W. & Navarro, R. 2006. Fungal responses to reactive oxygen species. *Med. Mycol.,* 44**,** S101-S107.

Al-Haq, M. I., Sugiyama, J. & Isobe, S. 2005. Applications of electrolyzed water in agriculture & food industries. *J. Food Sci. Technol.,* 11**,** 135-150.

Albrich, J. M., McCarthy, C. A. & Hurst, J. K. 1981. Biological reactivity of hypochlorous acid: implications for microbicidal mechanisms of leukocyte myeloperoxidase. *Proc. Natl. Acad. Sci. USA,* 78**,** 210-214.

Alhebshi, A. 2014. The essential iron-sulphur protein Rli1 is a key determinant of oxidative stress resistance in *Saccharomyces cerevisiae*. *School of Biology, University of Nottingham,* PhD Thesis, Nottingham, UK**,** 160-172.

Alhebshi, A., Sideri, T. C., Holland, S. L. & Avery, S. V. 2012. The essential iron-sulfur protein Rli1 is an important target accounting for inhibition of cell growth by reactive oxygen species. *Mol. Biol. Cell,* 23**,** 3582-3590.

Ali, A., Yeoh, W. K., Forney, C. & Siddiqui, M. W. 2018. Advances in postharvest technologies to extend the storage life of minimally processed fruits and vegetables. *Crit. Rev. Food Sci. Nutr.,* 58**,** 2632-2649.

Allu, P. K., Marada, A., Boggula, Y., Karri, S., Krishnamoorthy, T. & Sepuri, N. B. V. 2015. Methionine sulfoxide reductase 2 reversibly regulates Mge1, a cochaperone of mitochondrial Hsp70, during oxidative stress. *Mol. Biol. Cell,* 26**,** 406-419.

Alshehri, B. & Palanisamy, M. 2020. Evaluation of molecular identification of *Aspergillus* species causing fungal keratitis. *Saudi J. Biol. Sci.,* 27**,** 751-756.

Altamura, E., Borgatti, M., Finotti, A., Gasparello, J., Gambari, R., Spinelli, M., Castaldo, R. & Altamura, N. 2016. Chemical-induced read-through at premature termination codons determined by a rapid dual-fluorescence system based on *S. cerevisiae*. *PLOS ONE,* 11**,** e0154260.

Amich, J., Schafferer, L., Haas, H. & Krappmann, S. 2013. Regulation of sulphur assimilation is essential for virulence and affects Iron homeostasis of the human-pathogenic mould *Aspergillus fumigatus*. *PLoS Pathog.,* 9**,** e1003573.

Amiri, F., Mesquita, M. M. F. & Andrews, S. A. 2010. Disinfection effectiveness of organic chloramines, investigating the effect of pH. *Water Res.,* 44**,** 845-853.

Anders, S., Pyl, P. T. & Huber, W. 2015. HTSeq--a Python framework to work with high-throughput sequencing data. *Bioinformatics,* 31**,** 166-9.

Andersen, B., Smedsgaard, J. & Frisvad, J. C. 2004. *Penicillium expansum*: consistent production of patulin, chaetoglobosins, and other secondary

metabolites in culture and their natural occurrence in fruit products. *J. Agric. Food Chem.,* 52**,** 2421-8.

Anderson, N. M., Larkin, J. W., Cole, M. B., Skinner, G. E., Whiting, R. C., Gorris, L. G., Rodriguez, A., Buchanan, R., Stewart, C. M., Hanlin, J. H., Keener, L. & Hall, P. A. 2011. Food safety objective approach for controlling *Clostridium botulinum* growth and toxin production in commercially sterile foods. *J. Food Prot.,* 74**,** 1956-89.

Angelova, M. B., Pashova, S. B., Spasova, B. K., Vassilev, S. V. & Slokoska, L. S. 2005. Oxidative stress response of filamentous fungi induced by hydrogen peroxide and paraquat. *Mycol. Res.,* 109**,** 150-8.

Arnhold, J., Mueller, S., Arnold, K. & Sonntag, K. 1993. Mechanisms of inhibition of chemiluminescence in the oxidation of luminol by sodium hypochlorite. *J. Biolumin. Chemilumin.,* 8**,** 307-313.

Arnitz, R., Nagl, M. & Gottardi, W. 2009. Microbicidal activity of monochloramine and chloramine T compared. *J. Hosp. Infect.,* 73**,** 164-170.

Artés, F., Gómez, P., Aguayo, E., Escalona, V. & Artés-Hernández, F. 2009. Sustainable sanitation techniques for keeping quality and safety of fresh-cut plant commodities. *Postharvest Biol. Technol.,* 51**,** 287-296.

Aruscavage, D., Lee, K., Miller, S. & LeJeune, J. T. 2006. Interactions affecting the proliferation and control of human pathogens on edible plants. *J. Food Sci.,* 71**,** R89-R99.

Ashu, E. E., Korfanty, G. A., Samarasinghe, H., Pum, N., You, M., Yamamura, D. & Xu, J. 2018. Widespread amphotericin B-resistant strains of *Aspergillus fumigatus* in Hamilton, Canada. *Infect. Drug Resist.,* 11**,** 1549-1555.

Asplund, J. & Wardle, D. A. 2017. How lichens impact on terrestrial community and ecosystem properties. *Biol. Rev. Camb. Philos. Soc.,* 92**,** 1720-1738.

Avery, A. M. & Avery, S. V. 2001. *Saccharomyces cerevisiae* expresses three phospholipid hydroperoxide glutathione peroxidases. *J. Biol. Chem.,* 276**,** 33730-5.

Avery, S. V. 2005. Phenotypic diversity and fungal fitness. *Mycologist,* 19**,** 74-80.

Avery, S. V. 2006. Microbial cell individuality and the underlying sources of heterogeneity. *Nat. Rev. Microbiol.,* 4**,** 577-587.

Avery, S. V. 2011. Molecular targets of oxidative stress. *Biochem. J.,* 434**,** 201-210.

Baggio, A., Marino, M., Innocente, N., Celotto, M. & Maifreni, M. 2020. Antimicrobial effect of oxidative technologies in food processing: an overview. *Eur. Food Res. and Technol.,* 246**,** 669-692.

Baker, S. E. 2006. *Aspergillus niger* genomics: past, present and into the future. *Med. Mycol.,* 44**,** S17-S21.

Baraibar, M. A., Ladouce, R. & Friguet, B. 2013. Proteomic quantification and identification of carbonylated proteins upon oxidative stress and during cellular aging. *J. Proteomics,* 92**,** 63-70.

Barden, L. & Decker, E. A. 2016. Lipid oxidation in low-moisture food: a review. *Crit. Rev. Food Sci. Nutr.,* 56**,** 2467-2482.

Barkai-Golan, R. 2008a. Chapter 6 - *Aspergillus* mycotoxins. *In:* Barkai-Golan, R. & Paster, N. (eds.) *Mycotoxins in Fruits and Vegetables.* San Diego: Academic Press.

Barkai-Golan, R. 2008b. Chapter 7 - *Penicillium* mycotoxins. *In:* Barkai-Golan, R. & Paster, N. (eds.) *Mycotoxins in Fruits and Vegetables.* San Diego: Academic Press.

Barkai-Golan, R. 2008c. Chapter 8 - *Alternaria* mycotoxins. *In:* Barkai-Golan, R. & Paster, N. (eds.) *Mycotoxins in Fruits and Vegetables.* San Diego: Academic Press.

Bastarrachea, L. J., Alborzi, S. & Tikekar, R. V. 2019. Chapter 12 - Control strategies for postharvest microbiological safety of produce during processing, marketing, and quality measures. *In:* Biswas, D. & Micallef, S.

A. (eds.) *Safety and Practice for Organic Food.* London, UK: Academic Press.
Beare, J. A., Archer, S. A. & Bell, J. N. B. 1999. *Marssonina* leafspot disease of poplar under elevated ozone: pre-fumigated host and in vitro studies. *Environ. Pollut.,* 105**,** 409-417.
Beinert, H., Kennedy, M. C. & Stout, C. D. 1996. Aconitase as iron-sulfur protein, enzyme, and iron-regulatory protein. *Chem. Rev.,* 96**,** 2335-2374.
Ben-Asher, R. & Lahav, O. 2016. Electrooxidation for simultaneous ammonia control and disinfection in seawater recirculating aquaculture systems. *Aquac. Eng.,* 72-73**,** 77-87.
Benjamini, Y. & Hochberg, Y. 1995. Controlling the false discovery rate: a practical and powerful approach to multiple testing. *J. Royal Statist. Soc. (B, Methodol.),* 57**,** 289-300.
Benjamini, Y., Krieger, A. M. & Yekutieli, D. 2006. Adaptive linear step-up procedures that control the false discovery rate. *Biometrika,* 93**,** 491-507.
Benzie, I. F. F. & Choi, S.-W. 2014. Chapter one - Antioxidants in food: content, measurement, significance, action, cautions, caveats, and research needs. *In:* Henry, J. (ed.) *Advances in Food and Nutrition Research.* Waltham, MA: Academic Press.
Bernat, M., Segarra, J., Casals, C., Torres, R., Teixidó, N. & Usall, J. 2017. Identification of fungal population in the environment and on surfaces of stone fruit packinghouses. *Eur. J. Plant Pathol.,* 148**,** 723-731.
Berns, A. E., Philipp, H., Narres, H. D., Burauel, P., Vereecken, H. & Tappe, W. 2008. Effect of gamma-sterilization and autoclaving on soil organic matter structure as studied by solid state NMR, UV and fluorescence spectroscopy. *Eur. J. Soil Sci.,* 59**,** 540-550.
Berry, D., Xi, C. & Raskin, L. 2009. Effect of growth conditions on inactivation of *Escherichia coli* with monochloramine. *Environ. Sci. Technol.,* 43**,** 884-889.
Bettinger, J. Q., Welle, K. A., Hryhorenko, J. R. & Ghaemmaghami, S. 2020. Quantitative analysis of *in vivo* methionine oxidation of the human proteome. *J. Proteome Res.,* 19**,** 624-633.
Beuchat, L. R. 1999. Survival of enterohemorrhagic *Escherichia coli* O157:H7 in bovine feces applied to lettuce and the effectiveness of chlorinated water as a disinfectant. *J. Food Prot.,* 62**,** 845-9.
Bhilwadikar, T., Pounraj, S., Manivannan, S., Rastogi, N. K. & Negi, P. S. 2019. Decontamination of microorganisms and pesticides from fresh fruits and vegetables: a comprehensive review from common household processes to modern techniques. *Compr. Rev. Food Sci. Food Saf.,* 18**,** 1003-1038.
Bin, P., Huang, R. & Zhou, X. 2017. Oxidation resistance of the sulfur amino acids: methionine and cysteine. *Biomed. Res. Int.,* 2017**,** 9584932.
Bing, S., Zang, Y. T., Li, Y. J. & Shu, D. Q. 2019. The synergistic effects of slightly acidic electrolyzed water and UV-C light on the inactivation of *Salmonella* Enteritidis on contaminated eggshells. *Poult. Sci.,* 98**,** 6914-6920.
Blackburn, C. d. W. 2006. *Food Spoilage Microorganisms,* Cambridge, UK, CRC Press, Woodhead Publishing Limited.
Blaiseau, P. L., Lesuisse, E. & Camadro, J. M. 2001. Aft2p, a novel iron-regulated transcription activator that modulates, with Aft1p, intracellular iron use and resistance to oxidative stress in yeast. *J. Biol. Chem.,* 276**,** 34221-6.
Bleichrodt, R.-J., Foster, P., Howell, G., Latgé, J.-P., Read, N. D. & Goldman, G. H. 2020. Cell wall composition heterogeneity between single cells in *Aspergillus fumigatus* leads to heterogeneous behavior during antifungal treatment and phagocytosis. *mBio,* 11**,** e03015-19.
Bleichrodt, R.-J., Hulsman, M., Wösten, H. A. B., Reinders, M. J. T., Fischer, R. & Turgeon, B. G. 2015. Switching from a unicellular to multicellular organization in an *Aspergillus niger* hypha. *mBio,* 6**,** e00111-15.
Bleichrodt, R.-J., van Veluw, G. J., Recter, B., Maruyama, J.-i., Kitamoto, K. & Wösten, H. A. B. 2012. Hyphal heterogeneity in *Aspergillus oryzae* is the

result of dynamic closure of septa by Woronin bodies. *Mol. Microbiol.,* 86**,** 1334-1344.

Bleichrodt, R.-J., Vinck, A., Krijgsheld, P., van Leeuwen, M. R., Dijksterhuis, J. & Wösten, H. A. B. 2013. Cytosolic streaming in vegetative mycelium and aerial structures of *Aspergillus niger*. *Stud. Mycol.,* 74**,** 31-46.

Block, S. S. 2001. *Disinfection, Sterilization and Preservation,* Philadelphia, PA, Lippincott Williams & Wilkins.

Bodas, R., Bartolome, D. J., Tabernero De Paz, M. J., Posado, R., Garcia, J. J., Rodriguez, L., Olmedo, S. & Martin-Diana, A. B. 2013. Electrolyzed water as novel technology to improve hygiene of drinking water for dairy ewes. *Res. Vet. Sci.,* 95**,** 1169-70.

Bodet, C., Sahr, T., Dupuy, M., Buchrieser, C. & Héchard, Y. 2012. *Legionella pneumophila* transcriptional response to chlorine treatment. *Water Res.,* 46**,** 808-816.

Boiteux, S., Coste, F. & Castaing, B. 2017. Repair of 8-oxo-7,8-dihydroguanine in prokaryotic and eukaryotic cells: properties and biological roles of the Fpg and OGG1 DNA N-glycosylases. *Free Radic. Biol. Med.,* 107**,** 179-201.

Bonde, M. R., Nester, S. E., Khayat, A., Smilanick, J. L., Frederick, R. D. & Schaad, N. W. 1999. Comparison of effects of acidic electrolyzed water and NaOCl on *Tilletia indica* teliospore germination. *Plant Dis.,* 83**,** 627-632.

Bongomin, F., Gago, S., Oladele, R. O. & Denning, D. W. 2017. Global and multi-national prevalence of fungal diseases-estimate precision. *J. Fungi (Basel),* 3**,** 57.

Boyce, J. M. 2016. Modern technologies for improving cleaning and disinfection of environmental surfaces in hospitals. *Antimicrob. Resist. Infect. Control,* 5**,** 10.

Brackett, R. E. 1987. Microbiological consequences of minimally processed fruits and vegetables. *J. Food Qual.,* 10**,** 195-206.

Bradford, W. L. 2011. The differences between on-site generated mixed-oxidant solution and sodium hypochlorite (aka the master features summary). *MIOX Master Features Summary (online).* https://www.google.com/url?sa=t&rct=j&q=&esrc=s&source=web&cd=&cad=rja&uact=8&ved=2ahUKEwi18_as4svyAhWMOcAKHcq_CLsQFnoECAQQAQ&url=http%3A%2F%2Fcdn2.hubspot.net%2Fhub%2F312816%2Ffile-357588552-pdf%2FDownloads%2Ftechnicaldownloads%2FMaster_Feat&usg=AOvVaw244HZB3ppBOPmYBdKWhUwU accessed January 2021.

Brasil, C. C. B., de Menezes, C. R., Jacob-Lopes, E., Barin, J. S., Zepka, L. Q., Campagnol, P. C. B., Wagner, R. & Cichoski, A. J. 2020. Combined application of electrolysed water and ultrasound to improve the sanitation of knives in the meat industry. *Int. J. Food Sci. Technol.,* 55**,** 1136-1144.

Braymer, J. J. & Lill, R. 2017. Iron-sulfur cluster biogenesis and trafficking in mitochondria. *J. Biol. Chem.,* 292**,** 12754-12763.

Breitenbach, M., Weber, M., Rinnerthaler, M., Karl, T. & Breitenbach-Koller, H. 2015. Oxidative stress in fungi: its function in signal transduction, interaction with plant hosts, and lignocellulose degradation. *Biomolecules,* 5**,** 318-42.

Bridge, P. & Spooner, B. 2001. Soil fungi: diversity and detection. *Plant Soil,* 232**,** 147-154.

Brock, M., Maerker, C., Schütz, A., Völker, U. & Buckel, W. 2002. Oxidation of propionate to pyruvate in *Escherichia coli*. Involvement of methylcitrate dehydratase and aconitase. *Eur. J. Biochem.,* 269**,** 6184-94.

Brodowska, A. J., Nowak, A. & Śmigielski, K. 2018. Ozone in the food industry: principles of ozone treatment, mechanisms of action, and applications: an overview. *Crit. Rev. Food Sci. Nutr.,* 58**,** 2176-2201.

Brot, N., Weissbach, L., Werth, J. & Weissbach, H. 1981. Enzymatic reduction of protein-bound methionine sulfoxide. *Proc. Natl. Acad. Sci. USA,* 78**,** 2155-2158.

Buck, J. W., van Iersel, M. W., Oetting, R. D. & Hung, Y.-C. 2002. *In vitro* fungicidal activity of acidic electrolyzed oxidizing water. *Plant Dis.,* 86**,** 278-281.

Bugener, E., Kump, A. W., Casteel, M. & Klein, G. 2014. Benefits of neutral electrolyzed oxidizing water as a drinking water additive for broiler chickens. *Poult Sci.,* 93**,** 2320-6.

Burger, R. 2012. EHEC O104:H4 in Germany 2011: large outbreak of bloody diarrhea and haemolytic uraemic syndrome by shiga toxin-producting *E. coli* via contaminated food. *In:* US Institute of Medicine (ed.). *Improving Food Safety Through a One Health Approach: Workshop Summary.* Washington, DC: National Academics Press (US).

Butler, M. J. & Day, A. W. 1998. Fungal melanins: a review. *Can. J. Microbiol.,* 44**,** 1115-1136.

Cabañes, F. J., Accensi, F., Bragulat, M. R., Abarca, M. L., Castellá, G., Minguez, S. & Pons, A. 2002. What is the source of ochratoxin A in wine? *Int. J. Food Microbiol.,* 79**,** 213-215.

Cai, Z., Wei, Q., Li, X., Luan, Y. & Dong, S. 2020. Chemical syntheses and biological evaluation of CXCL14 and its site-selectively modified methionine sulfoxide-containing derivatives. *J. Org. Chem.,* 85**,** 1740-1747.

Cao, W., Zhu, Z. W., Shi, Z. X., Wang, C. Y. & Li, B. M. 2009. Efficiency of slightly acidic electrolyzed water for inactivation of *Salmonella* Enteritidis and its contaminated shell eggs. *Int. J. Food Microbiol.,* 130**,** 88-93.

Cao, Z., Mitchell, L., Hsia, O., Scarpa, M., Caldwell, S. T., Alfred, A. D., Gennaris, A., Collet, J. F., Hartley, R. C. & Bulleid, N. J. 2018. Methionine sulfoxide reductase B3 requires resolving cysteine residues for full activity and can act as a stereospecific methionine oxidase. *Biochem. J.,* 475**,** 827-838.

Carr, A. C., Tijerina, T. & Frei, B. 2000. Vitamin C protects against and reverses specific hypochlorous acid- and chloramine-dependent modifications of low-density lipoprotein. *Biochem. J.,* 346**,** 491-499.

Carrasco, G. & Urrestarazu, M. 2010. Green chemistry in protected horticulture: the use of peroxyacetic acid as a sustainable strategy. *Int. J. Mol. Sci.,* 11**,** 1999-2009.

Ceragioli, M., Mols, M., Moezelaar, R., Ghelardi, E., Senesi, S. & Abee, T. 2010. Comparative transcriptomic and phenotypic analysis of the responses of *Bacillus cereus* to various disinfectant treatments. *Appl. Environ. Microbiol.,* 76**,** 3352-3360.

Cerioni, L., Rapisarda, V. A., Hilal, M., Prado, F. E. & Rodriguez-Montelongo, L. 2009. Synergistic antifungal activity of sodium hypochlorite, hydrogen peroxide, and cupric sulfate against *Penicillium digitatum*. *J. Food Prot.,* 72**,** 1660-1665.

Cerqueira, G. C., Arnaud, M. B., Inglis, D. O., Skrzypek, M. S., Binkley, G., Simison, M., Miyasato, S. R., Binkley, J., Orvis, J., Shah, P., Wymore, F., Sherlock, G. & Wortman, J. R. 2014. The *Aspergillus* Genome Database: multispecies curation and incorporation of RNA-Seq data to improve structural gene annotations. *Nucleic Acids Res.,* 42**,** D705-10.

Chacón, J. M., Möbius, W. & Harcombe, W. R. 2018. The spatial and metabolic basis of colony size variation. *ISME J.,* 12**,** 669-680.

Chang, R. L., Stanley, J. A., Robinson, M. C., Sher, J. W., Li, Z., Chan, Y. A., Omdahl, A. R., Wattiez, R., Godzik, A. & Matallana-Surget, S. 2020. Protein structure, amino acid composition and sequence determine proteome vulnerability to oxidation-induced damage. *EMBO J.,* 39**,** e104523.

Charles, M. T. & Arul, J. 2007. UV treatment of fresh fruits and vegetables for improved quality: a status report. *Stewart Postharvest Rev.,* 3**,** 1-8.

Chen, S., Rillig, M. C. & Wang, W. 2009. Improving soil protein extraction for metaproteome analysis and glomalin-related soil protein detection. *Proteomics,* 9**,** 4970-4973.

Chen, X., Xue, S. J., Shi, J., Kostrzynska, M., Tang, J., Guévremont, E., Villeneuve, S. & Mondor, M. 2018. Red cabbage washing with acidic electrolysed water: effects on microbial quality and physicochemical properties. *Food Qual. Saf.,* 2**,** 229-237.

Clayton, G. E., Thorn, R. M. S. & Reynolds, D. M. 2019. Comparison of trihalomethane formation using chlorine-based disinfectants within a model system; applications within point-of-use drinking water treatment. *Front. Environ. Sci.,* 7**,** 35.

Cravero, F., Englezos, V., Rantsiou, K., Torchio, F., Giacosa, S., Río Segade, S., Gerbi, V., Rolle, L. & Cocolin, L. 2018. Control of *Brettanomyces bruxellensis* on wine grapes by post-harvest treatments with electrolyzed water, ozonated water and gaseous ozone. *Innov. Food Sci. Emerg. Technol.,* 47**,** 309-316.

D'Aoust, J. Y., Park, C. E., Szabo, R. A., Todd, E. C. D., Emmons, D. B. & McKellar, R. C. 1988. Thermal inactivation of *Campylobacter* species, *Yersinia enterocolitica*, and hemorrhagic *Escherichia coli* 0157:H7 in fluid milk. *J. Dairy Sci.,* 71**,** 3230-3236.

Dagnas, S., Gougouli, M., Onno, B., Koutsoumanis, K. P. & Membré, J.-M. 2017. Quantifying the effect of water activity and storage temperature on single spore lag times of three moulds isolated from spoiled bakery products. *Int. J. Food Microbiol.,* 240**,** 75-84.

Daly, P., Peng, M., Mitchell, H. D., Kim, Y. M., Ansong, C., Brewer, H., de Gijsel, P., Lipton, M. S., Markillie, L. M., Nicora, C. D., Orr, G., Wiebenga, A., Hildén, K. S., Kabel, M. A., Baker, S. E., Mäkelä, M. R. & de Vries, R. P. 2020. Colonies of the fungus *Aspergillus niger* are highly differentiated to adapt to local carbon source variation. *Environ. Microbiol.,* 22**,** 1154-1166.

Davies, M. J. 2005. The oxidative environment and protein damage. *Biochim. Biophys. Acta Proteins Proteom.,* 1703**,** 93-109.

Degala, H. L., Scott, J. R., Espinoza, F. I. R., Mahapatra, A. K. & Kannan, G. 2020. Synergistic effect of ozonated and electrolyzed water on the inactivation kinetics of *Escherichia coli* on goat meat. *J. Food Saf.,* 40**,** e12740.

Delaye, L., Becerra, A., Orgel, L. & Lazcano, A. 2007. Molecular evolution of peptide methionine sulfoxide reductases (MsrA and MsrB): on the early development of a mechanism that protects against oxidative damage. *J. Mol. Evol.,* 64**,** 15-32.

Delmar, J. A., Buehler, E., Chetty, A. K., Das, A., Quesada, G. M., Wang, J. & Chen, X. 2021. Machine learning prediction of methionine and tryptophan photooxidation susceptibility. *Mol. Ther. Methods Clin. Dev.,* 21**,** 466-477.

Demirci, A., Feng, H. & Krishnamurthy, K. 2020. *Food Safety Engineering.,* Cham, Switzerland, Springer International Publishing.

Demirci, E., Arentshorst, M., Yilmaz, B., Swinkels, A., Reid, I. D., Visser, J., Tsang, A. & Ram, A. F. J. 2021. Genetic characterization of mutations related to conidiophore stalk length development in *Aspergillus niger* laboratory strain N402. *Front. Genet.,* 12**,** 666684.

Deng, L.-Z., Mujumdar, A. S., Pan, Z., Vidyarthi, S. K., Xu, J., Zielinska, M. & Xiao, H.-W. 2019. Emerging chemical and physical disinfection technologies of fruits and vegetables: a comprehensive review. *Crit. Rev. Food Sci. Nutr.,* 60**,** 2481-2508.

Devi, P. & Dalai, A. K. 2021. Implications of breakpoint chlorination on chloramines decay and disinfection by-products formation in brine solution. *Desalination,* 504**,** 114961.

Devi, Y., Thirumdas, R., Sarangapani, C., Deshmukh, R. R. & Annapure, U. S. 2017. Influence of cold plasma on fungal growth and aflatoxins production on groundnuts. *Food Control,* 77**,** 187-191.

Deza, M. A., Araujo, M. & Garrido, M. J. 2005. Inactivation of *Escherichia coli*, *Listeria monocytogenes*, *Pseudomonas aeruginosa* and *Staphylococcus aureus* on stainless steel and glass surfaces by neutral electrolysed water. *Lett. Appl. Microbiol.,* 40**,** 341-346.

Deza, M. A., Araujo, M. & Garrido, M. J. 2007. Efficacy of neutral electrolyzed water to inactivate *Escherichia coli*, *Listeria monocytogenes*, *Pseudomonas aeruginosa*, and *Staphylococcus aureus* on plastic and wooden kitchen cutting boards. *J. Food Prot.,* 70**,** 102-8.

Dhall, R. K. 2013. Advances in edible coatings for fresh fruits and vegetables: a review. *Crit. Rev. Food Sci. Nutr.,* 53**,** 435-50.

Dighton, J. 2016. *Fungi in Ecosystem Processes,* Boca Raton, FL, CRC Press, Taylor & Francis Group, LLC.

Dijksterhuis, J. 2007. Heat-resistant ascospores. *In:* Dijksterhuis, J. & Samson, R. A. (eds.) *Food Mycology: A Multifaceted Approach to Fungi and Food.* 1 ed. Boca Raton: CRC Press.

Dijksterhuis, J. 2017. The fungal spore and food spoilage. *Curr. Opin. Food Sci.,* 17**,** 68-74.

Dijksterhuis, J. 2019. Fungal spores: highly variable and stress-resistant vehicles for distribution and spoilage. *Food Microbiol.,* 81**,** 2-11.

Ding, T. & Liao, X. 2019. Decontamination efficacy and principles of electrolyzed water. *In:* Ding, T., Oh, D.-H. & Liu, D. (eds.) *Electrolyzed Water in Food: Fundamentals and Applications.* Singapore: Springer Singapore.

Ding, T., Rahman, S. M. E. & Oh, D.-H. 2011. Inhibitory effects of low concentration electrolyzed water and other sanitizers against foodborne pathogens on oyster mushroom. *Food Control,* 22**,** 318-322.

Donnermair, M. M. & Blatchley, E. R. 2003. Disinfection efficacy of organic chloramines. *Water Res.,* 37**,** 1557-1570.

Drazic, A., Miura, H., Peschek, J., Le, Y., Bach, N. C., Kriehuber, T. & Winter, J. 2013. Methionine oxidation activates a transcription factor in response to oxidative stress. *Proc. Natl. Acad. Sci. USA,* 110**,** 9493.

Duan, D., Liu, G., Yao, P. & Wang, H. 2016. The effects of organic compounds on inactivation efficacy of *Artemia salina* by neutral electrolyzed water. *Ocean Eng.,* 125**,** 31-37.

Duarte-Molina, F., Gómez, P. L., Castro, M. A. & Alzamora, S. M. 2016. Storage quality of strawberry fruit treated by pulsed light: fungal decay, water loss and mechanical properties. *Innov. Food Sci. Emerg. Technol.,* 34**,** 267-274.

Dukan, S. & Touati, D. 1996. Hypochlorous acid stress in *Escherichia coli*: resistance, DNA damage, and comparison with hydrogen peroxide stress. *J. Bacteriol.,* 178**,** 6145-50.

Dusny, C. & Schmid, A. 2015. Microfluidic single-cell analysis links boundary environments and individual microbial phenotypes. *Environ. Microbiol.,* 17**,** 1839-1856.

Ellena, V., Sauer, M. & Steiger, M. G. 2020. The fungal sexual revolution continues: discovery of sexual development in members of the genus *Aspergillus* and its consequences. *Fungal Biol. Biotechnol.,* 7**,** 17.

Ellison, C. E., Kowbel, D., Glass, N. L., Taylor, J. W. & Brem, R. B. 2014. Discovering functions of unannotated genes from a transcriptome survey of wild fungal isolates. *mBio,* 5**,** e01046.

Emri, T., Szarvas, V., Orosz, E., Antal, K., Park, H., Han, K.-H., Yu, J.-H. & Pócsi, I. 2015. Core oxidative stress response in *Aspergillus nidulans*. *BMC Genomics,* 16**,** 478.

Ersoy, Z. G., Dinc, O., Cinar, B., Gedik, S. T. & Dimoglo, A. 2019. Comparative evaluation of disinfection mechanism of sodium hypochlorite, chlorine dioxide and electroactivated water on *Enterococcus faecalis*. *LWT-Food Sci. Technol.,* 102**,** 205-213.

EU 1998. Council directive 98/83/EC on the quality of water intended for human consumption (CELEX31998L0083). *Official Journal,* L 330**,** 32-54.

EU 2020a. Commission regulation (EU) 2020/749 amending Annex III to Regulation (EC) No 396/2005 of the European Parliament and of the Council as regards maximum residue levels for chlorate in or on certain products. *Official Journal,* L 178**,** 7-20.

EU 2020b. Proposal for a directive of the European parliament and of the council on the quality of water intended for human consumption (recast) - Political agreement. *Publications Office EU,* 6060/1/20 REV 1**,** 1-110.

Eustice, R. F. 2018. Global status and commercial applications of food irradiation. *In:* Ferreira, I. C. F. R., Antonio, A. L. & Cabo Verde, S. (eds.) *Food Irradiation Technologies: Concepts, Applications and Outcomes.* Croydon, UK: The Royal Society of Chemistry.

Everette, J. D., Bryant, Q. M., Green, A. M., Abbey, Y. A., Wangila, G. W. & Walker, R. B. 2010. Thorough study of reactivity of various compound classes toward the Folin−Ciocalteu reagent. *J. Agric. Food Chem.,* 58**,** 8139-8144.

Fakruddin, M., Chowdhury, A., Hossain, M. N. & Ahmed, M. M. 2015. Characterization of aflatoxin producing *Aspergillus flavus* from food and feed samples. *SpringerPlus,* 4**,** 159.

FAO 2011. Global food losses and food waste - extent, causes and prevention. *In:* Gustavsson, J., Cederberg, C., Sonesson, U., van Otterdijk, R. & Meybeck, A. (eds.) *Study conducted for the International Congress SAVE FOOD!, Interpack2011, Düsseldorf.* Rome, Italy.

FAO 2019. The state of food and agriculture 2019. Moving forward on food loss and waste reduction. Rome, Italy: Licence CC BY-NC-SA 3.0 IGO.

FAO 2020. The state of food and agriculture 2020. Overcoming water challenges in agriculture. Rome, Italy: Licence CC BY-NC-SA 3.0 IGO.

FAO, IFAC, UNICEF, WFP & WHO 2017. The state of food security and nutrition in the world 2017. Building resilience for peace and food security. *FAO (ed.),* Rome, Italy.

Fazius, F., Shelest, E., Gebhardt, P. & Brock, M. 2012. The fungal α-aminoadipate pathway for lysine biosynthesis requires two enzymes of the aconitase family for the isomerization of homocitrate to homoisocitrate. *Mol. Microbiol.,* 86**,** 1508-1530.

FDA 1998. Guidance for industry. Guide to minimize microbial food safety hazards for fresh fruits and vegetables. Washington, DC: U.S. Department of Health and Human Services, Food and Drug Administration, Center for Food Safety and Applied Nutrition (CFSAN).

FDA 2001. 21 CFR Part 173: Secondary direct food additives permitted in food for human consumption. §173.368. *e-CFR (online).* https://www.ecfr.gov/cgi-bin/retrieveECFR?gp=1&SID=f4a5e3158d923a799dbeba14976553dc&ty=HTML&h=L&mc=true&r=SECTION&n=se21.3.173_1368 accessed March 2021.

FDA 2019. 21 CFR Part 178: Indirect food additives: adjuvants, production aids, and sanitizers. §178.1010. *e-CFR (online).* https://www.ecfr.gov/cgi-bin/text-idx?SID=838e6233bc6ebeae32a63704f0109b00&mc=true&node=pt21.3.178&rgn=div5#se21.3.178_11010 accessed March 2021.

Fedorova, M., Bollineni, R. C. & Hoffmann, R. 2014. Protein carbonylation as a major hallmark of oxidative damage: update of analytical strategies. *Mass Spectrom. Rev.,* 33**,** 79-97.

Ferecatu, I., Gonçalves, S., Golinelli-Cohen, M.-P., Clémancey, M., Martelli, A., Riquier, S., Guittet, E., Latour, J.-M., Puccio, H., Drapier, J.-C., Lescop, E. & Bouton, C. 2014. The diabetes drug target MitoNEET governs a novel trafficking pathway to rebuild an Fe-S cluster into cytosolic aconitase/iron regulatory protein 1. *J. Biol. Chem.,* 289**,** 28070-28086.

Fernández-Niño, M., Pulido, S., Stefanoska, D., Pérez, C., González-Ramos, D., van Maris, A. J. A., Marchal, K., Nevoigt, E. & Swinnen, S. 2018. Identification of novel genes involved in acetic acid tolerance of

Saccharomyces cerevisiae using pooled-segregant RNA sequencing. *FEMS Yeast Res.,* 18.
Ferrier, P. 2010. Irradiation as a quarantine treatment. *Food Policy,* 35**,** 548-555.
Filtenborg, O., Frisvad, J. C. & Thrane, U. 1996. Moulds in food spoilage. *Int. J. Food Microbiol.,* 33**,** 85-102.
Fischer, G., Liti, G. & Llorente, B. 2020. The budding yeast life cycle: more complex than anticipated? *Yeast,* 38**,** 5-11.
Flemmig, J., Zschaler, J., Remmler, J. & Arnhold, J. 2012. The fluorescein-derived dye aminophenyl fluorescein is a suitable tool to detect hypobromous acid (HOBr)-producing activity in eosinophils. *J. Biol. Chem.,* 287**,** 27913-27923.
Folkes, L. K., Candeias, L. P. & Wardman, P. 1995. Kinetics and mechanisms of hypochlorous acid reactions. *Arch. Biochem. Biophys.,* 323**,** 120-126.
Foster, D. S. 2019. Changes in phenotypic heterogeneity as an adaptation of fungi to environmental stress. *School of Life Sciences, University of Nottingham,* PhD Thesis, Nottingham, UK**,** 104-108.
Fountain, J. C., Bajaj, P., Nayak, S. N., Yang, L., Pandey, M. K., Kumar, V., Jayale, A. S., Chitikineni, A., Lee, R. D., Kemerait, R. C., Varshney, R. K. & Guo, B. 2016a. Responses of *Aspergillus flavus* to oxidative stress are related to fungal development regulator, antioxidant enzyme, and secondary metabolite biosynthetic gene expression. *Front. Microbiol.,* 7.
Fountain, J. C., Bajaj, P., Pandey, M. K., Nayak, S. N., Yang, L., Kumar, V., Jayale, A. S., Chitikineni, A., Zhuang, W., Scully, B. T., Lee, R. D., Kemerait, R. C., Varshney, R. K. & Guo, B. 2016b. Oxidative stress and carbon metabolism influence *Aspergillus flavus* transcriptome composition and secondary metabolite production. *Sci. Rep.,* 6**,** 38747.
Foyer, C. H. & Noctor, G. 2005. Redox homeostasis and antioxidant signaling: a metabolic interface between stress perception and physiological responses. *Plant Cell,* 17**,** 1866-1875.
Fraise, A. P. 2008. European norms for disinfection testing. *J. Hosp. Infect.,* 70 Suppl 1**,** 8-10.
Fraser, A., Anderson, J., Goncalves, J., Black, E., Starobin, A., Buckley, D., Grinstead, D., Manuel, C. & Hollingsworth, J. 2021. Sanitizers and disinfectants: a retail food and foodservice perspective. *Food Prot. Trends,* 41**,** 358.
Fricker, M. D., Heaton, L. L. M., Jones, N. S. & Boddy, L. 2017. The mycelium as a network. *In:* Heitman, J., Howlett, B. J., Crous, P. W., Stukenbrock, E. H., James, T. Y. & Gow, N. A. R. (eds.) *The Fungal Kingdom.* Washington, DC: American Society for Microbiology.
Frølund, B., Griebe, T. & Nielsen, P. H. 1995. Enzymatic activity in the activated-sludge floc matrix. *Appl. Microbiol. Biotechnol.,* 43**,** 755-761.
Fujikawa, H., Morozumi, S., Smerage, G. H. & Teixeira, A. A. 2000. Comparison of capillary and test tube procedures for analysis of thermal inactivation kinetics of mold spores. *J. Food Prot.,* 63**,** 1404-9.
Gabrielli, M., Englezos, V., Rolle, L., Río Segade, S., Giacosa, S., Cocolin, L., Paissoni, M. A., Lambri, M., Rantsiou, K. & Maury, C. 2020. Chloroanisoles occurrence in wine from grapes subjected to electrolyzed water treatments in the vineyard. *Food Res. Int.,* 137**,** 109704.
Galdeano, M. C., Wilhelm, A. E., Goulart, I. B., Tonon, R. V., Freitas-Silva, O., Germani, R. & Hidalgo-Chávez, D. W. 2018. Effect of water temperature and pH on the concentration and time of ozone saturation. *Braz. J. Food Technol.,* 21**,** e2017156.
Gallmetzer, A., Silvestrini, L., Schinko, T., Gesslbauer, B., Hortschansky, P., Dattenböck, C., Muro-Pastor, M. I., Kungl, A., Brakhage, A. A., Scazzocchio, C. & Strauss, J. 2015. Reversible oxidation of a conserved methionine in the nuclear export sequence determines subcellular

distribution and activity of the fungal nitrate regulator NirA. *PLOS Genet.,* 11**,** e1005297.

Garin-Bastuji, B., Perrin, B., Thorel, M.-F. & Martel, J. L. 1990. Evaluation of γ-rays irradiation of cows' colostrum for *Brucella abortus*, *Escherichia coli* K99, *Salmonella* Dublin and *Mycobacterium paratuberculosis* decontamination. *Letters Appl. Microbiol.,* 11**,** 163-166.

Garrido, Y., Marín, A., Tudela, J. A., Truchado, P., Allende, A. & Gil, M. I. 2020. Chlorate accumulation in commercial lettuce cultivated in open field and irrigated with reclaimed water. *Food Control,* 114**,** 107283.

Geoghegan, I. A., Stratford, M., Bromley, M., Archer, D. B. & Avery, S. V. 2020. Weak Acid Resistance A (WarA), a novel transcription factor required for regulation of weak-acid resistance and spore-spore heterogeneity in *Aspergillus niger*. *mSphere,* 5**,** e00685-19.

Giacosa, S., Gabrielli, M., Torchio, F., Río Segade, S., Moar Grobas, A. M., Ricauda Aimonino, D., Gay, P., Gerbi, V., Maury, C. & Rolle, L. 2019. Relationships among electrolyzed water postharvest treatments on winegrapes and chloroanisoles occurrence in wine. *Food Res. Int.,* 120**,** 235-243.

Gibbs, P. A., Chambers, B. J., Chaudri, A. M., McGrath, S. P., Carlton-Smith, C. H., Bacon, J. R., Campbell, C. D. & Aitken, M. N. 2006. Initial results from a long-term, multi-site field study of the effects on soil fertility and microbial activity of sludge cakes containing heavy metals. *Soil Use Manag.,* 22**,** 11-21.

Gietz, R. D. & Woods, R. A. 2002. Transformation of yeast by lithium acetate/single-stranded carrier DNA/polyethylene glycol method. *In:* Guthrie, C. & Fink, G. R. (eds.) *Methods in Enzymology. Guide to Yeast Genetics and Molecular and Cell Biology - Part B.* New York, NY: Academic Press.

Gil, M. I., Gómez-López, V. M., Hung, Y.-C. & Allende, A. 2015. Potential of electrolyzed water as an alternative disinfectant agent in the fresh-cut industry. *Food Bioproc. Tech.,* 8**,** 1336-1348.

Gil, M. I., López-Gálvez, F., Andújar, S., Moreno, M. & Allende, A. 2019. Disinfection by-products generated by sodium hypochlorite and electrochemical disinfection in different process wash water and fresh-cut products and their reduction by activated carbon. *Food Control,* 100**,** 46-52.

Gimeno, C. & Fink, G. 1992. The logic of cell division in the life cycle of yeast. *Science,* 257**,** 626-626.

Gits, J. J. & Grenson, M. 1967. Multiplicity of the amino acid permeases in *Saccharomyces cerevisiae*. 3. Evidence for a specific methionine-transporting system. *Biochim. Biophys. Acta,* 135**,** 507-516.

Goemans, C. V. & Collet, J. F. 2019. Stress-induced chaperones: a first line of defense against the powerful oxidant hypochlorous acid. *F1000Res,* 8(F1000 Faculty Rev)**,** 1678.

Gomes, A. C., Kordala, A. J., Strack, R., Wang, X., Geslain, R., Delaney, K., Clark, W. C., Keenan, R. & Pan, T. 2016. A dual fluorescent reporter for the investigation of methionine mistranslation in live cells. *RNA,* 22**,** 467-76.

Gómez-Espinosa, D., Cervantes-Aguilar, F. J., del Río-García, J. C., Villarreal-Barajas, T., Vázquez-Durán, A. & Méndez-Albores, A. 2017. Ameliorative effects of neutral electrolyzed water on growth performance, biochemical constituents, and histopathological changes in turkey poults during aflatoxicosis. *Toxins (Basel),* 9**,** 104.

Gómez-López, V. M., Gil, M. I., Pupunat, L. & Allende, A. 2015. Cross-contamination of *Escherichia coli* O157:H7 is inhibited by electrolyzed water combined with salt under dynamic conditions of increasing organic matter. *Food Microbiol.,* 46**,** 471-478.

Gomez, M., Pérez-Gallardo, R. V., Sánchez, L. A., Díaz-Pérez, A. L., Cortés-Rojo, C., Meza Carmen, V., Saavedra-Molina, A., Lara-Romero, J., Jiménez-

Sandoval, S., Rodríguez, F., Rodríguez-Zavala, J. S. & Campos-García, J. 2014. Malfunctioning of the iron–sulfur cluster assembly machinery in *Saccharomyces cerevisiae* produces oxidative stress via an iron-dependent mechanism, causing dysfunction in respiratory complexes. *PLoS ONE,* 9**,** e111585.

Gonçalves Lemos, J., Stefanello, A., Olivier Bernardi, A., Valle Garcia, M., Nicoloso Magrini, L., Cichoski, A. J., Wagner, R. & Venturini Copetti, M. 2020. Antifungal efficacy of sanitizers and electrolyzed waters against toxigenic *Aspergillus*. *Food Res. Int.,* 137**,** 109451.

Gougouli, M. & Koutsoumanis, K. P. 2013. Relation between germination and mycelium growth of individual fungal spores. *Int. J. Food Microbiol.,* 161**,** 231-239.

Gougouli, M. & Koutsoumanis, K. P. 2017. Risk assessment of fungal spoilage: a case study of *Aspergillus niger* on yogurt. *Food Microbiol.,* 65**,** 264-273.

Gould, G. W. 1996. Methods for preservation and extension of shelf life. *Int. J. Food Microbiol.,* 33**,** 51-64.

Graça, A., Santo, D., Pires-Cabral, P. & Quintas, C. 2020. The effect of UV-C and electrolyzed water on yeasts on fresh-cut apple at 4°C. *J. Food Eng.,* 282**,** 110034.

Gracia, A. & de-Magistris, T. 2016. Consumer preferences for food labeling: what ranks first? *Food Control,* 61**,** 39-46.

Grimaud, R., Ezraty, B., Mitchell, J. K., Lafitte, D., Briand, C., Derrick, P. J. & Barras, F. 2001. Repair of oxidized proteins. Identification of a new methionine sulfoxide reductase. *J. Biol. Chem.,* 276**,** 48915-20.

Grünberger, A., Schöler, K., Probst, C., Kornfeld, G., Hardiman, T., Wiechert, W., Kohlheyer, D. & Noack, S. 2017. Real-time monitoring of fungal growth and morphogenesis at single-cell resolution. *Eng. Life Sci.,* 17**,** 86-92.

Guerreiro, T. C. d. S., Meng, X., Dacheux, E., Firczuk, H. & McCarthy, J. 2021. Translational control of gene expression noise and its relationship to ageing in yeast. *FEBS J.,* 288**,** 2278-2293.

Gunaydin, M., Esen, S., Karadag, A., Unal, N., Yanik, K., Odabasi, H. & Birinci, A. 2014. *In vitro* antimicrobial activity of Medilox® super-oxidized water. *Ann. Clin. Microbiol. Antimicrob.,* 13**,** 29-29.

Hage, H., Rosso, M.-N. & Tarrago, L. 2021. Distribution of methionine sulfoxide reductases in fungi and conservation of the free-methionine-R-sulfoxide reductase in multicellular eukaryotes. *Free Radic. Biol. Med.,* 169**,** 187-215.

Hageskal, G., Lima, N. & Skaar, I. 2009. The study of fungi in drinking water. *Mycol. Res.,* 113**,** 165-172.

Hagiwara, D., Sakai, K., Suzuki, S., Umemura, M., Nogawa, T., Kato, N., Osada, H., Watanabe, A., Kawamoto, S., Gonoi, T. & Kamei, K. 2017. Temperature during conidiation affects stress tolerance, pigmentation, and trypacidin accumulation in the conidia of the airborne pathogen *Aspergillus fumigatus*. *PLOS ONE,* 12**,** e0177050.

Hallen-Adams, H. E. & Suhr, M. J. 2017. Fungi in the healthy human gastrointestinal tract. *Virulence,* 8**,** 352-358.

Han, D., Hung, Y.-C., Bratcher, C. L., Monu, E. A., Wang, Y. & Wang, L. 2018. Formation of sublethally injured *Yersinia enterocolitica*, *Escherichia coli* O157:H7, and *Salmonella enterica* serovar Enteritidis cells after neutral electrolyzed oxidizing water treatments. *Appl. Environ. Microbiol.,* 84**,** e01066-18.

Hansen, J. & Johannesen, P. F. 2000. Cysteine is essential for transcriptional regulation of the sulfur assimilation genes in *Saccharomyces cerevisiae*. *Mol. Gen. Genet.,* 263**,** 535-42.

Hao, X. X., Li, B. M., Wang, C. Y., Zhang, Q. & Cao, W. 2013. Application of slightly acidic electrolyzed water for inactivating microbes in a layer breeding house. *Poult Sci.,* 92**,** 2560-6.

Harvey, H. J., Wildman, R. D., Mooney, S. J. & Avery, S. V. 2020. Soil aggregates by design: manufactured aggregates with defined microbial composition for interrogating microbial activities in soil microhabitats. *Soil Biol. Biochem.,* 148**,** 107870.

Hasan, H. A. H. 1995. *Alternaria* mycotoxins in black rot lesion of tomato fruit: conditions and regulation of their production. *Mycopathologia,* 130**,** 171-177.

Hashisaka, A. E., Matches, J. R., Batters, Y., Hungate, F. P. & Dong, F. M. 1990. Effects of gamma irradiation at -78°C on microbial populations in dairy products. *J. Food Sci.,* 55**,** 1284-1289.

Hawkins, C. L. & Davies, M. J. 1999. Hypochlorite-induced oxidation of proteins in plasma: formation of chloramines and nitrogen-centred radicals and their role in protein fragmentation. *Biochem. J.,* 340**,** 539-548.

Hawkins, C. L., Pattison, D. I. & Davies, M. J. 2002. Reaction of protein chloramines with DNA and nucleosides: evidence for the formation of radicals, protein–DNA cross-links and DNA fragmentation. *Biochem. J.,* 365**,** 605-615.

Hawkins, C. L., Pattison, D. I. & Davies, M. J. 2003. Hypochlorite-induced oxidation of amino acids, peptides and proteins. *Amino Acids,* 25**,** 259-274.

Hawkins, C. L., Pattison, D. I., Whiteman, M. & Davies, M. J. 2007. Chlorination and nitration of DNA and nucleic acid components. *In:* Evans, M. D. & Cooke, M. S. (eds.) *Oxidative Damage to Nucleic Acids.* New York, NY: Springer New York.

Hawksworth, D. L. 1991. The fungal dimension of biodiversity: magnitude, significance, and conservation. *Mycol. Res.,* 95**,** 641-655.

Hayer, K., Stratford, M., Archer David, B. & Brakhage, A. A. 2014. Germination of *Aspergillus niger* conidia Is triggered by nitrogen compounds related to L-amino acids. *Appl. Environ. Microbiol.,* 80**,** 6046-6053.

Hayer, K., Stratford, M. & Archer, D. B. 2013. Structural features of sugars that trigger or support conidial germination in the filamentous fungus *Aspergillus niger*. *Appl. Environ. Microbiol.,* 79**,** 6924-6931.

Held, A. M., Halko, D. J. & Hurst, J. K. 1978. Mechanisms of chlorine oxidation of hydrogen peroxide. *J. Am. Chem. Soc.,* 100**,** 5732-5740.

Hentchel, K. L., Escalante-Semerena, J. C. & Metcalf, W. W. 2015. In *Salmonella enterica*, the Gcn5-related acetyltransferase MddA (formerly YncA) acetylates methionine sulfoximine and methionine sulfone, blocking their toxic effects. *J. Bacteriol.,* 197**,** 314-325.

Hermant, B. M. & Basu, O. D. 2013. Comparison of reaction rates and relative efficiencies for various dechlorination chemicals. *J. Environ. Eng.,* 139**,** 522-529.

Hewitt, S. K., Foster, D. S., Dyer, P. S. & Avery, S. V. 2016. Phenotypic heterogeneity in fungi: importance and methodology. *Fungal Biol. Rev.,* 30**,** 176-184.

Hibben, C. R. & Stotzky, G. 1969. Effects of ozone on the germination of fungus spores. *Can. J. Microbiol.,* 15**,** 1187-1196.

Hinkle, B. 2017. Ozone as an added protection in food processing chain. *Food Quality and Safety (online).* https://www.foodqualityandsafety.com/article/ozone-added-protection-food-processing-chain/ accessed June 2020.

Hoelzer, K., Pouillot, R., Gallagher, D., Silverman, M. B., Kause, J. & Dennis, S. 2012. Estimation of *Listeria monocytogenes* transfer coefficients and efficacy of bacterial removal through cleaning and sanitation. *Int. J. Food Microbiol.,* 157**,** 267-277.

Hoffman, J. R. & Falvo, M. J. 2004. Protein - which is best? *J. Sports Sci. Med.,* 3**,** 118-130.

Holland, S. L., Reader, T., Dyer, P. S. & Avery, S. V. 2014. Phenotypic heterogeneity is a selected trait in natural yeast populations subject to environmental stress. *Environ. Microbiol.,* 16**,** 1729-1740.

Hong, P., Hao, W., Luo, J., Chen, S., Hu, M. & Zhong, G. 2014. Combination of hot water, *Bacillus amyloliquefaciens* HF-01 and sodium bicarbonate treatments to control postharvest decay of mandarin fruit. *Postharvest Biol. Technol.,* 88**,** 96-102.

Hong, Y., Zeng, J., Wang, X., Drlica, K. & Zhao, X. 2019. Post-stress bacterial cell death mediated by reactive oxygen species. *Proc. Natl. Acad. Sci. USA,* 116**,** 10064-10071.

Horvitz, S. & Cantalejo, M. J. 2014. Application of ozone for the postharvest treatment of fruits and vegetables. *Crit. Rev. Food Sci. Nutr.,* 54**,** 312-339.

How, Z. T., Kristiana, I., Busetti, F., Linge, K. L. & Joll, C. A. 2017. Organic chloramines in chlorine-based disinfected water systems: a critical review. *J. Environ. Sci.,* 58**,** 2-18.

How, Z. T., Linge, K. L., Busetti, F. & Joll, C. A. 2016. Organic chloramines in drinking water: an assessment of formation, stability, reactivity and risk. *Water Res.,* 93**,** 65-73.

How, Z. T., Linge, K. L., Busetti, F. & Joll, C. A. 2018. Formation of odorous and hazardous by-products from the chlorination of amino acids. *Water Res.,* 146**,** 10-18.

Hricova, D., Stephan, R. & Zweifel, C. 2008. Electrolyzed water and its application in the food industry. *J. Food Prot.,* 71**,** 1934-1947.

Hu, Y., Xie, G. & Stanbury, D. M. 2017. Oxidations at sulfur centers by aqueous hypochlorous acid and hypochlorite: Cl^+ versus O atom transfer. *Inorg. Chem.,* 56**,** 4047-4056.

Huang, C. T., Yu, F. P., McFeters, G. A. & Stewart, P. S. 1995. Nonuniform spatial patterns of respiratory activity within biofilms during disinfection. *Appl. Environ. Microbiol.,* 61**,** 2252-2256.

Huang, Y.-R., Hung, Y.-C., Hsu, S.-Y., Huang, Y.-W. & Hwang, D.-F. 2008. Application of electrolyzed water in the food industry. *Food Control,* 19**,** 329-345.

Huis in't Veld, J. H. J. 1996. Microbial and biochemical spoilage of foods: an overview. *Int. J. Food Microbiol.,* 33**,** 1-18.

Hurst, J. K., Barrette Jr, W. C., Michel, B. R. & Rosen, H. 1991. Hypochlorous acid and myeloperoxidase-catalyzed oxidation of iron-sulfur clusters in bacterial respiratory dehydrogenases. *Eur. J. Biochem.,* 202**,** 1275-1282.

Hussain, P. R., Rather, S. A., Suradkar, P. P. & Ayob, O. 2019. Gamma irradiation treatment of quince fruit (*Cydonia oblonga* Mill): effect on post-harvest retention of storage quality and inhibition of fungal decay. *J. Radiat. Res. Appl. Sci.,* 12**,** 118-131.

Imlay, J. A. 2006. Iron-sulphur clusters and the problem with oxygen. *Mol. Microbiol.,* 59**,** 1073-1082.

Imlay, J. A., Sethu, R. & Rohaun, S. K. 2019. Evolutionary adaptations that enable enzymes to tolerate oxidative stress. *Free Radic. Biol. Med.,* 140**,** 4-13.

Isnard, A. D., Thomas, D. & Surdin-Kerjan, Y. 1996. The study of methionine uptake in *Saccharomyces cerevisiae* reveals a new family of amino acid permeases. *J. Mol. Biol.,* 262**,** 473-484.

Izumi, H. 1999. Electrolyzed water as a disinfectant for fresh-cut vegetables. *J. Food Sci.,* 64**,** 536-539.

Jackman, T. & Hughes, C. 2010. Formation of trihalomethanes in soil and groundwater by the release of sodium hypochlorite. *Ground Water Monit. Remediat.,* 30**,** 74-78.

Jang, H.-J., Nde, C., Toghrol, F. & Bentley, W. E. 2009. Global transcriptome analysis of the *Mycobacterium bovis* BCG response to sodium hypochlorite. *Appl. Microbiol. Biotechnol.,* 85**,** 127-140.

Jang, H. H., Lee, K. O., Chi, Y. H., Jung, B. G., Park, S. K., Park, J. H., Lee, J. R., Lee, S. S., Moon, J. C., Yun, J. W., Choi, Y. O., Kim, W. Y., Kang, J. S., Cheong, G. W., Yun, D. J., Rhee, S. G., Cho, M. J. & Lee, S. Y. 2004. Two enzymes in one; two yeast peroxiredoxins display oxidative stress-dependent switching from a peroxidase to a molecular chaperone function. *Cell,* 117**,** 625-35.

Jang, S. & Imlay, J. A. 2007. Micromolar intracellular hydrogen peroxide disrupts metabolism by damaging iron-sulfur enzymes. *J. Biol. Chem.,* 282**,** 929-37.

Jaroszeski, M. J. & Radcliff, G. 1999. Fundamentals of flow cytometry. *Mol. Biotechnol.,* 11**,** 37-53.

Jay, J. M. 1995. Low-temperature food preservation and characteristics of psychrotrophic microorganisms. *In:* Jay, J. M. (ed.) *Modern Food Microbiology.* Boston, MA: Springer US.

Jeong, J., Kim, C. & Yoon, J. 2009. The effect of electrode material on the generation of oxidants and microbial inactivation in the electrochemical disinfection processes. *Water Res.,* 43**,** 895-901.

Jeong, J., Kim, J. Y., Cho, M., Choi, W. & Yoon, J. 2007. Inactivation of *Escherichia coli* in the electrochemical disinfection process using a Pt anode. *Chemosphere,* 67**,** 652-659.

Jeong, M.-A. & Jeong, R.-D. 2018. Applications of ionizing radiation for the control of postharvest diseases in fresh produce: recent advances. *Plant Pathol.,* 67**,** 18-29.

Jiménez-Pichardo, R., Hernández-Martínez, I., Regalado-González, C., Santos-Cruz, J., Meas-Vong, Y., Wacher-Rodarte, M. D. C., Carrillo-Reyes, J., Sánchez-Ortega, I. & García-Almendárez, B. E. 2021. Innovative control of biofilms on stainless steel surfaces using electrolyzed water in the dairy industry. *Foods,* 10**,** 103.

Jo, H.-Y., Tango, C. N. & Oh, D.-H. 2018. Influence of different organic materials on chlorine concentration and sanitization of slightly acidic electrolyzed water. *LWT-Food Sci. Technol.,* 92**,** 187-194.

Jo, I., Kim, D., No, T., Hong, S., Ahn, J., Ryu, S. & Ha, N.-C. 2019. Structural basis for HOCl recognition and regulation mechanisms of HypT, a hypochlorite-specific transcriptional regulator. *Proc. Natl. Acad. Sci. USA,* 116**,** 3740-3745.

Ju, S.-Y., Ko, J.-J., Yoon, H.-S., Seon, S.-J., Yoon, Y.-R., Lee, D.-I., Kim, S.-Y. & Chang, H.-J. 2017. Does electrolyzed water have different sanitizing effects than sodium hypochlorite on different vegetable types? *Br. Food J.,* 119**,** 342-356.

Jung, Y. J., Baek, K. W., Oh, B. S. & Kang, J.-W. 2010. An investigation of the formation of chlorate and perchlorate during electrolysis using Pt/Ti electrodes: the effects of pH and reactive oxygen species and the results of kinetic studies. *Water Res.,* 44**,** 5345-5355.

Kaczmarek, M., Avery, S. V. & Singleton, I. 2019. Microbes associated with fresh produce: sources, types and methods to reduce spoilage and contamination. *Adv. Appl. Microbiol.,* 107**,** 29-82.

Kawasaki, L. & Aguirre, J. 2001. Multiple catalase genes are differentially regulated in *Aspergillus nidulans*. *J. Bacteriol.,* 183**,** 1434-1440.

Keppler-Ross, S., Noffz, C. & Dean, N. 2008. A new purple fluorescent color marker for genetic studies in *Saccharomyces cerevisiae* and *Candida albicans*. *Genetics,* 179**,** 705-10.

Khalili, R., Ayoobian, N., Jafarpour, M. & Shirani, B. 2017. The effect of gamma irradiation on the properties of cucumber. *J. Food Sci. Technol.,* 54**,** 4277-4283.

Khor, H. K., Fisher, M. T. & Schöneich, C. 2004a. Potential role of methionine sulfoxide in the inactivation of the chaperone GroEL by hypochlorous acid (HOCl) and peroxynitrite ($ONOO^-$). *J. Biol.Chem.,* 279**,** 19486-93.

Khor, H. K., Fisher, M. T. & Schöneich, C. 2004b. Potential role of methionine sulfoxide in the inactivation of the chaperone GroEL by hypochlorous acid (HOCl) and peroxynitrite (ONOO−)*. *J. Biol. Chem.,* 279**,** 19486-19493.

Khoshnevis, S., Gross, T., Rotte, C., Baierlein, C., Ficner, R. & Krebber, H. 2010. The iron-sulphur protein RNase L inhibitor functions in translation termination. *EMBO Rep.,* 11**,** 214-219.

Killick, K. A. 1971. Modification of the composition and structure of the yeast cell wall by culture in the presence of sulfur amino acids. *J. Bacteriol.,* 106**,** 931-7.

Kim, C., Hung, Y.-C. & Brackett, R. E. 2000a. Efficacy of electrolyzed oxidizing (EO) and chemically modified water on different types of foodborne pathogens. *Int. J. Food Microbiol.,* 61**,** 199-207.

Kim, C., Hung, Y.-C. & Brackett, R. E. 2000b. Roles of oxidation-reduction potential in electrolyzed oxidizing and chemically modified water for the inactivation of food-related pathogens. *J. Food Prot.,* 63**,** 19-24.

Kim, G., Weiss, S. J. & Levine, R. L. 2014. Methionine oxidation and reduction in proteins. *Biochim. Biophys. Acta,* 1840**,** 901-905.

Kim, H., Ryu, J. H. & Beuchat, L. R. 2006. Survival of *Enterobacter sakazakii* on fresh produce as affected by temperature, and effectiveness of sanitizers for its elimination. *Int. J. Food Microbiol.,* 111**,** 134-43.

Kim, H. S., Choi, S. J. & Yoon, K. S. 2018. Efficacy evaluation of control measures on the reduction of *Staphylococcus aureus* in salad and *Bacillus cereus* in fried rice served at restaurants. *Foodborne Pathog. Dis.,* 15**,** 198-209.

Kispal, G., Sipos, K., Lange, H., Fekete, Z., Bedekovics, T., Janaky, T., Bassler, J., Aguilar Netz, D. J., Balk, J., Rotte, C. & Lill, R. 2005. Biogenesis of cytosolic ribosomes requires the essential iron-sulphur protein Rli1p and mitochondria. *EMBO J.,* 24**,** 589-598.

Klich, M. A. 2006. Identification of clinically relevant aspergilli. *Med. Mycol.,* 44**,** S127-S131.

Klich, M. A. 2007. *Aspergillus flavus*: the major producer of aflatoxin. *Mol. Plant Pathol.,* 8**,** 713-722.

Klich, M. A. 2009. Health effects of *Aspergillus* in food and air. *Toxicol. Ind. Health,* 25**,** 657-67.

Kögel-Knabner, I. 2002. The macromolecular organic composition of plant and microbial residues as inputs to soil organic matter. *Soil Biol. Biochem.,* 34**,** 139-162.

Koide, S., Takeda, J.-i., Shi, J., Shono, H. & Atungulu, G. G. 2009. Disinfection efficacy of slightly acidic electrolyzed water on fresh cut cabbage. *Food Control,* 20**,** 294-297.

Koseki, M., Tanaka, Y., Noguchi, H. & Nishikawa, T. 2007. Effect of pH on the taste of alkaline electrolyzed water. *J. Food Sci.,* 72**,** S298-302.

Koseki, S. & Isobe, S. 2007. Microbial control of fresh produce using electrolyzed water. *Jpn. Agric. Res. Q.,* 41**,** 273-282.

Koseki, S., Yoshida, K., Isobe, S. & Itoh, K. 2004. Efficacy of acidic electrolyzed water for microbial decontamination of cucumbers and strawberries. *J. Food Prot.,* 67**,** 1247-1251.

Koseki, S., Yoshida, K., Kamitani, Y. & Itoh, K. 2003. Influence of inoculation method, spot inoculation site, and inoculation size on the efficacy of acidic electrolyzed water against pathogens on lettuce. *J. Food Prot.,* 66**,** 2010-2016.

Kovačević, G., Ostafe, R., Fischer, R. & Prodanović, R. 2019. Influence of methionine residue position on oxidative stability of glucose oxidase from *Aspergillus niger*. *Biochem. Eng. J.,* 146**,** 143-149.

Kryukov, G. V., Kumar, R. A., Koc, A., Sun, Z. & Gladyshev, V. N. 2002. Selenoprotein R is a zinc-containing stereo-specific methionine sulfoxide reductase. *Proc. Natl. Acad. Sci. USA,* 99**,** 4245-4250.

Kumar, V., Neeraj, Sharma, S. & Sagar, N. A. 2015. Post harvest management of fungal diseases in onion - a review. *Int. J. Curr. Microbiol. Appl. Sci.,* 4**,** 737-752.

Kuncha, S. K., Kruparani, S. P. & Sankaranarayanan, R. 2019. Chiral checkpoints during protein biosynthesis. *J. Biol. Chem.,* 294**,** 16535-16548.

Kurucz, V., Krüger, T., Antal, K., Dietl, A.-M., Haas, H., Pócsi, I., Kniemeyer, O. & Emri, T. 2018. Additional oxidative stress reroutes the global response of *Aspergillus fumigatus* to iron depletion. *BMC Genomics,* 19**,** 357.

Kvitek, D. J., Will, J. L. & Gasch, A. P. 2008. Variations in stress sensitivity and genomic expression in diverse *S. cerevisiae* isolates. *PLOS Genet.,* 4**,** e1000223.

Lade, P. V. 2001. Basic soil mechanics. *In:* Rowe, R. K. (ed.) *Geotechnical and Geoenvironmental Engineering Handbook.* New York: Springer Science+Business Media, LLC.

Lado, B. H. & Yousef, A. E. 2002. Alternative food-preservation technologies: efficacy and mechanisms. *Microbes Infect.,* 4**,** 433-440.

Lalève, A., Vallières, C., Golinelli-Cohen, M.-P., Bouton, C., Song, Z., Pawlik, G., Tindall, S. M., Avery, S. V., Clain, J. & Meunier, B. 2016. The antimalarial drug primaquine targets Fe-S cluster proteins and yeast respiratory growth. *Redox biol.,* 7**,** 21-29.

Landfeld, A., Erban, V., Kováříková, E., Houška, M., Kýhos, K., Průchová, J. & Novotná, P. 2010. Decontamination of cut carrot by Persteril® agent based on the action of peroxyacetic acid. *Czech J. Food Sci.,* 28**,** 564-571.

Langmead, B. & Salzberg, S. L. 2012. Fast gapped-read alignment with Bowtie 2. *Nat. Methods,* 9**,** 357-9.

Laothanachareon, T., Tamayo-Ramos, J. A., Nijsse, B. & Schaap, P. J. 2018. Forward genetics by genome sequencing uncovers the central role of the *Aspergillus niger* goxB locus in hydrogen peroxide induced glucose oxidase expression. *Front. Microbiol.,* 9**,** 2269.

Larosa, V. & Remacle, C. 2018. Insights into the respiratory chain and oxidative stress. *Biosci. Rep.,* 38**,** BSR20171492.

Lau, A. T. Y., Wang, Y. & Chiu, J.-F. 2008. Reactive oxygen species: current knowledge and applications in cancer research and therapeutic. *J. Cell. Biochem.,* 104**,** 657-667.

Le, D. T., Lee, B. C., Marino, S. M., Zhang, Y., Fomenko, D. E., Kaya, A., Hacioglu, E., Kwak, G. H., Koc, A., Kim, H. Y. & Gladyshev, V. N. 2009. Functional analysis of free methionine-R-sulfoxide reductase from *Saccharomyces cerevisiae*. *J. Biol. Chem.,* 284**,** 4354-4364.

Lee, J., Shon, M.-B., Cha, H.-G. & Choi, K.-H. 2017. The impact of adding organic carbon on the concentrations of total residual oxidants and disinfection by-products in approval tests for ballast water management systems. *Sci. Total Environ.,* 605-606**,** 852-859.

Lee, J. Y., Kim, D. G., Kim, B. G., Yang, W. S., Hong, J., Kang, T., Oh, Y. S., Kim, K. R., Han, B. W., Hwang, B. J., Kang, B. S., Kang, M. S., Kim, M. H., Kwon, N. H. & Kim, S. 2014a. Promiscuous methionyl-tRNA synthetase mediates adaptive mistranslation to protect cells against oxidative stress. *J. Cell. Sci.,* 127**,** 4234-4245.

Lee, S. C., Billmyre, R. B., Li, A., Carson, S., Sykes, S. M., Huh, E. Y., Mieczkowski, P., Ko, D. C., Cuomo, C. A. & Heitman, J. 2014b. Analysis of a food-borne fungal pathogen outbreak: virulence and genome of a *Mucor circinelloides* isolate from yogurt. *MBio,* 5**,** e01390-14.

Lee, S. J., Choi, W. S., Park, G. H., Kim, T. H., Oh, C., Heo, S. J. & Kang, D. H. 2018. Flocculation effect of alkaline electrolyzed water (AEW) on harvesting of marine microalga *Tetraselmis* sp. *J. Microbiol. Biotechnol.,* 28**,** 432-438.

Lee, W.-N., Huang, C.-H. & Zhu, G. 2019. Analytical methods for conventional and emerging disinfection by-products in fresh-cut produce. *Food Chem.,* 291**,** 30-37.

Lehmann, J. & Kleber, M. 2015. The contentious nature of soil organic matter. *Nature,* 528**,** 60-68.

Leistner, L. 1992. Food preservation by combined methods. *Food Res. Int.,* 25**,** 151-158.

Leistner, L. & Gould, G. W. 2002. The hurdle concept. *In:* Leistner, L. & Gould, G. W. (eds.) *Hurdle Technologies: Combination Treatments for Food Stability, Safety and Quality.* Boston, MA: Springer US.

Levin, A. M., de Vries, R. P., Conesa, A., de Bekker, C., Talon, M., Menke, H. H., van Peij, N. N. M. E. & Wösten, H. A. B. 2007. Spatial differentiation in the vegetative mycelium of *Aspergillus niger*. *Eukaryot. Cell,* 6**,** 2311-2322.

Levine, R. L., Moskovitz, J. & Stadtman, E. R. 2000. Oxidation of methionine in proteins: roles in antioxidant defense and cellular regulation. *IUBMB Life,* 50**,** 301-307.

Levine, R. L., Mosoni, L., Berlett, B. S. & Stadtman, E. R. 1996. Methionine residues as endogenous antioxidants in proteins. *Proc. Natl. Acad. Sci. USA,* 93**,** 15036-15040.

Li, C. H., Cervantes, M., Springer, D. J., Boekhout, T., Ruiz-Vazquez, R. M., Torres-Martinez, S. R., Heitman, J. & Lee, S. C. 2011. Sporangiospore size dimorphism is linked to virulence of *Mucor circinelloides*. *PLOS Pathog.,* 7**,** e1002086.

Li, J., Lin, T., Lu, Q., Wang, J. J., Liao, C., Pan, Y. & Zhao, Y. 2014. Changes in physicochemical properties and bactericidal efficiency of acidic electrolyzed water ice and available chlorine decay kinetics during storage. *LWT-Food Sci. Technol.,* 59**,** 43-48.

Li, L., Hao, J., Song, S., Nirasawa, S., Jiang, Z. & Liu, H. 2018. Effect of slightly acidic electrolyzed water on bioactive compounds and morphology of broccoli sprouts. *Food Res. Int.,* 105**,** 102-109.

Liguori, I., Russo, G., Curcio, F., Bulli, G., Aran, L., Della-Morte, D., Gargiulo, G., Testa, G., Cacciatore, F., Bonaduce, D. & Abete, P. 2018. Oxidative stress, aging, and diseases. *Clin. Interv. Aging,* 13**,** 757-772.

Lill, R., Dutkiewicz, R., Freibert, S. A., Heidenreich, T., Mascarenhas, J., Netz, D. J., Paul, V. D., Pierik, A. J., Richter, N., Stümpfig, M., Srinivasan, V., Stehling, O. & Mühlenhoff, U. 2015. The role of mitochondria and the CIA machinery in the maturation of cytosolic and nuclear iron-sulfur proteins. *Eur. J. Cell Biol.,* 94**,** 280-91.

Lill, R. & Freibert, S. A. 2020. Mechanisms of mitochondrial iron-sulfur protein biogenesis. *Annu. Rev. Biochem.,* 89**,** 471-499.

Lim, J. C., You, Z., Kim, G. & Levine, R. L. 2011. Methionine sulfoxide reductase A is a stereospecific methionine oxidase. *Proc. Natl. Acad. Sci. USA,* 108**,** 10472-7.

Lin, D. & Zhao, Y. 2007. Innovations in the development and application of edible coatings for fresh and minimally processed fruits and vegetables. *Compr. Rev. Food Sci. Food Saf.,* 6**,** 60-75.

Lin, S., Yang, X., Jia, S., Weeks, A. M., Hornsby, M., Lee, P. S., Nichiporuk, R. V., Iavarone, A. T., Wells, J. A., Toste, F. D. & Chang, C. J. 2017. Redox-based reagents for chemoselective methionine bioconjugation. *Science,* 355**,** 597-602.

Lipus, D., Vikram, A., Gulliver, D. & Bibby, K. 2019. Upregulation of peroxide scavenging enzymes and multidrug efflux proteins highlight an active sodium hypochlorite response in *Pseudomonas fluorescens* biofilms. *Biofouling,* 35**,** 329-339.

Liu, Q., Cedric Tan, C. S., Yang, H. & Wang, S. 2017. Treatment with low-concentration acidic electrolysed water combined with mild heat to sanitise

fresh organic broccoli (*Brassica oleracea*). *LWT-Food Sci. Technol.,* 79**,** 594-600.

Liu, R. & Yu, Z.-L. 2017. Application of electrolyzed water on reducing the microbial populations on commercial mung bean sprouts. *J Food Sci. Technol.,* 54**,** 995-1001.

Liu, Z., Lin, Y.-L., Xu, B., Hu, C.-Y., Wang, A.-Q., Gao, Z.-C., Xia, S.-J. & Gao, N.-Y. 2018. Formation of iodinated trihalomethanes during breakpoint chlorination of iodide-containing water. *J. Hazard. Mater.,* 353**,** 505-513.

Liu, Z., Swem, B., Cheng, Y. & Li, Y. 2006. Disinfection of recirculated bacon chilling brine using flow-through electrolyzing treatment chambers. *Appl. Eng. Agric.,* 22**,** 737-745.

Ljungdahl, P. O. & Daignan-Fornier, B. 2012. Regulation of amino acid, nucleotide, and phosphate metabolism in *Saccharomyces cerevisiae*. *Genetics.,* 190**,** 885-929.

Loenen, W. A. 2006. S-adenosylmethionine: jack of all trades and master of everything? *Biochem. Soc. Trans.,* 34**,** 330-3.

Logrieco, A., Ferracane, R., Haidukowsky, M., Cozzi, G., Visconti, A. & Ritieni, A. 2009. Fumonisin B2 production by *Aspergillus niger* from grapes and natural occurrence in must. *Food Addit. Contam. Part A* 26**,** 1495-1500.

Loi, V. V., Busche, T., Tedin, K., Bernhardt, J., Wollenhaupt, J., Huyen, N. T. T., Weise, C., Kalinowski, J., Wahl, M. C., Fulde, M. & Antelmann, H. 2018. Redox-sensing under hypochlorite stress and infection conditions by the Rrf2-family repressor HypR in *Staphylococcus aureus*. *Antioxid. Redox Signal.,* 29**,** 615-636.

Longfield, J. 2017. Into the cold abyss of food waste. *Food Safety Magazine (online).* https://www.food-safety.com/articles/5545-into-the-cold-abyss-of-food-waste accessed March 2021.

Lontsi Djimeli, C., Tamsa Arfao, A., Noah Ewoti, O. V., Nougang, M. E., Moungang, M. L., Bricheux, G., Nola, M. & Sime-Ngando, T. 2014. Mixture of sodium hypochlorite and hydrogen peroxide on adhered *Aeromonas hydrophila* to solid substrate in water: impact of concentration and assessment of the synergistic effect. *Int. J. Bacteriol.,* 2014**,** 121367.

López-Gálvez, F., Tudela, J. A., Allende, A. & Gil, M. I. 2019. Microbial and chemical characterization of commercial washing lines of fresh produce highlights the need for process water control. *Innov. Food Sci. Emerg. Technol.,* 51**,** 211-219.

López-Gálvez, F., Andújar, S., Marín, A., Tudela, J. A., Allende, A. & Gil, M. I. 2018. Disinfection by-products in baby lettuce irrigated with electrolysed water. *J. Sci. Food Agric.,* 98**,** 2981-2988.

Lorbeer, J. W., Ransom, V. E. & Tuffley, J. J. 2000. Nature and source of inoculum of *Aspergillus niger* causing the *Aspergillus* black mold disease of onions in New York. *Research Report for the New York State Integrated Pest Management Grants Program.* New York: Department of Plant Pathology, Cornell University.

Lowther, W. T., Brot, N., Weissbach, H., Honek, J. F. & Matthews, B. W. 2000. Thiol-disulfide exchange is involved in the catalytic mechanism of peptide methionine sulfoxide reductase. *Proc. Natl. Acad. Sci. USA,* 97**,** 6463-6468.

Lu, C., Brauer, M. J. & Botstein, D. 2009. Slow growth induces heat-shock resistance in normal and respiratory-deficient yeast. *Mol. Biol. Cell,* 20**,** 891-903.

Luo, S. & Levine, R. L. 2009. Methionine in proteins defends against oxidative stress. *FASEB J.,* 23**,** 464-472.

Luo, Y., Zhou, B., Van Haute, S., Nou, X., Zhang, B., Teng, Z., Turner, E. R., Wang, Q. & Millner, P. D. 2018. Association between bacterial survival and free chlorine concentration during commercial fresh-cut produce wash operation. *Food Microbiol.,* 70**,** 120-128.

Lutz, C. D., Booth, J. D., Boudreau, D. J., Lauder, N. R., Zarrin, H., Roster, W. & Federico, R. A. 2017. *Apparatus for producing and delivering ozonated water (US Patent Number US9540259B2)*.

Lux, C. A., Johnston, J., Biswas, K. & Douglas, R. G. 2021. Efficacy of neutral electrolyzed water in postoperative chronic rhinosinusitis patients—a pilot study. *Int. Forum Allergy Rhinol.,* 11**,** 81-83.

Lyu, F., Gao, F., Zhou, X., Zhang, J. & Ding, Y. 2018. Using acid and alkaline electrolyzed water to reduce deoxynivalenol and mycological contaminations in wheat grains. *Food Control,* 88**,** 98-104.

Madeira, F., Park, Y. M., Lee, J., Buso, N., Gur, T., Madhusoodanan, N., Basutkar, P., Tivey, A. R. N., Potter, S. C., Finn, R. D. & Lopez, R. 2019. The EMBL-EBI search and sequence analysis tools APIs in 2019. *Nucleic Acids Res.,* 47**,** W636-W641.

Magistà, D., Cozzi, G., Gambacorta, L., Logrieco, A. F., Solfrizzo, M. & Perrone, G. 2021. Studies on the efficacy of electrolysed oxidising water to control *Aspergillus carbonarius* and ochratoxin A contamination on grape. *Int. J. Food Microbiol.,* 338**,** 108996.

Mahajan, P. V., Caleb, O. J., Singh, Z., Watkins, C. B. & Geyer, M. 2014. Postharvest treatments of fresh produce. *Phil. Trans. R. Soc. A,* 372**,** 20130309.

Mahawar, M., Tran, V., Sharp, J. S. & Maier, R. J. 2011. Synergistic roles of *Helicobacter pylori* methionine sulfoxide reductase and GroEL in repairing oxidant-damaged catalase. *J. Biol. Chem.,* 286**,** 19159-69.

Mahto, R. & Das, M. 2013. Effect of gamma irradiation on the physico-chemical and visual properties of mango (*Mangifera indica* L.), cv. 'Dushehri' and 'Fazli' stored at 20°C. *Postharvest Biol. Technol.,* 86**,** 447-455.

Malleshappa Gowder, S., Chatterjee, J., Chaudhuri, T. & Paul, K. 2014. Prediction and analysis of surface hydrophobic residues in tertiary structure of proteins. *Sci. World J.,* 2014**,** 971258.

Marada, A., Allu, P. K., Murari, A., PullaReddy, B., Tammineni, P., Thiriveedi, V. R., Danduprolu, J. & Sepuri, N. B. 2013. Mge1, a nucleotide exchange factor of Hsp70, acts as an oxidative sensor to regulate mitochondrial Hsp70 function. *Mol. Biol. Cell,* 24**,** 692-703.

Margenot, A. J., Calderón, F. J., Bowles, T. M., Parikh, S. J. & Jackson, L. E. 2015. Soil organic matter functional group composition in relation to organic carbon, nitrogen, and phosphorus fractions in organically managed tomato fields. *Soil Sci. Soc. Am. J.,* 79**,** 772-782.

Martin, M. 2011. Cutadapt removes adapter sequences from high-throughput sequencing reads. *EMBnet J,* 17**,** 10-12.

Martín, M. Á., Pachepsky, Y. A., García-Gutiérrez, C. & Reyes, M. 2018. On soil textural classifications and soil-texture-based estimations. *Solid Earth,* 9**,** 159-165.

Martínez-Hernández, G. B., Artés-Hernández, F., Gómez, P. A., Formica, A. C. & Artés, F. 2013. Combination of electrolysed water, UV-C and superatmospheric O_2 packaging for improving fresh-cut broccoli quality. *Postharvest Biol. Technol.,* 76**,** 125-134.

Martinez-Romero, D., Bailen, G., Serrano, M., Guillen, F., Valverde, J. M., Zapata, P., Castillo, S. & Valero, D. 2007. Tools to maintain postharvest fruit and vegetable quality through the inhibition of ethylene action: a review. *Crit. Rev. Food Sci. Nutr.,* 47**,** 543-60.

Martinović, T., Andjelković, U., Gajdošik, M. Š., Rešetar, D. & Josić, D. 2016. Foodborne pathogens and their toxins. *J. Proteomics,* 147**,** 226-235.

Massi, F. P., Iamanaka, B. T., Barbosa, R. L., Sartori, D., Ferrranti, L., Taniwaki, M. H. & Fungaro, M. H. P. 2021. Molecular analysis of *Aspergillus* section *Nigri* isolated from onion samples reveals the prevalence of *A. welwitschiae*. *Braz. J. Microbiol.,* 52**,** 387–392.

Maxin, P., Weber, R. W. S., Pedersen, H. L. & Williams, M. 2012. Control of a wide range of storage rots in naturally infected apples by hot-water dipping and rinsing. *Postharvest Biol. Technol.,* 70**,** 25-31.

McIsaac, R. S., Petti, A. A., Bussemaker, H. J. & Botstein, D. 2012. Perturbation-based analysis and modeling of combinatorial regulation in the yeast sulfur assimilation pathway. *Mol. Biol. Cell,* 23**,** 2993-3007.

Meakin, N. S., Bowman, C., Lewis, M. R. & Dancer, S. J. 2012. Comparison of cleaning efficacy between in-use disinfectant and electrolysed water in an English residential care home. *J. Hosp. Infect.,* 80**,** 122-7.

Measday, V., Baetz, K., Guzzo, J., Yuen, K., Kwok, T., Sheikh, B., Ding, H., Ueta, R., Hoac, T., Cheng, B., Pot, I., Tong, A., Yamaguchi-Iwai, Y., Boone, C., Hieter, P. & Andrews, B. 2005. Systematic yeast synthetic lethal and synthetic dosage lethal screens identify genes required for chromosome segregation. *Proc. Natl. Acad. Sci. USA,* 102**,** 13956-61.

Medina-Gudiño, J., Rivera-Garcia, A., Santos-Ferro, L., Ramirez-Orejel, J. C., Agredano-Moreno, L. T., Jimenez-Garcia, L. F., Paez-Esquiliano, D., Martinez-Vidal, S., Andrade-Esquivel, E. & Cano-Buendia, J. A. 2020. Analysis of neutral electrolyzed water anti-bacterial activity on contaminated eggshells with *Salmonella enterica* or *Escherichia coli*. *Int. J. Food Microbiol.,* 320**,** 108538.

Meireles, A., Ferreira, C., Melo, L. & Simões, M. 2017. Comparative stability and efficacy of selected chlorine-based biocides against *Escherichia coli* in planktonic and biofilm states. *Food Res. Int.,* 102**,** 511-518.

Melnyk, R. A., Youngblut, M. D., Clark, I. C., Carlson, H. K., Wetmore, K. M., Price, M. N., Iavarone, A. T., Deutschbauer, A. M., Arkin, A. P., Coates, J. D. & Moran, M. A. 2015. Novel mechanism for scavenging of hypochlorite involving a periplasmic methionine-rich peptide and methionine sulfoxide reductase. *mBio,* 6**,** e00233-15.

Menant, A., Barbey, R. & Thomas, D. 2006. Substrate-mediated remodeling of methionine transport by multiple ubiquitin-dependent mechanisms in yeast cells. *EMBO J.,* 25**,** 4436-47.

Meng, X., Khoso, S. A., Jiang, F., Zhang, Y., Yue, T., Gao, J., Lin, S., Liu, R., Gao, Z., Chen, P., Wang, L., Han, H., Tang, H., Sun, W. & Hu, Y. 2020. Removal of chemical oxygen demand and ammonia nitrogen from lead smelting wastewater with high salts content using electrochemical oxidation combined with coagulation–flocculation treatment. *Sep. Purif. Technol.,* 235**,** 116233.

Mikutta, R., Kleber, M., Kaiser, K. & Jahn, R. 2005. Review: organic matter removal from soils using hydrogen peroxide, sodium hypochlorite, and disodium peroxodisulfate. *Soil Sci. Soc. Am. J.,* 69**,** 120-135.

Milisavljevic, M. & Kojic, M. 2020. A comparative study of liquid holding restitution of viability after oxidative stress in *Ustilago maydis* and *Saccharomyces cerevisiae* cell populations. *Fungal Genet. Biol.,* 134**,** 103284.

Mishra, V., Abrol, G. S. & Dubey, N. 2018. Chapter 14 - Sodium and calcium hypochlorite as postharvest disinfectants for fruits and vegetables. *In:* Siddiqui, M. W. (ed.) *Postharvest Disinfection of Fruits and Vegetables.* London, UK: Academic Press.

Misra, N. N., Moiseev, T., Patil, S., Pankaj, S. K., Bourke, P., Mosnier, J. P., Keener, K. M. & Cullen, P. J. 2014. Cold plasma in modified atmospheres for post-harvest treatment of strawberries. *Food Bioprocess Technol.,* 7**,** 3045-3054.

Mokudai, T., Kanno, T. & Niwano, Y. 2015. Postantifungal-like effect of sublethal treatment of *Candida albicans* with acid-electrolyzed water. *Arch. Oral Biol.,* 60**,** 479-487.

Mons, C., Botzanowski, T., Nikolaev, A., Hellwig, P., Cianférani, S., Lescop, E., Bouton, C. & Golinelli-Cohen, M.-P. 2018. The H_2O_2-resistant Fe–S redox

switch MitoNEET acts as a pH sensor to repair stress-damaged Fe–S protein. *Biochemistry,* 57**,** 5616-5628.
Mood, E. W. 1950. Effect of free and combined available residual chlorine upon bacteria in swimming pools. *Am. J. Public Health Nations Health,* 40**,** 459-466.
Moreira, M. R., Álvarez, M. V., Martín-Belloso, O. & Soliva-Fortuny, R. 2017. Effects of pulsed light treatments and pectin edible coatings on the quality of fresh-cut apples: a hurdle technology approach. *J. Sci. Food Agric.,* 97**,** 261-268.
Morita, C., Nishida, T. & Ito, K. 2011. Biological toxicity of acid electrolyzed functional water: effect of oral administration on mouse digestive tract and changes in body weight. *Arch. Oral. Biol.,* 56**,** 359-66.
Moulis, J. M. & Meyer, J. 1982. Characterization of the selenium-substituted 2[4Fe-4Se] ferredoxin from *Clostridium pasteurianum*. *Biochemistry,* 21**,** 4762-4771.
Mullaney, E. J., Daly, C. B. & Ullah, A. H. J. 2000. Advances in phytase research. *Adv. Appl. Microbiol.,* 47**,** 157-199.
Musich, R., Cadle-Davidson, L. & Osier, M. V. 2021. Comparison of short-read sequence aligners indicates strengths and weaknesses for biologists to consider. *Front. Plant Sci.,* 12.
Nagy, P. & Ashby, M. T. 2005. Reactive sulfur species: kinetics and mechanism of the oxidation of cystine by hypochlorous acid to give N,N`-dichlorocystine. *Chem. Res. Toxicol.,* 18**,** 919-923.
Nanba, M., Nomura, K., Nasuhara, Y., Hayashi, M., Kido, M., Hayashi, M., Iguchi, A., Shigematsu, T., Hirayama, M., Ueno, S. & Fujii, T. 2013. Importance of cell damage causing growth delay for high pressure inactivation of *Saccharomyces cerevisiae*. *High Press. Res.,* 33**,** 299-307.
Narahari, J., Ma, R., Wang, M. & Walden, W. E. 2000. The aconitase function of iron regulatory protein 1. Genetic studies in yeast implicate its role in iron-mediated redox regulation. *J. Biol. Chem.,* 275**,** 16227-34.
Navarro-Rico, J., Artés-Hernández, F., Gómez, P. A., Núñez-Sánchez, M. Á., Artés, F. & Martínez-Hernández, G. B. 2014. Neutral and acidic electrolysed water kept microbial quality and health promoting compounds of fresh-cut broccoli throughout shelf life. *Innov. Food Sci. Emerg. Technol.,* 21**,** 74-81.
Nelder, J. A. & Wedderburn, R. W. M. 1972. Generalized linear models. *J. R. Stat. Soc. Ser. A,* 135**,** 370-384.
Netzer, N., Goodenbour, J. M., David, A., Dittmar, K. A., Jones, R. B., Schneider, J. R., Boone, D., Eves, E. M., Rosner, M. R., Gibbs, J. S., Embry, A., Dolan, B., Das, S., Hickman, H. D., Berglund, P., Bennink, J. R., Yewdell, J. W. & Pan, T. 2009. Innate immune and chemically triggered oxidative stress modifies translational fidelity. *Nature,* 462**,** 522-526.
Niazmand, R. & Yeganehzad, S. 2020. Capability of oxygen-scavenger sachets and modified atmosphere packaging to extend fresh barberry shelf life. *Chem. Biol. Technol. Agric.,* 7**,** 28.
Nicklow, E. E. & Sevier, C. S. 2020. Activity of the yeast cytoplasmic Hsp70 nucleotide-exchange factor Fes1 is regulated by reversible methionine oxidation. *J. Biol. Chem.,* 295**,** 552-569.
Noonim, P., Mahakarnchanakul, W., Nielsen, K. F., Frisvad, J. C. & Samson, R. A. 2009. Fumonisin B2 production by *Aspergillus niger* in Thai coffee beans. *Food Addit. Contam. Part A,* 26**,** 94-100.
Novodvorska, M., Hayer, K., Pullan, S. T., Wilson, R., Blythe, M. J., Stam, H., Stratford, M. & Archer, D. B. 2013. Trancriptional landscape of *Aspergillus niger* at breaking of conidial dormancy revealed by RNA-sequencing. *BMC Genomics,* 14**,** 246.
Novodvorska, M., Stratford, M., Blythe, M. J., Wilson, R., Beniston, R. G. & Archer, D. B. 2016. Metabolic activity in dormant conidia of *Aspergillus niger* and

developmental changes during conidial outgrowth. *Fungal Genet. Biol.,* 94**,** 23-31.

O'Gorman, C. M., Fuller, H. T. & Dyer, P. S. 2009. Discovery of a sexual cycle in the opportunistic fungal pathogen *Aspergillus fumigatus*. *Nature,* 457**,** 471-474.

Ogunniyi, A. D., Dandie, C. E., Brunetti, G., Drigo, B., Aleer, S., Hall, B., Ferro, S., Deo, P., Venter, H., Myers, B., Donner, E. & Lombi, E. 2021. Neutral electrolyzed oxidizing water is effective for pre-harvest decontamination of fresh produce. *Food Microbiol.,* 93**,** 103610.

Ogunniyi, A. D., Dandie, C. E., Ferro, S., Hall, B., Drigo, B., Brunetti, G., Venter, H., Myers, B., Deo, P., Donner, E. & Lombi, E. 2019. Comparative antibacterial activities of neutral electrolyzed oxidizing water and other chlorine-based sanitizers. *Sci. Rep.,* 9**,** 19955.

Oh, D.-H., Khan, I. & Tango, C. N. 2019. Hurdle enhancement of electrolyzed water with other techniques. *In:* Ding, T., Oh, D.-H. & Liu, D. (eds.) *Electrolyzed Water in Food: Fundamentals and Applications.* Singapore: Springer Singapore.

Okull, D. O. & Laborde, L. F. 2004. Activity of electrolyzed oxidizing water against *Penicilium expansum* in suspension and on wounded apples. *J. Food Sci.,* 69**,** FMS23-FMS27.

Olaimat, A. N. & Holley, R. A. 2012. Factors influencing the microbial safety of fresh produce: a review. *Food Microbiol.,* 32**,** 1-19.

Olin-Sandoval, V., Yu, J. S. L., Miller-Fleming, L., Alam, M. T., Kamrad, S., Correia-Melo, C., Haas, R., Segal, J., Peña Navarro, D. A., Herrera-Dominguez, L., Méndez-Lucio, O., Vowinckel, J., Mülleder, M. & Ralser, M. 2019. Lysine harvesting is an antioxidant strategy and triggers underground polyamine metabolism. *Nature,* 572**,** 249-253.

Ollagnier-de-Choudens, S., Mattioli, T., Takahashi, Y. & Fontecave, M. 2001. Iron-sulfur cluster assembly: characterization of IscA and evidence for a specific and functional complex with ferrodoxin. *J. Biol. Chem.,* 276**,** 22604-22607.

Oms-Oliu, G., Rojas-Graü, M. A., González, L. A., Varela, P., Soliva-Fortuny, R., Hernando, M. I. H., Munuera, I. P., Fiszman, S. & Martín-Belloso, O. 2010. Recent approaches using chemical treatments to preserve quality of fresh-cut fruit: a review. *Postharvest Biol. Technol.,* 57**,** 139-148.

Oomori, T., Oka, T., Inuta, T. & Arata, Y. 2000. The efficiency of disinfection of acidic electrolyzed water in the presence of organic materials. *Anal. Sci.,* 16**,** 365-369.

Ouni, I., Flick, K. & Kaiser, P. 2010. A transcriptional activator is part of an SCF ubiquitin ligase to control degradation of its cofactors. *Mol. Cell,* 40**,** 954-64.

Ovissipour, M., Shiroodi, S. G., Rasco, B., Tang, J. & Sablani, S. S. 2018. Electrolyzed water and mild-thermal processing of Atlantic salmon (*Salmo salar*): reduction of *Listeria monocytogenes* and changes in protein structure. *Int. J. Food Microbiol.,* 276**,** 10-19.

Paege, N., Jung, S., Schäpe, P., Müller-Hagen, D., Ouedraogo, J.-P., Heiderich, C., Jedamzick, J., Nitsche, B. M., van den Hondel, C. A., Ram, A. F. & Meyer, V. 2016. A transcriptome meta-analysis proposes novel biological roles for the antifungal protein AnAFP in *Aspergillus niger*. *PLOS ONE,* 11**,** e0165755.

Palou, L. 2014. Chapter 2 - *Penicillium digitatum*, *Penicillium italicum* (green mold, blue mold). *In:* Bautista-Baños, S. (ed.) *Postharvest Decay.* San Diego: Academic Press.

Palou, L., Valencia-Chamorro, S. A. & Pérez-Gago, M. B. 2015. Antifungal edible coatings for fresh citrus fruit: a review. *Coatings,* 5**,** 962-986.

Panasenko, O. M., Gorudko, I. V. & Sokolov, A. V. 2013. Hypochlorous acid as a precursor of free radicals in living systems. *Biochemistry (Mosc.),* 78**,** 1466-1489.

Pandey, N., Joshi, S. K., Singh, C. P., Kumar, S., Rajput, S. & Khandal, R. K. 2013. Enhancing shelf life of litchi (*Litchi chinensis*) fruit through integrated approach of surface coating and gamma irradiation. *Radiat. Phys. Chem. Oxf. Engl. 1993,* 85**,** 197-203.

Pankaj, S. K., Shi, H. & Keener, K. M. 2018. A review of novel physical and chemical decontamination technologies for aflatoxin in food. *Trends Food Sci. Technol.,* 71**,** 73-83.

Papageorgiou, A., Stylianou, S. K., Kaffes, P., Zouboulis, A. I. & Voutsa, D. 2017. Effects of ozonation pretreatment on natural organic matter and wastewater derived organic matter – possible implications on the formation of ozonation by-products. *Chemosphere,* 170**,** 33-40.

Pappen, F. G., Qian, W., Aleksejūnienė, J., de Toledo Leonardo, R., Leonardo, M. R. & Haapasalo, M. 2010. Inhibition of sodium hypochlorite antimicrobial activity in the presence of bovine serum albumin. *J. Endod.,* 36**,** 268-271.

Park, C.-M., Hung, Y.-C., Lin, C.-S. & Brackett, R. E. 2005. Efficacy of electrolyzed water in inactivating *Salmonella* Enteritidis and *Listeria monocytogenes* on shell eggs. *J. Food Prot.,* 68**,** 986-990.

Pattison, D. I. & Davies, M. J. 2001. Absolute rate constants for the reaction of hypochlorous acid with protein side chains and peptide bonds. *Chem. Res. Toxicol.,* 14**,** 1453-1464.

Pattison, D. I. & Davies, M. J. 2005. Kinetic analysis of the role of histidine chloramines in hypochlorous acid mediated protein oxidation. *Biochemistry,* 44**,** 7378-7387.

Pattison, D. I., Hawkins, C. L. & Davies, M. J. 2007. Hypochlorous acid-mediated protein oxidation: how important are chloramine transfer reactions and protein tertiary structure? *Biochemistry,* 46**,** 9853-9864.

Paul, V. D., Mühlenhoff, U., Stümpfig, M., Seebacher, J., Kugler, K. G., Renicke, C., Taxis, C., Gavin, A.-C., Pierik, A. J. & Lill, R. 2015. The deca-GX3 proteins Yae1-Lto1 function as adaptors recruiting the ABC protein Rli1 for iron-sulfur cluster insertion. *eLife,* 4**,** e08231.

Pazouki, M. & Panda, T. 2000. Understanding the morphology of fungi. *Bioprocess Engineering,* 22**,** 127-143.

Peñalosa-Ruiz, G., Aranda, C., Ongay-Larios, L., Colon, M., Quezada, H. & Gonzalez, A. 2012. Paralogous ALT1 and ALT2 retention and diversification have generated catalytically active and inactive aminotransferases in *Saccharomyces cerevisiae*. *PLoS One,* 7**,** e45702.

Perrone, G., Susca, A., Cozzi, G., Ehrlich, K., Varga, J., Frisvad, J. C., Meijer, M., Noonim, P., Mahakarnchanakul, W. & Samson, R. A. 2007. Biodiversity of *Aspergillus* species in some important agricultural products. *Stud. Mycol.,* 59**,** 53-66.

Peskin, A. V. & Winterbourn, C. C. 2001. Kinetics of the reactions of hypochlorous acid and amino acid chloramines with thiols, methionine, and ascorbate. *Free Radic. Biol. Med.,* 30**,** 572-579.

Petti, A. A., Crutchfield, C. A., Rabinowitz, J. D. & Botstein, D. 2011. Survival of starving yeast is correlated with oxidative stress response and nonrespiratory mitochondrial function. *Proc. Natl. Acad. Sci. USA,* 108**,** E1089-98.

Petti, A. A., McIsaac, R. S., Ho-Shing, O., Bussemaker, H. J. & Botstein, D. 2012. Combinatorial control of diverse metabolic and physiological functions by transcriptional regulators of the yeast sulfur assimilation pathway. *Mol. Biol. Cell,* 23**,** 3008-24.

Pfuntner, A. 2011. Sanitizers and disinfectants: the chemicals of prevention. *Food Safety Magazine (online).* https://www.food-safety.com/articles/6707-sanitizers-and-disinfectants-the-chemicals-of-prevention accessed March 2021.

Pichel, N., Vivar, M. & Fuentes, M. 2019. The problem of drinking water access: a review of disinfection technologies with an emphasis on solar treatment methods. *Chemosphere,* 218**,** 1014-1030.

Piedrafita, G., Keller, M. A. & Ralser, M. 2015. The impact of non-enzymatic reactions and enzyme promiscuity on cellular metabolism during (oxidative) stress conditions. *Biomolecules,* 5**,** 2101-22.

Pierrel, F., Hamelin, O., Douki, T., Kieffer-Jaquinod, S., Mühlenhoff, U., Ozeir, M., Lill, R. & Fontecave, M. 2010. Involvement of mitochondrial ferredoxin and para-aminobenzoic acid in yeast coenzyme Q biosynthesis. *Chem. Biol.,* 17**,** 449-59.

Pinto, C. A., Moreira, S. A., Fidalgo, L. G., Inácio, R. S., Barba, F. J. & Saraiva, J. A. 2020. Effects of high-pressure processing on fungi spores: factors affecting spore germination and inactivation and impact on ultrastructure. *Compr. Rev. Food Sci. Food Saf.,* 19**,** 553-573.

Pischetsrieder, M., Larisch, B. & Severin, T. 1998. The Maillard Reaction of ascorbic acid with amino acids and proteins - identification of products. *In:* O'Brien, J., Nursten, H. E., Crabbe, M. J. C. & Ames, J. M. (eds.) *The Maillard Reaction in Foods and Medicine.* Cambridge, UK: The Royal Society of Chemistry.

Poole, L. B. 2015. The basics of thiols and cysteines in redox biology and chemistry. *Free Radic. Biol. Med.,* 80**,** 148-157.

Pradhan, S., Flores, F. J., Melouk, H., Walker, N. R., Molineros, J. E. & Garzon, C. D. 2017. Chemical hormesis on plant pathogenic fungi and oomycetes. *In:* Duke, S. O., Kudsk, P. & Solomon, K. (eds.) *Pesticide Dose: Effects on the Environment and Target and Non-Target Organisms.* Washington, DC: American Chemical Society.

Priyadarshini, E., Priyadarshini, S. S., Cousins, B. G. & Pradhan, N. 2021. Metal-fungus interaction: review on cellular processes underlying heavy metal detoxification and synthesis of metal nanoparticles. *Chemosphere,* 274**,** 129976.

Punt, M., van den Brule, T., Teertstra, W. R., Dijksterhuis, J., den Besten, H. M. W., Ohm, R. A. & Wösten, H. A. B. 2020. Impact of maturation and growth temperature on cell-size distribution, heat-resistance, compatible solute composition and transcription profiles of *Penicillium roqueforti* conidia. *Food Res. Int.,* 136**,** 109287.

Qi, H., Huang, Q. & Hung, Y.-C. 2018. Effectiveness of electrolyzed oxidizing water treatment in removing pesticide residues and its effect on produce quality. *Food Chem.,* 239**,** 561-568.

Qiu, T. A., Nguyen, T. H. T., Hudson-Smith, N. V., Clement, P. L., Forester, D.-C., Frew, H., Hang, M. N., Murphy, C. J., Hamers, R. J., Feng, Z. V. & Haynes, C. L. 2017. Growth-based bacterial viability assay for interference-free and high-throughput toxicity screening of nanomaterials. *Anal. Chem.,* 89**,** 2057-2064.

Raftery, M. J. 2007. Detection and characterization of N-α-chloramines by electrospray tandem mass spectrometry. *Anal. Biochem.,* 366**,** 218-227.

Rahman, S. M. E., Jin, Y.-G. & Oh, D.-H. 2011. Combination treatment of alkaline electrolyzed water and citric acid with mild heat to ensure microbial safety, shelf-life and sensory quality of shredded carrots. *Food Microbiol.,* 28**,** 484-491.

Rahman, S. M. E., Khan, I. & Oh, D. H. 2016. Electrolyzed water as a novel sanitizer in the food industry: current trends and future perspectives. *Compr. Rev. Food Sci. Food Saf.,* 15**,** 471-490.

Rahman, S. M. E., Park, J., Wang, J. & Oh, D.-H. 2012. Stability of low concentration electrolyzed water and its sanitization potential against foodborne pathogens. *J. Food Eng.,* 113**,** 548–553.

Rainer, J., Peintner, U. & Pöder, R. 2001. Biodiversity and concentration of airborne fungi in a hospital environment. *Mycopathologia,* 149**,** 87.

Ramírez Orejel, J. C. & Cano-Buendía, J. A. 2020. Applications of electrolyzed water as a sanitizer in the food and animal-by products industry. *Processes,* 8**,** 534.

Redmile-Gordon, M. A., Armenise, E., White, R. P., Hirsch, P. R. & Goulding, K. W. T. 2013. A comparison of two colorimetric assays, based upon Lowry and Bradford techniques, to estimate total protein in soil extracts. *Soil Biol. Biochem.,* 67**,** 166-173.

Reis, R., Sipahi, H., Dinc, O., Kavaz, T., Charehsaz, M., Dimoglo, A. & Aydın, A. 2020. Toxicity, mutagenicity and stability assessment of simply produced electrolyzed water as a wound healing agent in vitro. *Hum. Exp. Toxicol.,* 40**,** 452-463.

Ribeiro, M. S. S., Freitas-Silva, O., Castro, I. M., Teixeira, A., Marques-da-Silva, S. H., Sales-Moraes, A. C. S., Abreu, L. F. & Sousa, C. L. 2020. Efficacy of sodium hypochlorite and peracetic acid against *Aspergillus nomius* in Brazil nuts. *Food Microbiol.,* 90**,** 103449.

Richardson, S. D., Plewa, M. J., Wagner, E. D., Schoeny, R. & Demarini, D. M. 2007. Occurrence, genotoxicity, and carcinogenicity of regulated and emerging disinfection by-products in drinking water: a review and roadmap for research. *Mutat. Res.,* 636**,** 178-242.

Rimmer, D. L. 2006. Free radicals, antioxidants, and soil organic matter recalcitrance. *Eur. J. Soil Sci.,* 57**,** 91-94.

Riquelme, M., Aguirre, J., Bartnicki-García, S., Braus, G. H., Feldbrügge, M., Fleig, U., Hansberg, W., Herrera-Estrella, A., Kämper, J., Kück, U., Mouriño-Pérez, R. R., Takeshita, N. & Fischer, R. 2018. Fungal morphogenesis, from the polarized growth of hyphae to complex reproduction and infection structures. *Microbiol. Mol. Biol. Rev.,* 82**,** e00068-17.

Rivera-Garcia, A., Santos-Ferro, L., Ramirez-Orejel, J. C., Agredano-Moreno, L. T., Jimenez-Garcia, L. F., Paez-Esquiliano, D., Andrade-Esquivel, E. & Cano-Buendia, J. A. 2019. The effect of neutral electrolyzed water as a disinfectant of eggshells artificially contaminated with *Listeria monocytogenes*. *Food Sci. Nutr.,* 7**,** 2252-2260.

Robinson, G., Thorn, R. & Reynolds, D. 2013. The effect of long-term storage on the physiochemical and bactericidal properties of electrochemically activated solutions. *Int. J. Mol. Sci.,* 14**,** 457-469.

Robinson, M. D., McCarthy, D. J. & Smyth, G. K. 2010. edgeR: a Bioconductor package for differential expression analysis of digital gene expression data. *Bioinformatics,* 26**,** 139-140.

Roche, R., Bain, R. & Cumming, O. 2017. A long way to go – estimates of combined water, sanitation and hygiene coverage for 25 sub-Saharan African countries. *PLOS ONE,* 12**,** e0171783.

Romanos, M. A., Scorer, C. A. & Clare, J. J. 1992. Foreign gene expression in yeast: a review. *Yeast,* 8**,** 423-88.

Romsang, A., Duang-Nkern, J., Khemsom, K., Wongsaroj, L., Saninjuk, K., Fuangthong, M., Vattanaviboon, P. & Mongkolsuk, S. 2018. *Pseudomonas aeruginosa ttcA* encoding tRNA-thiolating protein requires an iron-sulfur cluster to participate in hydrogen peroxide-mediated stress protection and pathogenicity. *Sci. Rep.,* 8**,** 11882-11882.

Rosen, H., Klebanoff, S. J., Wang, Y., Brot, N., Heinecke, J. W. & Fu, X. 2009. Methionine oxidation contributes to bacterial killing by the myeloperoxidase system of neutrophils. *Proc. Natl. Acad. Sci. USA,* 106**,** 18686-18691.

Ross, R. P., Morgan, S. & Hill, C. 2002. Preservation and fermentation: past, present and future. *Int. J. Food Microbiol.,* 79**,** 3-16.

Ruijter, G. J. G., Bax, M., Patel, H., Flitter, S. J., van de Vondervoort, P. J. I., de Vries, R. P., Vankuyk, P. A. & Visser, J. 2003. Mannitol is required for stress tolerance in *Aspergillus niger* conidiospores. *Eukaryot. Cell,* 2**,** 690-698.

Sadhu, M. J., Moresco, J. J., Zimmer, A. D., Yates, J. R. r. & Rine, J. 2014. Multiple inputs control sulfur-containing amino acid synthesis in *Saccharomyces cerevisiae*. *Mol. Biol. Cell,* 25**,** 1653-1665.

Sakurai, Y., Nakatsu, M., Sato, Y. & Sato, K. 2003. Endoscope contamination from HBV- and HCV-positive patients and evaluation of a cleaning/disinfecting method using strongly acidic electrolyzed water. *Dig. Endosc.,* 15**,** 19-24.

Sandle, T. 2017. The European approach to disinfectant qualification. *La Vague,* 52**,** 45-48.

Savary, S., Ficke, A., Aubertot, J.-N. & Hollier, C. 2012. Crop losses due to diseases and their implications for global food production losses and food security. *Food Sec.,* 4**,** 519-537.

Schindeldecker, M. & Moosmann, B. 2015. Protein-borne methionine residues as structural antioxidants in mitochondria. *Amino Acids,* 47**,** 1421-1432.

Schuller, A. P. & Green, R. 2017. The ABC(E1)s of ribosome recycling and reinitiation. *Mol. Cell,* 66**,** 578-580.

Schuster, E., Dunn-Coleman, N., Frisvad, J. & van Dijck, P. 2002. On the safety of *Aspergillus niger* – a review. *Appl. Microbiol. Biotechnol.,* 59**,** 426-435.

Schwabe, A. & Bruggeman, F. J. 2014. Single yeast cells vary in transcription activity not in delay time after a metabolic shift. *Nat. Commun.,* 5**,** 4798.

Sekido, K. & Kitaori, N. 2008. Development of a small-sized generator of ozonated water using an electro-conductive diamond electrode. *Biocontrol Sci.,* 13**,** 119-123.

Setsukinai, K., Urano, Y., Kakinuma, K., Majima, H. J. & Nagano, T. 2003. Development of novel fluorescence probes that can reliably detect reactive oxygen species and distinguish specific species. *J. Biol. Chem.,* 278**,** 3170-3175.

Shaner, N. C., Campbell, R. E., Steinbach, P. A., Giepmans, B. N. G., Palmer, A. E. & Tsien, R. Y. 2004. Improved monomeric red, orange and yellow fluorescent proteins derived from *Discosoma* sp. red fluorescent protein. *Nat. Biotechnol.,* 22**,** 1567-1572.

Sharma, V. K. & Graham, N. J. D. 2010. Oxidation of amino acids, peptides and proteins by ozone: a review. *Ozone Sci. Eng.,* 32**,** 81-90.

Sheehan, G., Nagl, M. & Kavanagh, K. 2019. Exposure to N-chlorotaurine induces oxidative stress responses in *Aspergillus fumigatus*. *J. Med. Microbiol.,* 68**,** 279-288.

Sheng, L., Shen, X., Ulloa, O., Suslow, T. V., Hanrahan, I. & Zhu, M.-J. 2020. Evaluation of JC9450 and neutral electrolyzed water in controlling *Listeria monocytogenes* on fresh apples and preventing cross-contamination. *Front. Microbiol.,* 10**,** 3128.

Sideri, T. C., Willetts, S. A. & Avery, S. V. 2009. Methionine sulphoxide reductases protect iron-sulphur clusters from oxidative inactivation in yeast. *Microbiology,* 155**,** 612-623.

Sies, H., Berndt, C. & Jones, D. P. 2017. Oxidative stress. *Annu. Rev. Biochem.,* 86**,** 715-748.

Singh, J. 1994. Nature and extent of deterioration in buildings due to fungi. *In:* Singh, J. (ed.) *Building Mycology: Management of Decay and Health in Buildings.* London, UK: Chapman & Hall.

Singh, Z., Khan, A., Zhu, S. & Payne, A. 2013. Nitric oxide in the regulation of fruit ripening: challenges and thrusts. *Stewart Postharvest Rev.,* 9**,** 1-11.

Slavin, J. L. & Lloyd, B. 2012. Health benefits of fruits and vegetables. *Adv. Nutr.,* 3**,** 506-516.

Sleutel, S., Leinweber, P., Ara Begum, S., Kader, M. A. & De Neve, S. 2009. Shifts in soil organic matter composition following treatment with sodium hypochlorite and hydrofluoric acid. *Geoderma,* 149**,** 257-266.

Small, D. A., Chang, W., Toghrol, F. & Bentley, W. E. 2007. Toxicogenomic analysis of sodium hypochlorite antimicrobial mechanisms in *Pseudomonas aeruginosa*. *Appl. Microbiol. Biotechnol.,* 74**,** 176-185.

Smith, M. C., Sumner, E. R. & Avery, S. V. 2007. Glutathione and Gts1p drive beneficial variability in the cadmium resistances of individual yeast cells. *Mol. Microbiol.,* 66**,** 699-712.

Snyder, A. B. & Worobo, R. W. 2018. Fungal spoilage in food processing. *J. Food Prot.,* 81**,** 1035-1040.

Spooner, R. & Yilmaz, Ö. 2011. The role of reactive-oxygen-species in microbial persistence and inflammation. *Int. J. Mol. Sci.,* 12**,** 334-352.

Srinivasan, R. & Sorial, G. A. 2009. Treatment of perchlorate in drinking water: a critical review. *Sep. Purif. Technol.,* 69**,** 7-21.

Stadtman, E. R. 1991. Ascorbic acid and oxidative inactivation of proteins. *Am. J. Clin. Nutr.,* 54**,** 1125s-1128s.

Stadtman, E. R. & Levine, R. L. 2003. Free radical-mediated oxidation of free amino acids and amino acid residues in proteins. *Amino Acids,* 25**,** 207-218.

Steele, M. & Odumeru, J. 2004. Irrigation water as source of foodborne pathogens on fruit and vegetables. *J. Food Prot.,* 67**,** 2839-2849.

Stefán, D., Erdélyi, N., Izsák, B., Záray, G. & Vargha, M. 2019. Formation of chlorination by-products in drinking water treatment plants using breakpoint chlorination. *Microchem. J.,* 149**,** 104008.

Stehling, O., Vashisht, A. A., Mascarenhas, J., Jonsson, Z. O., Sharma, T., Netz, D. J. A., Pierik, A. J., Wohlschlegel, J. A. & Lill, R. 2012. MMS19 assembles iron-sulfur proteins required for DNA metabolism and genomic integrity. *Science,* 337**,** 195.

Stemmler, T. L., Lesuisse, E., Pain, D. & Dancis, A. 2010. Frataxin and mitochondrial FeS cluster biogenesis. *J. Biol. Chem.,* 285**,** 26737-43.

Sterflinger, K. 2010. Fungi: their role in deterioration of cultural heritage. *Fungal Biol. Rev.,* 24**,** 47-55.

Sterflinger, K. & Pinzari, F. 2012. The revenge of time: fungal deterioration of cultural heritage with particular reference to books, paper and parchment. *Environ. Microbiol.,* 14**,** 559-566.

Storkey, C., Davies, M. J. & Pattison, D. I. 2014. Reevaluation of the rate constants for the reaction of hypochlorous acid (HOCl) with cysteine, methionine, and peptide derivatives using a new competition kinetic approach. *Free Radic. Biol. Med.,* 73**,** 60-66.

Stratford, M., Steels, H., Nebe-von-Caron, G., Avery, S. V., Novodvorska, M. & Archer, D. B. 2014. Population heterogeneity and dynamics in starter culture and lag phase adaptation of the spoilage yeast *Zygosaccharomyces bailii* to weak acid preservatives. *Int. J. Food Microbiol.,* 181**,** 40-47.

Stratford, M., Vallières, C., Geoghegan, I. A., Archer, D. B. & Avery, S. V. 2020. The preservative sorbic acid targets respiration, explaining the resistance of fermentative spoilage yeast species. *mSphere,* 5**,** e00273-20.

Sumner, E. R., Shanmuganathan, A., Sideri, T. C., Willetts, S. A., Houghton, J. E. & Avery, S. V. 2005. Oxidative protein damage causes chromium toxicity in yeast. *Microbiology,* 151**,** 1939-1948.

Szabó, M., Simon, F. & Fábián, I. 2019. The formation of N-chloramines with proteinogenic amino acids. *Water Res.,* 165**,** 114994.

Takeda, Y., Uchiumi, H., Matsuda, S. & Ogawa, H. 2020. Acidic electrolyzed water potently inactivates SARS-CoV-2 depending on the amount of free available chlorine contacting with the virus. *Biochem. Biophys. Res. Commun.,* 530**,** 1-3.

Tamura, S., Wada, C., Hase, A., Kanamitsu, K. & Ikeda, S. 2010. A simple growth test of a *Saccharomyces cerevisiae* Cu, Zn-superoxide dismutase-deficient mutant in hypertonic medium for biological evaluation of antioxidants. *Food Sci. Technol. Res.,* 16**,** 267-272.

Tanaka, Y., Saihara, Y., Izumotani, K. & Nakamura, H. 2019. Daily ingestion of alkaline electrolyzed water containing hydrogen influences human health, including gastrointestinal symptoms. *Med. Gas Res.,* 8**,** 160-166.

Taniwaki, M. H., Pitt, J. I. & Magan, N. 2018. *Aspergillus* species and mycotoxins: occurrence and importance in major food commodities. *Curr. Opin. Food Sci.,* 23**,** 38-43.

Tarrago, L., Grosse, S., Lemaire, D., Faure, L., Tribout, M., Siponen, M. I., Kojadinovic-Sirinelli, M., Pignol, D., Arnoux, P. & Sabaty, M. 2020. Reduction of protein bound methionine sulfoxide by a periplasmic dimethyl sulfoxide reductase. *Antioxidants (Basel),* 9**,** 616.

Tarrago, L., Kaya, A., Weerapana, E., Marino, S. M. & Gladyshev, V. N. 2012. Methionine sulfoxide reductases preferentially reduce unfolded oxidized proteins and protect cells from oxidative protein unfolding. *J. Biol. Chem.,* 287**,** 24448-24459.

Tazebay, U. H., Sophianopoulou, V., Cubero, B., Scazzocchio, C. & Diallinas, G. 1995. Post-transcriptional control and kinetic characterization of proline transport in germinating conidiospores of *Aspergillus nidulans*. *FEMS Microbiol. Lett.,* 132**,** 27-37.

Tchobanoglous, G., Burton, F. L. & Stensel, H. D. 2003. *Wastewater Engineering: Treatment and Reuse,* China, McGraw-Hill Companies, Inc.

Teertstra, W. R., Tegelaar, M., Dijksterhuis, J., Golovina, E. A., Ohm, R. A. & Wösten, H. A. B. 2017. Maturation of conidia on conidiophores of *Aspergillus niger*. *Fungal Genet. Biol.,* 98**,** 61-70.

Tegelaar, M., Bleichrodt, R.-J., Nitsche, B., Ram, A. F. J. & Wösten, H. A. B. 2020. Subpopulations of hyphae secrete proteins or resist heat stress in *Aspergillus oryzae* colonies. *Environ. Microbiol.,* 22**,** 447-455.

The World Bank, Natural Resources Institute (UK) & FAO 2011. Missing food: the case of postharvest grain losses in sub-saharan Africa. *The International Bank for Reconstruction and Development.* Washington, DC: The World Bank.

Thostenson, J. O., Mourouvin, R., Hawkins, B. T., Ngaboyamahina, E., Sellgren, K. L., Parker, C. B., Deshusses, M. A., Stoner, B. R. & Glass, J. T. 2018. Improved blackwater disinfection using potentiodynamic methods with oxidized boron-doped diamond electrodes. *Water Res.,* 140**,** 191-199.

Tian, F., Lee, S. Y., Woo, S. Y., Choi, H. Y., Heo, S., Nah, G. & Chun, H. S. 2021. Transcriptomic responses of *Aspergillus flavus* to temperature and oxidative stresses during aflatoxin production. *Sci. Rep.,* 11**,** 2803.

Timmermans, R., Hayrapetyan, H., Vollebregt, M. & Dijksterhuis, J. 2020. Comparing thermal inactivation to a combined process of moderate heat and high pressure: effect on ascospores in strawberry puree. *Int. J. Food Microbiol.,* 325**,** 108629.

Trinci, A. P. J. 1971. Influence of the width of the peripheral growth zone on the radial growth rate of fungal colonies on solid media. *Microbiology,* 67**,** 325-344.

Tudela, J. A., López-Gálvez, F., Allende, A., Hernández, N., Andújar, S., Marín, A., Garrido, Y. & Gil, M. I. 2019. Operational limits of sodium hypochlorite for different fresh produce wash water based on microbial inactivation and disinfection by-products (DBPs). *Food Control,* 104**,** 300-307.

Ünal, N., Karadağ, A., Yanık, K., Bilgin, K., Günaydın, M. & Birinci, A. 2014. Analysis of *in vitro* efficiency of electrolyzed water against fungi species frequently detected in nosocomial infections. *Univers. J. Microbiol. Res.,* 2**,** 50-55.

USEPA 2009. Safe drinking water act (SDWA): national primary drinking water regulations. *EPA 816-F-09-004 (online).* https://www.epa.gov/ground-water-and-drinking-water/national-primary-drinking-water-regulations accessed 22 May 2020.

Vallières, C., Holland, S. L. & Avery, S. V. 2017. Mitochondrial ferredoxin determines vulnerability of cells to copper excess. *Cell Chem. Biol.,* 24**,** 1228-1237.

Vallières, C., Singh, N., Alexander, C. & Avery, S. V. 2020. Repurposing nonantifungal approved drugs for synergistic targeting of fungal pathogens. *ACS Infect. Dis.,* 6**,** 2950-2958.

Valverde, H., Cantón, F. R. & Aledo, J. C. 2019. MetOSite: an integrated resource for the study of methionine residues sulfoxidation. *Bioinformatics,* 35**,** 4849-4850.

van den Brule, T., Lee, C. L. S., Houbraken, J., Haas, P.-J., Wösten, H. A. B. & Dijksterhuis, J. 2020. Conidial heat resistance of various strains of the food spoilage fungus *Paecilomyces variotii* correlates with mean spore size, spore shape and size distribution. *Food Res. Int.,* 137**,** 109514.

van der Does, H. C. & Rep, M. 2017. Adaptation to the host environment by plant-pathogenic fungi. *Annu. Rev. Phytopathol.,* 55**,** 427-450.

Van Haute, S., López-Gálvez, F., Gómez-López, V. M., Eriksson, M., Devlieghere, F., Allende, A. & Sampers, I. 2015. Methodology for modeling the disinfection efficiency of fresh-cut leafy vegetables wash water applied on peracetic acid combined with lactic acid. *Int. J. Food Microbiol.,* 208**,** 102-113.

Van Haute, S., Tryland, I., Escudero, C., Vanneste, M. & Sampers, I. 2017. Chlorine dioxide as water disinfectant during fresh-cut iceberg lettuce washing: disinfectant demand, disinfection efficiency, and chlorite formation. *LWT-Food Sci. Technol.,* 75**,** 301-304.

Van Haute, S., Uyttendaele, M. & Sampers, I. 2013. Organic acid based sanitizers and free chlorine to improve the microbial quality and shelf-life of sugar snaps. *Int. J. Food Microbiol.,* 167**,** 161-169.

van Leeuwen, M. R., Krijgsheld, P., Bleichrodt, R.-J., Menke, H., Stam, H., Stark, J., Wösten, H. A. B. & Dijksterhuis, J. 2013. Germination of conidia of *Aspergillus niger* is accompanied by major changes in RNA profiles. *Stud. Mycol.,* 74**,** 59-70.

Veredas, F. J., Urda, D., Subirats, J. L., Cantón, F. R. & Aledo, J. C. 2020. Combining feature engineering and feature selection to improve the prediction of methionine oxidation sites in proteins. *Neural Comput. & Applic.,* 32**,** 323-334.

Villanueva, C. M., Cordier, S., Font-Ribera, L., Salas, L. A. & Levallois, P. 2015. Overview of disinfection by-products and associated health effects. *Curr. Envir. Health Rpt.,* 2**,** 107-115.

Vinck, A., de Bekker, C., Ossin, A., Ohm, R. A., de Vries, R. P. & Wösten, H. A. B. 2011. Heterogenic expression of genes encoding secreted proteins at the periphery of *Aspergillus niger* colonies. *Environ. Microbiol.,* 13**,** 216-225.

Voth, W. & Jakob, U. 2017. Stress-activated chaperones: a first line of defense. *Trends Biochem. Sci.,* 42**,** 899-913.

Voth, W., Schick, M., Gates, S., Li, S., Vilardi, F., Gostimskaya, I., Southworth, D. R., Schwappach, B. & Jakob, U. 2014. The protein targeting factor Get3 functions as ATP-independent chaperone under oxidative stress conditions. *Mol. Cell,* 56**,** 116-27.

Waak, M. B., Hozalski, R. M., Hallé, C. & LaPara, T. M. 2019. Comparison of the microbiomes of two drinking water distribution systems—with and without residual chloramine disinfection. *Microbiome,* 7**,** 87.

Wai, H. H., Vu, L., Oakes, M. & Nomura, M. 2000. Complete deletion of yeast chromosomal rDNA repeats and integration of a new rDNA repeat: use of rDNA deletion strains for functional analysis of rDNA promoter elements in vivo. *Nucleic Acids Res.,* 28**,** 3524-34.

Walker, G. M. & White, N. A. 2017. Introduction to fungal physiology. *In:* Kavanagh, K. (ed.) *Fungi: Biology and Applications.* 3 ed. Hoboken, NJ: John Wiley & Sons, Inc.

Wallace, M. A., Liou, L. L., Martins, J., Clement, M. H., Bailey, S., Longo, V. D., Valentine, J. S. & Gralla, E. B. 2004. Superoxide inhibits 4Fe-4S cluster

enzymes involved in amino acid biosynthesis: cross-compartment protection by CuZn-superoxide dismutase. *J. Biol. Chem.,* 279**,** 32055-62.
Walvekar, A. S. & Laxman, S. 2019. Methionine at the heart of anabolism and signaling: perspectives from budding yeast. *Front. Microbiol.,* 10**,** 2624-2624.
Wang, F., Sethiya, P., Hu, X., Guo, S., Chen, Y., Li, A., Tan, K. & Wong, K. H. 2021. Transcription in fungal conidia before dormancy produces phenotypically variable conidia that maximize survival in different environments. *Nat. Microbiol.,* 6**,** 1066-1081.
Wang, H., Duan, D., Wu, Z., Xue, S., Xu, X. & Zhou, G. 2019. Primary concerns regarding the application of electrolyzed water in the meat industry. *Food Control,* 95**,** 50-56.
Wang, H., Ge, D., Cheng, Z., Zhu, N., Yuan, H. & Lou, Z. 2020. Improved understanding of dissolved organic matter transformation in concentrated leachate induced by hydroxyl radicals and reactive chlorine species. *J. Hazard. Mater.,* 387**,** 121702.
Wang, J. & Fan, L. 2019. Effect of ultrasound treatment on microbial inhibition and quality maintenance of green asparagus during cold storage. *Ultrason. Sonochem.,* 58**,** 104631.
Wang, S., Deng, K., Zaremba, S., Deng, X., Lin, C., Wang, Q., Tortorello, M. L. & Zhang, W. 2009. Transcriptomic response of *Escherichia coli* O157:H7 to oxidative stress. *Appl. Environ. Microbiol.,* 75**,** 6110-23.
Wang, X. & Pan, T. 2016. Methionine mistranslation bypasses the restraint of the genetic code to generate mutant proteins with distinct activities. *PLOS Genet.,* 11**,** e1005745.
Wei, W., Wang, X., Xie, Z., Wang, W., Xu, J., Liu, Y., Gao, H. & Zhou, Y. 2017. Evaluation of sanitizing methods for reducing microbial contamination on fresh strawberry, cherry tomato, and red bayberry. *Front. Microbiol.,* 8**,** 2397.
White, T. J., Bruns, T., Lee S. & J., T. 1990. Amplification and direct sequencing of fungal ribosomal RNA genes for phylogenetics. *In:* Innis M.A., G., D.H., Sninsky J.J., White T.J. (ed.) *PCR Protocols: A Guide to Methods and Applications.* London, UK: Academic Press, Inc.
WHO 2015. WHO estimates of the global burden of foodborne diseases. *Foodborne Disease Burden Epidemiology Reference Group 2007-2015.* Geneva, Switzerland: World Health Organization.
WHO 2017. Guidelines for drinking-water quality (GDWQ), incorporating the 1st addendum. *Licence: CC BY-NC-SA 3.0 IGO.* Geneva, Switzerland.
Wilks, S. S. 1938. The large-sample distribution of the likelihood ratio for testing composite hypotheses. *Ann. Math. Stat.,* 9**,** 60-62.
Wiltrout, E., Goodenbour, J., Frechin, M. & Pan, T. 2012. Misacylation of tRNA with methionine in *Saccharomyces cerevisiae*. *Nucleic Acids Res.,* 40**,** 10494-10506.
Winterbourn, C. C. & Metodiewa, D. 1999. Reactivity of biologically important thiol compounds with superoxide and hydrogen peroxide. *Free Radic. Biol. Med.,* 27**,** 322-328.
Wösten, H. A. B., van Veluw, G. J., de Bekker, C. & Krijgsheld, P. 2013. Heterogeneity in the mycelium: implications for the use of fungi as cell factories. *Biotechnol. Lett.,* 35**,** 1155-1164.
Wu, Q.-Y., Zhou, Y.-T., Li, W., Zhang, X., Du, Y. & Hu, H.-Y. 2019a. Underestimated risk from ozonation of wastewater containing bromide: both organic byproducts and bromate contributed to the toxicity increase. *Water Res.,* 162**,** 43-52.
Wu, Y., An, Q., Li, D., Wu, J. & Pan, C. 2019b. Comparison of different home/commercial washing strategies for ten typical pesticide residue removal effects in kumquat, spinach and cucumber. *Int. J. Environ. Res. Public Health,* 16**,** 472.

Wuyts, J., Van Dijck, P. & Holtappels, M. 2018. Fungal persister cells: the basis for recalcitrant infections? *PLOS Pathog.,* 14**,** e1007301.

Wynn, J. P., Hamid, A. b. A. & Ratledge, C. 1999. The role of malic enzyme in the regulation of lipid accumulation in filamentous fungi. *Microbiology,* 145**,** 1911-1917.

Wynn, J. P. & Ratledge, C. 1997. Malic enzyme is a major source of NADPH for lipid accumulation by *Aspergillus nidulans*. *Microbiology,* 143**,** 253-257.

Xiong, K., Li, X.-t., Guo, S., Li, L.-t. & Liu, H.-j. 2014. The antifungal mechanism of electrolyzed oxidizing water against *Aspergillus flavus*. *Food Sci. Biotechnol.,* 23**,** 661-669.

Xiong, K., Liu, H.-j., Liu, R. & Li, L.-t. 2010. Differences in fungicidal efficiency against *Aspergillus flavus* for neutralized and acidic electrolyzed oxidizing waters. *Int. J. Food Microbiol.,* 137**,** 67-75.

Xu, G. & Chance, M. R. 2005. Radiolytic modification and reactivity of amino acid residues serving as structural probes for protein footprinting. *Anal. Chem.,* 77**,** 4549-4555.

Xuan, X. T., Wang, M. M., Ahn, J., Ma, Y. N., Chen, S. G., Ye, X. Q., Liu, D. H. & Ding, T. 2016. Storage stability of slightly acidic electrolyzed water and circulating electrolyzed water and their property changes after application. *J. Food Sci.,* 81**,** E610-7.

Yan, P., Daliri, E. B. & Oh, D.-H. 2021. New clinical applications of electrolyzed water: a review. *Microorganisms,* 9**,** 136.

Yao, J., Pan, B., Shen, R., Yuan, T. & Wang, J. 2019. Differential control of anode/cathode potentials of paired electrolysis for simultaneous removal of chemical oxygen demand and total nitrogen. *Sci. Total Environ.,* 687**,** 198-205.

Young, D. J., Guydosh, N. R., Zhang, F., Hinnebusch, A. G. & Green, R. 2015. Rli1/ABCE1 recycles terminating ribosomes and controls translation reinitiation in 3'UTRs *in vivo*. *Cell,* 162**,** 872-884.

Youssef, K. & Hussien, A. 2020. Electrolysed water and salt solutions can reduce green and blue molds while maintain the quality properties of 'Valencia' late oranges. *Postharvest Biol. Technol.,* 159**,** 111025.

Yukihiro, S., Masami, N., Yuko, S. & Kinuko, S. 2003. Endoscope contamination from HBV- and HCV-positive patients and evaluation of a cleaning/disinfecting method using strongly acidic electrolysed water. *Dig. Endosc.,* 15**,** 19-24.

Zadrąg-Tęcza, R., Maślanka, R., Bednarska, S. & Kwolek-Mirek, M. 2018. Response mechanisms to oxidative stress in yeast and filamentous fungi. *In:* Skoneczny, M. (ed.) *Stress Response Mechanisms in Fungi: Theoretical and Practical Aspects.* Cham, Switzerland: Springer International Publishing.

Zhang, C., Zhang, Y., Zhao, Z., Liu, W., Chen, Y., Yang, G., Xia, X. & Cao, Y. 2019. The application of slightly acidic electrolyzed water in pea sprout production to ensure food safety, biological and nutritional quality of the sprout. *Food Control,* 104**,** 83-90.

Zhang, G., Ma, L., Phelan, V. H. & Doyle, M. P. 2009. Efficacy of antimicrobial agents in lettuce leaf processing water for control of *Escherichia coli* O157:H7. *J. Food Prot.,* 72**,** 1392-7.

Zhang, J., Yang, H. & Chan, J. Z. Y. 2018. Development of portable flow-through electrochemical sanitizing unit to generate near neutral electrolyzed water. *J. Food Sci.,* 83**,** 780-790.

Zhang, W. & Jiang, W. 2019. UV treatment improved the quality of postharvest fruits and vegetables by inducing resistance. *Trends Food Sci. Technol.,* 92**,** 71-80.

Zhao, F., Li, J., Lin, K., Chen, H., Lin, Y., Zheng, S., Liang, S. & Han, S. 2019. Genome-wide screening of *Saccharomyces cerevisiae* deletion mutants

reveals cellular processes required for tolerance to the cell wall antagonist calcofluor white. *Biochem. Biophys. Res. Commun.,* 518**,** 1-6.

Zou, K., Ouyang, Q., Li, H. & Zheng, J. 2017. A global characterization of the translational and transcriptional programs induced by methionine restriction through ribosome profiling and RNA-seq. *BMC Genomics,* 18**,** 189.

Zukiewicz-Sobczak, W. A. 2013. The role of fungi in allergic diseases. *Postepy Dermatol. Alergol.,* 30**,** 42-45.

6 Appendix

6.1 Appendix A: ITS sequencing results

6.1.1 Raw sequences

>seq1: isolate 1
TGCAAGGTCTTTGGGCCAACCTCCCATCCGTGTCTATTGTACCCTGTTGCTTCGGCGGGCCCGCC
GCTTGTCGGCCGCCGGGGGGGCGCCTCTGCCCCCCGGGCCCGTGCCCGCCGGAGACCCCAACA
CGAACACTGTCTGAAAGCGTGCAGTCTGAGTTGATTGAATGCAATCAGTTAAAACTTTCAACAATG
GATCTCTTGGTTCCGGCATCGATGAAGAACGCAGCGAAATGCGATAACTAATGTGAATTGCAGAA
TTCAGTGAATCATCGAGTCTTTGAACGCACATTGCGCCCCCTGGTATTCCGGGGGGCATGCCTGT
CCGAGCGTCATTGCTGCCCTCAAGCCCGGCTTGTGTGTTGGGTCGCCGTCCCCCTCTCCGGGGG
GACGGGCCCGAAAGGCAGCGGCGGCACCGCGTCCGATCCTCGAGCGTATGGGGCTTTGTCACAT
GCTCTGTAGGATTGGCCGGCGCCTGCCGACGTTTTCCAACCATTCTTTCCAGGTTGACCTCGGAT
CAGGTAGGGATACCCGCTGAACTTAAGCATATCAATAAGGCGGAAAGAAATCATTACCGAGTGCG
GGTCCTTTGGGCCCAACCTCCCATCCGTGTCTATTGTACCCTGTTGCTTCGGCGGGCCCGCCGCT
TGTCGGCCGCCGGGGGGGCGCCTCTGCCCCCGGGCCGTGCCGCCGGAGACCCAACACGAACAC
TGTCTGAAAGCGTGCAGTCTGAGTTGATTGAATGCAATCAGTTAAAACTTTCACAATGGATCTCTT
GGGTTCGGCATCGATGAAGAACGCAGCGAAATGCGATAACTAATGTGAATTGCAGAATTCGTGAA
TCATCGAGTCTTTGAACGCCATTGGG

>seq2: isolate 2
AGGCCCGAACCTCCCATCCGTGTCTATTGTACCCTGTTGCTTCGGCGGGCCCGCCGCTTGTCGGC
CGCCGGGGGGGCGCCTCTGCCCCCCGGGCCCGTGCCCGCCGGAGACCCCAACACGAACACTGT
CTGAAAGCGTGCAGTCTGAGTTGATTGAATGCAATCAGTTAAAACTTTCAACAATGGATCTCTTGG
TTCCGGCATCGATGAAGAACGCAGCGAAATGCGATAACTAATGTGAATTGCAGAATTCAGTGAAT
CATCGAGTCTTTGAACGCACATTGCGCCCCCTGGTATTCCGGGGGGCATGCCTGTCCGAGCGTCA
TTGCTGCCCTCAAGCCCGGCTTGTGTGTTGGGTCGCCGTCCCCCTCTCCGGGGGGACGGGCCCG
AAAGGCAGCGGCGGCACCGCGTCCGATCCTCGAGCGTATGGGGCTTTGTCACATGCTCTGTAGG
ATTGGCCGGCGCCTGCCGACGTTTTCCAACCATTCTTTCCAGGTTGACCTCGGATCAGGTAGGGA
TACCCGCTGAACTTAAGCATATCATAAGGCGGAGGAATCATTACCGAGTGCGGGTCCTTTGGGCC
CAACCTCCCATCCGTGTCTATTGTACCCTGTTGCTTCGGCGGGCCCGCGCTTGTCGGCGCCGGGG
GGCGCCTCTGCCCGGGCCGG

>seq3: isolate 3
GGCGGGCCCGCCGCTTGTCGGCCGCCGGGGGGGCGCCTCTGCCCCCCGGGCCCGTGCCCGCC
GGAGACCCCAACACGAACACTGTCTGAAAGCGTGCAGTCTGAGTTGATTGAATGCAATCAGTTAA
AACTTTCAACAATGGATCTCTTGGTTCCGGCATCGATGAAGAACGCAGCGAAATGCGATAACTAAT
GTGAATTGCAGAATTCAGTGAATCATCGAGTCTTTGAACGCACATTGCGCCCCCTGGTATTCCGG
GGGGCATGCCTGTCCGAGCGTCATTGCTGCCCTCAAGCCCGGCTTGTGTGTTGGGTCGCCGTCC
CCCTCTCCGGGGGGACGGGCCCGAAAGGCAGCGGCGGCACCGCGTCCGATCCTCGAGCGTATG
GGGCTTTGTCACATGCTCTGTAGGATTGGCCGGCGCCTGCCGACGTTTTCCAACCATTCTTTCCA
GGTTGACCTCGGATCAGGTAGGGATACCCGCTGAACTTAAGCATATCAATAAGCGGAGGAAACAT
AC

>seq4: isolate 4
ACTCGAACACTGTCTGAAAGCGTGCAGTCTGAGTTGATTGAATGCAATCAGTTAAAACTTTCATCA
ATGGATCTCTTGGTTCCGGCATCAATGAAGAACGCAGCGAAATGCGATAACTAATGTGAATTGCA
GAATTCAGTGAATCATCGAGTCTTTGAACGCACATTGCGCCCCCTGGTATTCCGGGGGGCATGCC
TGTCCGAGCGTCATTGCTGCCCTCAAGCCCGGCTTGTGTGTTGGGTCGCCGTCCCCCTCTCCGGG
GGGACGGGCCCGAAAGGCAGCGGCGGCACCGCGTCCGATCCTCGAGCGTATGGGGCTTTGTCA
CATGCTCTGTAGGATTGGCCGGCGCCTGCCGACGTTTTCCAACCATTCTTTCCAGGTTGACCTCG
GATCAGGTAGGGATACCCGCTGAACTTAAGCATATCAATAAGCGGAGGAACATT

>seq5: isolate 5
AGCTAATGTGAATTGCACAATTCAGTG

>seq6: isolate 6
GAAGGTCCTTTGGGCCAACCTCCCATCCGTGTCTATTGTACCCTGTTGCTTCGGCGGGCCCGCCG
CTTGTCGGCCGCCGGGGGGGCGCCTCTGCCCCCCGGGCCCGTGCCCGCCGGAGACCCCAACAC
GAACACTGTCTGAAAGCGTGCAGTCTGAGTTGATTGAATGCAATCAGTTAAAACTTTCAACAATGG
ATCTCTTGGTTCCGGCATCGATGAAGAACGCAGCGAAATGCGATAACTAATGTGAATTGCAGAAT
TCAGTGAATCATCGAGTCTTTGAACGCACATTGCGCCCCCTGGTATTCCGGGGGGCATGCCTGTC
CGAGCGTCATTGCTGCCCTCAAGCCCGGCTTGTGTGTTGGGTCGCCGTCCCCCTCTCCGGGGGGG
ACGGGCCCGAAAGGCAGCGGCGGCACCGCGTCCGATCCTCGAGCGTATGGGGCTTTGTCACATG
CTCTGTAGGATTGGCCGGCGCCTGCCGACGTTTTCCAACCATTCTTTCCAGGTTGACCTCGGATC
AGGTAGGGATACCCGCTGAACTTAAGCATATCAATAAGCGGAGGAATCATTACCGAGTGCGGGTC
CTTTGGGCGAA

>seq7: isolate 7
GGCATCAATGAAGAACGCAGCGAAATGCGATAACTAATGTGAATTGCAAAATTCAGTGAATCATC
GAGTCTTTGAACGCACATTGCGCCCCCTGGTATTCCGGGGGGCATGCCTGTCCGAGCGTCATTGC
TGC

>seq8: isolate 8
GAAGGTCCTTTGGGCCAACCTCCCATCCGTGTCTATTGTACCCTGTTGCTTCGGCGGGCCCGCCG
CTTGTCGGCCGCCGGGGGGGCGCCTCTGCCCCCCGGGCCCGTGCCCGCCGGAGACCCCAACAC
GAACACTGTCTGAAAGCGTGCAGTCTGAGTTGATTGAATGCAATCAGTTAAAACTTTCAACAATGG
ATCTCTTGGTTCCGGCATCGATGAAGAACGCAGCGAAATGCGATAACTAATGTGAATTGCAGAAT
TCAGTGAATCATCGAGTCTTTGAACGCACATTGCGCCCCCTGGTATTCCGGGGGGCATGCCTGTC
CGAGCGTCATTGCTGCCCTCAAGCCCGGCTTGTGTGTTGGGTCGCCGTCCCCCTCTCCGGGGGG
ACGGGCCCGAAAGGCAGCGGCGGCACCGCGTCCGATCCTCGAGCGTATGGGGCTTTGTCACATG
CTCTGTAGGATTGGCCGGCGCCTGCCGACGTTTTCCAACCATTCTTTCCAGGTTGACCTCGGATC
AGGTAGGGATACCCGCTGAACTTAAGCATATCAATAAGCGGAGGAATCATTACCGAGTGCGGGTC
CTTTGGGCCCAACCTCCCATCCGTGTCTATTGTACCCTGTTGCTTCGGCGGGCCCGCCGCTTGTC
GGCCGCCGGGGGGGCGCCTCTGCCCCCGGGCCCGTGCCG

>N402: *A. niger* N402
TGAAGGTCCTTTGGGCCAACCTCCCATCCGTGTCTATTGTACCCTGTTGCTTCGGCGGGCCCGCC
GCTTGTCGGCCGCCGGGGGGGCGCCTCTGCCCCCCGGGCCCGTGCCCGCCGGAGACCCCAACA
CGAACACTGTCTGAAAGCGTGCAGTCTGAGTTGATTGAATGCAATCAGTTAAAACTTTCAACAATG
GATCTCTTGGTTCCGGCATCGATGAAGAACGCAGCGAAATGCGATAACTAATGTGAATTGCAGAA
TTCAGTGAATCATCGAGTCTTTGAACGCACATTGCGCCCCCTGGTATTCCGGGGGGCATGCCTGT
CCGAGCGTCATTGCTGCCCTCAAGCCCGGCTTGTGTGTTGGGTCGCCGTCCCCCTCTCCGGGGG
GACGGGCCCGAAAGGCAGCGGCGGCACCGCGTCCGATCCTCGAGCGTATGGGGCTTTGTCACAT
GCTCTGTAGGATTGGCCGGCGCCTGCCGACGTTTTCCAACCATTCTTTCCAGGTTGACCTCGGAT
CAGGTAGGGATACCCGCTGAACTTAAGCATATCAATAAGCCGGAAGAATCATTACCGAGTGCGGG
TCCTTTGGGCCCAACCTCCCATCCGTGTCTATTGTACCCTGTTGCTTCGGCGGGCCCGCCGCTTG
TCGGCCGCCGGGGGGGCGCCTCTGCCCCCGGGCCGTGCCCGCCG

6.1.2 Multiple sequence alignment

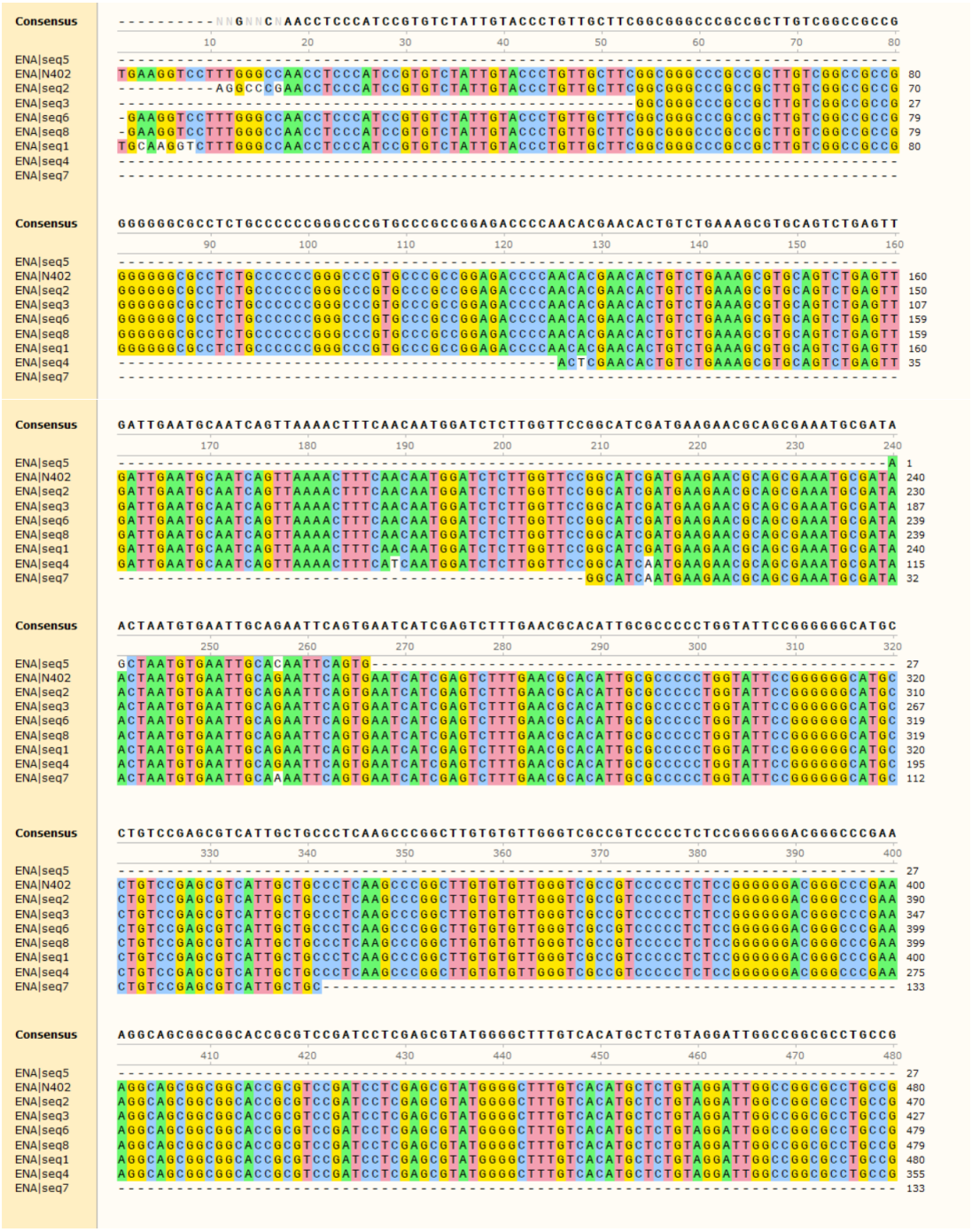

Figure_Apx 1: Multiple sequence alignment of ITS sequences. The ITS regions of *A. niger* isolates from Indian onions and the lab strain *A. niger* N402 were sequenced as described previously (White et al., 1990). The alignment was performed with the EMBL-EBI Clustal Omega tool (Madeira et al., 2019). The consensus sequence was added in SnapGene® Viewer with a threshold of >50% consensus. The coloured bases represent bases that match the N402 sequence. Seq1–8: ITS sequence of isolates 1–8 (see 2.2.2, 2.3.1.1).

6.1.3 NCBI BLAST® blastn results

Table_Apx 1: NCBI BLAST® blastn search results for the ITS sequences of isolates 1–8 and lab strain *A. niger* N402.

Strain	Sequence length [bp]	Best hits[a]	E value	Query cover [%]	Identity [%]	Most frequent organism[b]
isolate 1	867	*Aspergillus niger* strain MBL1511 internal transcribed spacer 1, partial sequence; 5.8S ribosomal RNA gene and internal transcribed spacer 2, complete sequence; and 28S ribosomal RNA gene, partial sequence *Aspergillus niger* strain BFW internal transcribed spacer 1, partial sequence; 5.8S ribosomal RNA gene and internal transcribed spacer 2, complete sequence; and large subunit ribosomal RNA gene, partial sequence	0.0 0.0	99 99	94.79 94.32	*A. niger* (74 out of 102 hits)
isolate 2	667	*Aspergillus tubingensis* strain Hoba5-41 internal transcribed spacer 1, partial sequence; 5.8S ribosomal RNA gene and internal transcribed spacer 2, complete sequence; and 28S ribosomal RNA gene, partial sequence *Aspergillus niger* small subunit ribosomal RNA gene, partial sequence; internal transcribed spacer 1, 5.8S ribosomal RNA gene, and internal transcribed spacer 2, complete sequence; and large subunit ribosomal RNA gene, partial sequence	0.0 0.0	98 98	98.92 98.61	*A. niger* (78 out of 102 hits)

isolate 3	517	*Aspergillus niger* isolate Asp-7136 internal transcribed spacer 1, partial sequence; 5.8S ribosomal RNA gene and internal transcribed spacer 2, complete sequence; and large subunit ribosomal RNA gene, partial sequence *Aspergillus niger* isolate AR2 internal transcribed spacer 1, partial sequence; 5.8S ribosomal RNA gene and internal transcribed spacer 2, complete sequence; and large subunit ribosomal RNA gene, partial sequence	0.0 0.0	100 99	99.81 100	*A. niger* (84 out of 142 hits)
isolate 4	443	*Aspergillus niger* strain An3-2 small subunit ribosomal RNA gene, partial sequence; internal transcribed spacer 1, 5.8S ribosomal RNA gene, and internal transcribed spacer 2, complete sequence; and large subunit ribosomal RNA gene, partial sequence *Aspergillus niger* strain JS-1 small subunit ribosomal RNA gene, partial sequence; internal transcribed spacer 1, 5.8S ribosomal RNA gene, and internal transcribed spacer 2, complete sequence; and large subunit ribosomal RNA gene, partial sequence	0.0 0.0	100 99	99.10 99.10	*A. niger* (68 out of 103 hits)
isolate 5	27	*Penicillium* sp. isolate F0.05 internal transcribed spacer 1 and 5.8S ribosomal RNA gene, partial sequence	0.002	92	100	"unculture d fungus" (17 out of 100 hits)

		Aspergillus tubingensis isolate A_9 internal transcribed spacer 1, partial sequence; 5.8S ribosomal RNA gene and internal transcribed spacer 2, complete sequence; and large subunit ribosomal RNA gene, partial sequence	0.002	92	100	
isolate 6	593	Fungal sp. AM2013 strain 232_Mbmp internal transcribed spacer 1, partial sequence; 5.8S ribosomal RNA gene and internal transcribed spacer 2, complete sequence; and 28S ribosomal RNA gene, partial sequence *Aspergillus niger* voucher MSR3 18S ribosomal RNA gene, partial sequence; internal transcribed spacer 1, 5.8S ribosomal RNA gene, and internal transcribed spacer 2, complete sequence; and 28S ribosomal RNA gene, partial sequence	0.0 0.0	98 98	99.49 99.49	*A. niger* (59 out of 103 hits)
isolate 7	133	Uncultured *Aspergillus* clone 22 small subunit ribosomal RNA gene, partial sequence; internal transcribed spacer 1 and 5.8S ribosomal RNA gene, complete sequence; and internal transcribed spacer 2, partial sequence *Aspergillus terreus* internal transcribed spacer 1, partial sequence; 5.8S ribosomal RNA gene and internal transcribed spacer 2, complete sequence; and large subunit ribosomal RNA gene, partial sequence	3e-58 3e-58	100 100	99.25 99.25	*Penicillium spinulosum* (17 out of 102 hits) [14 *A. niger* hits]

isolate 8	686	*Aspergillus tubingensis* strain Hoba5-41 internal transcribed spacer 1, partial sequence; 5.8S ribosomal RNA gene and internal transcribed spacer 2, complete sequence; and 28S ribosomal RNA gene, partial sequence *Aspergillus niger* voucher MSR4 internal transcribed spacer 1, partial sequence; 5.8S ribosomal RNA gene and internal transcribed spacer 2, complete sequence; and 28S ribosomal RNA gene, partial sequence	0.0 0.0	99 99	98.96 98.54	*A. niger* (66 out of 102 hits)
A. niger N402	691	*Aspergillus tubingensis* strain Hoba5-41 internal transcribed spacer 1, partial sequence; 5.8S ribosomal RNA gene and internal transcribed spacer 2, complete sequence; and 28S ribosomal RNA gene, partial sequence *Aspergillus niger* voucher MSR4 internal transcribed spacer 1, partial sequence; 5.8S ribosomal RNA gene and internal transcribed spacer 2, complete sequence; and 28S ribosomal RNA gene, partial sequence	0.0 0.0	100 99	99.11 98.54	*A. niger* (69 out of 99 hits)

[a] Results of the blastn algorithm were sorted by E value and the first two hits are listed for each strain.
[b] The most frequent organism found among the significant hits is listed.

6.2 Appendix B: Raw data tables for heatmap graphs

6.2.1 Inactivation of fungicidal EW activity by amino acids

Table_Apx 2: Related to Figure 2-10 A: Inactivation of fungicidal EW activity by amino acids.

Amino acid	Gly		Ala		Leu		Ile	
conc.	mean[a]	SD	mean	SD	mean	SD	mean	SD
7mM	79.73	3.38	80.23	7.15	100.53	13.08	87.92	7.18
5mM	76.70	11.32	85.25	11.19	96.81	11.91	86.45	7.33
3.5mM	21.39	17.69	75.88	12.99	84.63	14.86	90.34	6.18
2.5mM	8.19	0.38	7.78	0.68	9.09	0.99	12.41	7.50
1.75mM	8.68	3.17	8.07	0.98	8.07	0.56	6.27	2.30
1.25mM	8.23	1.10	8.07	0.60	9.35	2.53	8.11	0.56
0.9mM	7.07	1.35	8.02	1.39	7.64	0.93	6.60	0.50
0.625mM	7.73	2.33	7.91	0.98	8.08	1.32	7.49	1.01

Amino acid	Val		Pro		Phe		Tyr	
conc.	mean	SD	mean	SD	mean	SD	mean	SD
7mM	83.05	8.55	94.80	6.04	61.12	8.40	na[b]	
5mM	77.43	19.59	72.30	3.52	50.83	3.88	na	
3.5mM	68.81	27.47	7.63	0.16	34.63	5.10	na	
2.5mM	11.58	4.16	8.77	1.02	8.80	2.46	na	
1.75mM	7.38	0.28	7.64	0.53	7.41	0.30	40.75	15.95
1.25mM	8.03	0.94	8.80	1.19	7.37	1.06	10.46	1.27
0.9mM	7.77	1.08	14.26	10.65	6.90	1.38	9.18	0.58
0.625mM	7.24	0.35	7.50	1.17	7.92	0.58	11.78	3.49

Amino acid	Trp		Ser		Thr		Met (I)	
conc.	mean	SD	mean	SD	mean	SD	mean	SD
7mM	55.80	14.15	85.58	9.05	81.79	19.80	94.14	10.23
5mM	57.33	3.77	62.31	18.31	49.59	12.77	95.27	17.31
3.5mM	89.23	20.73	34.12	10.63	23.14	4.30	80.54	16.13
2.5mM	111.42	9.77	8.08	0.44	7.06	0.69	77.44	27.60
1.75mM	84.77	21.26	7.50	0.96	7.62	0.68	61.57	33.26
1.25mM	81.29	6.68	7.87	0.73	8.14	0.26	7.62	0.99
0.9mM	82.79	22.72	7.47	0.89	7.16	0.77	7.29	0.55
0.625mM	35.86	44.10	7.53	0.88	7.03	0.63	8.87	1.06

Amino acid	Met (II)		Cys		Lys		Arg	
conc.	mean	SD	mean	SD	mean	SD	mean	SD
7mM	97.69	7.76	102.76	12.47	75.07	20.57	89.59	9.05
5mM	90.82	6.02	104.06	8.87	76.14	17.56	98.37	15.17
3.5mM	85.00	17.69	103.46	11.87	72.40	15.71	95.01	14.23
2.5mM	84.44	16.81	86.52	4.95	40.76	43.50	92.63	13.22
1.75mM	66.32	22.34	80.10	16.85	7.51	0.65	15.98	11.45
1.25mM	6.74	1.70	9.74	0.45	7.30	1.37	4.67	1.63
0.9mM	5.90	2.46	7.65	0.79	6.65	0.28	4.84	4.76
0.625mM	9.11	1.82	7.04	0.89	7.25	1.99	3.47	2.70

Amino acid	His		Asn		Gln		Asp	
conc.	mean	SD	mean	SD	mean	SD	mean	SD
7mM	94.86	27.20	105.88	26.45	89.38	12.49	61.65	27.51
5mM	24.67	16.81	87.02	9.06	73.18	9.79	52.11	23.90
3.5mM	20.41	10.54	63.56	15.56	72.30	8.66	50.84	32.15
2.5mM	25.13	19.11	29.60	23.67	17.09	18.49	11.75	3.80
1.75mM	7.64	1.31	7.99	0.13	7.45	0.73	6.14	4.81
1.25mM	10.94	3.29	8.07	1.47	7.89	0.41	8.32	0.42
0.9mM	7.38	0.58	7.33	0.71	8.50	0.64	8.09	1.32
0.625mM	7.06	0.45	7.16	0.48	15.06	11.38	8.84	1.28

Amino acid	Glu		water control (I)		water control (II)	
conc.	mean	SD	mean	SD	mean	SD
7mM	96.28	8.09	7.44	0.28	6.92	0.64
5mM	91.40	10.00	7.85	0.70	12.08	4.36
3.5mM	92.03	12.27	7.27	0.63	8.43	0.88
2.5mM	47.01	34.37	7.34	0.64	9.45	3.72
1.75mM	8.41	1.30	5.89	2.22	7.62	0.56
1.25mM	7.75	0.80	7.68	0.75	6.81	3.84
0.9mM	7.72	1.34	7.15	1.03	6.77	2.77
0.625mM	6.76	0.74	6.58	1.67	7.71	1.56

[a] Growth in all cases was determined in YEPD broth by OD_{600} readings after 24 h. Values shown are for % growth relative to control (no EW treatment). Mean values are shown from biological triplicates (except lysine, where n = 2).
[b] Not tested due to limited solubility of Tyr in water.

Table_Apx 3: Related to Figure 2-10 B: Inactivation of fungicidal EW activity by certain amino acids determined from subsequent growth for extended periods.

Amino acid	Arg, 24h		Arg, 48h		Arg, 72h	
conc.	mean[a]	SD	mean	SD	mean	SD
7mM	89.59	9.05	96.11	0.35	96.33	0.86
5mM	98.37	15.17	99.88	2.21	99.76	2.35
3.5mM	95.01	14.23	96.74	3.37	97.30	1.93
2.5mM	92.63	13.22	94.35	3.67	95.84	1.75
1.75mM	15.98	11.45	53.24	32.31	95.61	3.44
1.25mM	4.67	1.63	8.55	14.11	32.44	55.60
0.9mM	4.84	4.76	0.49	0.49	0.40	0.41
0.625mM	3.47	2.70	0.30	0.29	0.28	0.22

Amino acid	His, 24h		His, 48h		His, 72h	
conc.	mean	SD	mean	SD	mean	SD
7mM	94.86	27.20	104.67	3.91	104.61	4.17
5mM	24.67	16.81	79.35	27.15	101.74	2.93
3.5mM	20.41	10.54	76.50	31.54	102.46	2.27
2.5mM	25.13	19.11	69.90	35.35	100.38	1.20
1.75mM	7.64	1.31	19.91	33.25	35.40	58.45
1.25mM	10.94	3.29	30.41	26.04	69.43	57.77
0.9mM	7.38	0.58	29.47	18.74	99.65	1.69
0.625mM	7.06	0.45	14.70	24.08	36.40	60.65

Amino acid	Asn, 24h		Asn, 48h		Asn, 72h	
conc.	mean	SD	mean	SD	mean	SD
7mM	105.88	26.45	104.26	9.29	102.59	5.52
5mM	87.02	9.06	105.04	1.63	103.90	2.73
3.5mM	63.56	15.56	88.06	12.39	97.20	4.28
2.5mM	29.60	23.67	37.05	21.67	94.40	4.89
1.75mM	7.99	0.13	10.07	4.48	93.28	9.69
1.25mM	8.07	1.47	6.52	3.51	92.28	2.94
0.9mM	7.33	0.71	6.60	5.02	70.85	50.70
0.625mM	7.16	0.48	4.25	6.06	34.10	57.99

Amino acid	Met (II), 24h		Met (II), 48h		Met (II), 72h	
conc.	mean	SD	mean	SD	mean	SD
7mM	97.69	7.76	102.71	4.35	100.71	5.16
5mM	90.82	6.02	104.84	2.94	103.23	2.20
3.5mM	85.00	17.69	90.86	12.64	97.43	1.97
2.5mM	84.44	16.81	88.72	14.10	99.54	1.58
1.75mM	66.32	22.34	87.05	26.35	101.00	6.66
1.25mM	6.74	1.70	16.60	12.22	91.89	11.64
0.9mM	5.90	2.46	22.30	25.98	65.90	57.07
0.625mM	9.11	1.82	10.71	17.30	34.26	58.25

Amino acid conc.	Ala, 24h		Ala, 48h		Ala, 72h	
	mean	SD	mean	SD	mean	SD
7mM	80.23	7.15	97.25	4.16	98.97	2.22
5mM	85.25	11.19	96.62	8.67	99.36	4.43
3.5mM	75.88	12.99	93.91	3.06	99.22	1.60
2.5mM	7.78	0.68	4.26	6.13	28.90	47.13
1.75mM	8.07	0.98	0.77	0.02	1.23	0.92
1.25mM	8.07	0.60	0.71	0.05	1.21	0.94
0.9mM	8.02	1.39	0.72	0.09	1.03	0.68
0.625mM	7.91	0.98	0.89	0.13	0.81	0.23

Amino acid conc.	water control (I+II)		water control (I+II)		water control (I+II)	
	mean	SD	mean	SD	mean	SD
7mM	7.18	0.42	15.81	16.44	52.12	50.60
5mM	9.96	1.85	19.22	17.46	51.08	48.71
3.5mM	7.85	0.75	9.27	9.72	33.12	28.11
2.5mM	8.39	1.78	13.16	21.57	17.45	28.92
1.75mM	6.76	1.12	2.20	2.79	17.85	30.05
1.25mM	7.24	1.55	0.65	0.21	0.68	0.32
0.9mM	6.96	1.18	3.39	4.48	16.21	26.90
0.625mM	7.14	1.31	0.76	0.12	0.60	0.12

[a] Growth in all cases was determined in YEPD broth by OD_{600} readings after 24 h, 48 h and 72 h. Values shown are for % growth relative to control (no EW treatment). Mean values are shown from biological triplicates (water control: mean value from the replicates [2 technical x 3 biological for each given mean value]).

6.2.2 Inactivation of fungicidal EW activity by Met and MetO

Table_Apx 4: Related to Figure 2-11 A,B: Inactivation of fungicidal EW activity by Met and MetO; 40 h and 72 h time points.

Amino acid conc.	Met - 20% EW (40 h)		MetO – 20% EW (40 h)	
	mean[a]	SD	mean	SD
7mM	0.96	0.05	0.27	0.43
5mM	1.02	0.09	0.48	0.36
3.5mM	0.85	0.16	0.79	0.09
2.5mM	0.85	0.07	0.81	0.12
1.75mM	0.71	0.16	0.20	0.18
1.25mM	0.06	0.03	0.01	0.01
0.9mM	0.01	0.01	0.01	0.01
0mM	0.33	0.54	0.01	0.01

Amino acid conc.	Met - 20% EW (72 h)		MetO – 20% EW (72 h)	
	mean	SD	mean	SD
7mM	0.96	0.00	0.58	0.44
5mM	0.97	0.01	1.02	0.06
3.5mM	0.94	0.03	1.01	0.02
2.5mM	0.97	0.02	1.01	0.04
1.75mM	0.98	0.01	0.68	0.58
1.25mM	0.33	0.55	0.01	0.01
0.9mM	0.01	0.01	0.01	0.01
0mM	0.33	0.56	0.01	0.01

Amino acid conc.	Met – 6400 ppm NaOCl (40 h)		MetO – 6400 ppm NaOCl (40 h)	
	mean	SD	mean	SD
7mM	0.20	0.17	0.12	0.09
5mM	0.20	0.15	0.16	0.03
3.5mM	0.23	0.15	0.06	0.09
2.5mM	0.09	0.13	0.01	0.00
1.75mM	0.01	0.01	0.01	0.01
1.25mM	0.01	0.01	0.01	0.01
0.9mM	0.01	0.01	0.01	0.01
0.625mM	0.01	0.01	0.01	0.01

Amino acid conc.	Met – 6400 ppm NaOCl (72 h)		MetO – 6400 ppm NaOCl (72 h)	
	mean	SD	mean	SD
7mM	0.85	0.04	0.90	0.07
5mM	0.91	0.06	0.86	0.06
3.5mM	0.89	0.04	0.31	0.51
2.5mM	0.57	0.49	0.01	0.01
1.75mM	0.16	0.26	0.01	0.01
1.25mM	0.01	0.01	0.01	0.00
0.9mM	0.01	0.01	0.01	0.01
0.625mM	0.01	0.01	0.01	0.01

[a] Growth in all cases was determined in YEPD broth by OD_{600} readings after 40 h and 72 h. Values shown are for % growth relative to control (no EW treatment). Mean values are shown from biological triplicates.

Table_Apx 5: Related to Figure 2-12: Inactivation of fungicidal EW activity by Met and MetO (II).

Amino acid conc.	i) Met - 20% EW		i) MetO - 20% EW		i) Met - water ctrl	
	mean[a]	SD	mean	SD	mean	SD
7mM (1:2)	10.20	0.56	4.16	0.28	9.44	0.35
5mM (1:2)	9.54	0.40	4.75	0.83	9.15	0.95
3.5mM (1:2)	8.15	0.11	6.89	0.74	9.08	0.88
0mM (1:2)	0.05	0.04	0.05	0.04	9.36	0.89
7mM (1:10)	7.92	0.52	7.93	0.11	9.00	0.45
5mM (1:10)	7.29	0.30	8.13	0.37	8.06	0.41
3.5mM (1:10)	7.74	0.52	9.69	1.21	8.75	0.08
0mM (1:10)	0.02	0.01	0.02	0.00	7.31	1.27

Amino acid conc.	i) MetO - water ctrl		ii) Met - 20% EW (inactiv.)		ii) MetO - 20% EW (inactiv.)	
	mean	SD	mean	SD	mean	SD
7mM (1:2)	8.92	0.27	10.68	0.34	4.21	0.27
5mM (1:2)	10.29	0.24	11.14	0.19	4.98	0.42
3.5mM (1:2)	9.85	0.57	10.50	1.21	8.05	1.53
0mM (1:2)	9.74	0.22	11.35	0.06	11.50	0.61
7mM (1:10)	8.05	0.52	9.89	2.15	9.86	0.84
5mM (1:10)	8.56	1.22	10.05	1.21	10.71	1.97
3.5mM (1:10)	7.20	1.01	9.85	0.55	10.16	1.70
0mM (1:10)	8.41	0.42	9.70	0.14	9.04	0.21

Amino acid conc.	ii) Met - water ctrl		ii) MetO - water ctrl	
	mean	SD	mean	SD
7mM (1:2)	8.66	0.43	9.06	1.90
5mM (1:2)	9.47	0.70	10.08	0.69
3.5mM (1:2)	9.32	1.12	10.51	0.81
0mM (1:2)	10.45	0.57	10.27	0.61
7mM (1:10)	10.27	1.20	10.77	0.77
5mM (1:10)	10.07	0.67	10.24	1.55
3.5mM (1:10)	9.64	2.21	10.16	1.27
0mM (1:10)	9.21	0.45	8.86	0.12

[a] Growth in all cases was determined in YEPD broth by OD_{600} readings after 40 h. Mean values are shown from biological duplicates.

6.3 Appendix C: The pH of the amino acid solutions was not correlated with their effect on EW activity

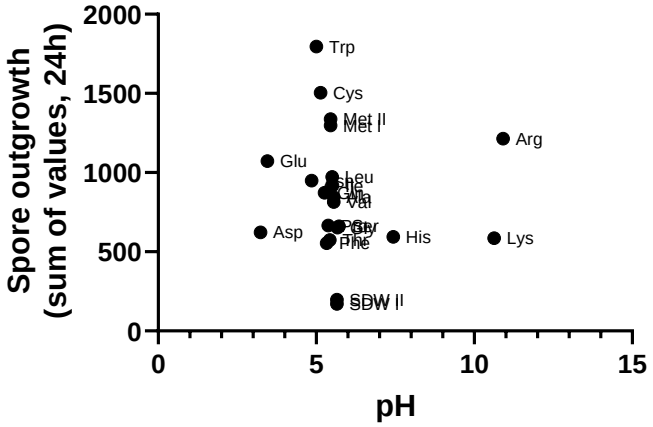

Figure_Apx 2: pH of amino acid solutions used to inactivate EW. EW was mixed with amino acids (0.625–7 mM) and used to treat *A. niger* spores. The relative survival was determined by outgrowth in YEPD broth, OD_{600} readings after 24 h and calculated relative to an EW-free control (see Figure 2-10 and Table_Apx 2 for data and experimental details). The relative growth values obtained from treatments that included different amino acid concentrations were summed up for all concentrations and all 3 biological replicates to obtain one single value for each amino acid, and plotted against the pH of the amino acid stock solutions (10 mM in water). No correlation was observed. SDW, sterile distilled water.

6.4 Appendix D: NaOCl + H_2O_2 checkerboard

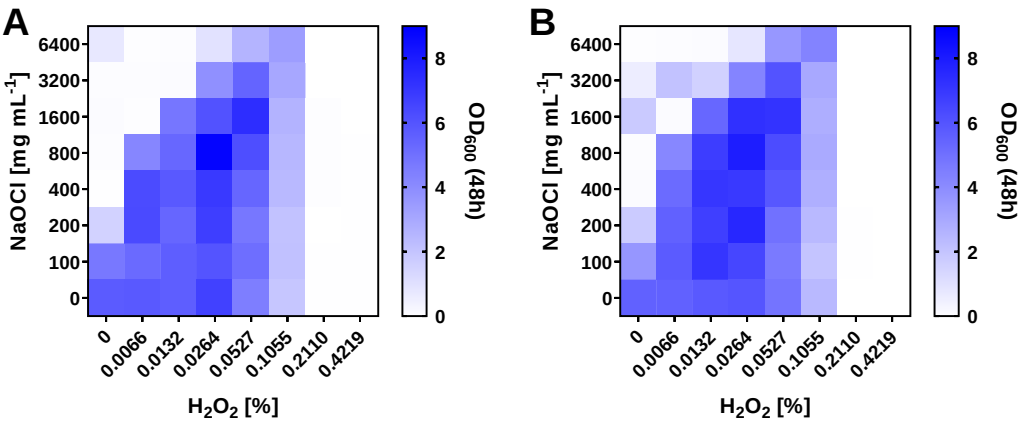

Figure_Apx 3: Combining NaOCl and H_2O_2 to treat *A. niger* spores. NaOCl and H_2O_2 were mixed for 5 min (A) or 1 h (B), and then used to treat *A. niger* spores for 5 min, followed by mixing 1:1 with 2X YEPD. Outgrowth from viable spores was determined in YEPD broth by OD_{600} readings after 48 h. Data from 1 biological replicate. Spores treated with 400–6400 mg L^{-1} NaOCl showed more outgrowth when increasing concentrations of H_2O_2 were included in the treatment, possibly due to reactions between the two chemicals ($NaOCl + H_2O_2 \rightarrow O_2 + Cl^- + Na^+ + H_2O$) (Held et al., 1978) that interfere with the sanitising activity. Regarding the NaOCl concentration, it should be noted that this concentration was calculated after diluting a purchased 5% NaOCl solution but was not confirmed by FAC measurement. In other experiments, the measured FAC of dilutions of the purchased NaOCl solution was lower than the calculated FAC, therefore it is likely that the actual NaOCl concentration was lower than stated. H_2O_2 solutions were dilutions of a purchased 30% H_2O_2 solution.

6.5 Appendix E: Sequenced region of the yEmRG plasmid

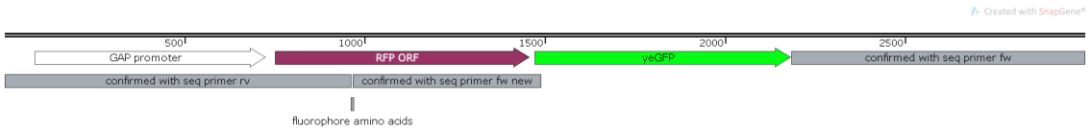

Figure_Apx 4: Map of the sequenced region of yEmRG including the mCherry-GFP fusion protein. Image generated in SnapGene® Viewer 5.1.7.

Features:

84	…	727	GAP promoter (*S. cerevisiae* TDH3)
751	…	1458	yEmRFP ORF (mCherry)
961	…	969	mCherry fluorophore
1471	…	2184	yEGFP ORF

Sequences confirmed by sequencing:

1	…	1487
2185	…	2994

Sequence:

```
   1 CCCCGCGCGT TGGCCGATTC ATTAATGCAC GGATCCGGTA GAATCATTTT
  51 GAATAAAAAA CACGCTTTTT CAGTTCGAGT TTATCATTAT CAATACTGCC
 101 ATTTCAAAGA ATACGTAAAT AATTAATAGT AGTGATTTTC CTAACTTTAT
 151 TTAGTCAAAA AATTAGCCTT TTAATTCTGC TGTAACCCGT ACATGCCCAA
 201 AATAGGGGGC GGGTTACACA GAATATATAA CATCGTAGGT GTCTGGGTGA
 251 ACAGTTTATT CCTGGCATCC ACTAAATATA ATGGAGCCCG CTTTTTAAGC
 301 TGGCATCCAG AAAAAAAAAG AATCCCAGCA CCAAAATATT GTTTTCTTCA
 351 CCAACCATCA GTTCATAGGT CCATTCTCTT AGCGCAACTA CAGAGAACAG
 401 GGGCACAAAC AGGCAAAAAA CGGGCACAAC CTCAATGGAG TGATGCAACC
 451 TGCCTGGAGT AAATGATGAC ACAAGGCAAT TGACCCACGC ATGTATCTAT
 501 CTCATTTTCT TACACCTTCT ATTACCTTCT GCTCTCTCTG ATTTGGAAAA
 551 AGCTGAAAAA AAAGGTTGAA ACCAGTTCCC TGAAATTATT CCCCTACTTG
 601 ACTAATAAGT ATATAAAGAC GGTAGGTATT GATTGTAATT CTGTAAATCT
 651 ATTTCTTAAA CTTCTTAAAT TCTACTTTTA TAGTTAGTCT TTTTTTTAGT
 701 TTTAAAACAC CAAGAACTTA GTTTCGAATA AACACACATA AACAGAATTC
 751 ATGGTTTCAA AAGGTGAAGA AGATAATATG GCTATTATTA AAGAATTTAT
 801 GAGATTTAAA GTTCATATGG AAGGTTCAGT TAATGGTCAT GAATTTGAAA
 851 TTGAAGGTGA AGGTGAAGGT AGACCATATG AAGGTACTCA AACTGCTAAA
 901 TTGAAAGTTA CTAAAGGTGG TCCATTACCA TTTGCTTGGG ATATTTTGTC
 951 ACCACAATTT ATGTATGGTT CAAAAGCTTA TGTTAAACAT CCAGCTGATA
1001 TTCCAGATTA TTTAAAATTG TCATTTCCAG AAGGTTTTAA ATGGGAAAGA
1051 GTTATGAATT TTGAAGATGG TGGTGTTGTT ACTGTTACTC AAGATTCATC
1101 ATTACAAGAT GGTGAATTTA TTTATAAAGT TAAATTGAGA GGTACTAATT
1151 TTCCATCAGA TGGTCCAGTT ATGCAAAAAA AAACTATGGG TTGGGAAGCT
1201 TCATCAGAAA GAATGTATCC AGAAGATGGT GCTTTAAAAG GTGAAATTAA
1251 ACAAAGATTG AAATTAAAAG ATGGTGGTCA TTATGATGCT GAAGTTAAAA
1301 CTACTTATAA AGCTAAAAAA CCAGTTCAAT TACCAGGTGC TTATAATGTT
1351 AATATTAAAT TGGATATTAC TTCACATAAT GAAGATTATA CTATTGTTGA
1401 ACAATATGAA AGAGCTGAAG GTAGACATTC AACTGGTGGT ATGGATGAAT
1451 TATATAAAGG TACCCGACCC TCTAAAGGTG AAGAATTATT CACTGGTGTT
1501 GTCCCAATTT TGGTTGAATT AGATGGTGAT GTTAATGGTC ACAAATTTTC
1551 TGTCTCCGGT GAAGGTGAAG GTGATGCTAC TTACGGTAAA TTGACCTTAA
1601 AATTTATTTG TACTACTGGT AAATTGCCAG TTCCATGGCC AACCTTAGTC
1651 ACTACTTTCG GTTATGGTGT TCAATGTTTT GCTAGATACC CAGATCATAT
1701 GAAACAACAT GACTTTTTCA AGTCTGCCAT GCCAGAAGGT TATGTTCAAG
1751 AAAGAACTAT TTTTTTCAAA GATGACGGTA ACTACAAGAC CAGAGCTGAA
1801 GTCAAGTTTG AAGGTGATAC CTTAGTTAAT AGAATCGAAT TAAAAGGTAT
1851 TGATTTTAAA GAAGATGGTA ACATTTTAGG TCACAAATTG GAATACAACT
1901 ATAACTCTCA CAATGTTTAC ATCATGGCTG ACAAACAAAA GAATGGTATC
1951 AAAGTTAACT TCAAAATTAG ACACAACATT GAAGATGGTT CTGTTCAATT
2001 AGCTGACCAT TATCAACAAA ATACTCCAAT TGGTGATGGT CCAGTCTTGT
2051 TACCAGACAA CCATTACTTA TCCACTCAAT CTGCCTTATC CAAAGATCCA
2101 AACGAAAAGA GAGACCACAT GGTCTTGTTA GAATTTGTTA CTGCTGCTGG
2151 TATTACCCAT GGTATGGATG AATTGTACAA ATAACTGGTC GAGTCATGTA
2201 ATTAGTTATG TCACGCTTAC ATTCACGCCC TCGAGCAGCT GTGATTGATT
2251 GAGTCGACTT GGTTGAACAC GTTGCCAAGG CTTAAGTGAA TTTACTTTAA
2301 ATCTTGCATT TAAATAAATT TTCTTTTTAT AGCTTTATGA CTTAGTTTCA
2351 ATTTATATAC TATTTTAATG ACATTTTCGA TTCGGATCCG CTGGCGTAAT
2401 AGCGAAGAGG CCCGCACCGA TCGCCCTTCC CAACAGTTGC GCAGCCTGAA
2451 TGGCGAATGG CGCCTGATGC GGTATTTTCT CCTTACGCAT CTGTGCGGTA
2501 TTTCACACCG CATAGGGTAA TAACTGATAT AATTAAATTG AAGCTCTAAT
2551 TTGTGAGTTT AGTATACATG CATTTACTTA TAATACAGTT TTTTAGTTTT
2601 GCTGGCCGCA TCTTCTCAAA TATGCTTCCC AGCCTGCTTT TCTGTAACGT
2651 TCACCCTCTA CCTTAGCATC CCTTCCCTTT GCAAATAGTC CTCTTCCAAC
2701 AATAATAATG TCAGATCCTG TAGAGACCAC ATCATCCACG GTTCTATACT
2751 GTTGACCCAA TGCGTCTCCC TTGTCATCTA AACCCACACC GGGTGTCATA
2801 ATCAACCAAT CGTAACCTTC ATCTCTTCCA CCCATGTCTC TTTGAGCAAT
2851 AAAGCCGATA ACAAAATCTT TGTCGCTCTT CGCAATGTCA ACAGTACCCT
2901 TAGTATATTC TCCAGTAGAT AGGGAGCCCT TGCATGACAA TTCTGCTAAC
2951 ATCAAAAGGC CTCTAGGTTC CTTTGTTACT TCTTCTGCCG CCTG
```

6.6 Appendix F: R code for y-intercept determination

```
## Set working directory (final csv table will be saved there)
setwd("C:/…")


## Read the data file
# Has to be a csv file and should contain all OD readings for all
wells as columns.
# First column has to contain the time points.
# Can have a header (first row with column titles). If NOT change
code to "header=F".

dataset <- read.csv(file="… .csv", header=T, sep=",")


## If necessary, eliminate negative values by replacing them with
0.01
# First column needs “Hours” as a header, if not the case, change
header or code.

dataset[dataset<=0] <- 0.01
dataset$Hours[1] <- 0


## Defining time and vectors

time.name <- colnames(dataset[1])
time <- dataset[, time.name[1]]
y.int <- vector("numeric")
OD <- vector("numeric")
col.names <- colnames(dataset[2:(ncol(dataset))])
all.col.names <- colnames(dataset[1:(ncol(dataset))])



## Replace data from wells without growth
# If the max value in the column is lower than OD 0.5, the values
are replaced by 1,2,3,...
# This is to prevent misleading y-intercept values.
# This will return y-intercept "1.270907" and will later be
replaced by NA.
# Can be skipped if necessary (inactivate by preceding each line
by #).

max.value <- vector("numeric")
for(k in 1:(ncol(dataset))){
  max.value[k] <- max(dataset[, all.col.names[k]])
}
df.max <- data.frame(max.value,1:(ncol(dataset)))
index <- df.max$max.value<0.5
dataset[index] <- 1:(nrow(dataset))
```

```
## Loop for all columns: determine phase of highest exponential
growth and y-intercept of the exponential regression
# For each possible string of 6 consecutive values, the linear
regression of the logged OD values (natural logarithm) over time is
calculated and the slope is saved (gradients[i]).
# Gradients and their time points (corresponding to the last one of
the six time points in one string) are stored (df.gradients) and
the maximum gradient and the corresponding OD are determined for
all columns (row.max.gradient.stored[j] and OD.max.stored[j]). This
corresponds to the phase of highest exponential growth.
# For the determined 6 values that resulted in the highest gradient
(OD.exp.range), the linear regression of the logged OD values is
calculated again and the y-intercept is back-transformed to the
exponential scale and stored (y-int[j]).
# IF values in the first few hours are missing in your csv file,
change "for (i in 6:rows)": change from 6 into (your first row with
values)+6

col=((ncol(dataset))-1)
rows=nrow(dataset)
y.int <- vector("numeric")
row.max.gradient.stored <- vector("numeric")
OD.max.stored <- vector("numeric")

for(j in 1:col){
  OD <- dataset[, col.names[j]]
  gradients <- vector("numeric")
  for (i in 6:rows){
    OD.range <- OD[i:(i-5)]
    time.range <- time[i:(i-5)]
    OD.range.log <- log(OD.range)
    gradients[i] <- coef(lm(OD.range.log ~ time.range))[2]
  }
    df.gradients <- data.frame(gradients,time)
    row.max.gradient <- which(df.gradients$gradients == (max(df.gra
dients$gradients, na.rm=TRUE)))
    row.max.gradient.stored[j] <- which(df.gradients$gradients == (
max(df.gradients$gradients, na.rm=TRUE)))
    OD.max.stored[j] <- OD[row.max.gradient]
    OD.exp.range <- OD[(row.max.gradient-5):row.max.gradient]
    OD.exp.range.log <- log(OD.exp.range)
    time.exp.range <- time[(row.max.gradient-5):row.max.gradient]
    fit.exp.OD <- lm(OD.exp.range.log ~ time.exp.range)
    y.int.lin.OD <- coef(fit.exp.OD)["(Intercept)"]
    y.int.OD <- exp(y.int.lin.OD)
    y.int[j] <- y.int.OD
  }

# All y-intercepts are stored in the linear vector y.int (same
order as the columns in your csv table).
# row.max.gradient.stored and OD.max.stored contain the row and OD
corresponding to value 6 in the string of 6 values that make up the
maximum exponential phase (can be used to determine the time points
and ODs corresponding to the maximum exponential phase for all
```

```
columns, if needed).


## Compile the y-intercept results into a matrix
# The matrix will be formatted like a well-plate.
# ncol = 12 is the number of columns on the well plate (=12 for 96-
well plate - change for other layouts/48-well plates etc.)
# This relies on the csv file being formatted like a well plate (A1
-A12 followed by B1-B12 and so on)
# Example: If the csv table only contains data for wells A1-H8,
ncol = 8
# If the csv file skips some columns (e.g., A1 is next to A3) or
has a very different layout, this will not work. The vector y-int
contains the y-intercepts of all columns in the order of the
columns in the csv file, this can be used to access the results.

# The row and column titles are formatted for a 96-well plate.
Change to match different formats.

y.int.matrix <- matrix(y.int, ncol=12, byrow=T)

colnames(y.int.matrix) <- c("1","2","3","4","5","6","7","8","9","10
","11","12")
rownames(y.int.matrix) <- c("A","B","C","D","E","F","G","H")

y.int.matrix


## Replace y-intercepts of wells without growth (OD<0.5 or as
defined above) with “NA”

index2 <- y.int.matrix>1.27
y.int.matrix[index2] <- "NA"


## Save a csv table of the y-intercept data matrix

write.csv(y.int.matrix, file = "… .csv")
```

6.7 Appendix G: Attempt to reconstitute the aconitase FeS cluster

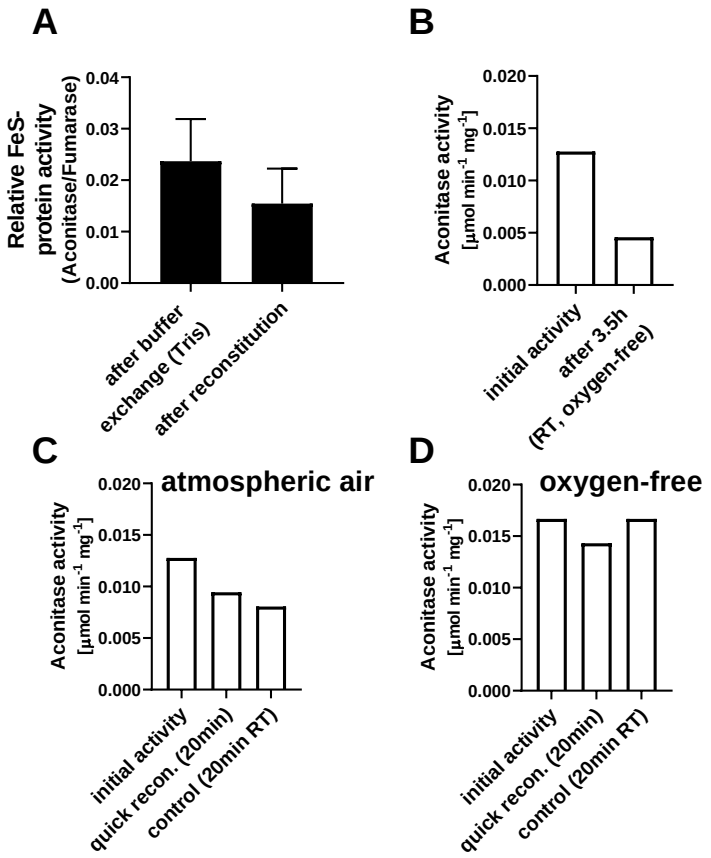

Figure_Apx 5: FeS cluster reconstitution experiments. Crude protein extracts were obtained from exponentially growing *S. cerevisiae* BY4741 cells after treatment with EW (0.3% [v/v] EW; 5.4–6 mg L^{-1} FAC, 5 min, see Figure 3-16 for details and yeast survival). A) The extraction buffer (MES) was replaced by Tris buffer (0.1 M, pH 8), followed by a reconstitution step. Enzyme activities were determined before and after the reconstitution. Aconitase activity is normalised against fumarase activity (non-FeS protein) to account for protein losses during the buffer exchange step. The relative aconitase activity (aconitase/fumarase) was decreased, rather than increased, after the reconstitution compared to after the buffer exchange step. Mean values ± SD are shown for 2 replicates. B) Aconitase activity of a crude protein extract sample from EW treated cells (as in A) was determined immediately after thawing the sample and after 3.5 h (room temperature, anaerobic conditions, see note below) to test the stability of aconitase. After 3.5 h, aconitase activity was decreased by ~64% vs. ~90% decrease after reconstitution in panel A (buffer exchange + reconstitution took ~3.5 h), suggesting that the observed decrease in aconitase activity during the reconstitution protocol cannot be fully explained by the 3.5 h incubation at room temperature. C,D) The reconstitution (see A) was adapted to a shorter protocol (20 min) without buffer exchange. The aconitase activity was measured before (initial activity) and after the reconstitution ("quick recon.") and in a control that was incubated for 20 min with water instead of the reconstitution mix. In anaerobic conditions (D), the reconstitution did not result in higher aconitase activity than the control (incubated in anaerobic conditions for 20 min) or the initial activity, suggesting that the positive effect of 'reconstitution' compared to the water-control in aerobic conditions (C) may be a protection of the FeS cluster from oxygen (protecting the cluster from further damage) by the reconstitution buffer rather than a successful repair of EW induced damage

to the cluster. Data from 1 replicate each in B-D. Note that all buffer exchange and reconstitution steps were performed in plastic tubes which do not guarantee anaerobic conditions, so conditions were not truly "oxygen-free", which likely had a negative effect on the aconitase stability and reconstitution. RT, room temperature.

6.8 Appendix H: Macro for colony size image analysis

Images were opened in ImageJ 1.49k and a square selection of the plate area was performed manually. Colony areas were then measured using the following macro script. If colonies with a size outside of the script's limits (<10,000 or >100,000 pxs) were noticed on a given plate, the "Analyze Particle" command was changed accordingly. Where necessary, colonies were separated from background features of the YEPD agar using the command "Process/Binary/Watershed" after running the macro. Five randomly selected plates were also analysed by manually drawing circles around colonies and measuring the area. The macro's estimates were in close agreement to the manual measurements (automated measurements were 98–110% of the manual measurements; mean ± SD = 103.5 ± 4.4%).

Macro script:

```
run("Duplicate...", " ");
run("Subtract Background...", "rolling=300");
run("Enhance Contrast...", "saturated=4");
run("Color Threshold...");
// Color Thresholder 2.0.0-rc-15/1.49k
// Autogenerated macro, single images only!
min=newArray(3);
max=newArray(3);
filter=newArray(3);
a=getTitle();
run("HSB Stack");
run("Convert Stack to Images");
selectWindow("Hue");
rename("0");
selectWindow("Saturation");
rename("1");
selectWindow("Brightness");
rename("2");
min[0]=0;
max[0]=255;
```

```
filter[0]="pass";
min[1]=0;
max[1]=255;
filter[1]="pass";
min[2]=50;
max[2]=255;
filter[2]="pass";
for (i=0;i<3;i++){
  selectWindow(""+i);
  setThreshold(min[i], max[i]);
  run("Convert to Mask");
  if (filter[i]=="stop")  run("Invert");
}
imageCalculator("AND create", "0","1");
imageCalculator("AND create", "Result of 0","2");
for (i=0;i<3;i++){
  selectWindow(""+i);
  close();
}
selectWindow("Result of 0");
close();
selectWindow("Result of Result of 0");
rename(a);
// Colour Thresholding-------------
run("Median...", "radius=10");
run("Analyze Particles...", "size=10000-100000 circularity=0.5-1.00 display add");
String.copyResults();
```

6.9 Appendix I: Transcriptome analysis

6.9.1 GO Slim terms

Table_Apx 6: GO Slim terms: processes. Percentage of genes mapping to the GO term, number of genes in brackets.

GO Slim term	All detected genes (12243)	All DE genes (660)	All DE up-regulated (251)	All DE down-regulated (409)
Biological process unknown	52.6% (6437)	60% (396)	42.2% (106)	70.9% (290)
Regulation of biological process	10.9% (1338)	7.4% (49)	9.2% (23)	6.4% (26)
Transport	9.9% (1207)	9.4% (62)	13.5% (34)	6.8% (28)
RNA metabolic process	5.9% (725)	4.8% (32)	7.6% (19)	3.2% (13)
Organelle organisation	5.6% (680)	5.5% (36)	8.8% (22)	3.4% (14)

Response to stress	5.0% (613)	5.5% (36)	8.4% (21)	3.7% (15)
Response to chemical	4.2% (515)	3.6% (24)	5.2% (13)	2.7% (11)
Cellular protein modification process	4% (488)	3.9% (26)	5.2% (13)	3.2% (13)
Developmental process	3.4% (413)	3.9% (26)	6% (15)	2.7% (11)
Lipid metabolic process	3.2% (393)	3.2% (21)	3.6% (9)	2.9% (12)
Cell cycle	3.2% (391)	3.5% (23)	6.4% (16)	1.7% (7)
Carbohydrate metabolic process	3% (367)	2.3% (15)	3.6% (9)	1.5% (6)
Filamentous growth	3% (363)	2.7% (18)	3.6% (9)	2.2% (9)
Transcription (DNA-templated)	2.9% (355)	2.3% (15)	3.2% (8)	1.7% (7)
DNA metabolic process	2.1% (262)	3.2% (21)	4.4% (11)	2.4% (10)
Secondary metabolic process	2.1% (261)	1.4% (9)	2.8% (7)	0.5% (2)
Cellular amino acid metabolic process	2% (249)	1.7% (11)	1.6% (4)	1.7% (7)
Vesicle-mediated transport	1.8% (218)	2% (13)	2.4% (6)	1.7% (7)
Translation	1.7% (203)	1.1% (7)	2.4% (6)	0.2% (1)
Signal transduction	1.6% (202)	1.8% (12)	2.8% (7)	1.2% (5)
Asexual sporulation	1.5% (184)	1.4% (9)	2.4% (6)	0.7% (3)
Ribosome biogenesis	1.5% (181)	1.4% (9)	2.4% (6)	0.7% (3)
Cellular homeostasis	1.3% (156)	0.8% (5)	1.2% (3)	0.5% (2)
Protein catabolic process	1.2% (152)	1.2% (8)	2.4% (6)	0.5% (2)
Pathogenesis	1.1% (140)	1.1% (7)	0.8% (2)	1.2% (5)
Sexual sporulation	1.1% (129)	1.5% (10)	2% (5)	1.2% (5)
Cytoskeleton organisation	1% (127)	1.2% (8)	2.4% (6)	0.5% (2)
Toxin metabolic processes	0.8% (96)	0.6% (4)	1.6% (4)	/
Cytokinesis	0.6% (77)	0.5% (3)	0.4% (1)	0.5% (2)
Protein folding	0.5% (66)	0.3% (2)	/	0.5% (2)
Cellular respiration	0.4% (53)	0.3% (2)	0.4% (1)	0.2% (1)
Conjugation	0.3% (40)	0.3% (2)	0.4% (1)	0.2% (1)
Vitamin metabolic process	0.3% (34)	0.3% (2)	0.4% (1)	0.2% (1)
Nucleus organisation	0.3% (34)	0.2% (1)	/	0.2% (1)
Cell adhesion	0.2% (24)	/	/	/
Establishment of vesicle localisation	0% (6)	/	/	/
Transposition	0% (6)	/	/	/
Establishment of nucleus organisation	0% (1)	0.2% (1)	/	0.2% (1)
cannot be mapped to a GO Slim term	10% (1223)	7.4% (49)	10% (25)	5.9% (24)

Table_Apx 7: GO Slim terms: functions. Percentage of genes mapping to the GO term, number of genes in brackets.

GO Slim term	All detected genes (12243)	All DE genes (660)	All DE up-regulated (251)	All DE down-regulated (409)
Molecular function unknown	53.7% (6576)	61.8% (408)	47.4% (119)	70.7% (289)
Hydrolase activity	9.8% (1203)	7.9% (52)	12.4% (31)	5.1% (21)
Oxidoreductase activity	9.0% (1107)	6.1% (40)	8.4% (21)	4.6% (19)
Transferase activity	7.8% (961)	7.3% (48)	9.6% (24)	5.9% (24)
DNA binding	4.9% (605)	4.8% (32)	6.8% (17)	3.7% (15)
Transporter activity	4% (495)	3.2% (21)	4% (10)	2.7% (11)
Protein binding	3.3% (398)	2.3% (15)	3.2% (8)	1.7% (7)
RNA binding	2.2% (269)	2.1% (14)	3.2% (8)	1.5% (6)
Peptidase activity	1.5% (180)	1.2% (8)	2.8% (7)	0.2% (1)
Lyase activity	1.4% (172)	1.1% (7)	1.2% (3)	1% (4)
Protein kinase activity	1.4% (169)	1.7% (11)	2.4% (6)	1.2% (5)
Structural molecule activity	1.4% (166)	0.8% (5)	1.6% (4)	0.2% (1)
Ligase activity	1.2% (141)	1.7% (11)	2% (5)	1.5% (6)
Enzyme regulator activity	0.9% (113)	0.9% (6)	1.2% (3)	0.7% (3)
Helicase activity	0.8% (99)	0.5% (3)	0.8% (2)	0.2% (1)
Isomerase activity	0.7% (82)	0.5% (3)	0.8% (2)	0.2% (1)
Phosphatase activity	0.6% (78)	0.8% (5)	1.2% (3)	0.5% (2)
Nucleotidyl-transferase activity	0.6% (77)	0.9% (6)	1.2% (3)	0.7% (3)
Translation regulator activity	0.4% (54)	0.5% (3)	1.2% (3)	/
Lipase activity	0.3% (33)	0.3% (2)	/	0.5% (2)
Motor activity	0.2% (23)	0.2% (1)	/	0.2% (1)
Cannot be mapped to a GO Slim term	6.4% (785)	6.1% (40)	7.6% (19)	5.1% (21)

Table_Apx 8: GO Slim terms: components. Percentage of genes mapping to the GO term, number of genes in brackets.

GO Slim term	All detected genes (12243)	All DE genes (660)	All DE up-regulated (251)	All DE down-regulated (409)
Cellular component unknown	66.8% (8184)	69.4% (458)	53.8% (135)	79% (323)
Membrane	11.7% (1434)	11.2% (74)	16.7% (42)	7.8% (32)
Nucleus	10.9% (1331)	10.5% (69)	14.3% (36)	8.1% (33)
Mitochondrion	4% (488)	4.1% (27)	5.6% (14)	3.2% (13)
Endomembrane system	3.6% (435)	3.5% (23)	5.2% (13)	2.4% (10)
Plasma membrane	2.6% (315)	2.3% (15)	4% (10)	1.2% (5)
Chromosome	2.5% (312)	2% (13)	3.6% (9)	1% (4)
Extracellular region	2.2% (269)	2% (13)	3.2% (8)	1.2% (5)
Cytosol	2.1% (260)	2.9% (19)	5.2% (13)	1.5% (6)
Cytoskeleton	1.5% (184)	1.2% (8)	1.2% (3)	1.2% (5)

Ribosome	1.2% (147)	0.8% (5)	1.6% (4)	0.2% (1)
Vacuole	1.2% (144)	1.8% (12)	2.4% (6)	1.5% (6)
Endoplasmatic reticulum	1% (128)	0.9% (6)	0.8% (2)	1% (4)
Cell cortex	1% (124)	0.6% (4)	0.4% (1)	0.7% (3)
Site of polarised growth	1% (123)	1.4% (9)	2% (5)	1% (4)
Nucleolus	1% (120)	1.1% (7)	2.4% (6)	0.2% (1)
Golgi apparatus	1% (120)	0.5% (3)	1.2% (3)	/
Microtubule skeleton	1% (118)	0.9% (6)	1.2% (3)	0.7% (3)
Peroxisome	0.8% (93)	0.6% (4)	0.8% (2)	0.5% (2)
Cell wall	0.8% (103)	1.1% (7)	2% (5)	0.5% (2)
Actin cytoskeleton	0.6% (69)	0.3% (2)	/	0.5% (2)
Cannot be mapped to a GO Slim term	3.8% (462)	3.2% (21)	5.6% (14)	1.7% (7)

6.9.2 List of DE genes with unknown functions detected at two or three time points

Table_Apx 9: List of DE genes found at more than one time point, with orthologs of unknown function in other *Aspergillus* species. LogFC values are plotted in Figure 4-30 A.

Gene ID[a]	Orthologs in other *Aspergillus* species (function unknown)
An07g07680	Ortholog of *A. nidulans* FGSC A4 : AN4506, *A. fumigatus* Af293 : Afu2g03250, A. oryzae RIB40 : AO090120000262, *Aspergillus wentii* : Aspwe1_0059757 and *Aspergillus sydowii* : Aspsy1_0073302
An11g00580	Ortholog of *A. oryzae* RIB40 : AO090023000204, Neosartorya fischeri NRRL 181 : NFIA_056440, *Aspergillus wentii* : Aspwe1_0171161 and *Aspergillus versicolor* : Aspve1_0147930
An07g06990	Ortholog of *A. nidulans* FGSC A4 : AN4556, *A. fumigatus* Af293 : Afu2g02670, *A. oryzae* RIB40 : AO090026000612, *Aspergillus wentii* : Aspwe1_0036732 and *Aspergillus sydowii* : Aspsy1_0154947
An09g04310	Ortholog of *Aspergillus brasiliensis* : Aspbr1_0057159 and *Aspergillus acidus* : Aspfo1_0084546
An07g05100	Ortholog of *Aspergillus tubingensis* : Asptu1_0151353, *Aspergillus flavus* NRRL 3357 : AFL2T_12157*, Aspergillus kawachii* : Aspka1_0175431 and *Aspergillus acidus* : Aspfo1_0040960
An03g04610	Ortholog of *A. fumigatus* Af293 : Afu5g08360*, A. oryzae* RIB40 : AO090701000757, *Aspergillus wentii* : Aspwe1_0035166, *Aspergillus sydowii* : Aspsy1_0046236 and *Aspergillus terreus* NIH2624 : ATET_08268
An16g04370	Ortholog of *A. nidulans FGSC A4* : AN2806, *A. niger CBS 513.88* : An14g05270, An11g10010, An14g07230, An15g00800, *A. oryzae RIB40* : AO090103000150, AO090113000067 and *Aspergillus wentii* : Aspwe1_0117492
An08g01010	Ortholog of *Aspergillus acidus* : Aspfo1_0079546
An18g03420	Ortholog of *Aspergillus tubingensis* : Asptu1_0052118
An02g06340	Ortholog of *A. nidulans FGSC A4* : AN4921, *A. fumigatus Af293* : Afu3g10680, *A. oryzae RIB40* : AO090003000613, *Aspergillus wentii* : Aspwe1_0360214 and *Aspergillus sydowii* : Aspsy1_0056501 (uncharacterised)

An02g14000	Ortholog of *Aspergillus tubingensis* : Asptu1_0055440, *Aspergillus brasiliensis* : Aspbr1_0051229 and *Aspergillus acidus* : Aspfo1_0057718
An08g04330	Ortholog of *Aspergillus tubingensis* : Asptu1_0037715, *Aspergillus brasiliensis* : Aspbr1_0053866, *Aspergillus kawachii* : Aspka1_0178640 and *Aspergillus acidus* : Aspfo1_0129898
An17g01915	Ortholog of *Aspergillus niger* ATCC 1015 : 45202-mRNA
An08g02680	Ortholog of *A. nidulans FGSC A4* : AN1221, *A. fumigatus Af293* : Afu1g10620, *A. oryzae RIB40* : AO090038000358, *Aspergillus wentii* : Aspwe1_0049022 and *Aspergillus sydowii* : Aspsy1_0139464
An07g03490	Ortholog of *Aspergillus acidus* : Aspfo1_0056732 (uncharacterised)
An02g08680	Ortholog of *A. nidulans FGSC A4* : AN3114, *A. fumigatus Af293* : Afu3g12710, *A. oryzae RIB40* : AO090012000852, *Aspergillus wentii* : Aspwe1_0105294 and *Aspergillus sydowii* : Aspsy1_0056161 (uncharacterised)
An18g03400	Ortholog of *Aspergillus tubingensis* : Asptu1_0052114

[a] Genes in bold were significantly differentially expressed at three time points (all other genes were significantly expressed at two time points).

Searchable list of DE genes that were significant at more than one time point and whose function is unknown (bold: significant at three time points, others where significant at two time points). LogFC values are plotted in Figure 4-30 B.

An17g00380, An08g06860, An04g04220, An11g07850, An09g05500, An14g03380, An07g04740, An11g02310, An18g05410, An01g11030, An04g03230, An12g00150, An11g06910, An15g01090, An07g03510, **An09g04450**, An09g04610, An07g04910, An18g06100, An08g04210, An07g01610, An04g09880, **An16g04360**, An16g00360, An02g08500, An16g08960, An12g00190, An01g04350, **An02g10290**, **An07g07080**, An08g08810, **An02g14420**, **An12g08990**, An18g01920, An04g06550, An02g12190, **An18g06080**, An02g12580, An12g00430, An02g13990, An01g05720

6.10 Appendix J: ROS detection by flow cytometry in *A. niger*

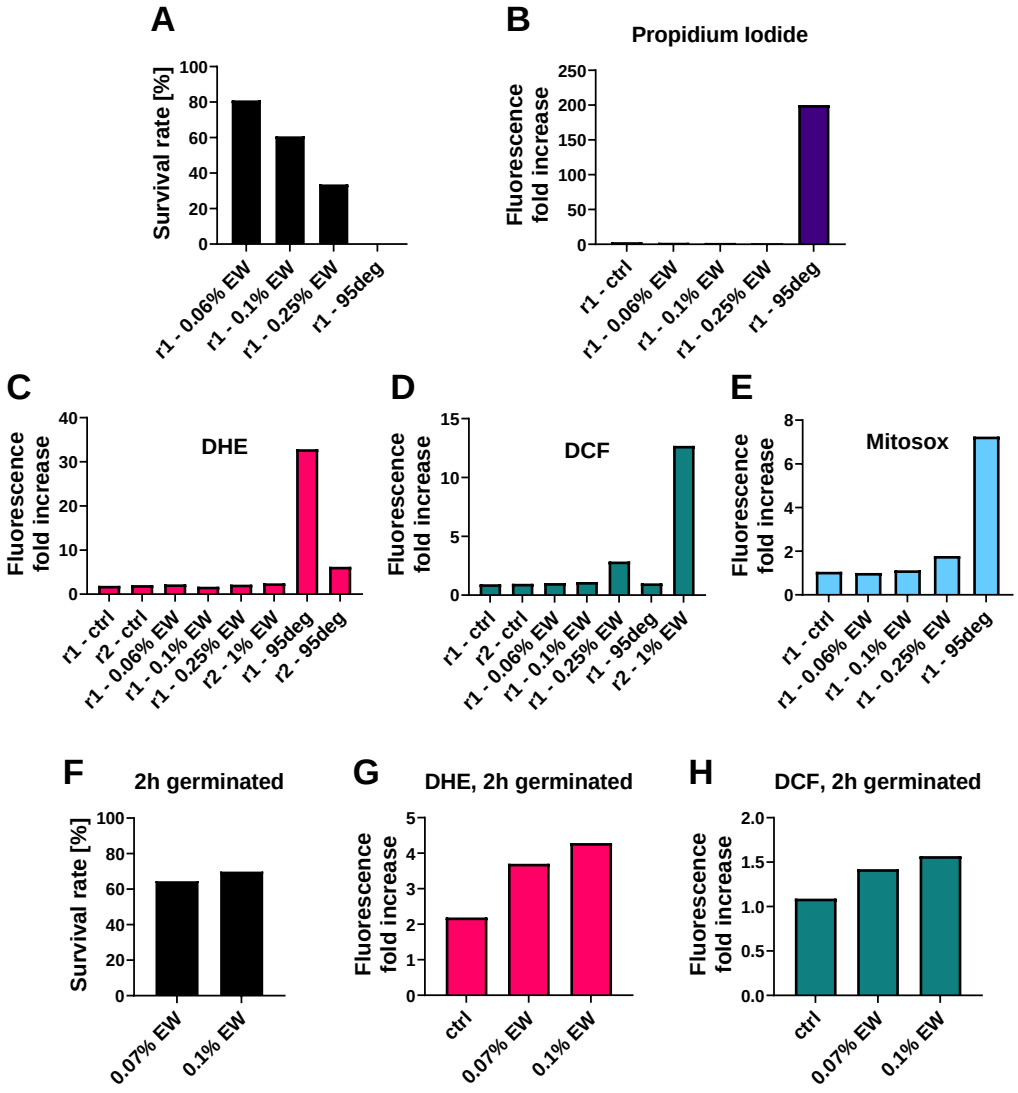

Figure_Apx 6: ROS detection by flow cytometry in *A. niger*. Spore suspensions (A–E) or conidia from 2 h-germination cultures harvested by filtration (F–H) were suspended in Tween 80 (0.1%) and treated or not with EW dilutions in sterile tap water (33–50 mL treatment volume; 0.06–1% EW; full strength EW was 1900–2000 mg L^{-1} FAC for r1 in panels A–E and ~1600 mg L^{-1} FAC for r2 and panels F–H). Treatments were stopped by centrifugation and resuspension in YEPD as before (4.2.5.1). Heat treatments ("95deg") were performed at 95°C for 10 min (400–500 µL spore suspensions, 10^7 spores mL^{-1}) and stopped by YEPD addition (10 mL). "r1" and "r2" refer to 2 biological replicates on different days. Data in panel F–H (1 biological replicate) was obtained in the same experiment as r2 data in A–E. A,F) Appropriate dilutions were plated onto YEPD agar for colony enumeration. Survival [%] was calculated relative to untreated controls. Survival could not be determined for r2 due to very dense colony growth on control and EW treatment plates (no growth on heat treatment plates). B–E,G,H) Samples were washed in PBS and stained with ROS dyes before flow cytometry analysis (staining was for 30 min in the dark [30°C] followed by washing in PBS; except propidium iodide which was added in the final resuspension step before flow cytometry). Samples were analysed in a BD FACS Canto™ A flow cytometer

(gating single spore events based on light scatter properties [SSC-A/FSC-A] and doublet exclusion [FSC-H/FSC-A]). Fluorescence was recorded with 488 nm excitation and 564–606 nm emission filter (DHE, MitoSOX™ or PI) or 515–545 nm emission filter (DCF). 10,000 single spore events were usually recorded (if possible; at least 2000 events were recorded in samples with low spore levels). The fluorescence in unstained samples was increased in EW-treated samples compared to untreated controls, therefore the fold increase of median fluorescence was calculated for each stained sample relative to its unstained control. B) Propidium iodide staining (5 µg mL^{-1}) was performed in experiment r1 only. C,G) Staining with 5 µM DHE (dihydroethidium). D,H) Staining with 50 µM (r2 in D; H) or 10 µM (r1 in D) DCF (2',7'-dichloro-dihydro-fluorescein diacetate). E) Staining with 5 µM MitoSOX™ was performed in experiment r1 only.